

**Combinatorial regulation of bZIP10
dependent stress responses in
*Arabidopsis thaliana***

Dissertation

der Mathematisch-Naturwissenschaftlichen Fakultät
der Eberhard Karls Universität Tübingen
zur Erlangung des Grades eines
Doktors der Naturwissenschaften
(Dr. rer. nat.)

vorgelegt von
Abhroop Garg
aus Ujjain, Madhya Pradesh, Indien

Tübingen
2018

Tag der mündlichen Qualifikation:

15.03.2018

Dekan:

Prof. Dr. Wolfgang Rosenstiel

1. Berichterstatter:

Prof. Dr. Klaus Harter

2. Berichterstatter:

Prof. Dr. Ulrike Zentgraf

Declaration

The research work described in this thesis has been carried out under the supervision of Dr. Christina Chaban during the period of October 2011 - Jan 2018 at Zentrum für Molekularbiologie der Pflanzen, Eberhard-Karls-University, Tuebingen. I hereby declare that unless otherwise specified, all sample preparation and downstream gene/protein characterization or analyses have been independently performed by me.

1. The *Mamestra* infection assay was performed by me under the guidance of Ms. Merel Steenberg at the laboratory of Dr. A.C.M. (Saskia) van Wees, Institute of Environmental Biology, Utrecht University, Netherlands.
2. The sample preparation for qPCR and root growth assay was done by Ms. Kerstin Haible (TA).
3. The *Pseudomonas* infection assay was performed by Dr. Lorenzo Pedrotti, University of Wuerzburg, Germany.
4. Part of the sample preparation and complete analysis of GC-MS data for the hormone measurement was performed by Dr. Joachim Kilian, Analytics, ZMBP, Tuebingen University.
5. Part of the sample preparation for the proteomics analysis, the MS/MS runs and data processing were done by the Proteome Centre Tuebingen.
6. The library preparation for ChIP-Seq was performed by me under the guidance of Ms. Christa Lanz at MPI Developmental biology, Tuebingen. The analysis of the ChIP-Seq data was performed by Dr. Stefan Czemmel at Quantitative Biology Centre, Tuebingen University (Figures 52-56).

Abhroop Garg

February 03, 2018

Table of Contents

List of Abbreviations	1
Summary	3
Zusammenfassung	5
1. Introduction	7
1.1. Transcription factors	8
1.2. The bZIP transcription factors	9
1.3. Regulation of transcription by phosphorylation	14
1.4. Plant immune reponses	15
1.4.1. SA-dependent defense responses	17
1.4.2. JA-dependent defense responses	19
1.4.3. Cross talk between SA and JA pathways.....	21
1.5. Redox regulation in plants	26
1.5.1. Redox PTMs of protein thiols.....	29
1.5.2. Functional significance of redox PTMs	31
2. Aim of Thesis	34
3. Materials and Methods	35
3.1. Materials	35
3.1.1. List of Chemicals and Consumables:	35
3.1.2. List of Primers:	37
3.1.3. List of DNA constructs:	40
3.2. Methods	43
3.2.1. Polymerase chain reaction (PCR).....	43
3.2.2. Cloning of genes of interest.....	44
3.2.3. Site-directed mutagenesis.....	44
3.2.4. Bacterial transformation.....	46
3.2.5. Plasmid isolation (Mini prep)	46
3.2.6. Plasmid isolation (Maxi prep).....	47
3.2.7. Sequencing of plasmids	47
3.2.8. <i>Arabidopsis</i> leaf mesophyll protoplasts isolation by tape-sandwich method and transfection.....	47
3.2.9. GUS-NAN Assay.....	51
3.2.10. Sub-cellular localization	52
3.2.11. FRET-FLIM (Förster Resonance Energy Transfer - Fluorescence Lifetime Imaging)	52
3.2.12. Yeast 2-hybrid and Split ubiquitin system.....	52
3.2.13. Yeast β -gal assay.....	55
3.2.14. Generation of transgenic lines of <i>Arabidopsis</i>	56
3.2.15. Pathogen assays	57
3.2.16. RNA isolation.....	60

3.2.17. cDNA synthesis.....	61
3.2.18. Quantitative polymerase chain reaction (qPCR).....	61
3.2.19. Hormone measurement	61
3.2.20. Arabidopsis root growth assay.....	62
3.2.21. Reporter gene assay in tobacco leaf cells.....	63
3.2.22. Immunoprecipitation of GFP-tagged bZIP10.....	64
3.2.23. Polyacryl amide gel electrophoresis (PAGE).....	67
3.2.24. Western blotting.....	68
3.2.25. Proteomics analysis of bZIP10	70
3.2.26. Chromatin Immunoprecipitation (ChIP).....	70
3.2.27. ChIP library preparation.....	74
4. Results.....	76
4.1. Analysis of regulation of bZIP10 using phosphorylation mutants.....	76
4.1.1. Transactivation capacity of bZIP10 phosphorylation mutants	76
4.1.2. bZIP10 phospho-mimetic mutant heterodimer formation	78
4.1.3. Sub-cellular localization of bZIP10 phosphorylation mutants	81
4.2. Functional characterization of bZIP10.....	86
4.2.1. <i>Mamestra brassicae</i> infection assay	87
4.2.2. <i>Botrytis cinerea</i> infection assay.....	92
4.2.3. <i>Pseudomonas syringae</i> infection assay.....	94
4.2.4. Hormone measurement.....	95
4.2.5. Effect of SA on bZIP10 transactivity	98
4.2.6. Effect of SA on bZIP10-dependent root growth	101
4.3. Redox regulation of bZIP10.....	104
4.3.1. MS-based proteomics analysis of bZIP10.....	105
4.3.2. Effect of oxidative stress on bZIP10 activity	111
4.3.3. Effect of oxidative stress on bZIP10 heterodimerization.....	114
4.3.4. Effect of oxidative stress on sub-cellular localization of bZIP10	116
4.3.5. LSD1 dependent sub-cellular localization of bZIP10.....	117
4.3.6. Interaction of bZIP10 and LSD1 under oxidative stress.....	119
4.3.7. Effect of LSD1 on bZIP10-bZIP53 transactivation capacity	122
4.4. Identification of direct targets of bZIP10	125
4.4.1 Screening for appropriate conditions and positive controls.....	125
4.4.2. ChIP-qPCR pilot experiment	129
4.4.3. Chromatin Immunoprecipitation (ChIP-Seq).....	131
4.5. Proteomic screen for bZIP10 interaction partners	142
5. Discussion.....	144
5.1. Regulation of bZIP10 by phosphorylation	144
5.2. The antagonistic role of bZIP10 in the <i>Arabidopsis</i> defense responses	147
5.3. Redox regulation of bZIP10	153
5.4. Identification of ASN1 as a direct target of bZIP10	159

5.5. Target gene identification attempt by Chromatin Immunoprecipitation (ChIP-Seq)	162
5.6. Proteomic screen for bZIP10 interaction partners	166
6. Conclusion	169
7. References	171
8. List of Publications	180
9. Curriculum Vitae	181
10. Acknowledgements	182

List of Abbreviations

ABA	Abscisic acid
AD	Activation domain
Ala	Alanine
Asp	Aspartate
BD	Binding domain
bHLH	Basic helix-loop-helix
bZIP	Basic region leucine zipper
CAT	Catalase
ChIP-Seq	Chromatin immunoprecipitation sequencing
COI1	Coronatine insensitive 1
CPK	Calcium-dependent protein kinase
CPRFs	Common Plant Regulatory Factors
Cub	C-terminal ubiquitin half
Cys	Cysteine
DAMPs	Danger-associated molecular patterns
DBD	DNA-binding domain
ET	Ethylene
ETI	Effector triggered immunity
GFP	Green fluorescent protein
GSH	Glutathione
HR	Hyper-sensitive response
IC	Isochorismate
Ile	Isoleucine
IP	Immunoprecipitation
JA	Jasmonic acid
JAZ	Jasmonate zim domain
LES	Low energy syndrome
LSD1	Lesion simulating disease 1

MAMPs	Microbe-associated molecular patterns
NEM	N-ethylmaleimide
NES	Nuclear export sequence
NLS	Nuclear localization signal
NO	Nitric oxide
NPR1	Non-expressor of pathogenesis related genes 1
Nub	N-terminal ubiquitin half
ORA59	Octadecanoid-responsive Arabidopsis 59
PAMPs	Pathogen-associated molecular patterns
PCD	Programmed cell death
PDF1.2	Plant defensin 1.2
PR	Pathogenesis related
ProDH1	Proline Dehydrogenase 1
PRRs	Pattern recognition receptors
PTI	Pattern triggered immunity
PTMs	Post-translational modifications
RNS	Reactive nitrogen species
ROS	Reactive oxygen species
SA	Salicylic acid
SABP	Salicylic acid binding protein
SAR	Systemic acquired resistance
Ser	Serine
SIRT	Sucrose induced repression of translation
SUS	Split ubiquitin system
TAF	TBP associated factors
TBP	TATA-box binding proteins
TF(s)	Transcription factors(s)
TPL	Topless
TRX	Thioredoxins
VSP2	Vegetative storage protein 2

Summary

For plants to survive, it is of utmost importance that they respond to different environmental stimuli appropriately. These responses mostly arise from an altered gene expression, which is regulated by transcription factors. The bZIP transcription factors, found in all eukaryotes from yeast to humans, form an important part of different metabolic processes and stress responses in plants. I focused on bZIP10, a C-group bZIP in the model plant *Arabidopsis thaliana* with the objective of unraveling its involvement in plant processes and its mode of regulation. The pathogen assays performed on bZIP10 transgenic lines of *Arabidopsis* revealed that bZIP10 is involved in the biotic stress responses in *Arabidopsis*. The over-expression of bZIP10 in *Arabidopsis* resulted in enhanced tolerance of the plants towards the biotrophic pathogen *Pseudomonas syringae*, while exhibiting an increased susceptibility against the necrotrophic pathogen *Botrytis cinerea* and the herbivore *Mamestra brassicae*. It seems that bZIP10 plays a positive role in the salicylic acid mediated defense responses against biotrophic pathogens while indirectly antagonizing the jasmonic acid mediated defense responses against the necrotrophs and herbivory, thereby facilitating a cross talk between SA- and JA-defense pathways in *Arabidopsis thaliana*. The mass spectrometry based proteomic analysis of bZIP10 revealed that the Cys residues in bZIP10 might be involved in its redox based regulation. In the line with this, the Cys-to-Ala substitutions in bZIP10 sequence caused the alteration in *ProDH1* (*PROLINE DEHYDROGENASE 1*) transactivation by the heterodimers of bZIP10 and bZIP53, a known interaction partner of C-group bZIPs, in the leaf mesophyll protoplasts. However, the transactivation capacity of the bZIP10 Cys mutants did not coincide with their heterodimerization capacity with bZIP53, thus indicating a role of another protein in the regulation of activity of bZIP10. Using ChIP-qPCR and gene expression analysis, I identified *ASN1* (*ASPARAGINE SYNTHETASE 1*) as a possible direct target of bZIP10. The phenotypes obtained in our pathogen assays correlate well with the reported phenotypes of *Arabidopsis* plants with modified levels of *ASN1*, indicating that, at least partially, bZIP10 could be regulating pathogen defense responses via its regulation of *ASN1*. Finally, several proteins were identified in the mass

spectrometry based proteomics screen as putative bZIP10 interaction candidates, thus providing valuable clues regarding the function and regulation of bZIP10.

Zusammenfassung

Um überleben zu können ist es äußerst wichtig, dass Pflanzen angemessen auf verschiedene Reize aus ihrer Umwelt reagieren. Dies wird meistens durch Änderungen der Expression verschiedener Gene ermöglicht. Expressionsänderungen werden durch Transkriptionsfaktoren reguliert. bZIP-Transkriptionsfaktoren finden sich in Eukaryoten, von der Hefe hin zu Menschen, und spielen in Pflanzen bei verschiedenen metabolischen Prozessen und bei der Reaktion auf unterschiedliche Stressfaktoren eine wichtige Rolle. Den Schwerpunkt meiner Untersuchungen legte ich auf bZIP10, ein bZIP aus der C-Gruppe der Modellpflanze *Arabidopsis thaliana*, mit dem Ziel den Einfluss und die Art der Regulation dieses Transkriptionsfaktors in pflanzlichen Prozessen aufzuklären. Pathogenexperimente mit *Arabidopsis* bZIP10-Überexpressionslinien zeigten, dass dieser Transkriptionsfaktor in der biotischen Stressantwort involviert ist. Die Überexpression von bZIP10 führte zur erhöhten Toleranz der Pflanzen gegenüber dem biotrophen Pflanzenschädling *Pseudomonas syringae* und zur erhöhten Sensitivität gegenüber dem nekrotrophen Schädling *Botrytis cinerea* und dem herbivoren Fraßfeind *Mamestra brassicae*. Es scheint, dass bZIP10 einen positiven Einfluss auf Salicylsäure-vermittelte Abwehrreaktionen gegen biotrophe Pathogene und indirekt eine antagonistische Rolle bei Jasmonat-vermittelten Reaktionen auf nekrotrophe Pathogene und Herbivoren hat. Daher scheint bZIP10 ein weiterer wichtiger Faktor bei der Wechselwirkung zwischen SA- und JA-vermittelten Abwehrmechanismen zu sein. Durch massenspektrometrische Proteomanalysen von bZIP10 konnte gezeigt werden, dass Cystein-Reste eventuell eine Rolle bei der Redox-basierten Regulation dieses Proteins spielen. Dies stimmt mit dem Ergebnis über ein, dass ein Austausch von Cystein- zu Alanin-Resten, in der bZIP10 Proteinsequenz, zu einer Veränderung der ProDH1 (PROLINE DEHYDROGENASE 1) Transaktivierung, durch bZIP10 und bZIP53 Heterodimere in Protoplasten aus Mesophyllzellen, führt. bZIP53 ist dabei ein bekannter Interaktionspartner von bZIP Transkriptionsfaktoren der C-Gruppe. Allerdings stimmte bei diesen Mutanten die Fähigkeit der Transaktivierung nicht mit der Fähigkeit Heterodimere zu bilden überein. Dies weist darauf hin, dass ein weiteres Protein eine Rolle bei der Regulation von bZIP10 spielen könnte. ChIP-qPCR und

Genexpressionsanalysen weisen darauf hin, dass ASN1 (ASPARAGINE SYNTHETASE 1) möglicherweise direkt durch bZIP10 reguliert wird. Die von uns beobachteten Phänotypen stimmen dabei mit den veröffentlichten Daten von *Arabidopsis*-Pflanzen mit veränderten ASN1 Gehalten überein. Dies weist darauf hin, dass bZIP10 die Pathogenantwort über die Regulation von ASN1 verändert. Abschließend konnten durch massenspektrometrische Proteomanalysen einige weitere Proteine als potentielle bZIP10 Interaktionspartner identifiziert werden. Diese Analysen liefern wertvolle Hinweise auf die Funktion und Regulation von bZIP10.

1. Introduction

Plants are very important for sustaining life on Earth as they fix the solar energy that is subsequently used by almost all living organisms on our planet. For plants to survive, it is of utmost importance that they respond to different environmental stimuli appropriately. Environmental stimuli may include abiotic factors such as light, drought, high and low temperature, soil salinity, and biotic factors such as pathogen and pest attack. On perception of these signals or cues, specific responses are induced that are tightly regulated from physiological to cellular and all the way down to the molecular level. Most of these responses are the result of altered gene expression. Upregulation or downregulation of a gene could regulate the amount of enzymes and proteins present in the cell, consequently modulating the intracellular biochemical reactions, leading to amplification of the original signal, which could in the end upregulate or downregulate other genes. Therefore identifying the signaling components of a transduction pathway and unraveling their function is imperative for understanding the plant responses. In this regard, model organisms provide some distinctive advantages in that they are easily manipulated, relatively inexpensive, have short regeneration time and are easy to propagate (Edison, Hall et al. 2016).

Arabidopsis thaliana, a member of Brassicaceae family, was the first flowering plant whose genome was sequenced (Kramer 2015). It is comprised of about 25,500 genes and 11,000 protein families. The sequencing of *Arabidopsis* paved the way for a much better understanding of plant responses (Arabidopsis Genome Initiative 2000). A little over 1500 transcription factors were identified in the *Arabidopsis* genome, which forms almost 6 % of the total genes. Comparative analysis of *Arabidopsis* genome with the genomes of *Caenorhabditis elegans*, *Drosophila melanogaster* and *Saccharomyces cerevisiae* revealed that 45 % of these transcription factors belonged to plant specific families. Transcriptional control of gene expression regulates most of the biological processes in a living organism, ranging from development to environmental stimuli. Transcription factors act as regulatory switches through which an organism modulates its cellular pathways (Riechmann, Heard et al. 2000).

1.1. Transcription factors

Transcription factors (TFs) are proteins that bind to their target DNA in order to activate or repress the transcription of the corresponding genes. This binding is mediated by a highly conserved specific domain in the transcription factor known as the DNA-binding domain (DBD). Apart from this, the transactivation domain and the interaction domain, by mediating interactions with other proteins, also play an important role in TF function (Frankel and Kim 1991, Phillips 2008). TFs also contain other functional domains, which could play diverse roles such as nuclear transport or localization, oligomerization or mediation of protein degradation (Ptashne 1988, Johnson and McKnight 1989, Pabo and Sauer 1992).

The DBD of TF recognizes specific DNA sequences known as *cis*-acting elements or boxes present in the promoters of the corresponding genes (Phillips and Hoopes 2008). Different TFs bind *cis*-acting elements with varying affinities dependent on the properties of their DBD. For example, the basal TFs, TBP (TATA-box binding proteins) and TAF (TBP associated factors), both belonging to the TFII transcription factor family can bind to the TATA-box (Breathnach and Chambon 1981, Buratowski, Hahn et al. 1989, Dynlacht, Hoey et al. 1991, Zhou, Boyer et al. 1993). Together with RNA polymerase II and other proteins, they form what is called a transcription initiation complex that is responsible for initiating the transcription. This basal complex can be regulated by sequence motifs present upstream to the TATA-box (Buratowski 1994, Tjian and Maniatis 1994), e.g., the LREs (Light Responsive Elements) comprising of G-box and C-box in the plant promoters. It has been shown that these sequences are recognized by the members of the bZIP transcription factor family (Izawa, Foster et al. 1993, Suckow, von Wilcken-Bergmann et al. 1993, Foster, Izawa et al. 1994).

Based on their characteristic structural motifs, plant TFs have been classified into different classes. For example, the basic helix-loop-helix (bHLH) proteins comprise a basic DBD and a HLH domain. The α -helix in the basic region is responsible for the interaction with DNA while the HLH region, as the name suggests, comprises two α -helices separated by a loop and is responsible for its homo- and heterodimerization

(Meshi and Iwabuchi 1995). Another class of transcription factors classified based on their structural motif is bZIP, which is discussed in more detail below.

1.2. The bZIP transcription factors

The basic region leucine zipper (bZIP) transcription factors consist of two structural features: an ~16 amino acid residues long basic region composed of a nuclear localization signal followed by N-x7-R/K motif responsible for interaction with DNA; and a zipper domain formed by repetition of hydrophobic amino acid leucine at every seventh position, known as the heptad repeats (**Figure 1A**) (Lupas 1996). Also, the leucine residue could be substituted by other hydrophobic amino acid residues (Jakoby, Weisshaar et al. 2002). The side-chains of these hydrophobic amino acid residues are exposed to the same side of the α -helix generating an amphipathic structure. The hydrophobic interaction between two α -helices leads to dimerization of bZIPs. Upon dimerization, the bZIP dimer assumes a Y-shape, with the C-terminal leucine zipper forming the stem and the N-terminal DBD of each monomer forming the two arms. Both the arms interact with the major groove of the double helix on the opposite sides (**Figure 1B**). The bZIPs can either form homodimers or heterodimers leading to specific functionalities (Llorca, Potschin et al. 2014).

The bZIP transcription factors are found in all eukaryotes ranging from *Saccharomyces cerevisiae* to *Homo sapiens*. In plants, they regulate important processes such as energy metabolism, hormone signaling, and biotic and abiotic stress responses (Choi, Hong et al. 2000, Fujita, Fujita et al. 2005, Baena-Gonzalez, Rolland et al. 2007, Alves, Dadalto et al. 2013). They are also known to be involved in plant developmental processes such as maturation of seedling and flowering (Abe, Kobayashi et al. 2005, Alonso, Onate-Sanchez et al. 2009). In 1989, Katagiri *et al* and Tabata *et al* described the first plant bZIP proteins, namely TGA1a and TGA1b from tobacco (Katagiri, Lam et al. 1989) and HBP1 (Histone DNA Binding Protein 1) from wheat (Tabata, Takase et al. 1989). In 1991, three CPRFs (Common Plant Regulatory Factors), CPRF1, CPRF2 and CPRF3, belonging to the bZIP family were identified to be interacting with the LRE present in the chalcone synthase (CHS) promoter in parsley (Weisshaar, Armstrong et al. 1991).

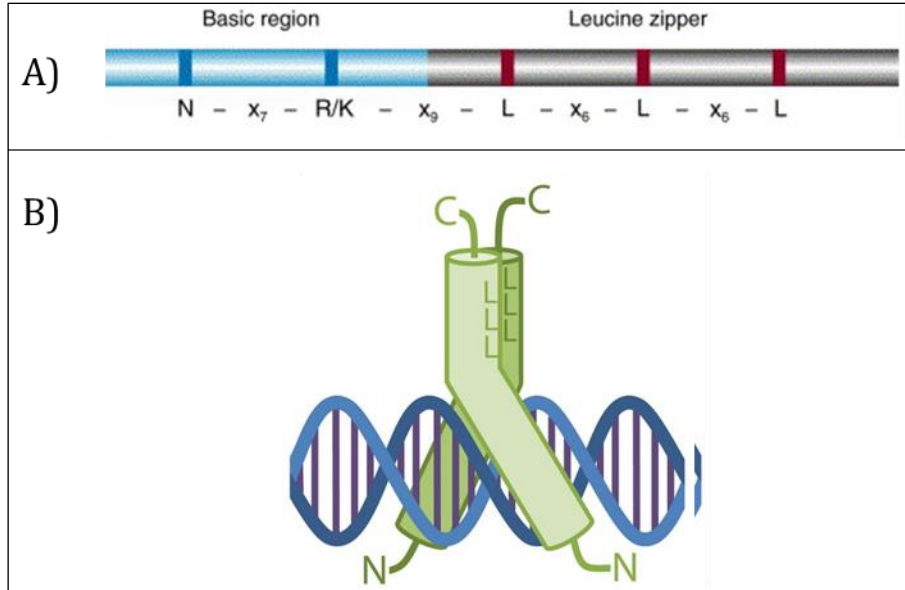


Figure 1: (A) Schematic representation of a bZIP domain. The basic region comprising of the NLS and the DBD is shown in blue. The α -helical domain containing the heptad repeats is shown in grey. The blue and red bars depict the conserved residues (Jakoby, Weisshaar et al. 2002). (B) Schematic representation of a DNA bound bZIP dimer (Llorca, Potschin et al. 2014).

In *Arabidopsis*, about 75 bZIP TFs have been identified which, based on the sequence similarities in their basic region, are divided into 10 groups from A to I and S (Figure 2) (Jakoby, Weisshaar et al. 2002). The group nomenclature is based on either the known members (e.g. C for CPRF2 homolog, G for GBF1, H for HY5) or the size of the protein (B for big, S for small) or just alphabetically. The functions of many of the *Arabidopsis* bZIPs still remain to be elucidated.

The A-group consists of abscisic acid (ABA) response element (ABRE) binding factors (ABFs/AREBs). There are seven members in this group that are known to regulate ABA-mediated abiotic stress responses (Choi, Hong et al. 2000, Correa, Riano-Pachon et al. 2008, Xu, Kim et al. 2013, Yoshida, Fujita et al. 2015). One of the most studied group members ABI5 (bZIP39) is involved in the regulation of seed development and germination. The S-nitrosylation of ABI5 leads to its proteasomal degradation, thereby lifting up the growth arrest induced by ABA (Albertos, Romero-Puertas et al. 2015).

The D-group bZIPs (also known as TGA factors) are involved in plant development and pathogen defense (Jakoby, Weisshaar et al. 2002). The interaction of NPR1 (Non-

expressor of pathogenesis related genes 1) with TGA TFs has been reported to regulate the expression of salicylic acid (SA) mediated defense responsive genes. In the absence of SA, the expression of PR1 is repressed by TGA2, TGA5 and TGA6 while the presence of SA induces its expression mediated by these TGAs (Seyfferth and Tsuda 2014). The role of these TFs is discussed in a bit more detail later in this section.

The G-group bZIPs, homologues of CPRF1, CPRF3, CPRF4a and CPRF5 from parsley (Jakoby, Weisshaar et al. 2002), generally bind to the G-boxes in the promoters of genes regulated by different environmental signals. For example, GBF3 (G-box binding factor 3) has been reported to impart tolerance to plants against drought, salinity and osmotic stress (Ramegowda, Gill et al. 2017). GBF1, another G-group member, regulates photomorphogenesis in two ways: it positively regulates the growth of cotyledon, while negatively regulating light dependent inhibition of hypocotyl elongation. It has also been shown that GBF1 heterodimerises with H-group bZIPs, HY5/bZIP56 (Elongated hypocotyl 5) and HYH/bZIP64 (HY5 homologue) (Ram and Chattopadhyay 2013).

The S-group with 17 members is the largest one of the ten bZIP groups. It is further subdivided into 3 sub-groups based on bZIP domain homology, namely S1, S2 and S3 (Ehlert, Weltmeier et al. 2006). The sub-group S1 includes five bZIPs; bZIP1, bZIP2, bZIP11, bZIP44 and bZIP53. These bZIPs contain a long 5' leader sequence bearing upstream open reading frames (uORFs). These uORFs are highly conserved in the S1-group bZIPs (Weltmeier 2009) and play a regulatory role in sucrose induced repression of translation (SIRT) of these bZIPs. Thus, the nutrient status of the cell might be under the control of these bZIPs (Weltmeier, Rahmani et al. 2009). It has been proposed that bZIP1, bZIP11 and bZIP53 could mediate the SnRK1 (SNF1-related kinase 1) signaling pathway-induced transcriptional reprogramming and thereby being involved in LES (Low Energy Syndrome) in *Arabidopsis* (Tome, Nagele et al. 2014). Recently, bZIP11 was shown to negatively regulate primary root growth upon starvation (Weiste, Pedrotti et al. 2017).

AtbZIPno.	Gene code	Published name	GenBank Acc.	AtbZIPno.	Gene code	Published name	GenBank Acc.
AtbZIP12	At2g41070	DPBF4	AF334209	AtbZIP16	At2g35530		AV559248*
AtbZIP13	At5g44080		BN000023	AtbZIP41	At4g36730	GBF1	X63894
AtbZIP14	At4g35900		BN000021	AtbZIP54	At4g01120	GBF2	AF053228
AtbZIP15	At5g42910		AJ419599	AtbZIP55	At2g46270	GBF3	U51850
AtbZIP27	At2g17770		BN000022	AtbZIP68	At1g32150		-
AtbZIP35	At1g49720	ABF1	AF093544	AtbZIP56	At5g11260	HY5	AB005295
AtbZIP36	At1g?	ABF2/ AREB1	AF093545	AtbZIP64	At3g17609	HYH	AF453477
AtbZIP37	At4g34000	ABF3	AF093546	AtbZIP18	At2g40620		AY0744269
AtbZIP38	At3g19290	ABF4/AREB2	AF093547	AtbZIP29	At4g38900		AF401297
AtbZIP39	At2g36270	ABI5	AF334206	AtbZIP30	At2g21230		AF401298
AtbZIP40	At1g03970	GBF4	U01823	AtbZIP31	At2g13150		AF401301
AtbZIP66	At3g56850	AREB3	AB017162	AtbZIP32	At2g12980		AV566578*
AtbZIP67	At3g44460	DPBF2	AJ419600	AtbZIP33	At2g12900		-
AtbZIP17	At2g40950		AV551374*	AtbZIP51	At1g43700	VIP1	AF225983
AtbZIP28	At3g10800		AJ419850	AtbZIP52	At1g06850		AJ419852/53
AtbZIP49	At3g56660		AJ419851	AtbZIP59	At2g31370	PosF21	X61031
AtbZIP9	At5g24800	BZO2H2	AF310223	AtbZIP69	At1g06070		AJ419854
AtbZIP10	At4g02640	BZO2H1	AF310222	AtbZIP71	At2g24340		-
AtbZIP25	At3g54620		AJ010860	AtbZIP73	At2g13130		-
AtbZIP63	At5g28770	BZO2H3	AF310224	AtbZIP74	At2g21235		-
AtbZIP20	At5g06950	AHBP-1b/TGA2	D10042	AtbZIP1	At5g49450		AF400618
AtbZIP21	At1g08320		AJ314757	AtbZIP2	At2g18160	GBF5	AF053939
AtbZIP22	At1g22070	TGA3	L10209	AtbZIP3	At5g15830		AV549429*
AtbZIP26	At5g06960	OBF5/TGA5	X69900	AtbZIP4	At1g59530		AF400619
AtbZIP45	At3g12250	TGA6	AJ320540	AtbZIP5	At3g49760		-
AtbZIP46	At1g68640	PAN	AF111711	AtbZIP6	At2g22850		-
AtbZIP47	At5g65210	TGA1	X68053	AtbZIP7	At4g37730		AI992458
AtbZIP50	At1g77920		AJ315736	AtbZIP8	At1g68880		AF400621
AtbZIP57	At5g10030	OBF4/TGA4	X69899	AtbZIP11	At4g34590	ATB2	X99747
AtbZIP65	At5g06839		AJ314787	AtbZIP42	At3g30530		-
AtbZIP34	At2g42380		AF401299	AtbZIP43	At5g38800		-
AtbZIP61	At3g58120		AF401300	AtbZIP44	At1g75390		AV566155*
AtbZIP19	At4g35040		N65677*	AtbZIP48	At2g04038		-
AtbZIP23	At2g16770		AV544638*	AtbZIP53	At3g62420		AF400620
AtbZIP24	At3g51960		AI994442*	AtbZIP58	At1g13600		AF332430
				AtbZIP70	At5g60830		-
				AtbZIP75	At5g08141		-
				AtbZIP60	At1g42990		AY045964
				AtbZIP62	At1g19490		-
				AtbZIP72	At5g07160		-

Figure 2: Classification of *Arabidopsis* bZIP transcription factors, adapted from (Jakoby, Weisshaar et al. 2002).

The C-group comprises four members: bZIP9, bZIP10, bZIP25 and bZIP63. These TFs share structural similarities with Opaque2 from maize and CPRF2 from parsley. The members of this group contain up to nine heptads in their leucine zipper domain (Jakoby, Weisshaar et al. 2002). bZIP9, bZIP25 and bZIP63 exhibit an exclusive nuclear localization. bZIP63 was recently demonstrated to regulate the starvation response in *Arabidopsis*. The authors also reported that bZIP63 is a direct target of the SnRK1 kinase. Upon phosphorylation by SnRK1, the dimerization preferences of bZIP63 changes,

subsequently leading to the differential regulation of its target genes (Mair, Pedrotti et al. 2015).

bZIP10 (protein of interest in my thesis, **Figure 3**), unlike the other three members of the group, localizes to the nucleus as well as cytoplasm. The first 105 amino acids in bZIP10 form the interaction site of XPO1 (Protein exportin 1A). This interaction leads to XPO1-mediated active transport of bZIP10 from the nucleus to the cytoplasm. LSD1 (Lesion simulating disease 1) was identified as the protein responsible for retaining bZIP10 in the cytoplasm. LSD1 is a plant specific zinc-finger protein, which functions as a negative regulator of plant cell death induced by ROS (Reactive Oxygen Species). It has been suggested that LSD1 could regulate the transcriptional activity of bZIP10 by retaining it in the cytoplasm (Kaminaka, Nake et al. 2006).

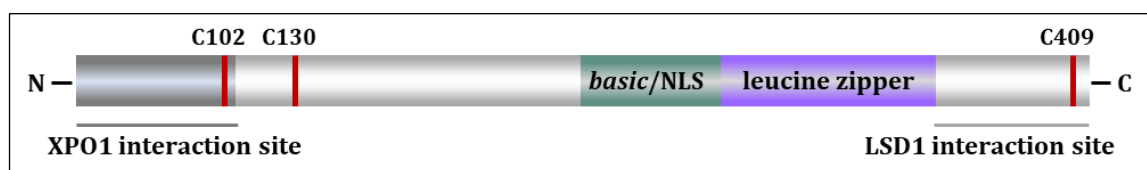


Figure 3: Schematic diagram depicting the functional domains of bZIP10.

The very C-terminus of bZIP10 is required for its interaction with LSD1. The specific interaction of LSD1 with only bZIP10 can be ascribed to the least similarity of this C-terminal domain among the C-group bZIPs. Binding of LSD1 to bZIP10 also blocks the latter's ability to bind to DNA *in vitro*. It has been proposed that LSD1 regulates the nuclear transport of bZIP10 by masking the NLS of bZIP10 (Kaminaka, Nake et al. 2006). It is also possible that LSD1 interacts with bZIP10 in the nucleus, thereby making it incompetent to bind to DNA. Under conditions leading to oxidative stress, ROS-mediated signaling might result in dissociation of bZIP10 from LSD1 by a mechanism not known yet. The dissociated bZIP10 could then be transported to the nucleus where it can activate the expression of its target genes (Schutze, Harter et al. 2008). The direct genomic targets of bZIP10 are not yet known. However, it has been shown that bZIP10, functioning antagonistically to LSD1, acts as a positive regulator of ROS induced cell death and hyper-sensitive response (HR) induced by pathogens. The *Arabidopsis* transgenic lines over-expressing bZIP10 and *lsd1* mutant exhibited an improved

resistance towards *Hyaloperonospora parasitica* (biotrophic fungus) (Kaminaka, Nake et al. 2006).

The S1-group is known to specifically dimerize with the C-group bZIPs (Ehlert, Weltmeier et al. 2006). This so-called C/S1 bZIP network have been shown to be involved in amino acid metabolism, stress response, energy homeostasis and sink specific gene expression. For example, bZIP53, upon dimerization with bZIP10 or bZIP25 (both C-group bZIPs) has been shown to enhance the expression of the *MAT* (*MATURATION*) genes (Alonso, Onate-Sanchez et al. 2009). bZIP53 has also been shown to be involved in abiotic stress response by regulating the expression of several genes including *ProDH1* (*PROLINE DEHYDROGENASE 1*), a direct target of heterodimers of C/S1 bZIPs (Weltmeier, Rahmani et al. 2009). Upon heterodimerization, a synergistic increase could be seen in the reporter gene activation, which was highest for bZIP10/bZIP53 heterodimers (Weltmeier, Ehlert et al. 2006).

1.3. Regulation of transcription by phosphorylation

Protein phosphorylation is one of the most ubiquitous post-translational modifications involved in the regulation of almost all cellular processes and responses. It involves a transfer of a phosphate group from ATP to mostly serine (Ser), threonine (Thr) and tyrosine (Tyr), consequently leading to a change in the structure or function of a protein. Enzymes known as kinases mediate this reversible reaction, while phosphatases catalyze the reverse reaction. Due to its reversible nature, phosphorylation plays an important role in cellular signaling (Cheng, Deng et al. 2014).

Owing to the extensive studies performed in the previous years, phosphorylation of transcription factors is now known to be one of the major means of regulating transcription factors. It can affect transcription factors in various ways. Phosphorylation can lead to a change in the stability of a transcription factor. For example, it has been shown that phosphorylation of MyoD (a bHLH animal transcription factor) and E2F-1 (an E2F family transcription factor in humans) leads to their degradation, while the degradation of ATF2 (a human bZIP) and p53 is prevented upon phosphorylation. Phosphorylation can also affect the sub-cellular localization of a transcription factor, as

in the case of NFAT (Nuclear factor of activated T cells family of transcription factors in humans) and FKHRL1 (transcription factor of human Forkhead family). Phosphorylation of these proteins restricts their movement to the nucleus. As seen for CREB-CBP (CREB is a human bZIP transcription factor) interaction and dimerization of STAT (Signal transducers and activators of transcription) proteins, phosphorylation can also affect protein-protein interaction and oligomerization respectively. Phosphorylation has also been known to modulate the DNA-binding ability of transcription factors. The STAT proteins and c-Jun (a human bZIP) are good examples of this regulation (Holmberg, Tran et al. 2002). Phosphorylation is also known to regulate the activity of plant bZIPs by the above-mentioned mechanisms. For example, phosphorylation of HY5 prevents its E3-ubiquitin-protein ligase COP1 mediated degradation (Hardtke, Gohda et al. 2000). Phosphorylation dependent sub-cellular localization has been shown for the tobacco bZIP RSG (Repression of shoot growth) (Ishida, Yuasa et al. 2008) and *Arabidopsis* bZIP51 (aka VIP1) (Djamei, Pitzschke et al. 2007). Finally, phosphorylation of bZIPs have been shown to prevent them from binding to their target DNA sequences (Kirchler, Briesemeister et al. 2010).

1.4. Plant immune responses

Broadly classified, plant pathogens are of two types: necrotrophs and biotrophs. The pathogens that kill the host cells and feed on its contents are known as the necrotrophs. The pathogens, which follow biotrophic lifestyle, derive their nutrition from the host cells without killing them. Some pathogens, however, have necrotrophic and biotrophic growth stages in their life cycle. Such pathogens are known as hemi-biotrophs (Pieterse, Van der Does et al. 2012).

During the course of evolution, plants have developed a two-tiered innate immune system: PTI (Pattern triggered immunity) and ETI (Effector triggered immunity). The recognition of PAMPs or MAMPs (pathogen- or microbe-associated molecular patterns) such as flagellin, chitin and glycoproteins or endogenous DAMPs (danger-associated molecular patterns) by PRRs (pattern recognition receptors) leads to the activation of PTI. This forms the first line of defense against various adapted and non-adapted

pathogens. Some pathogens have evolved a way of either suppressing or bypassing PTI by injecting effector proteins (Avr) into their hosts. In response to this, plants have developed what are called the resistance (R) proteins, which can recognize these Avr proteins or the changes carried out by them in the host resulting in the activation of ETI, the second line of defense (**Figure 4**). ETI is responsible for resistance against specific pathogens. In general, PTI and ETI are very similar responses, except that ETI is a much faster and stronger response than PTI, and ETI may involve programmed cell death near the infection site, known as the hyper-sensitive response (HR), to restrict the spread of pathogen to other parts of the plant.

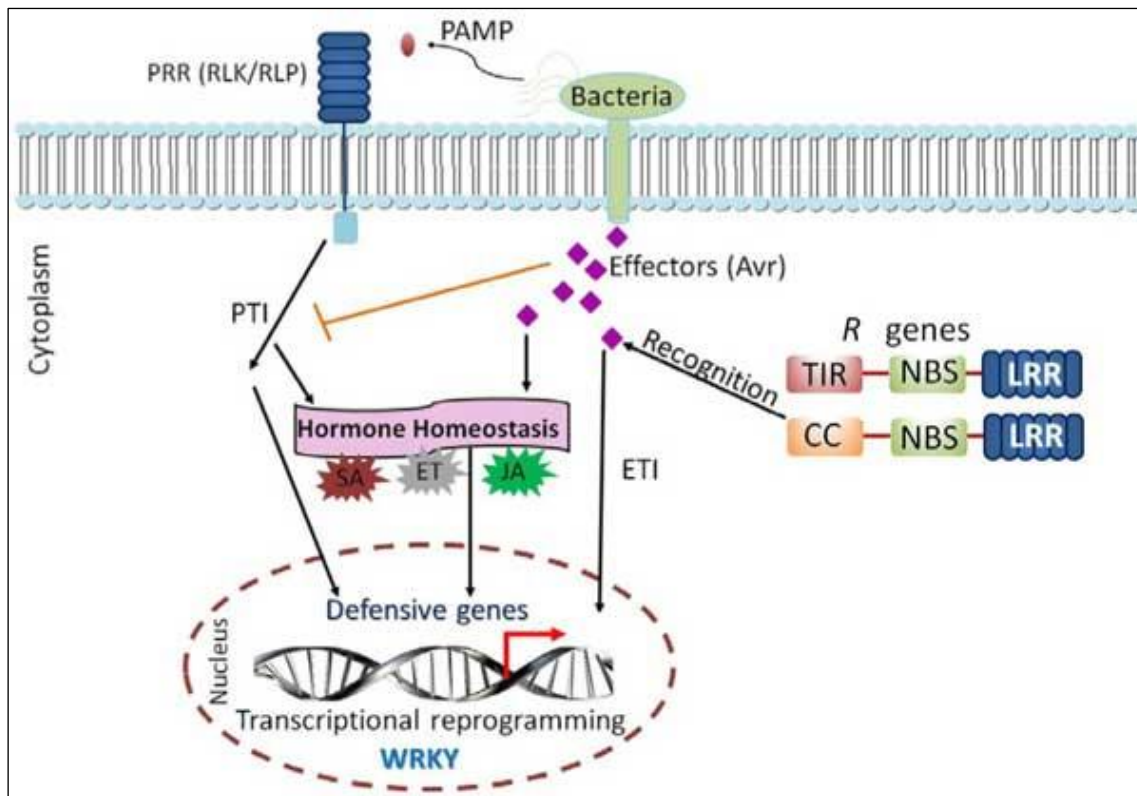


Figure 4: Different modes of pathogen recognition in plants leading to the induction of defense responses. The perception of PAMPs by PRRs induces PTI. Some pathogens release Avr proteins to suppress PTI. These Avr proteins are recognized by R proteins leading to ETI. Adapted from (Amorim, da Fonseca Dos Santos et al. 2017).

The plant immune signaling network is largely controlled by the plant hormones. While salicylic acid (SA) and jasmonic acid (JA) are the two major hormones involved in the regulation of plant defense responses, other hormones such as ethylene (ET), abscisic

acid (ABA), cytokinins (CKs), gibberelins (GAs), auxins, brassinosteroids and nitric oxide (NO) are also known to participate in this regulation (Pieterse, Van der Does et al. 2012, Li, Meng et al. 2016, Amorim, da Fonseca Dos Santos et al. 2017).

1.4.1. SA-dependent defense responses

In general, the SA defense pathway imparts resistance to plants against the biotrophic pathogens. SA can be synthesized in plants via either isochorismate (IC) or phenylalanine ammonia-lyase (PAL) pathways, both of which use chorismate as the precursor. The enzyme ICS (isochorismate synthase) catalyzes the conversion of chorismate to isochorismate, from which SA is synthesized in the chloroplasts. In the latter pathway, PAL catalyzes the conversion of phenylalanine to *trans*-cinnamic acid, which is then further converted to SA. The MATE (Multidrug and toxin)-transporter EDS5 (Enhanced disease susceptibility 5) then transports SA to the cytosol (Seyfferth and Tsuda 2014, Dempsey and Klessig 2017). The accumulation of SA leads to the activation of NPR1 (Non-expressor of pathogenesis related genes 1), which then initiates the transcription of *PR* (*PATHOGENESIS RELATED*) genes. Although a diverse group, a lot of *PR* genes are known to encode anti-microbial proteins (Pieterse, Van der Does et al. 2012).

Under basal conditions, NPR1 resides in the cytoplasm in its oligomeric form. The oligomers are formed because of the intermolecular disulfide bonds between the Cys residues of NPR1. Upon pathogen invasion, SA causes a change in the redox state of the cell, thereby resulting in TRX-H3 (Thioredoxin H3) and TRX-H5 mediated reduction of the intermolecular disulfide bonds of NPR1. The monomerized NPR1 then translocates to the nucleus via the nuclear pore proteins such as MOS (Modifier of *snc1*). The SA levels determine the NPR1 monomer levels inside the nucleus. NPR3 and NPR4, both homologs of NPR1, are SA receptors, which participate in the proteasomal degradation of NPR1 by behaving as CUL3 ligase adapter proteins. They both differ in their binding affinities for SA with NPR4 possessing a higher affinity for SA and NPR3 lower. Low SA level causes the binding of NPR4 with NPR1 resulting in its degradation and avoiding the unwarranted transcription of its target genes. High SA level results in the degradation of NPR1 via its interaction with NPR3. Since NPR1 is a negative regulator of PCD

(programmed cell death), this degradation is thought to be important for PCD activation. Only the intermediate levels of SA allow the accumulation of NPR1 in the nucleus. Once inside the nucleus, NPR1 interacts with the TGA factors (D-group bZIPs) such as TGA2 and TGA3 to form a complex, which then initiates the transcription of SA-dependent defense genes such as *PR-1*. NPR1 is then phosphorylated, ubiquitinated and ultimately targeted for proteasomal degradation, thus allowing new NPR1 monomers to reinitiate the transcription (**Figure 5**). Very often, a similar response is triggered in plant parts distant from the infection site which renders resistance to the healthy parts against subsequent infections, known as SAR (Systemic Acquired Resistance) (Pieterse, Van der Does et al. 2012, Seyfferth and Tsuda 2014, Caarls, Pieterse et al. 2015).

Several proteins are known to negatively regulate this pathway. For example, NIMIN1 (Non-inducible immunity (NIM)1-interacting protein 1) most likely targets the TGA factors for repressing the transcription of the defense genes. NIMIN1 has been shown to form a ternary complex with NPR1 and TGA2 in yeast, which dissociates in the presence of SA. SNI1 (Suppressor of *npr1* inducible 1) is another repressor identified in a suppressor screen of *npr1* mutant. It has been suggested that SNI1 could repress SA-responsive genes by binding to the transcriptional repressor CBNAC (CaM-binding NAC) because SNI1-CBNAC interaction enhances latter's ability to bind to the *PR1* promoter. Upon SA induction, SNI1 gets replaced by the DNA repair protein SSN2 (Suppressor of *sni1* 2). Apart from SSN2, other DNA repair proteins such as BRCA2A (Breast cancer 2A) and RAD51D (RAS associated with diabetes 51D) are also a part of the SA-dependent defense responses as SA has been known to cause damage to DNA (**Figure 5**) (Pieterse, Van der Does et al. 2012, Seyfferth and Tsuda 2014). Additionally, SA also induces expression of several WRKY transcription factors, which can either repress or activate the SA responses. Furthermore, the promoters of *NPR1* and *ICS1* contain WRKY factors responsive W-boxes, indicating WRKY-dependent regulation of *NPR1* and *ICS1* to further fine-tune the SA-mediated responses (Seyfferth and Tsuda 2014, Dempsey and Klessig 2017).

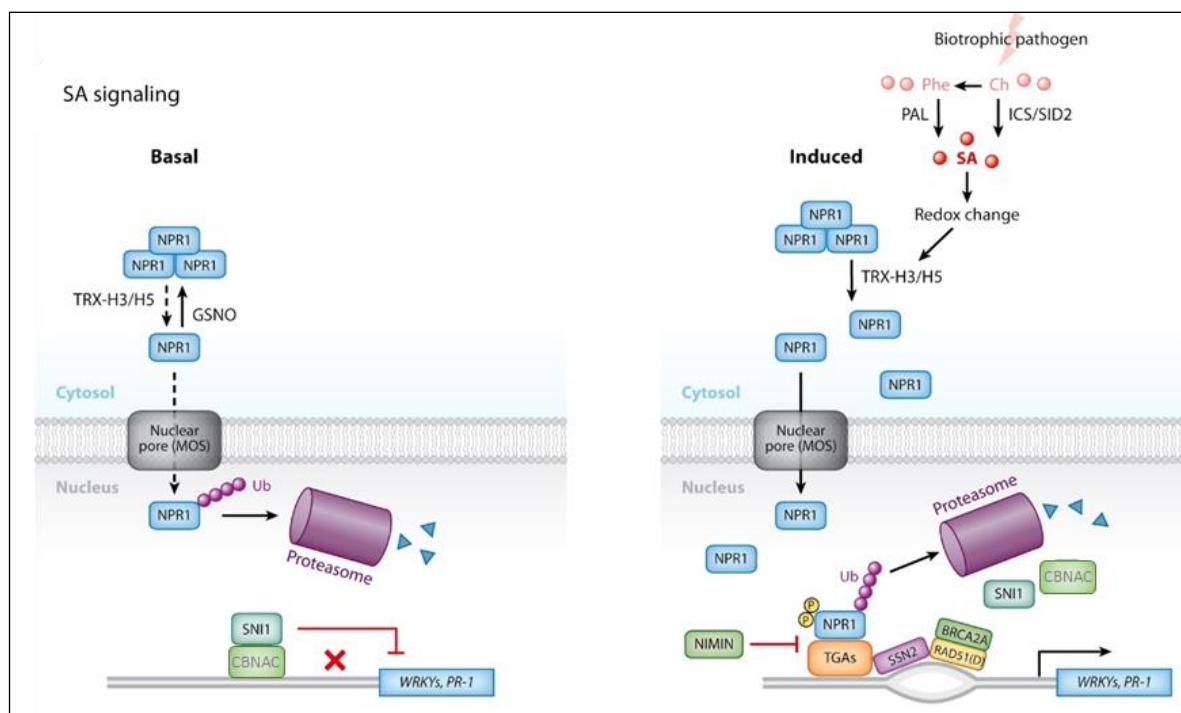


Figure 5: Schematic representation of SA-dependent signaling pathway. Solid arrows represent either known activity or accumulation of compound. Arrows with dotted lines represent low relative activity and the red lines and crosses represent inhibition and transcriptional repression respectively. CBNAC (in grey)-mediated repression of SA-responsive genes by SNI1 in unstressed conditions is hypothetical. Ch: chorismate, P: phosphorylated protein, Ub: ubiquitinated protein. Adapted from (Pieterse, Van der Does et al. 2012).

1.4.2. JA-dependent defense responses

Generally, the defense responses of plants against necrotrophic pathogens and herbivores are mediated by JA-dependent immune pathway. The biosynthesis of JA takes place via the oxylipin pathway in plants starting with α -linolenic acid. In the end, JA is either converted to methyl jasmonate (MeJA) by JMT (JA carboxyl methyl transferase) or combined with isoleucine (Ile) by JAR1 (Jasmonoyl isoleucine conjugate synthase 1) to form JA-Ile, both of which are bioactive forms of JA (Pieterse, Van der Does et al. 2012, Wasternack and Hause 2013).

The JA perception and signaling is mediated by the SCF (Skp1/Cullin/F-box) complex. This complex, an E3 ubiquitin ligase, has COI1 (Coronatine insensitive 1) as the F-box protein which along with the JAZ (Jasmonate zim domain) proteins perceives JA-Ile leading to the ubiquitinylation and subsequent proteasomal degradation of JAZ proteins.

Under non-induced conditions, the binding of the JAZ proteins to the transcriptional activators such as MYC2/3/4 represses the JA defense pathway. The ZIM domain of the JAZ proteins binds to NINJA (Novel interactor of JAZ), which in turn, via its EAR (ERF-associated amphiphilic repression) domain recruits the corepressor TPL (Topless), thus deactivating the JA-responsive genes. The JA-Ile perception causes the dissociation of JAZ proteins and transcriptional activators, and the inhibition on the JA-responsive genes is lifted. In *Arabidopsis*, there are two parallel branches in the JA signaling pathway: the MYC branch (co-regulated by ABA) and the ERF branch (co-regulated by ET). As the name suggests and described above, the MYC transcription factors such as MYC2 regulate the MYC branch which consists of *VSP2* (*VEGETATIVE STORAGE PROTEIN 2*) and *LOX2* (*LIPOXYGENASE 2*) as the JA-responsive marker genes. The ERF branch is controlled by AP2/ERF (APETALA2/Ethylene response factor) transcription factors such as ERF1 and ORA59 (Octadecanoid-responsive Arabidopsis 59) with *PDF1.2* (*PLANT DEFENSIN 1.2*) as the JA-responsive marker gene. In resting cells, the ethylene (ET) responsive transcription factors EIN3 (Ethylene insensitive 3) and EIL1 (EIN3-like 1) interact with the JAZ proteins which in turn recruit the corepressor HDA6 (Histone deacetylase 6) consequently leading to the inhibition of transcription. Upon induction of JA and ET, the JAZ proteins are degraded resulting in the activation of EIN3/EIL1, which further leads to the activation of *ERF1*, *ORA59* and *PDF1.2* (**Figure 6**). The ERF branch is responsible for imparting resistance to plants against necrotrophs while the MYC branch renders resistance against the herbivores and is involved in the wound response as well (Pieterse, Van der Does et al. 2012, Wasternack and Hause 2013, Caarls, Pieterse et al. 2015).

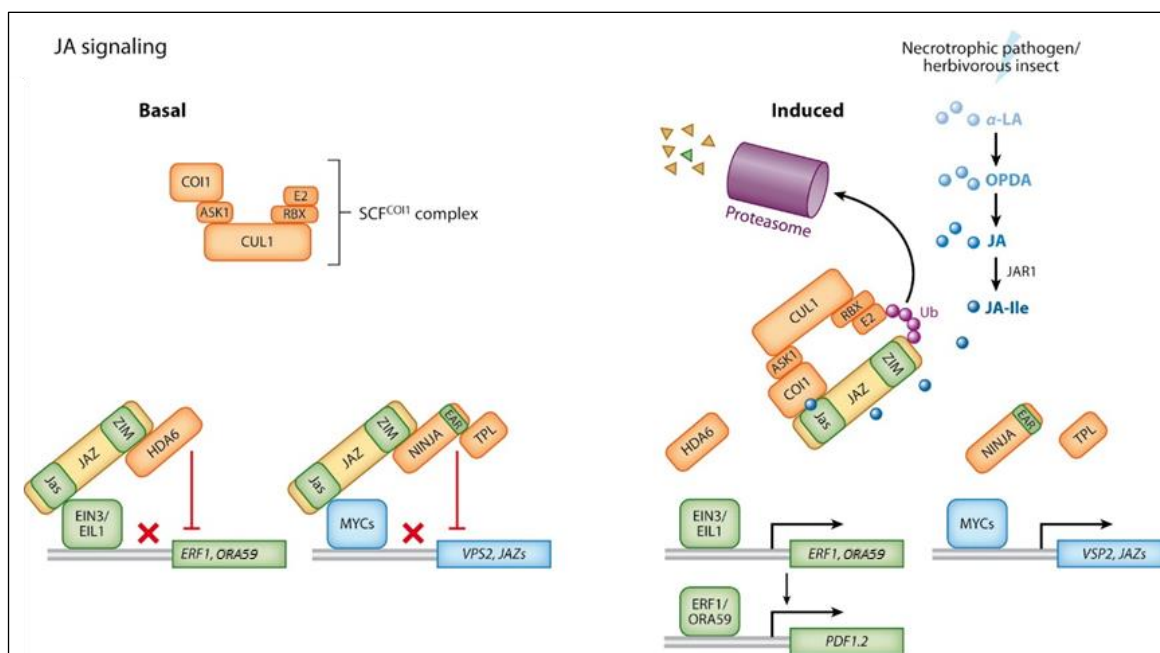


Figure 6: Schematic representation of JA-dependent signaling pathway. Solid arrows represent either known activity or accumulation of compound. The red lines and crosses represent inhibition and transcriptional repression respectively. Ub: ubiquitinated protein. Adapted from (Pieterse, Van der Does et al. 2012).

1.4.3. Cross talk between SA and JA pathways

The SA- and JA-dependent defense pathways form a complex network in which other plant hormones such as ET and ABA also participate in deciding the final outcome. The SA-JA cross talk was first revealed when SA and aspirin (acetylated SA) were shown to repress the JA-mediated response upon wounding in tomato. Since then, this antagonism has been reported to be functional in different plant species. This communication between the different hormones may help the plants to mount a finely tuned, tailor-made response against the invader. For example, *Pseudomonas syringae*, in the early stages of the infection, induces both, SA and JA pathways. However, the SA-dependent suppression of JA pathway results in granting the plants resistance against the pathogen. In nature, plants are not attacked by a single enemy at a time. There can be a simultaneous or sequential invasion of attackers employing different tactics to overpower their host. In situations like these, there might be a need for plants to prioritize one pathway over the other in order to survive, and the hormonal cross talk can be an important mechanism to do that. The JA-dependent susceptibility against the necrotrophs or herbivores has been

reported to be the price paid for the SA-dependent resistance against the biotrophs (Pieterse, Van der Does et al. 2012). For example, *Arabidopsis* leaves infected with *Pseudomonas syringae* induce the SA pathway, which in turn suppresses the JA-dependent responses and makes the leaves susceptible to the necrotrophic fungus *Alternaria brassicicola* (Spoel, Johnson et al. 2007). Similarly, upon *Pieris rapae* (induces JA pathway) caterpillar feeding, the JA-dependent defenses are suppressed in plants pre-inoculated with the biotroph *Hyaloperonospora arabidopsidis* (induces SA pathway) (Koornneef, Leon-Reyes et al. 2008). Conversely, JA-dependent signaling can result in the suppression of the SA pathway as well. The biotrophic pathogen *Pseudomonas syringae* produces coronatine (COR), a phytotoxin that mimics JA-Ile leading to activation of JA pathway, which in turn suppresses the SA pathway. The bacterium employs this as a strategy to make its host plants susceptible (Pieterse, Van der Does et al. 2012).

The SA-JA cross talk does not always lead to the suppression of one pathway or the other. Upon treatment with low amounts of SA and JA, a synergistic increase in *PR-1* (SA responsive) and *PDF1.2* (JA responsive) gene expression was seen. The authors observed that this synergism turned into antagonism upon prolongation of the treatment times or upon increasing the SA and JA amounts (Mur, Kenton et al. 2006). In a very recent report, the SA receptors NPR3 and NPR4 were shown to activate JA-dependent defense genes and *de novo* synthesis of JA. The authors suggested that this activation was the result of NPR3- and NPR4-mediated degradation of JAZ proteins. This synergism between SA and JA pathway may also aid plants in defending against biotrophic pathogens without becoming defenseless against the necrotrophs (Liu, Sonbol et al. 2016).

Although the SA-JA interaction has been shown to be antagonistic and synergistic, it does appear to show antagonism predominantly (Pieterse, Van der Does et al. 2012, Caarls, Pieterse et al. 2015). It was thought earlier that SA exerted its repression of JA pathway by targeting JA biosynthesis as it was shown that genes of many enzymes of JA biosynthetic machinery are SA-repressible. However, it was demonstrated that in the *aos/dde2* mutant (no biosynthesis of JA), there was a similar repression of MeJA-induced *PDF1.2* expression by SA as compared to the wild-type plants, thus indicating that SA-mediated repression of JA pathway is functioning, maybe additionally, downstream to

the JA biosynthesis. Next, it was shown that SA could suppress the expression of *PDF1.2* in the *coi1-1* (JA receptor) mutant. The JA-responsive genes were activated by expressing ERF1 ectopically. This suggests that the SA-mediated repression takes place downstream of COI1, i.e., in the central components of JA signal transduction. The proteins that could be implicated in the repression of JA-dependent immune signaling by SA pathway are discussed below (Pieterse, Van der Does et al. 2012, Caarls, Pieterse et al. 2015).

As described earlier, NPR1 plays an important role in activation of SA-mediated defense responses. The *npr1* mutant in *Arabidopsis* is unable to activate the SA pathway. Additionally, SA-mediated JA pathway repression does not occur in these plants. Furthermore, it was demonstrated that although the nuclear localization of NPR1 is indispensable for the activation of SA pathway, this re-localization was not required for the suppression of JA pathway by SA. This was confirmed in rice (*Oryza sativa*) where the suppression of JA pathway and reduced resistance against herbivores were reported upon cytosolic OsNPR1 over-expression. On the contrary, mutated OsNPR1 constitutively present in the nucleus resulted in no effect on JA pathway and herbivore resistance. However, the molecular mechanism behind this differential response of nuclear and cytosolic NPR1-mediated regulation of SA-JA cross talk still needs to be elucidated (**Figure 7**) (Pieterse, Van der Does et al. 2012, Caarls, Pieterse et al. 2015).

Apart from its role in SA signal transduction, redox-dependent regulation also plays a role in SA-JA cross talk. GRXs (Glutaredoxins) and TRXs (thioredoxins) can reduce the Cys disulfide bonds in proteins thus modulating their activity. This makes them indispensable for redox-dependent regulation of proteins. Both the hormones are known for influencing the redox state of the cell. While SA causes an increase in the amounts of glutathione, the cellular redox buffer, and shifts the reduced/oxidized glutathione ratio towards the reduced side, JA, on the other hand, triggers a decrease in glutathione amounts and shifting of the reduced/oxidized glutathione ratio towards the oxidized side. After SA treatment, the time frame that marks the increase in glutathione levels coincides with *PDF1.2* (JA induced) suppression. This SA-mediated suppression did not happen in the presence of BSO (L-buthionine-sulfoximine, an inhibitor of glutathione biosynthesis), suggesting the importance of redox regulation in SA-JA cross talk. When

SA and JA were applied simultaneously, glutathione levels rose similarly to that in SA treatment alone, indicating that redox regulation gives precedence to the SA pathway. The involvement of GRXs further supports the redox-based suppression of JA pathway by SA pathway. GRXs are known to reduce their target proteins by using glutathione. It has been shown that in plants over-expressing GRX480, JA did not induce the expression of *PDF1.2*, and the plants over-expressing GRXS13 showed more susceptibility towards *Botrytis cinerea* (necrotrophic fungus). The expression of both the GRXs is known to be induced by SA. Furthermore, it has been reported that GRXs can inhibit the expression of *ORA59*. GRX480 exhibits a reduced expression in *npr1-1* mutant and over-expressing it in the *npr1-1* mutant background suppresses the expression of *PDF1.2*, indicating that GRX480 functions downstream to NPR1 in SA-mediated suppression of JA pathway, most probably by interacting with TGA factors (**Figure 7**) (Pieterse, Van der Does et al. 2012, Caarls, Pieterse et al. 2015).

In addition to their role in SA pathway as positive regulators, TGA factors also regulate, both positively and negatively, the JA/ET-dependent defense responses. In a microarray analysis of wild-type plants and *tga2/tga5/tga6* triple mutant, various ACC (1-aminocyclopropane-1-carboxylic acid, ethylene precursor)-induced TGA-dependent genes were found, out of which many were repressed by SA after the plants were subjected to a combined treatment of SA and ACC. TGA factors have also been shown to bind to the *ORA59* promoter and therefore activate *ORA59* expression upon ACC treatment, while inhibiting it upon SA treatment. It is possible that TGA factors interact with JA-dependent regulators that are not yet known, for activating the JA pathway. However, during the SA-JA cross talk, the interaction of TGAs with GRX480 may lead to the inhibition of the JA-responsive genes (**Figure 7**) (Pieterse, Van der Does et al. 2012, Caarls, Pieterse et al. 2015).

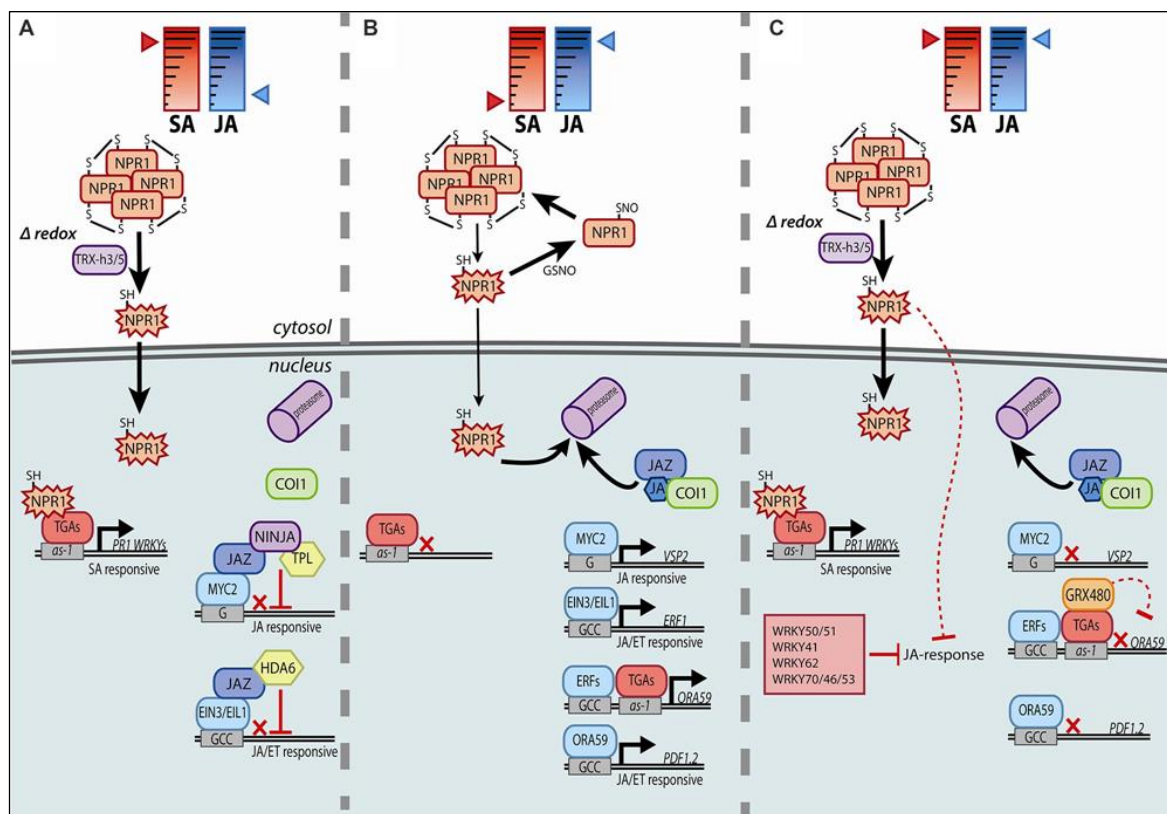


Figure 7: A model representing the different players involved in the regulation of (A) SA signaling pathway, (B) JA signaling pathway and (C) SA-mediated suppression of JA signaling pathway. Known activities are shown by solid arrows while dotted lines represent hypothesized activities. The red blocks and crosses indicate inhibition and repression of transcription respectively. Adapted from (Caarls, Pieterse et al. 2015).

WRKY transcription factors could be other proteins mediating the SA-dependent suppression of JA pathway. Being induced by SA and pathogens, WRKYs are known to regulate the SA-mediated defense gene expression. They bind to the W-box (C/TTGACC/T), a DNA element enriched in the promoters of the SA-suppressed JA-responsive genes indicating the probable role of WRKYs in the regulation of SA-JA cross talk. Several reports have shown the involvement of different WRKYs in the inhibition of JA pathway (Figure 7). It has been shown that upon treatment with MeJA, the expression of *PDF1.2* is inhibited in plants over-expressing WRKY70 (induced by SA). In the *wrky70* mutant, JA pathway was intact upon JA treatment but suppressed upon SA and JA treatment. This could be attributed to the redundancy between the WRKY factors as the expression of *PDF1.2* upon treatment with MeJA was indeed found to be upregulated in the single and double mutants of *wrky46* and *wrky53* in *wrky70* background (Hu, Dong et

al. 2012). Another SA inducible WRKY factor, WRKY62, has been proposed to be implicated in SA-JA cross talk as its over-expression led to an attenuation of the JA pathway while its mutant, *wrky62*, exhibited an increased JA-dependent gene expression (Mao, Duan et al. 2007). Although WRKY41 has also been shown to be involved in SA-JA cross talk because of an increased *PR-5* expression and lowered *PDF1.2* expression in plants over-expressing WRKY41, its expression upon SA treatment is very slightly induced, and it is highly likely that it is not targeted by NPR1 (Higashi, Ishiga et al. 2008). Two more WRKYs, WRKY50 and WRKY51, were implicated in SA-JA cross talk based on the studies performed on the *ssi2* mutant. In plant cells, the desaturation of stearic to oleic acid (18:1) is performed by an enzyme encoded by *SSI2* (*SUPPRESSOR OF SALICYLIC ACID INSENSITIVITY 2*). This mutant, identified in an *npr1* suppressor screen, exhibited elevated SA responses and lowered JA responses independent of NPR1 activation. The ectopic expression of *nahG* (encoding SA hydroxylase) reduced SA levels in *ssi2* mutant, but this did not have any effect on the repressed JA pathway. This indicates that *ssi2*-mediated (lowered 18:1 fatty acid levels dependent) repression of JA-responsive genes is acting downstream to SA. Further analysis revealed WRKY50 and WRKY51 to be involved in this process. The expression of *PDF1.2* was restored in the mutants of *wrky50* and *wrky51* in *ssi2* background without any alteration in the 18:1 fatty acid levels. Furthermore, no inhibition of *PDF1.2* and *VSP2* was detected in the single and double mutants of *wrky50* and *wrky51* upon SA and JA combined treatment (Pieterse, Van der Does et al. 2012, Caarls, Pieterse et al. 2015). In a report published recently, the interaction of WRKY51 and JAV1, a negative regulator of JA defense response, was demonstrated (Hu, Zhou et al. 2013). Thus it appears that WRKYs, after induction by SA, could directly or indirectly repress the expression of JA-responsive genes. However, the molecular mechanism behind this phenomenon is not yet known.

1.5. Redox regulation in plants

Partial reduction of oxygen leads to the formation of ROS such as hydrogen peroxide (H₂O₂), hydroxyl radical (HO•), singlet oxygen (¹O₂) and superoxide anion (O₂⁻). ROS production in plants results from the cellular processes such as respiration,

photosynthesis, folding of proteins and other metabolic reactions. Accumulation of large amounts of ROS can be injurious to cells and can result in denaturation of proteins, changes in carbohydrate oxidation, and even death. However, at lower concentrations, these ROS act as signaling molecules in the regulation of various plant processes ranging from growth and development to biotic and abiotic stress responses. Therefore, the regulation of ROS amounts in the cells is of utmost importance, and this is where the ROS processing systems come into play. During the course of evolution, plants have evolved ROS processing systems which protect them from the toxic effects of ROS while still being able to use ROS as signaling molecules. They are generally divided into enzymatic and non-enzymatic types. The enzymatic ROS processing system comprises the antioxidant enzymes such as catalase (CAT), superoxide dismutase (SOD), ascorbate peroxidase (APX), glutathione peroxidase (GPX), peroxiredoxin (PRX) and dehydroascorbate reductase (DHAR). Glutathione (GSH) and ascorbate (ASC), among others, are the two major antioxidant molecules which can convert H_2O_2 to H_2O and O_2 (Choudhury, Rivero et al. 2017, Liu and He 2017).

ROS are produced not just as the by-products of certain cellular processes. In plants, ROS are actively produced, to be used for signal transduction, at apoplast (by NADPH oxidases), and in mitochondria, chloroplasts and peroxisomes as well (Choudhury, Rivero et al. 2017). All ROS possess unique chemical properties resulting in their targets and signaling specificities. For example, $HO\bullet$ readily oxidizes cellular compounds such as proteins, lipids and carbohydrates. It is also the most unstable of the four ROS with a half-life of 1 ns. While $O_2\cdot^-$ interacts with the Fe-S centres in a protein, 1O_2 might be involved in the oxidation of guanine, certain amino acids and polyunsaturated fatty acids. Both these ROS, however, have a similar half-life of 1 μ s. Out of the four ROS, H_2O_2 is the most stable with a half-life of 1 ms and thus can be present in relatively higher amounts (Mignolet-Spruyt, Xu et al. 2016).

Apart from ROS, reactive nitrogen species (RNS) such as nitric oxide ($NO\bullet$), peroxynitrite ($ONOO^-$) and nitrous oxide (N_2O) have also been shown to be accumulating in plants under stress conditions, with similar implications as ROS (Akter, Huang et al. 2015). An

excess of RNS may lead to oxidative cell damage. RNS conferred toxicity can be a result of either their strong oxidizing effects or because of their ability to transfer an NO moiety to various biological molecules such as lipids, nucleic acids and proteins, and damaging them in the process (Zaffagnini, De Mia et al. 2016, Fancy, Bahlmann et al. 2017). Synthesis of NO is mediated by the enzyme NOS (NO synthase) in mammals, a reaction which involves oxidation of arginine to citrulline and NO. However, no NOS encoding gene has been identified yet in the terrestrial plants. The major biosynthetic pathway of NO in plants is believed to be the NR (Nitrate reductase)-mediated reduction of nitrite (NO_2^-). The ability of NR to reduce NO_2^- to peroxynitrite (ONOO^-), an NO derivative, has been shown *in vitro* and *in vivo* (Fancy, Bahlmann et al. 2017). Other proposed reductive pathways of enzymatic NO production in plants include mitochondrial electron system and the enzyme xanthine dehydrogenase/oxidase. In addition, several oxidative pathways for NO synthesis have also been proposed. For example, NO production by polyamines has been reported *in planta* (Tun, Santa-Catarina et al. 2006). The non-enzymatic production routes include production of NO by chemical reduction of NO_2^- at acidic pH. Taken together, it seems that the unavailability of a NOS-like enzyme in plants is devoid of major consequences with respect to NO production, at least under certain stress responses. NO solubilizes readily in both, water and hydrophobic solvents, thus it can just diffuse across the lipid bilayer without needing any membrane transporter which makes it an excellent signalling molecule (Fancy, Bahlmann et al. 2017).

ROS, together with RNS, by initiating and integrating with other signaling pathways, regulate a myriad of processes during plant growth and development such as root growth, pollen-tube growth and gravitropism; cellular processes such as photosynthesis, mitochondrial respiration, peroxisomal metabolism, fatty acid β -oxidation; and biotic and abiotic stress responses such as pathogen attack, light stress, wounding, and low temperature (Waszczak, Akter et al. 2015, Mignolet-Spruyt, Xu et al. 2016, Zaffagnini, De Mia et al. 2016). ROS/RNS signaling has also been shown to be an integral part of plant hormone responses mediated by salicylic acid, jasmonic acid, ethylene, abscisic acid and auxin, both in the hormone biosynthesis and further downstream signaling (**Figure 8**) (Mignolet-Spruyt, Xu et al. 2016, Zaffagnini, De Mia et al. 2016).

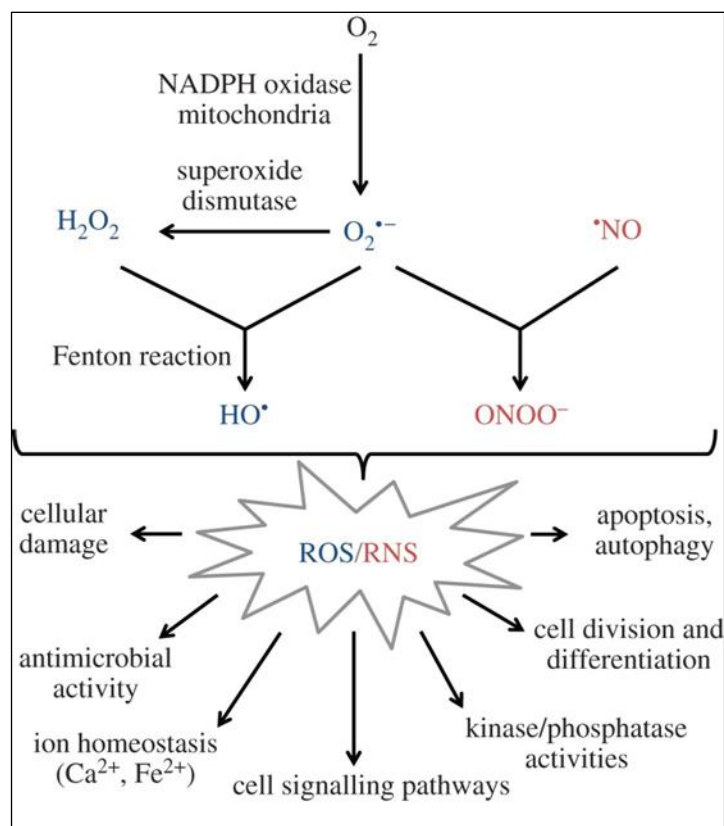


Figure 8: Origin and downstream effects of ROS/RNS. Superoxide anion ($O_2^{\bullet -}$) produced by the respiratory chain in mitochondria is converted to hydrogen peroxide (H_2O_2) by superoxide dismutase. Further reaction of H_2O_2 with Fe^{+2} leads to the generation of hydroxyl radical (HO^{\bullet}). Nitric oxide (NO^{\bullet}) can generate peroxynitrite ($ONOO^-$) upon its reaction with $O_2^{\bullet -}$. ROS ($O_2^{\bullet -}$, H_2O_2 , HO^{\bullet}) and RNS (NO^{\bullet} , $ONOO^-$) are involved in the regulation of different cell signalling pathways. Adapted from (Mone, Monnin et al. 2014).

ROS/RNS-dependent redox changes in the cells are generally perceived by redox reactions such as oxidation of a thiol group (-SH) of a Cys residue (Choudhury, Rivero et al. 2017). These post-translational modifications (PTMs) of proteins on specific Cys and Met residues can lead to the modulation of protein structure and/or function. Several oxidation states of sulfur in Cys residues allow for a number of different PTMs to be possible such as ROS-dependent sulfenylation (R-SOH), inter/intra-molecular disulfide bond formation (R-S-S-R/R-S-S-R'), S-glutathionylation (R-S-SG), sulfinylation (R-SO₂H) and sulfonylation (R-SO₃H), and NO-mediated S-nitrosylation (R-SNO) (Waszczak, Akter et al. 2015).

1.5.1. Redox PTMs of protein thiols

In the first step of ROS-mediated oxidation, the Cys thiolate ($-S^-$) gets oxidized to sulfenic acid ($-SOH$, **Figure 9**). Sulfenic acid is highly unstable, and thus undergoes further modification. If there are no other thiolate molecules in the vicinity, sulfenic acid can get further oxidized to sulfinic acid ($-SO_2H$) and then to sulfonic acid ($-SO_3H$) (Couturier, Chibani et al. 2013). In *Arabidopsis*, the ATP-dependent reduction of sulfinic acid back to sulfenic acid has been shown to be mediated by the enzyme sulfiredoxin (SRX). Only two substrates for this enzyme have been identified so far: 2-Cys Prx (2-cysteine peroxiredoxins) in chloroplasts and PrxIIF (Peroxiredoxin IIF) in mitochondria. Thus this reversion does not form a general mechanism. The oxidation to sulfonic acid is irreversible and mostly results in degradation of proteins (Akter, Huang et al. 2015, Waszczak, Akter et al. 2015). On the other hand, sulfenic acid can either form sulfenylamide by reacting with the nitrogen in the backbone of a neighboring residue or a thiosulfinate upon condensation with another sulfenic acid. However, the physiological relevance of these modifications is not known in plants. Alternatively, sulfenic acid can form intra/inter-molecular disulfide bonds by reacting with another thiolate of protein Cys, or it can be modified by addition of glutathione, known as S-glutathionylation (**Figure 9**) (Couturier, Chibani et al. 2013, Akter, Huang et al. 2015).

Two major PTMs mediated by NO are known: tyrosine nitration and S-nitrosylation. Both these PTMs can modify the function of their target proteins. As the name suggests, tyrosine nitration (NO_2 -Tyr) involves the addition of NO_2 radical to either of the ortho-carbons in the benzene ring of Tyr residue. A couple of reports did report a presence of a denitrase in mammals; however, no such enzyme has been identified in plants so far. Therefore, in context of plants, this PTM represents the presence of nitrosative stress but cannot be considered as a signaling modification. S-nitrosylation results in the formation of S-nitrosothiols (R-SNO) and involves the addition of an NO group to the thiol group of a Cys residue. GSNO (S-nitrosoglutathione) is the smallest, most abundant S-nitrosothiol in plants, formed by S-nitrosylation of glutathione and acts as the reservoir of NO in plant cells. The NO group of GSNO can be directly transferred to a Cys thiol group, called transnitrosylation, resulting in a formation of a new S-nitrosothiol. Because this PTM can be reversed enzymatically by TRXs (Thioredoxins) or non-enzymatically by antioxidants

such as glutathione or ascorbate, S-nitrosylation has come to be known as the major modification which transduces the bioactivity of NO (**Figure 9**) (Begara-Morales, Sánchez-Calvo et al. 2016, Begara-Morales, Sanchez-Calvo et al. 2016).

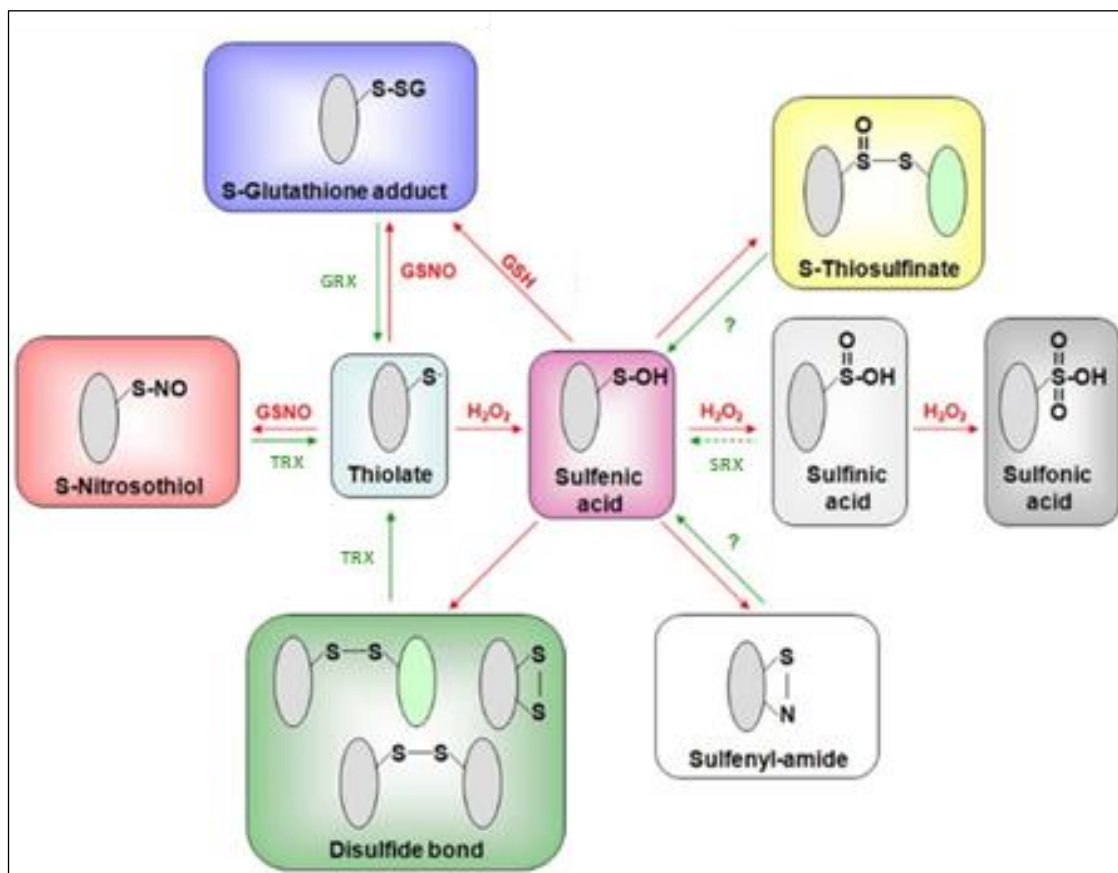


Figure 9: Representation of ROS/RNS-mediated PTMs of Cys residues, adapted from (Couturier, Chibani et al. 2013).

1.5.2. Functional significance of redox PTMs

The ROS-dependent PTMs have been studied extensively on the enzymes of Calvin cycle, and the enzymes involved in starch and sulfur metabolism. Apart from these, ROS-dependent PTMs also modulate various signaling pathway proteins such as transcription factors, proteases, kinases, phosphatases and RNA-binding proteins (Waszczak, Akter et al. 2015). There are many proteins known in which redox-induced disulfide bond formation takes place to regulate their activity and response to the oxidative stress. For example, OxyR and YAP1, transcription factors in *E. coli* and *S. cerevisiae* respectively, get activated due to the formation of disulfide bonds and initiate transcription of their target

genes (Zheng, Aslund et al. 1998, Tachibana, Okazaki et al. 2009). Another good example is GAPDH, enzyme of the glycolysis pathway. Upon the perception of oxidative stress, the Cys residue in the active site of GAPDH forms an intra-molecular disulfide bond with a nearby Cys resulting in the inactivation of the enzyme. This blocking of glycolysis is possibly the reason behind decreased ATP levels reported in different species upon oxidative stress. Consequently, glucose metabolism is redirected to pentose phosphate pathway resulting in the generation of NADPH instead of NADH. Because NADPH plays an important role in TRX and GRX reduction, increasing its amounts is good for cells under oxidative stress. The disulfide bond formation in GAPDH also leads to its translocation to the nucleus where it binds to DNA-binding complexes, thus indicating that GAPDH may be involved in transcriptional regulation upon oxidative stress (Cremers and Jakob 2013).

Similarly to ROS-mediated PTMs, S-nitrosylation has been shown to regulate the activity of enzymes of different signaling pathways, protein localization and structure, and protein-protein and protein-DNA interactions. The proteomic studies have revealed a plenty of S-nitrosylated plant proteins, a lot of which function as regulators in various signaling pathways, especially in plant defense pathways (Akter, Huang et al. 2015). The GSNO-mediated transnitrosylation of NPR1 is the best studied example in plants. As mentioned earlier, NPR1 plays a key role in the regulation of SA-dependent defense pathway. Upon pathogen infection and induction by SA, the oligomeric NPR1, stabilized by disulfide bonds between Cys82 and Cys216, is converted into its monomers by TRX5 resulting in its translocation to the nucleus where it bonds to TGA1 to start the transcription of defense genes. The activation of NPR1 also induces S-nitrosylation of its Cys156, which promotes its oligomerization. This keeps the NPR1 monomers from being depleted and tightly regulates the downstream signaling. Recently, selective denitrosylation of NPR1 was shown to be catalyzed by TRX5. Furthermore, GSNO-mediated S-nitrosylation of TGA1 has also been reported. Upon oxidation, an intra-molecular disulfide bond is formed between Cys260 and Cys266, and between Cys172 and Cys287 of TGA1 which blocks its interaction with NPR1. The GSNO-mediated S-nitrosylation and glutathionylation of these Cys residues protect them from getting

oxidized and hence, enhance the DNA-binding capacity of TGA1 (Waszczak, Akter et al. 2015, Zaffagnini, De Mia et al. 2016).

Taking into account the findings of recent years, it seems that oxidation of Cys residues in the transcription factors is more widespread phenomenon than it was assumed some years ago. There are indications that apart from TGA factors, other bZIPs may undergo redox-dependent changes via oxidation of exposed Cys residues. For example, three members of the G-group bZIPs, bZIP16, bZIP68 and GBF1, have been shown to regulated by redox-mediated changes in the cell. The reduction of a conserved Cys residue in their basic region was shown to be important for their DNA binding ability (Shaikhali, Noren et al. 2012). Based on the superoxide-induced cell death phenotype in *Arabidopsis lsd1* mutant plants overexpressing bZIP10 (Kaminaka, Nake et al. 2006), the posttranslational modification of Cys residues could be suggested as a potential regulatory mechanism also for bZIP10 protein.

2. Aim of Thesis

The main aim of this thesis is to elucidate the functional importance of bZIP10 in plant biotic stress responses and to unravel its mode of regulation in *Arabidopsis thaliana*, with the following specific objectives:

1. Utilizing the phospho-mimicking and phospho-ablative mutant forms of the Ser19 residue in the DNA-binding domain of bZIP10 to analyze the regulation of its localization, transactivation and heterodimerization capacity.
2. Generate *Arabidopsis* transgenic lines over-expressing bZIP10 and its above-mentioned phosphorylation mutants, and utilize them for the functional characterization of bZIP10.
3. Analyze redox status of cysteine residues in bZIP10 protein sequence and assess the potential redox-dependent bZIP10 regulation by mutational analysis of these residues. The importance of the Cys residues in bZIP10 will be experimentally analyzed with regards to bZIP10 localization, transactivation capacity, heterodimerization capacity and interaction with other proteins.
4. Identification of direct genomic targets of bZIP10.
5. Performing a mass spectrometry based proteomic screen to identify the novel interaction partners of bZIP10.

3. Materials and Methods

3.1. Materials

3.1.1. List of Chemicals and Consumables:

Note: The composition of all buffers are described along with the respective protocols.

Name	Company	Name	Company
2-(4-morpholino)ethanesulfonic acid (MES)	Roth	Calcium chloride	Merck
2'-(4-Methylumbeliferyl)- α -D-N-acetylneuraminic acid (sodium salt) (MUN)	Cayman Chemical	Cellulase R10	Yakult Pharmaceuticals
4- Methylumbeliferyl- β -D-Glucuronid (MUG)	Duchefa	cOmpete protease inhibitor cocktail	Roche
4-(2-hydroxyethyl)-1-piperazineethanesulfonic acid (HEPES)	Roth	CSM auxotrophy mix	MP Biomedicals
4-Nitroblue tetrazolium chloride (NBT)	Merck	Dimethylformamide	Roth
5-bromo-4-chloro-3'-indolyl-phosphate p-toluidine (BCIP)	Roche	Dipotassium hydrogen phosphate	Roth
Acetic acid	Merck	Disodium hydrogen phosphate	Merck
Acetosyringon	Sigma Aldrich	Dithiothreitol (DTT)	Sigma Aldrich
Agar	Oxoid	D-Luciferin	PJK
Ammonium persulphate	Bio-Rad	DpnI	Fermentas
Ammonium sulphate	Roth	Ethanol	Merck
Ampicillin	Roth	Ethylenediaminetetraacetic acid (EDTA)	Roth
AMV Reverse Transcriptase	EURx	Formaldehyde	Merck
Anti-GFP antibody	Roche	GFP-Trap [®] _MA	ChromoTek
Anti-GFP Ab290	Abcam	Glucose	Fluka
Anti-mouse-AP antibody	Bio-Rad	Glycerol	Roth
Bacto-peptone	Sigma Aldrich	Glycine	Roth
Beef extract	Becton	Hydrogen peroxide	Sigma Aldrich
β -mercaptoethanol	Sigma Aldrich	Igepal CA-630	Sigma Aldrich
Bovine serum albumin (BSA)	Appli-Chem	Lithium acetate	Roth

Bromophenol blue	Roth	LR-Clonase enzyme	Invitrogen
Lysogeny broth (LB)	Roth	Ribonuclease A	Sigma Aldrich
Macerozyme R10	Yakult Pharmaceuticals	RNeasy Plant Mini Kit	Qiagen
Magnesium chloride	Merck	Rotiphorese Gel 30	Roth
Magnesium sulfate	Merck	Saccharose/Sucrose	Sigma Aldrich
Mannitol	Merck	Salicylic acid	Sigma Aldrich
Methanol	Merck	Sarkosyl	Sigma Aldrich
Milk powder	Roth	Sodium chloride	Merck
MinElute Reaction Cleanup Kit	Qiagen	Sodium dihydrogen phosphate	Merck
M-MuLV Reverse Transcriptase	Fermentas	Sodium dodecyl sulphate (SDS)	Merck
NEB®5α competent cells	New England Biolabs	Sodium hydroxide	Merck
N-ethylmaleimide (NEM)	Thermo Fisher	Spectinomycin	Roth
N-Lauroylsarcosine sodium salt	Sigma Aldrich	Tetramethylethylenedi amine (TEMED)	Kulzer
pENTR™ Directional TOPO® Cloning Kit	Invitrogen	Tris base	Roth
Phusion HF DNA polymerase	New England Biolabs	Triton X-100	Sigma Aldrich
Polyethylene glycol Mn 4,000 (PEG)	Fluka	Tryptone	Becton
Potassium acetate	Roth	Tryptone, Peptone	Fluka
Potassium chloride	Roth	Tween 20	Sigma Aldrich
Protein A agarose beads	Bio-Rad	Urea	Merck
Proteinase K	Sigma Aldrich	Yeast extract	Roth
Proteose peptone #3	BD Biosciences	Yeast nitrogen base	BD Biosciences
PVDF membrane	Millipore	Zinc sulfate	Merck
QIAGEN® Plasmid Plus Maxi Kit	Qiagen		

3.1.2. List of Primers:

Note: Most of the primers listed below were designed by me while others were available at the Plant Physiology Department, ZMBP, Tuebingen University.

Gene/ Construct Name	Primer Name	Primer Sequence (5'- 3')
NES1-LSD1	NES1-LSD1-F	CACCATGTTGCAGAACGAGCTTGCTCTTAAGTTGGC TGGACTTGATATTAACAAGACTGGAGGACAGGACCA GCTGGTGTG
	LSD1-R	CTTTTTGTGTCAGTCGTCCTCCAACAACAACATTG
LSD1-NES1	LSD1-F	CACCATGCAGGACCAGCTTGTATGTCATG
	LSD1-NES1-R	TCCTCCAGTCTTGTTAATATCAAGTCCAGCCAACCTT AAGAGCAAGCTCGTTCTGCAACTTTTTGTGAGTTGT CACTCC
NES1-LSD1- NES1	NES1-LSD1-F	CACCATGTTGCAGAACGAGCTTGCTCTTAAGTTGGC TGGACTTGATATTAACAAGACTGGAGGACAGGACCA GCTGGTGTG
	LSD1-NES1-R	TCCTCCAGTCTTGTTAATATCAAGTCCAGCCAACCTT AAGAGCAAGCTCGTTCTGCAACTTTTTGTGAGTTGT CACTCC
NES-bZIP10	NES-bZIP10-F	CACCATGAAAGCGTTACAGCTGCCACCGATTGAGAG ACTTACGTTAAACAGTATCTTCTCCA
	2-2/fulenGWL (reverse)	GTCCACGCATTTTTTCGGCCATGC
<i>pProDH1</i>	pProDH1-F	CACCAAGTCCAGGTCCACATGTTGAATCC
	pProDH1-R	GCTAAAAGCGGGTAAACGGTAAGATCGCC
pENTR- D/bZIP10 C102,130,409A	bZIP10 C102,130,409A-F	GCATGGCCGAAAAAAGCCGTGGACAAGGGTGGG
	bZIP10 C102,130,409A-R	GTCCACGGCTTTTTTCGGCCATGC
pPR3-N/NES- bZIP10 S19A	2-2/Asp19F	GAGTCAGCTAGGCGAGCTAGAAGGAGAAAGCAG
	2-2/Asp19R	CTGCTTTCTCCTTCTAGCTCGCCTAGCTGACTC
pPR3-N/NES- bZIP10 S19D	2-2/Asp19F	GAGTCAGCTAGGCGAGATAGAAGGAGAAAGCAG
	2-2/Asp19R	CTGCTTTCTCCTTCTATCTCGCCTAGCTGACTC
psMAV4/bZIP1 0 S19A	2-2/Asp19F	GAGTCAGCTAGGCGAGCTAGAAGGAGAAAGCAG
	2-2/Asp19R	CTGCTTTCTCCTTCTAGCTCGCCTAGCTGACTC
psMAV4/bZIP1 0 S19D	2-2/Asp19F	GAGTCAGCTAGGCGAGATAGAAGGAGAAAGCAG
	2-2/Asp19R	CTGCTTTCTCCTTCTATCTCGCCTAGCTGACTC

pENTR-D/bZIP1 C125A	pENTR-D/bZIP1 C125A-F	ATAGCGGTTGGAGATGCTAGACGTACACCG
	pENTR-D/bZIP1 C125A-R	CGGTGTACGTCTAGCATCTCCAACCGCTAT
pENTR-D/bZIP1 C134A	pENTR-D/bZIP1 C134A-F	CCGTGGAAATTGAGTGCTGGTTCTCTACAACC
	pENTR-D/bZIP1 C134A-R	GGTTGTAGAGAACCAGCACTCAATTTCCACGG
pENTR-D/bZIP2 C128A	pENTR-D/bZIP2 C128A-F	ACCAGATCGACGGCGCTGGTTTTGATGATCG
	pENTR-D/bZIP2 C128A-R	CGATCATCAAAAACCAGCGCCGTCGATCTGGT
pENTR-D/bZIP11 C123A	pENTR-D/bZIP11 C123A-F	AACAACATGGGCATGGCTTCGAACCCCTCTGG
	pENTR-D/bZIP11 C123A-R	CCAGAGGGTTTGAAGCCATGCCCATGTTGTT
pENTR-D/bZIP11 C132A	pENTR-D/bZIP11 C132A-F	TTGGTTTGGAGGCTGATGATTTCTTCG
	pENTR-D/bZIP11 C132A-R	CGAAGAAATCATCAGCCTCCAAACCAA
pENTR-D/bZIP44 C173A	pENTR-D/bZIP44 C173A-F	ATGTTTTCAACGCTAAGGGTGGGCGCGCCG
	pENTR-D/bZIP44 C173A-R	CGGCGCGCCACCCTTAGCGTTGAAAACAT
pENTR-D/bZIP53 C132A	pENTR-D/bZIP53 C132A-F	CCCTTGGCAGATGCCTGCTCCAATGCAACC
	pENTR-D/bZIP53 C132A-R	GGTTGCATTGGAGCAGGCATCTGCCAAGGG
pENTR-D/bZIP53 C146A	pENTR-D/bZIP53 C146A-F	ATATGTTTGATGCCAAGGGTGGGCGCGCCG
	pENTR-D/bZIP53 C146A-R	CGGCGCGCCACCCTTGGCATCAAACATAT
Gene Expression Primers		
<i>bZIP10</i> (used in section 4.2.1.)	bZIP10-RTDB-F	TTTTTCGGCCATGCTGAATCGTTC
	bZIP10-RTDB-R	TTACTCCAAGCGCCAACCCGTA
<i>MYC2</i>	MYC2-F	TTGCTCCGTCGGATGACGCT
	MYC2-R	AATCCCGCACCGCAAGCGAA
<i>VSP2</i>	VSP2-F	ATGCCAAAGGACTTGCCCTA
	VSP2-R	CGGGTCGGTCTTCTCTGTTC
<i>ERF1</i>	ERF1-F	CGAGCAGTCCACGCAACAAACCT
	ERF1-R	ATGGCCGTCGTCTTACGCCTCT
<i>ORA59</i>	ORA59-F	TGTGGCTTGGGACATTTCGACACC
	ORA59-R	TCAAAGCGAAAGCCGCCTGA
<i>ProDH1</i>	ERD5#84-F	GCTGCCAAATCTTTACCAACA

	ERD5#84-R	TGAAGTTCGGACTTTTGTATTCC
<i>ProDH2</i>	ProDH2#137-F	AGCTACGCATAACACAGACTCG
	ProDH2#137-R	TTATTGATCCCTAGCTCACTTGC
<i>ASN1</i>	ASN1#65-F	CGATGACTGTGAGCATTTCG
	ASN1#65-R	AAACCCTCCTAATTTGCTTGAA
<i>BCAT2</i>	BCAT2#21-F	TCACAAATTATGCGCCAGTT
	BCAT2#21-R	CGAGATAAAGAACGTCTGAAAACC
<i>bZIP10</i> (used in section 4.4.1.)	bZIP10#89-F	TTGAAGCCAGAGGACGTTAAA
	bZIP10#89-R	CGCCTAGCTGACTCACGATT
<i>EF-1α</i>	EF-1intr-F	GTAACAAGATGGATGCCACCACCCC
	EF-1intr-R	TCCCTCGAATCCAGAGATTGGCACA
ChIP Promoter Primers		
<i>ASN1-P1</i>	ASN1-P1-F	ATCATGTTCGGATTGGGTCT
	ASN1-P1-R	GCCTCACACGTTGCTACAAT
<i>ASN1-P2</i>	ASN1-P2-F	CGTGATAACACGTGTACGGC
	ASN1-P2-R	GGCAAACCTCCGGTTTAGGG
<i>ProDH2-P1</i>	ProDH2-P1-F	GCATCCGATTCCACATCCAC
	ProDH2-P1-R	AGTCAGAGACACCAAGGACG
<i>ProDH2-P2</i>	ProDH2-P2-F	AGTCAACATCAAAAAGCCACG
	ProDH2-P2-R	GGAGGTTTAGGGGCTGGTTA
<i>BCAT2-P1</i>	BCAT2-P1-F	GGCTGTCAATCTCCACAACG
	BCAT2-P1-R	ATGTGAAAGCCACGTTGGAC
<i>BCAT2-P2</i>	BCAT2-P2-F	GGTAATTGCGTGCCGAAGAA
	BCAT2-P2-R	CGTCACTTGTGTCTATCTGCC
<i>Actin 1</i>	Act-1-F	ATTTGAACGATGTCCGAACC
	Act-1-R	GAGCCGTGACTGATGGTTAC
<i>Actin 2</i>	Act-2-F	CGTTTCGCTTTCCTTAGTGTTAGCT
	Act-2-R	AGCGAACGGATCTAGAGACTCACCTTG
<i>Actin 3</i>	Act-3-F	GCTGACCGTATGAGCAAAGA
	Act-3-R	GATCCTCCGATCCAGACACT

3.1.3. List of DNA constructs:

Construct Name	Resistance (<i>E.coli</i>)	Yeast Selection	Remarks	Experiment (Section no.)
pABindFRET/bZIP10	Spectinomycin		generated in this study	3.2.11.
pABindFRET/bZIP10 C102,130,409A	Spectinomycin		generated in this study	3.2.11.
pABindmCherry/NES1-LSD1	Spectinomycin		available in lab	3.2.10.; 3.2.21.
pABindmCherry/NLS-LSD1-NLS	Spectinomycin		available in lab	3.2.21.
pB7/ABARespromCherry-NLS	Spec		available in lab	3.2.8.; 3.2.10.
pBinAR/Lucmod	Kanamycin		available in lab	3.2.21.
pBT10-4xGal4-UAS/GUS	Ampicillin		available in lab	3.2.8.; 3.2.9.
pDHB1/bZIP53	Kanamycin	Leu	generated in this study	3.2.12.; 3.2.13.
pENTR-D/bZIP10 C102,130,409A	Kanamycin	-	generated in this study	
pENTR-D/LSD1-NES1	Kanamycin	-	generated in this study	
pENTR-D/NES-bZIP10	Kanamycin	-	generated in this study	
pENTR-D/NES1-LSD1	Kanamycin	-	generated in this study	
pENTR-D/NES1-LSD1-NES1	Kanamycin	-	generated in this study	
pENTR-D/pProDH1 full	Kanamycin	-	generated in this study	
pEXSG-mCherry/bZIP53	Ampicillin	-	generated in this study	3.2.8.; 3.2.9.; 3.2.10.
pEXSG-mCherry/LSD1	Ampicillin	-	generated in this study	3.2.8.; 3.2.9.; 3.2.10.; 3.2.11.
pGADT7/bZIP10	Ampicillin	Leu	available in lab	3.2.12.; 3.2.13.
pGADT7/bZIP10 C102,130A	Ampicillin	Leu	available in lab	3.2.12.; 3.2.13.
pGADT7/bZIP10 C409A	Ampicillin	Leu	available in lab	3.2.12.; 3.2.13.
pGADT7/bZIP10 Δ300	Ampicillin	Leu	available in lab	3.2.12.; 3.2.13.
pGBKT7/NLS-LSD1-NLS	Kanamycin	Trp	available in lab	3.2.12.; 3.2.13.

pH7FWG2/bZIP10	Spectinomycin	-	available in lab	3.2.8; 3.2.9; 3.2.10; 3.2.11.; 3.2.21.
pH7FWG2/bZIP10 C102,130,409A	Spectinomycin	-	generated in this study	3.2.8; 3.2.10.; 3.2.11.
pH7FWG2/bZIP10 S19A	Spectinomycin	-	available in lab	3.2.8; 3.2.9.; 3.2.10.
pH7FWG2/bZIP10 S19D	Spectinomycin	-	available in lab	3.2.8; 3.2.9.; 3.2.10.
pHBTL-AD/bZIP10	Ampicillin	-	available in lab	3.2.8; 3.2.9.
pHBTL-AD/bZIP10 C102,130,409A	Ampicillin	-	generated in this study	3.2.8; 3.2.9.
pHBTL-AD/bZIP10 C102,130A	Ampicillin	-	available in lab	3.2.8; 3.2.9.
pHBTL-AD/bZIP10 C409A	Ampicillin	-	available in lab	3.2.8; 3.2.9.
pHBTL-AD/bZIP10 S19A	Ampicillin	-	generated in this study	3.2.8; 3.2.9.
pHBTL-AD/bZIP10 S19D	Ampicillin	-	generated in this study	3.2.8; 3.2.9.
pHBTL-BD/bZIP53	Ampicillin	-	generated in this study	3.2.8; 3.2.9.
pHBTL-HA/bZIP10	Ampicillin	-	available in lab	3.2.8; 3.2.9.
pHBTL-HA/bZIP10 C102,130,409A	Ampicillin	-	generated in this study	3.2.8; 3.2.9.
pHBTL-HA/bZIP10 C102,130A	Ampicillin	-	available in lab	3.2.8; 3.2.9.
pHBTL-HA/bZIP10 C409A	Ampicillin	-	available in lab	3.2.8; 3.2.9.
pMDC163/pProDH1	Kanamycin	-	generated in this study	3.2.8; 3.2.9.; 3.2.21.
pPR3-N/NES-bZIP10	Ampicillin	Trp	generated in this study	3.2.12.; 3.2.13.
pPR3-N/NES-bZIP10 S19A	Ampicillin	Trp	generated in this study	3.2.12.; 3.2.13.
pPR3-N/NES-bZIP10 S19D	Ampicillin	Trp	generated in this study	3.2.12.; 3.2.13.
pROK219/Nan	Ampicillin	-	available in lab	3.2.8; 3.2.9.
psMAV4/bZIP10 Δ648	Ampicillin		available in lab	3.2.8; 3.2.10.
psMAV4/bZIP10 Δ648 S19A	Ampicillin		generated in this study	3.2.8; 3.2.10.
psMAV4/bZIP10 Δ648 S19D	Ampicillin		generated in this study	3.2.8; 3.2.10.

pUGT1/bZIP53	Spectinomycin		available in lab	3.2.8; 3.2.9; 3.2.21.
--------------	---------------	--	------------------	--------------------------

Note: 1. Vectors (construct backbone) mentioned in the above list were readily available at ZMBP, Plant Physiology Department, Tuebingen University.

2. psMAV4 vector has been cited in (Davis and Vierstra 1998)

3.2. Methods

3.2.1. Polymerase chain reaction (PCR)

The gene(s) of interest were amplified by performing polymerase chain reaction (PCR) on the genomic DNA of *Arabidopsis thaliana*. The following scheme was used for setting up the PCR reaction:

Components	Volume for 25 μ L reaction
5x Phusion HF Buffer	10 μ L
10 μ M Forward Primer	1 μ L
10 μ M Reverse Primer	1 μ L
10 mM dNTPs	1 μ L
Template DNA	1 – 3 μ L (~ 50-150 ng)
Phusion HF DNA polymerase (2000 units/mL)	0.3 μ L
Nuclease-free water	Volume made up to 25 μ L

Note: Primers used during the course of this study are listed in section 3.1.2.

After mixing the above components on ice, the tubes were placed in a thermal cycler with the following conditions:

Step	Temperature	Time
Initial Denaturation	95°C	2 min
30 cycles:	Denaturation	95°C
	Annealing	*55 – 65°C
	Extension	72°C
Final Extension	72°C	7 min

*The annealing temperatures (T_a) vary from primer to primer, and can be calculated from their melting temperature (T_m): $T_a = T_m_lower \pm 5^\circ\text{C}$.

3.2.2. Cloning of genes of interest

Note: Genes and constructs generated or used during the entire course of this study are all listed in section 3.1.3.

Generation of entry clone:

The entry clones were generated using the pENTR™ Directional TOPO® Cloning Kit as per the manufacturer's instructions.

Generation of expression clone:

The expression clones were generated by performing the LR recombination reaction using the Gateway™ technology (Invitrogen). The components were mixed as follows:

0,75 μL Entry-Clone

0,75 μL Destination Vector

0,5 μL 5x LR-Clonase Buffer

0,5 μL LR-Clonase enzyme

The concentrations of the entry clone and the destination vector were set such that the molar ratio of entry clone:destination vector was 1:1. The mixture was incubated either at 16°C overnight or 4-5 hours at room temperature. After the incubation, 1 μL Proteinase-K was added to the mixture and kept at 37°C for 10 minutes. The tubes were then put at 56°C for 10 minutes to denature the Proteinase-K. After cooling on ice, the mixture was transformed in NEB®5 α *E. coli* competent cells.

3.2.3. Site-directed mutagenesis

For performing site-directed mutagenesis, the following components of PCR were mixed together on ice:

Components	Volume for 50 μ L reaction
5x Phusion HF Buffer	10 μ L
10 μ M Forward/Reverse Primer	1 μ L
10 mM dNTPs	1 μ L
Template DNA	1 - 3 μ L (~ 50-150 ng)
Phusion HF DNA polymerase (2000 units/mL)	0.6 μ L
Nuclease-free water	Volume made up to 50 μ L

Note: Primers used during the course of this study are listed in section 3.1.2.

Because the primers designed for site-directed mutagenesis are complementary to each other, two separate reactions were set-up, each containing either primer and placed in a thermal cycler with the following conditions:

Step	Temperature	Time
Initial Denaturation	94°C	2 min
5 cycles:	Denaturation	94°C
	Annealing	54°C
	Extension	72°C
		30 s/kb

After the first 5 cycles of PCR, the two reactions were combined together and put in the thermal cycler again with following conditions:

Step	Temperature	Time
Initial Denaturation	94°C	2 min
19 cycles:	Denaturation	94°C
	Annealing	54°C
	Extension	72°C
		30 s/kb

This was followed by adding 2 μ L DpnI to the PCR reaction and incubating the mix at 37°C for 2 h. The tube was then kept at 80°C to deactivate the enzyme. 10 μ L PCR mixture was then transformed in 50 μ L competent cells, followed by plasmid isolation, restriction digestion analysis and sending the positive clones for sequencing.

3.2.4. Bacterial transformation

After the competent cells were thawed, the LR cloning reaction was added to the cells. The solution was mixed by gentle stirring using a pipette tip. The mixture was then left on ice for 15 minutes. This was followed by heat-shock at 42°C for 40 seconds. The tubes were then transferred back to ice for 1 minute and 200 μ L LB media was added to the mixture. The mixture was then kept at 37°C for 1 h with vigorous shaking. After 1 h, 200 μ L from the mixture was inoculated on LB plates containing appropriate antibiotics (Ampicillin, 100 mg/L; Kanamycin, 50 mg/L; Spectinomycin, 100 mg/L) and incubated at 37°C overnight.

3.2.5. Plasmid isolation (Mini prep)

Solutions and buffers:

- Solution 1:
 - 50 mM Tris pH 8.0
 - 10 mM EDTA
- Solution 2:
 - 0.2 M Sodium hydroxide
 - 1 % SDS (Sodium dodecyl sulfate)
- Solution 3:
 - 3 M Potassium acetate
 - 2 M Acetic acid
- RNase (200 μ g/mL)

Protocol:

1. A single colony was inoculated in 2 mL liquid LB media containing an appropriate antibiotic and incubated overnight at 37°C.
2. 1.5 mL from the overnight culture was taken in a 1.5 mL tube and centrifuged at full speed for 1 min.
3. After discarding the supernatant, 150 µL Solution 1 and 50 µL RNase was added to the tube and vortexed to resuspend the pellet. The tube was incubated at room temperature for 5 min.
4. 150 µL of Solution 2 was then added and mixed by inverting the tube upside down, followed by adding 150 µL of Solution 3 and mixing again by inverting the tube.
5. The mixture was then centrifuged at full speed for 5 min.
6. The supernatant was taken in a new tube containing 1 mL 100 % ethanol and centrifuged again at full speed for 10 min.
7. This time the supernatant was discarded and 70 % ethanol was added to the pellet, followed by another centrifugation step at full speed for 5 min.
8. The supernatant was discarded and the pellet was allowed to air-dry. 30 µL water was added after the pellet was dried.

3.2.6. Plasmid isolation (Maxi prep)

All the maxi preps required were performed using the QIAGEN® Plasmid *Plus* Maxi Kit, as per the manufacturer's instructions.

3.2.7. Sequencing of plasmids

All the plasmid sequencing was performed at GATC Biotech. About 100 ng of plasmid was sent for sequencing and the positive clones were used further.

3.2.8. *Arabidopsis* leaf mesophyll protoplasts isolation by tape-sandwich method and transfection

The leaf mesophyll protoplasts from *Arabidopsis* were isolated as described (Wu, Shen et al. 2009), with some minor modifications.

Plants:

Between 4-5 weeks old plants with fully expanded 2nd and 3rd true leaves, grown at 22°C, 50 % humidity and under 12/12 h light/dark photo-period were used.

Solutions and buffers:

- 0.8 M Mannitol
- 5 M Sodium chloride
- 2 M Potassium chloride
- 1 M Magnesium chloride
- 0.2 M MES buffer pH 5.7 (adjusted by KOH, stored at 4°C)
- 10 % BSA (stored at 4°C)
- W5 solution (stored at 4°C):
 - 154 mM Sodium chloride
 - 125 mM Calcium chloride
 - 2 mM Potassium chloride
 - 2 mM MES buffer
- MMG solution (prepared fresh, kept on ice):
 - 0.4 mM Mannitol
 - 15 mM Magnesium chloride
 - 4 mM MES buffer
- WI solution (prepared fresh):
 - 0.5 M Mannitol
 - 4 mM MES buffer
 - 20 mM Potassium chloride
- 40 % PEG solution (10 mL, prepared fresh):
 - 4 g PEG 4000
 - 3 mL water

- 2.5 mL 0.8 M mannitol
- 1 mL 1 M Calcium chloride

Protocol:

A. Protoplast isolation:

1. The enzyme solution was prepared as follows (10 mL):
 - 3.7 mL water
 - 0.4 M mannitol
 - 20 mM KCl
 - 20 mM MES buffer pH5.7 (KOH)
 - heat for 2 min at 70°C
 - add 1 % (w/v) cellulase R10 and 0.25 % (w/v) macerozyme R10
 - dissolve gently by inverting the tube
 - incubate for 10 min at 55°C
 - cool to room temperature on ice
 - 10 mM CaCl₂
 - 0.1 % BSA*
 - pass through a 0.45 µM filter into a petridish

*BSA was filter sterilized to keep it DNase and RNase free.

2. A strip of Time tape was used to stabilize the upper epidermal leaf surface while a strip of Cello tape was affixed to the lower epidermal leaf surface. This resulted in the leaf being sandwiched between the two strips of different tapes.
3. The strip of Cello tape was then carefully removed so as to peel the lower epidermis of the leaf.
4. About 7-10 leaves adhering to the Time tape were then transferred to a Petri dish with 10 mL enzyme solution, with the leaves facing down in the enzyme solution. The Petri dish was kept on a platform shaker at 40 rpm for ~60 min.

5. The protoplasts were then transferred to a round-bottom tube and centrifuged at $100 \times g$ for 3 min and washed twice with W5 solution. The protoplasts were recovered between the washes by centrifuging as before.
6. The protoplasts were then counted using a hemocytometer under a light microscope. The remaining protoplasts were kept on ice meanwhile.
7. This was followed by centrifugation of the protoplasts again and resuspending them in the MMG solution to a final concentration of 2×10^5 protoplasts/mL. The protoplasts solution was incubated on ice for 30 min.

B. Protoplast PEG- Ca^{+2} transfection:

1. The plasmid(s) to be transfected was/were pipetted together in a 2 mL round-bottom tube (Roth). In total, 12 μg maxi prep plasmid DNA was pipetted in each 2 mL tubes. The NAN vector was added in all the samples for the normalization of GUS activity (Kirby and Kavanagh 2002). The total DNA transfected was always maintained at the same level in each tube by using an unrelated plasmid when needed.
2. 100 μL protoplasts were then added to the tubes (by using cut tips) and mixed by gentle tapping.
3. The same volume (DNA + protoplasts) of 40 % PEG solution was added, mixed by gentle tapping and the clock was started.
4. After 5 min at room temperature, 2 volumes of W5 solution was added to dilute the solution and mixed by gentle tapping.
5. The solution was then spun for 3 min at $100 \times g$ and the supernatant removed leaving behind about 30-40 μL solution in the tube.
6. Then, 500 μL of the WI solution was added, and the pellet resuspended by gentle tapping.
7. The protoplasts solution was transferred to a round-bottom tube and incubated in light at room temperature for at least 6 h before starting any treatment (either 100 μM salicylic acid or 0.3 mM H_2O_2).

3.2.9. GUS-NAN Assay

Solutions and buffers:

- 1 M Sodium phosphate buffer (for 100 mL):
 - 28 mL 1 M NaH₂PO₄ + 72 mL 1 M Na₂HPO₄, pH 7.2
- GUS buffer
 - 50 mM Sodium phosphate buffer
 - 10 mM EDTA
- GUS extraction buffer
 - GUS buffer
 - 0.1 % (v/v) Triton X-100
 - 0.1 % (v/v) Sarkosyl
- MUG solution:
 - 4 mM 4- Methylumbeliferyl- β-D-Glucoronid in GUS buffer.
- MUN solution:
 - 0.2 mM 2'-(4-Methylumbeliferyl)-α-D-N-acetylneuraminic acid (sodium salt) in GUS buffer.

Protocol:

The protoplasts were taken in a 2 mL round bottom Eppendorf tube and centrifuged at room temperature (RT) for 3 min at 100 *x g*. 500 μL of the supernatant was removed and the pellet was re-suspended in 100 μL GUS extraction buffer. The protoplasts were then kept at -20 °C until frozen. The protoplasts were next thawed and spun again at full speed for 10 min. After centrifugation, the protoplast extract was added to the 96-well plate as per the following scheme:

100 μL MUG + 100 μL protoplast extract

50 μL MUN + 2 μL protoplast extract

The plate was then read in the plate reader (Fluoroskan Ascent FL, Thermo Labsystems) with the following conditions: every 10 min for 2 h at 37°C, excitation at 360 nm and emission at 460 nm.

3.2.10. Sub-cellular localization

All the images for sub-cellular localization of proteins were acquired on Leica TCS SP8 confocal microscope (Leica Microsystems) using a 63x /1.20 water-immersion objective. The laser settings used were as follows:

- GFP (Green fluorescent protein): excitation at 488 nm and emission from 500 nm to 550 nm.
- mCherry: excitation at 561 nm and emission from 600 nm to 640 nm.

3.2.11. FRET-FLIM (Förster Resonance Energy Transfer - Fluorescence Lifetime Imaging)

The FRET-FLIM data were acquired on Leica TCS SP8 confocal microscope (Leica Microsystems) connected to a FLIM unit (PicoQuant) using a 63x /1.20 water-immersion objective. A 470 nm pulsed laser (LDH-PC-470) was employed to excite the GFP-tagged proteins. A FLIM-compatible photomultiplier tube was used to detect the resulting emission from 500 nm to 550 nm by time-correlated single-proton counting using a PicoHarp 300 module (PicoQuant). The reconvolution of the time-correlated single-proton counting histogram with the instrument response function, followed by fitting it against a bi-exponential decay function resulted in the determination of the fluorescence lifetime of GFP.

3.2.12. Yeast 2-hybrid and Split ubiquitin system

Solutions and buffers:

- YPD medium (autoclaved):
 - 20 g Tryptone, Peptone
 - 20 g Glucose
 - 10 g Yeast extract

- 20 g Agar (for solid medium)
- CSM medium (pH 6.0 adjusted with KOH, autoclaved):
 - 1.7 g Yeast nitrogen base
 - 5 g Ammonium sulfate
 - 20 g Glucose
 - 1.5 g Auxotrophy mix (CSM-Leu-Trp or CSM-Ade-His-Leu-Trp)
 - 20 g Agar (for solid medium)
- Salmon sperm DNA: warmed to 95°C for 3 min before use. Placed on ice for 1-2 min.
- 1 M Lithium acetate (LiAc) pH 7.5 (adjusted with acetic acid, autoclaved)
- 50 % (w/v) PEG 4000 (autoclaved)
- 10x TE buffer (autoclaved):
 - 10 mM Tris
 - 1 mM EDTA, pH7.5

The volumes of the autoclaved solutions were adjusted after autoclaving.

- TE/LiAc buffer (1x TE + 0.1 M LiAc):
 - 5 mL LiAc solution
 - 5 mL 10x TE buffer
 - 40 mL sterile water
- PEG/LiAc buffer:
 - 80 mL 50 % PEG
 - 10 mL LiAc solution
 - 10 mL 10x TE buffer

Protocol:

A. Making competent cells:

1. A single colony of *Saccharomyces cerevisiae* (THY.AP4 strain for Split ubiquitin system; AH109 strain for Yeast 2-hybrid) was inoculated in 4 mL liquid YPD and incubated overnight at 28°C on a shaker.

2. The overnight culture was diluted in fresh YPD medium to obtain an optical density (OD) of 0.2 at 600 nm.
3. The cells were then allowed to grow to the OD₆₀₀ of 0.8 – 1.0.
4. The yeast cells were then harvested by centrifuging for 1 min at 1500 *x g* for 5 min in falcon tubes.
5. The resulting supernatant was discarded and the yeast pellet was resuspended in 500 µL TE/LiAc buffer followed by centrifugation as before twice.
6. The supernatant was discarded and resuspended in 300 µL TE/LiAc buffer. The resuspended cells were placed on ice for at least 20 min.

B. Transformation:

7. In a PCR tube, the following was pipetted:
 - 3.5 µL salmon sperm DNA
 - 200-500 ng plasmid
 - 16.5 µL yeast cells
8. Then, 100 µL PEG/LiAc buffer was added and incubated for 30-40 min at room temperature on a vertical rotator.
9. The cells were heat shocked at 42°C for 20 min followed by addition of 50 µL sterile water.
10. The solution is then mixed by pipetting and 50 µL plated out on an appropriate selective media plate.

C. Interaction test:

11. About 4-5 colonies of the transformed yeast were inoculated in 3 mL of an appropriate CSM liquid medium and incubated overnight at 28°C on a shaker.
12. Next morning, OD₆₀₀ of the culture was recorded after diluting it 1:9 in fresh medium.
13. 100 µL of the undiluted culture was centrifuged at 2000 *x g* for 10 min. After removing the supernatant, an appropriate amount of sterile water was added such that the OD₆₀₀ of the suspension became 1.

14. 7 μ L from this suspension was then pipetted on the square plates containing CSM-Leu-Trp solid medium (growth control) and CSM-Ade-His-Leu-Trp solid medium (interaction medium).
15. A dilution series was prepared from the remaining suspension and 7 μ L from each dilution was also pipetted on the plates.
16. The plates were incubated at 28°C and checked for growth every day.

3.2.13. Yeast β -gal assay

Solutions and buffers:

- Z-buffer (autoclaved):
 - 10 mM Potassium chloride
 - 0.1 M Sodium phosphate buffer pH 7.0
 - 1 mM Magnesium sulfate
- β -gal juice (PJK)
- Triggering solution (PJK)

Protocol:

1. 3-4 yeast colonies were inoculated in 3 mL of an appropriate CSM liquid medium and grown overnight shaking at 28°C.
2. The overnight cultures were diluted and their OD₆₀₀ was recorded.
3. The cultures were diluted in 3 ml fresh media to a final OD₆₀₀ of 0.3. This was done in duplicates- one set for mock treatment and one set for treatment (0.5 mM H₂O₂).
4. The diluted cultures were incubated again at 28°C shaking for 6 h.
5. After 6 h, 1 mL of culture was centrifuged at 11,000 \times *g* for 1 min followed by discarding of the supernatant and resuspending the pellet in 400 μ L water.
6. The cells were centrifuged again as before, the supernatant discarded and the pellet resuspended in 100 μ L Z-buffer.
7. The solution was further diluted 1:9 with Z-buffer in a final volume of 200 μ L, followed by measurement of OD₆₀₀ in a 96-well plate.

8. The remaining solution was then frozen in liquid nitrogen.
9. The yeast cells were lysed by alternating 6 times between freezing in liquid nitrogen and thawing at 37°C in a water bath. The tubes can explode easily during this procedure!
10. 20 µL of the lysed yeast cells were pipetted in a 96-well plate, followed by 100 µL of β-gal juice. The plate was incubated at 25°C for 30 min.
11. Then, 100 µL of Triggering solution was added to the wells and the plate was incubated at 25°C for further 5 min.
12. The luminescence was then measured in the plate reader (Fluoroskan Ascent FL from Thermo Labsystems) and the Miller units calculated as per the following formula:

$$\text{Miller units} = \text{luminescence} / \text{OD}_{600}$$

3.2.14. Generation of transgenic lines of *Arabidopsis*

Solutions and buffers:

- Sterilization solution:
 - 70 % ethanol
 - 0.05 % Triton X-100
- 100 % ethanol
- ½ MS medium
- Hygromycin (25 µg/mL)

Protocol:

The transformed plants were available in our laboratory. Further selection of plants was performed as follows:

1. The seeds were taken in a 1.5 mL tube and sterilized with 1 mL of sterilization solution by incubating it on a rotator for 10 min.
2. The solution was then replaced with 1 mL 100 % ethanol and put on a rotator mixer for another 5 min.

The following steps were performed under sterile conditions.

3. The seeds from the tube were pipetted on a sterile filter paper and allowed to dry.
4. After drying, the seeds were spread on Petri dish containing ½ MS solid media with appropriate antibiotic.
5. The plates were then kept in dark at 4°C for 2-3 days followed by transferring the plates to the plant growth room (22°C, 50 % humidity, 12/12 h light/dark photo-period).
6. The plants that grew were either checked under the epifluorescence microscope or by western blotting for the presence of the transformed insert.

This process was repeated until there was no segregation of plants.

3.2.15. Pathogen assays

3.2.15.1. *Mamestra brassicae* (cabbage moth) assay

This assay was performed in collaboration with Ms. Merel Steenbergen and Dr. A. C. M. (Saskia) van Wees, Utrecht University, Netherlands. Ms. Steenbergen, kindly arranged for the *Mamestra* caterpillars in addition to sowing of seeds, transfer of seedlings to individual pots and nursing the plants required for the assay. The plants were grown under standard growth conditions in the greenhouse as described earlier (Verhage, Vlaardingerbroek et al. 2011). About 30 plants per genotype were used in the performance assay, with ten extra plants of Col-0.

Performance assay:

1. Seeds (imbibed in 0.1 % agar at 4°C for at least 2 days) were sown in autoclaved sand mixed with nutrient solution (Van Wees, Van Pelt et al. 2013).
2. After about 11-12 days of sowing the seeds, the seedlings were transferred to individual pots containing soil. About five weeks old plants were used for the assay.

3. The pots were placed inside a plastic cup. Each plant was inoculated with one freshly hatched larva (L1 stage) of *Mamestra*. The plastic cups were then covered with a mesh so that caterpillars do not escape.
4. After 8-9 days, the caterpillars were weighed on a fine balance.

Gene expression analysis:

For the gene expression analysis, five freshly hatched (L1 stage) *Mamestra* larvae were inoculated on each plant. The leaf samples were harvested in triplicates after 6 h, 24 h, 30 h and 48 h post-inoculation and frozen in liquid nitrogen. About 20 plants per genotype (10 for control and 10 for treatment) were used in the gene expression analysis.

3.2.15.2. *Botrytis cinerea* assay

The spores of *Botrytis cinerea* isolate B0510 were kindly provided by Mrs. Margaux Kaster, ZMBP, Tuebingen University. The plants were grown at 22°C, 50 % humidity and under 12/12 h light/dark photo-period. About 6 plants per genotype were used in this assay. The spores were diluted to a concentration of 5×10^5 spores/mL in PDB (Potato dextrose broth; also provided by Mrs. Kaster). Five fully-grown leaves of each plant was inoculated with 5 μ L of spore solution. The pots were placed in trays with transparent lids. The inside of the transparent lids was sprayed with water and all the openings were closed with the help of a tape in order to maintain 100 % relative humidity inside the tray. The disease symptoms were recorded after 3-4 days and the leaves were classified in different categories depending on the severity of the symptoms, as described earlier (Van Wees, Van Pelt et al. 2013). The percentage of leaves per plant appearing in a class was calculated. The Chi-square test was used to determine if there was a difference in the distribution of classes between different genotypes.

3.2.15.3. *Pseudomonas syringae* assay

Spray inoculation:

This assay was performed in collaboration with Dr. Lorenzo Pedrotti, University of Wuerzburg, Germany. The plants were grown at 22°C during the light period and at 20°C

during the dark period, 60 % humidity and under 12/12 h light/dark photo-period. About 4-5 weeks old plants were used in this assay. The optical density at 600 nm (OD_{600}) of *Pseudomonas syringae* pv. *tomato* DC3000 (Pst DC3000) suspension was set to 1 and sprayed onto the plants. The bacteria were harvested at 0 h and 72 h time-points and quantified.

Leaf infiltration:

Solutions and buffers:

- Kings'B medium:
 - 20 g/L Glycerol
 - 40 g/L Proteose peptone #3
 - 15 g/L Agar (for solid media)After autoclaving, add the following:
 - 10 mL/L 10 % Dipotassium hydrogen phosphate
 - 10 mL/L 10 % Magnesium sulfate
- 50 µg/mL Rifampicin
- 50 µg/mL Cycloheximide
- 70 % Ethanol
- 10 mM Magnesium chloride (autoclaved)

Protocol:

1. *Pst* DC3000 was inoculated in 25 mL Kings'B liquid media containing rifampicin and cycloheximide and incubated overnight at 28°C while shaking.
2. The cells were centrifuged at 3220 $\times g$ for 5 min at 4°C and the supernatant discarded.
3. The cell pellet was washed with 10 mM $MgCl_2$.
4. The previous two steps were repeated two times more.
5. The solvent optical density at 600 nm (OD_{600}) was set to 0.2 ($OD_{600} = 1 \times 10^8$ cfu/mL).

6. The solvent was then diluted 1:9999 with 10 mM MgCl₂ (final concentration: 1 x 10⁴ cfu/mL).
7. 2 fully grown leaves per plant were infiltrated with a needle-less syringe on the abaxial side of the leaf.
8. The time-point 0 was harvested immediately after the infiltration was done.
 - The infiltrated leaf was cut, washed in 70 % ethanol for 1 min and blotted dry.
 - The leaf was then washed in water for 10 s to remove the ethanol and blotted dry.
 - 2 discs (0.6 cm diameter) were cut out from the leaf and transferred to 96-well Autotube vial box (Elkay) containing two autoclaved glass beads (ca. 2 mm) and 200 µL MgCl₂.
 - The leaf discs were then homogenized by using Mixer Mill MM 400 (Retsch) at maximum speed for 30 s.
 - The 96-well box was rotated 180°, homogenized again and centrifuged briefly.
9. The homogenate was mixed by pipetting up and down, and 10 µL of it was transferred to square plates containing Kings'B medium with rifampicin and cycloheximide. The homogenate was pipetted at the upper edge of the plate. The plate was left in upright position until the drop reached the opposite end.
10. The plates were then left for air-drying , packed in a plastic bag and incubated at 28°C for 24-72 h.
11. The colonies were counted and log cfu/cm² value was calculated using the following formula:
$$\text{cfu/cm}^2 = \Sigma(\text{colonies/spotted volume} * \text{total volume/number of discs/disc area})$$
12. For the remaining time-points, the following dilutions of the homogenate (from step 9) were used:
 - 1 d: undiluted, 1:9 and 1:99
 - 3 d: 1:99, 1:999 and 1:9999

3.2.16. RNA isolation

The RNA was isolated from the harvested samples using RNeasy Plant Mini Kit, as per the manufacturer's instructions.

3.2.17. cDNA synthesis

The cDNA synthesis from RNA was carried out using either oligodT or random hexamer primers with AMV Reverse Transcriptase (native) or with M-MuLV Reverse Transcriptase.

3.2.18. Quantitative polymerase chain reaction (qPCR)

The cDNA generated from the RNA isolated from the samples was used to quantify the expression of the genes by performing quantitative-PCR on Bio-Rad CFX384 Real-Time PCR Detection System under following conditions:

Step		Temperature	Time
Initial Denaturation		95°C	3 min
45 cycles:	Denaturation	95°C	15 s
	Annealing	59°C	25 s
	Extension	72°C	15 s

For preparing the reaction mixture of qPCR, either PerfeCta SYBR Green SuperMix (Quanta Biosciences) or qPCR Green-MasterMix (Genaxxon) was used. Primers used for the qPCR reactions are listed in section 3.1.2.

3.2.19. Hormone measurement

This assay was done in collaboration with Dr. Joachim Kilian, Analytics, ZMBP, Tuebingen University.

Salicylic acid measurement:

The plants were infiltrated with *Pst* DC3000 12 h prior to harvesting the leaves for salicylic acid measurement. 10 mM MgCl₂ was used for the mock treatment. In total, 12 plants per genotype per treatment were used, which were divided into 4 replicates (3

plants in each replicate). Two leaves per plant were infiltrated with either *Pst* DC3000 (1×10^7 cfu/mL) or mock solution. The leaves were harvested and weighed on a fine balance. These samples were then used by Dr. Kilian for further analysis.

Jasmonic acid measurement:

The plants were infected with *Botrytis cinerea* 24 h prior to harvesting the leaves for jasmonic acid measurement. Potato dextrose broth was used for the mock treatment. In total, 12 plants per genotype per treatment were used, which were divided into 4 replicates (3 plants in each replicate). Two leaves per plant were inoculated with 5 μ L of either *Botrytis* spores (5×10^5 spores/mL) or mock solution. The leaves were harvested and weighed on a fine balance. These samples were then used by Dr. Kilian for further analysis.

Water content determination:

The water content of leaves was determined for both the treatments mentioned above. For the determination of water content in leaves, the leaves were harvested after the treatment (*Pst* DC3000 or *Botrytis*) with the same scheme: 4 replicates per genotype per treatment, 3 plants per replicate, 2 leaves inoculated per plant. The leaves were harvested and weighed on a fine balance. These were then lyophilized and weighed again on a fine balance. The difference in the measured weights revealed the water content of the leaves.

3.2.20. Arabidopsis root growth assay

1. The *Arabidopsis* seeds were sterilized as mentioned above (see section 3.2.13.).
2. Under sterile conditions, the sterilized seeds were placed in rows on square plates containing $\frac{1}{2}$ MS solid media.
3. The plates were then incubated at 4°C in dark for 2-3 days.
4. The plates were then taken from the dark and placed in vertical position in the plant growth room (22°C, 50 % humidity, 12/12 h light/dark photo-period) for 4 days.

5. The seedlings were then transferred to new square plates containing $\frac{1}{2}$ MS solid medium with or without 50 μ M salicylic acid.
6. The end of primary root of the seedlings was marked on the plate with a marker, followed by placing the plates in vertical orientation in the plant growth room.
7. The plates were scanned after 1 week, 2 weeks and 3 weeks.

3.2.21. Reporter gene assay in tobacco leaf cells

Solutions and buffers:

- YEB medium:
 - 0.5 % Bacto-peptone
 - 0.1 % Yeast extract
 - 0.5 % Beef extract
 - 0.5 % Saccharose
 - 0.05 % Magnesium sulfate
- AS medium:
 - 10 mM Magnesium chloride
 - 10 mM MES buffer pH 5.6 (adjusted by KOH)
 - 0.15 mM Acetosyringon
- 0.1 M Potassium phosphate buffer pH 7.8
- Lysis buffer (Promega)
- 4 mM 4- Methylumbeliferyl- β -D-Glucoronid (MUG)
- D-Luciferin

Protocol:

A. Tobacco leaf infiltration:

1. 5 mL of YEB medium containing appropriate antibiotics was inoculated with *Agrobacterium tumefaciens* (GV3101) (available from the Harter lab) transformed with the required vectors and incubated overnight at 28°C on a shaker.

The tobacco plants were watered in excess (for 2-4 h).

2. The overnight culture was diluted 1:4 with fresh medium and incubated at 28°C on a shaker for 4 h.
3. The culture was then centrifuged at 3220 $\times g$ for 15 min at 4°C to pellet the cells.
4. The supernatant was discarded and the pellet was resuspended in 1 mL AS – medium. The OD₆₀₀ was set at 0.7- 0.8.
5. The different agrobacteria were mixed together in the same proportion. The p19 clone and the luciferase clone (used for normalization) were included in all the combinations.
6. The agrobacteria suspensions were incubated in AS-medium for 2 h before proceeding to infiltration.
7. The suspension was then infiltrated in the tobacco leaves (2 leaves per plant) on their abaxial side using a needle-less syringe.

B. Measurement of GUS activity:

8. After about 42 h of infiltration of the tobacco leaves, a 1.5 cm disc was cut out from the infiltrated leaf and crushed using glass beads.
9. 100 μ L of lysis buffer was added to the tube and kept on ice for 10 min, vortexing every 3 min.
10. The suspension was centrifuged full speed at 4°C for 5 min and the supernatant was transferred to a new tube.
11. The previous step was repeated once more, and 10 μ L of the extract was pipetted in 96-well plate followed by addition of 50 μ L D-Luciferin. The luminescence was then measured in the plate reader (Fluoroskan Ascent FL from Thermo LabSystems).
12. For the measurement of GUS activity, 10 μ L of the extract was pipetted in a 96-well plate and mixed with 40 μ L potassium buffer and 50 μ L MUG solution.
13. The plate was then read in the plate reader under following conditions: every 20 min for 1 h at 37°C, excitation at 360 nm and emission at 460 nm.

3.2.22. Immunoprecipitation of GFP-tagged bZIP10

Solutions and buffers:

-
- Extraction buffer 1:
 - 10 mM Tris pH 7.5
 - 150 mM Sodium chloride
 - 0.5 % Igepal CA-630
 - Protease inhibitor (cOmplete. EDTA –free Protease Inhibitor Cocktail)
 - 100 mM N-ethylmaleimide (NEM)
 - Extraction buffer 2:
 - 50 mM Tris pH 7.4
 - 150 mM Sodium chloride
 - Protease inhibitor (cOmplete. EDTA –free Protease Inhibitor Cocktail)
 - 100 mM N-ethylmaleimide (NEM)
 - Dilution buffer 1:
 - 10 mM Tris pH 7.5
 - 150 mM Sodium chloride
 - Protease inhibitor (cOmplete. EDTA –free Protease Inhibitor Cocktail)
 - Dilution buffer 2:
 - 50 mM Tris pH 7.4
 - 150 mM Sodium chloride
 - Protease inhibitor (cOmplete. EDTA –free Protease Inhibitor Cocktail)
 - Wash buffer 1:
 - 10 mM Tris pH 7.5
 - 150 mM Sodium chloride
 - 0.1 % Igepal CA-630
 - Wash buffer 2:
 - 50 mM Tris pH 7.4
 - 150 mM Sodium chloride
 - 0.1 % Tween 20
 - Elution buffer:
 - 0.1 M sodium phosphate buffer pH 7.5
 - 6 M Urea

- 0.1 % SDS

Protocol:

Unless mentioned otherwise, all the steps were performed on ice in a temperature controlled room (23°C).

1. 500 mg of harvested leaves were ground in liquid nitrogen using mortar and pestle.
2. The ground leaf material was then transferred to a cold 50 mL falcon tube containing 4 mL extraction buffer 1 or extraction buffer 2. The tube was vortexed to remove the clumps.
3. The tube was then incubated on ice for 20 min with vortexing every 5 min.
4. The suspension was then centrifuged at $3220 \times g$ for 10 min at 4°C. The supernatant was transferred to a new tube.
5. Step 4 was repeated once again.
6. To the supernatant, 4 mL of dilution buffer 1 or dilution buffer 2 was added.
7. The GFP-Trap®_MA beads were equilibrated by washing them 3 times with 1:1 extraction buffer:dilution buffer, recovering the beads magnetically between the washes. 20 µL of the equilibrated beads was added to the solution in step 6, followed by incubation on a rotator for 2 h at 4°C.
8. The beads were recovered by magnetic separation and the supernatant was discarded.
9. The beads were then washed 2 times with 1 mL wash buffer 1 or wash buffer 2 and once with wash buffer lacking the detergent (Igepal CA-630). The beads were recovered by magnetic separation between the washes.
10. 20 µL elution buffer was added to the beads and the tubes were heated at 60°C for 3 min.
11. The supernatant was transferred to a new 1.5 mL tube and stored -80°C.

3.2.23. Polyacryl amide gel electrophoresis (PAGE)

Solutions and buffers:

- 10X running buffer (1 L):
 - 30 g Tris
 - 144 g Glycine
 - 15 g SDS
- Loading buffer:
 - 125 mM Tris pH 6.8
 - 2.5 % SDS
 - 6 M Urea
 - 25 % Glycerol
 - 0.1 M Dithiothreitol (DTT)
 - traces of bromophenol blue
- 10 % Ammonium persulfate (APS)
- 10 % SDS
- Rotiphorese Gel 30
- 1.5 M Tris pH 8.8
- 0.5 M Tris pH 6.8
- Tetramethylethylenediamine (TEMED)

Protocol:

Samples were separated on a 12.5 % denaturing gel. Denaturing gels were manually cast by following the procedure briefly outlined below.

Glass plates that were to be used for casting the gels were cleaned with 70 % ethanol and assembled into the glass-plate-holding-device. The formulations to cast the required gel density are listed below. Samples were mixed with an appropriate volume of loading

buffer. Post sample loading, the gels were run at 10 - 15 mA/gel in the running buffer. The run was stopped before (or shortly after) the loading front ran out of the gel.

Components	Volume
<i>Resolving Gel</i>	
Rotiphorese gel 30	8.3 mL
1.5 M Tris, pH 8.8	5.0 mL
Water	6.4 mL
10 % SDS	200 μ L
10 % APS	150 μ L
<i>Stacking Gel</i>	
Rotiphorese gel 30	1.3 mL
0.5 M Tris, pH 6.8	2.0 mL
Water	3.2 mL
10 % SDS	80 μ L
10 % APS	80 μ L

Note: 12 μ L and 8 μ L of Tetramethylethylenediamine (TEMED) were added to the resolving and stacking gel mixtures respectively, to enable solidification of the gels.

3.2.24. Western blotting

Western blotting was used as an analytical technique to identify the specific proteins in a complex mixture.

Solutions and buffers:

- Transfer Buffer (1 L):
 - 14.3 g Glycine
 - 3.9 g Tris
 - 200 mL Ethanol
- 10x TBS-buffer:
 - 0.5 M Tris pH 7.4

- 1.5 M NaCl
- TBS-T:
 - 1x TBS
 - 0.1 % Tween 20
- Blocking buffer:
 - TBS-T
 - 5 % w/v milk powder
- Staining buffer A:
 - 100 mM Tris pH 9.5
 - 100 mM Sodium chloride
 - 5 mM Magnesium chloride
- NBT-solution:
 - 50 mg/mL nitro-blue tetrazolium chloride (NBT) in 70 % dimethylformamide, aliquots stored at -20°C
- BCIP-solution:
 - 50 mg/mL 5-bromo-4-chloro-3'-indolyl-phosphate p-toluidine (BCIP) in 100 % dimethylformamide (or in water if sodium-salt), aliquots stored at -20°C
- Staining solution (freshly prepared):
 - 66 µL NBT-solution
 - 33 µL BCIP-solution
 - 10 mL staining buffer A

Protocol:

1. A PVDF membrane (Immobilon-P, Millipore) was equilibrated in methanol.
2. The gel along with the membrane was placed in a blotting device with 1x transfer buffer.
3. The transfer was carried out at 4°C with 66 mA for ~16 - 17 h.
4. After the transfer of the proteins from the polyacrylamide gel to the PVDF membrane, the membrane was incubated in the blocking buffer for 1 h at room temperature.

5. The membrane was briefly rinsed in TBS-T.
6. The membrane was incubated next for 1 h at room temperature with anti-GFP antibody diluted 1:999 in TBS-T.
7. The membrane was subsequently washed 3 times for 5 min each in TBS-T at room temperature.
8. The membrane was incubated for 1 h at room temperature with alkaline phosphatase conjugated anti-mouse antibody (anti-mouse-AP) diluted 1:4999 in TBS-T.
9. The membrane was washed 3 times for 5 min each with TBS-T and subsequently equilibrated briefly in staining buffer A.
10. Lastly, the membrane was stained with 10 mL of the staining solution until the signal was clearly visible.
11. The reaction was stopped by rinsing the membrane twice in water.
12. The membrane was air-dried and scanned.

3.2.25. Proteomics analysis of bZIP10

The proteomics analysis of bZIP10 was done in collaboration with the Proteome Centre Tuebingen (PCT), Tuebingen University, Germany. Following the immunoprecipitation of the samples, they were submitted to the proteomics facility. Briefly, the samples were run shortly on NuPAGE® Bis-Tris 4-12 % gradient polyacrylamide gel and the band cut out from the gel. The proteins were then subjected to the in-gel digestion with either Trypsin or LysC endoproteases, followed by elution from the gel, after which the peptides were analyzed on the QExactive HF MS instrument (Thermo Fisher).

3.2.26. Chromatin Immunoprecipitation (ChIP)

Solutions and buffers:

- MC buffer:
 - 10 mM Sodium phosphate buffer pH 7.0
 - 50 mM Sodium chloride
 - 100 mM Sucrose

-
- Master-M-buffer:
 - 10 mM Sodium phosphate buffer pH 7.0
 - 100 mM Sodium chloride
 - 10 mM β -mercaptoethanol
 - Protease inhibitor tablets (cOmplete. EDTA –free Protease Inhibitor Cocktail)
 - M1 buffer (for 160 mL):
 - 18.4 mL 2-methyl-2,4-pentanediol
 - 141.6 mL Master-M-buffer
 - M2 buffer (for 120 mL):
 - 10 mM Magnesium chloride
 - 0.5 % Triton X-100
 - 112.8 mL Master-M-buffer
 - Sonic buffer:
 - 10 mM Sodium phosphate buffer pH 7.0
 - 100 mM Sodium chloride
 - 1 % Sarkosyl
 - 10 mM EDTA
 - 1x Protease inhibitor solution (cOmplete. EDTA –free Protease Inhibitor Cocktail)
 - IP buffer:
 - 50 mM HEPES buffer pH 7.5
 - 150 mM Potassium chloride
 - 5 mM Magnesium chloride
 - 10 μ M Zinc sulfate
 - 1 % Triton X-100
 - 0.05 % SDS
 - Elution buffer (pH 2.8, adjusted with HCl, prepared freshly):
 - 100 mM glycine
 - 500 mM Sodium chloride
 - 500 μ M Tween-20

Protocol:

1. The fresh leaf tissue was fixed with 1 % formaldehyde in the MC buffer for 30 min under vacuum-
 - a) The material was collected in a 50 mL falcon kept on ice.
 - b) The tissue was resuspended in 25 mL of MC buffer containing 1 % formaldehyde.
 - c) The vacuum was turned on and after 15 min turned off, the tissue was mixed and the procedure was repeated for another 15 min.
 - d) Fixation was stopped by adding 2.5 mL glycine (1.25 M stock), mixed well by inverting the tube several times and vacuum was applied for another 2 min.
2. The tissue was washed thrice with 25 mL of MC buffer, blot dried on paper towels and transferred into liquid nitrogen. The tissue can be stored at -80°C if necessary.
3. A Miracloth filter (Calibrochem) was wetted with 10 mL M1 buffer and the eluate was run through it 3x times.
4. The frozen tissue was intensely ground.
5. The ground powder was next transferred to a 50 mL falcon tube with 20 mL of M1 buffer. A very cold spoon was used for this purpose.
6. The slurry was filtered through the equilibrated Miracloth into a falcon tube.
7. The Miracloth was washed with an additional 5 mL of M1 buffer to quantitatively collect all nuclei in the filtrate.
8. The solution was spun at $1,000 \times g$ for 20 min at 4°C .
9. The pellet was washed 5 times with 5 mL M2-Buffer with intermittent spins of $1000 \times g$ for 10 min at 4°C . To avoid strong forces, pasteur pipettes were used for resuspending the pellet.
10. The pellet was washed with 1 mL Master-M-buffer at $1000 \times g$ for 10 min at 4°C .
11. The crude nuclear pellet was resuspended in 2 mL sonic buffer.
12. Chromatin shearing of was carried out by one of the two following methods-
 - a) Sonication with probe sonicator: The chromatin material was solubilized with the help of a Branson probe sonicator (Output 3; Continuous pulse; Power 50 %; Cycle 1 min). The samples were kept on ice and allowed to cool down between

each ultrasonic treatment. The aim was to achieve about 300-500 bp fragments via sonication.

b) Sonication with Covaris sonicator: the chromatin was solubilised with the help of Covaris sonicator (Duty Cycle: 20 %; Intensity: 5; Cycles per Burst: 200; Cycle time: 2 min). The samples were placed on ice and allowed to cool down after the ultrasonic treatment. Aim was to achieve about 200-500 bp fragments via this treatment. The sonication treatment was checked by running an aliquot of the reverse crosslinked input sample on a 1.5 % agarose gel.

13. The fragmented samples were then centrifuged at top speed for 5 min at 4°C.
14. The supernatant was transferred into a fresh tube. 750 µL of the supernatant was mixed with an equal amount of IP buffer and the rest of the sample (~250 µL) was used as the input DNA (stored at -20°C until Step 23).
15. 10 µL of GFP-Trap_MA beads equilibrated in 1:1 sonic buffer:IP buffer or 2.5 µL Anti-GFP Ab290 (1:999 diluted GFP antibody) was added to the sample.
16. The samples were incubated at 4°C on a rotating wheel for 2 h.
17. The DNA-protein-antibody complex was separated, either magnetically (in case of GFP-Trap_MA beads) or by using protein A agarose beads equilibrated in 1:1 sonic buffer:IP buffer (in case of GFP Ab290), from the solution and the supernatant was discarded.
18. The beads were washed 5 times for 10 min with 1 mL IP buffer on a rotator. (4 times at 4°C, last wash at room temperature).
19. Elution was performed with 100 µL of ice cold Elution buffer, vortexed for 30 s followed by magnetic separation (in case of GFP-Trap_MA beads) or by centrifugation at full speed (in case of GFP Ab290).
20. The supernatant was transferred to a tube containing 150 µL of Tris pH 9.0.
21. Steps 19-20 were repeated twice.
22. The sample was then centrifuged at maximum speed for 2 min and the s/n was transferred to a new tube.

The following procedures were performed on input and immunoprecipitated samples.

23. 1 μ L of RNase A (10 mg/mL) was added to each tube followed by incubation for 15 min at 37°C.
24. 1.5 μ L of proteinase K was added to the sample, briefly vortexed and incubated overnight at 37°C.
25. A second aliquot of proteinase K was added to the samples followed by incubation at 65°C for 6 h.
26. MinElute Reaction Cleanup Kit was used to column purify the samples as per the manufacturer's instructions.
27. The DNA was eluted from the column by using 30 μ L of Buffer EB (from the kit).
28. The DNA was further used for either qPCR to check the enrichment or to make the libraries for sequencing.

3.2.27. ChIP library preparation

The ChIP library preparation followed by the downstream sequencing and sequence analysis was done in collaboration with the Quantitative Biology Center (QBiC), Tuebingen University, Germany. The ChIP libraries were prepared using the TruSeq® ChIP Sample Preparation Guide (available at info/truseq-chip-sample-prep-guide-15023092-b.pdf) with the following exceptions:

1. The ligation products were purified on a 2 % gel using BluePippin (Sage Science) with 200-600 bp as the size selection range.
2. The DNA fragments were enriched after the purification by performing a PCR under following conditions:

Step		Temperature	Time
Initial Denaturation		98°C	30 s
18 cycles:	Denaturation	98°C	10 s
	Annealing	65°C	30 s
	Extension	72°C	30 s
Final Extension		72°C	5 min

The following scheme was used for setting up the PCR reaction:

Components	Volume for 25 μL reaction
Primer cocktail	5 μ L
PCR mix (PMM)	50 μ L
BluePippin eluate	40 μ L
RSB	5 μ L

4. Results

4.1. Analysis of regulation of bZIP10 using phosphorylation mutants

It had been shown that the serine (Ser, S) residue at position 19 in the DNA-binding domain (DBD) is very highly conserved in the plant bZIP transcription factors. Out of 74 genes coding for bZIP factors in *Arabidopsis thaliana*, 66 have a Ser residue at position 19. Reversible phosphorylation of certain serine, threonine or tyrosine residues can lead to a transient change in the function of a transcription factor either by altering its sub-cellular localization, stability, DNA-binding or transactivation capacity (Kirchler, Briesemeister et al. 2010). It is usually possible to mimic the phosphorylated state of serine residue by its substitution to aspartate, which similarly to phosphorylated serine confers a negative charge to protein molecule. It had been shown that upon substitution of Ser19 to aspartate (Asp, D) the *in vitro* binding of bZIP63 to cognate DNA sequence was completely disrupted, whereas mutating Ser19 to alanine (Ala, A) did not influence the affinity of bZIP63 to cognate DNA sequence (Kirchler, Briesemeister et al. 2010). The same result was seen in the case of bZIP53 (Kirchler 2014). The inhibitory effect on DNA binding upon mutating Ser19 to Asp was also shown for GBF1, a G-group bZIP from *Arabidopsis* (Smykowski, Fischer et al. 2015). Mimicking the phosphorylated status of Ser residue by its substitution with Asp residue might open a strong possibility of generating dominant negative mutants of often redundantly acting bZIP factors. Therefore, I used such an approach to analyze the effect of potential phosphorylation on bZIP10 behavior.

4.1.1. Transactivation capacity of bZIP10 phosphorylation mutants

To analyze the transactivation capacity of the phospho-mimetic mutant of bZIP10, a reporter gene assay in *Arabidopsis* leaf mesophyll protoplasts prepared from *bzip10ko* line was performed. bZIP10 and its mutants carrying substitution of Ser19 either with Ala or with Asp fused to GFP at their C-terminus and placed downstream of 35S promoter were used for this purpose. Since bZIP10 is known to heterodimerize with the S1-group bZIP factors and its *in vivo* target genes are yet unknown, the S1 member bZIP53 fused to mCherry at its C-terminus (*35S::bZIP53-mCherry*) was used as a co-effector. bZIP10

heterodimerizes with bZIP53 to synergistically activate the expression of *ProDH1* (*PROLINE DEHYDROGENASE 1*) and seed storage albumins (Weltmeier, Ehlert et al. 2006, Alonso, Onate-Sanchez et al. 2009). As a reporter, a UidA sequence under the control of *ProDH1* promoter (*pProDH1::GUS*) bearing the *in vivo* binding site for bZIP53 was used. Either bZIP10-GFP or one of its Ser19 mutants was co-transfected with bZIP53-mCherry and *pProDH1::GUS* in the protoplasts. The expression of bZIP10 and bZIP53 was confirmed by shortly examining the protoplasts under the epi-fluorescence microscope for GFP and mCherry signal respectively. In agreement with a previous report, bZIP10 alone did not possess the transactivation capacity towards *pProDH1*. Also, the activation of *pProDH1* by bZIP53 alone is considerably weaker as compared to the synergistic activation by bZIP10/bZIP53 heterodimers (Weltmeier, Ehlert et al. 2006). The reporter gene activation by bZIP10/bZIP53 heterodimers revealed that when compared to the wild-type bZIP10, the heterodimers of phospho- mimicking mutant bZIP10^{S19D} showed strongly reduced (p value: 6×10^{-6}) transactivation capacity. The heterodimers of phospho- ablative mutant bZIP10^{S19A} behaved similarly to the wild-type bZIP10 (**Figure 10**). To test whether such an inhibitory effect of Ser to Asp substitution was due to the disruption of interaction of bZIP10 with bZIP53 or not, the bZIP10 phosphorylation mutants were further analyzed for their dimerization capability with bZIP53.

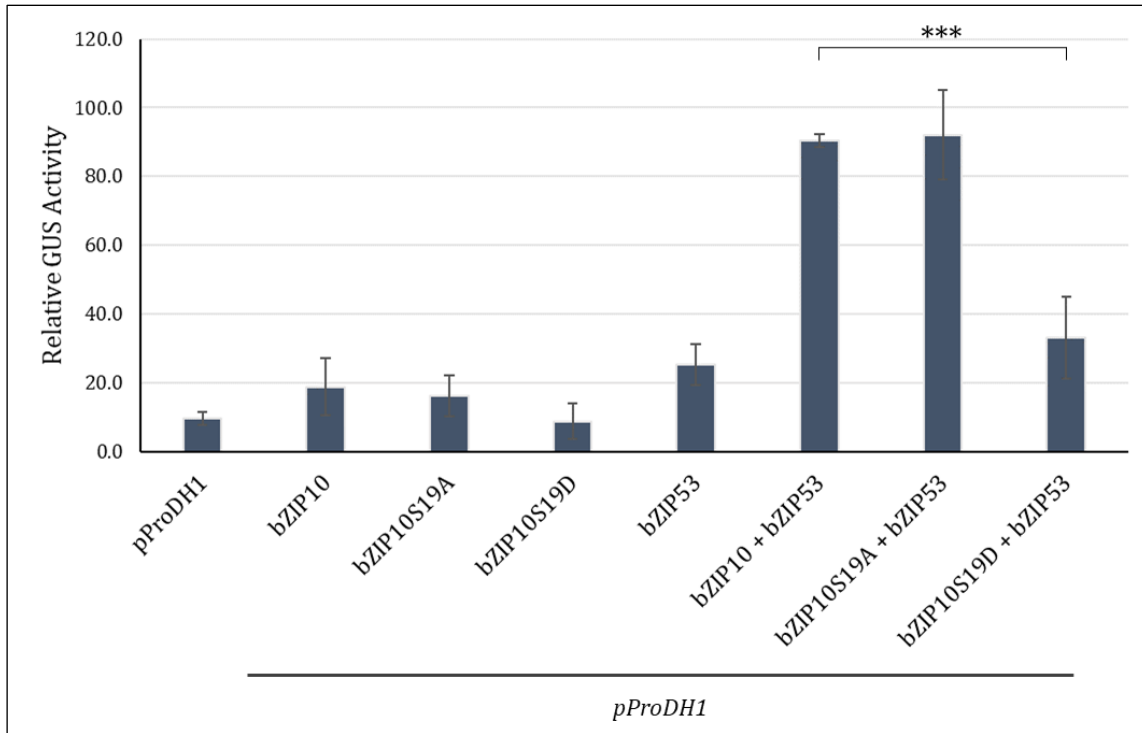


Figure 10: Relative GUS expression driven by pProDH1 promoter either alone or in the presence of bZIP10 or one of its Ser mutants and/or bZIP53, in *Arabidopsis thaliana* leaf mesophyll protoplasts prepared from *bzip10ko* line. *** denotes a significant change (p value ≤ 0.005). Statistical analysis was performed on at least four biological repeats.

4.1.2. bZIP10 phospho-mimetic mutant heterodimer formation

To test if mutating Ser19 affects the dimerization capability of bZIP10, a protoplast 2-hybrid experiment was performed where bZIP10 and its Ser19 mutants (bZIP10^{S19A} and bZIP10^{S19D}), N-terminally fused to the GAL4 Activation domain (AD) driven by 35S promoter were used. The interaction partner bZIP53 N-terminally fused to GAL4 DNA-binding domain (BD) was also expressed under 35S promoter. The GUS reporter driven by GAL4 Upstream Activating Sequence (*GAL4-UAS::GUS*) was used as the reporter gene for the quantification of heterodimerization capacity of the bZIPs. Then, either bZIP10 or one of its Ser19 mutants was co-transfected with bZIP53 and *GAL4-UAS::GUS* in *Arabidopsis* leaf mesophyll protoplasts prepared from *bzip10ko* line, followed by measurement of the reporter gene activity with the appropriate substrate. As seen in **Figure 11**, there is no difference in the heterodimerization capacity of bZIP10^{S19D} with bZIP53, as compared to native bZIP10 or bZIP10^{S19A}.

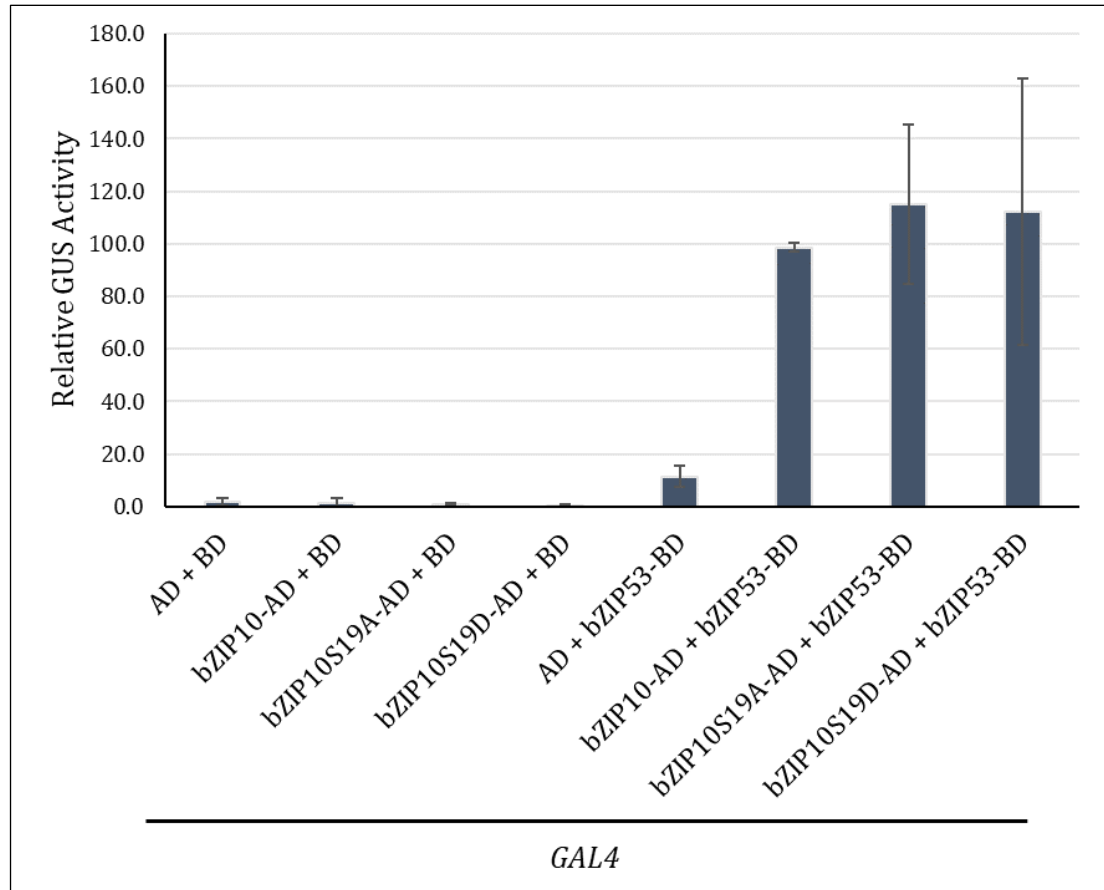


Figure 11: Relative GUS expression driven by GAL4 promoter either alone or in the presence of bZIP10-AD or one of its Ser mutants and/or bZIP53-BD, in *Arabidopsis thaliana* leaf mesophyll protoplasts prepared from *bzip10ko* line. AD and BD wherever mentioned alone in the graph (bar number 1-5 from left) are the empty vector negative controls. Statistical analysis was performed on four biological repeats.

The same results were obtained when the heterodimerization capacity was tested in yeast by using the Split Ubiquitin System (SUS) ((Grefen, Obrdlik et al. 2009), DUALhunter kit from Dualsystems Biotech). In this system, the N-terminus of a bait protein is fused to a small membrane anchor (the yeast ER protein Ost4), and C-terminal ubiquitin half (Cub) is fused at its C-terminus, followed by a transcription factor LexA-VP16. The C-terminus of a prey protein is fused to the mutated N-terminal ubiquitin half (NubG). Upon interaction, the split-ubiquitin (Cub + NubG) comes together leading to its recognition by the ubiquitin specific proteases that cleave between ubiquitin and LexA-VP16. This cleavage releases LexA from the membrane whereby it is transported to the nucleus where it activates the reporter genes, viz., *ADH2* (leading to synthesis of

adenine), *HIS3* (leading to synthesis of histidine) and *lacZ*. The growth of yeast on media lacking adenine and histidine indicates a successful interaction. In our experiment, bZIP53 was used as the bait protein and cloned as a fusion with Cub. A Nuclear Export Sequence (NES) was added to bZIP10 and its Ser19 mutants to ensure their presence in the cytoplasm. These served as the prey proteins and were cloned as fusions with NubG. Either of the prey proteins was co-transformed with the bait in yeast and its growth was monitored on growth control media and selective interaction media. There were no differences in the growth of yeast expressing either bZIP10 or its Ser19 mutants with bZIP53 (**Figure 12**). In addition, the *lacZ* activity was measured by performing the β -Gal assay. Again, no significant differences were observed between the heterodimerization capacity of bZIP10 and its Ser19 mutants with bZIP53 (**Figure 13**).

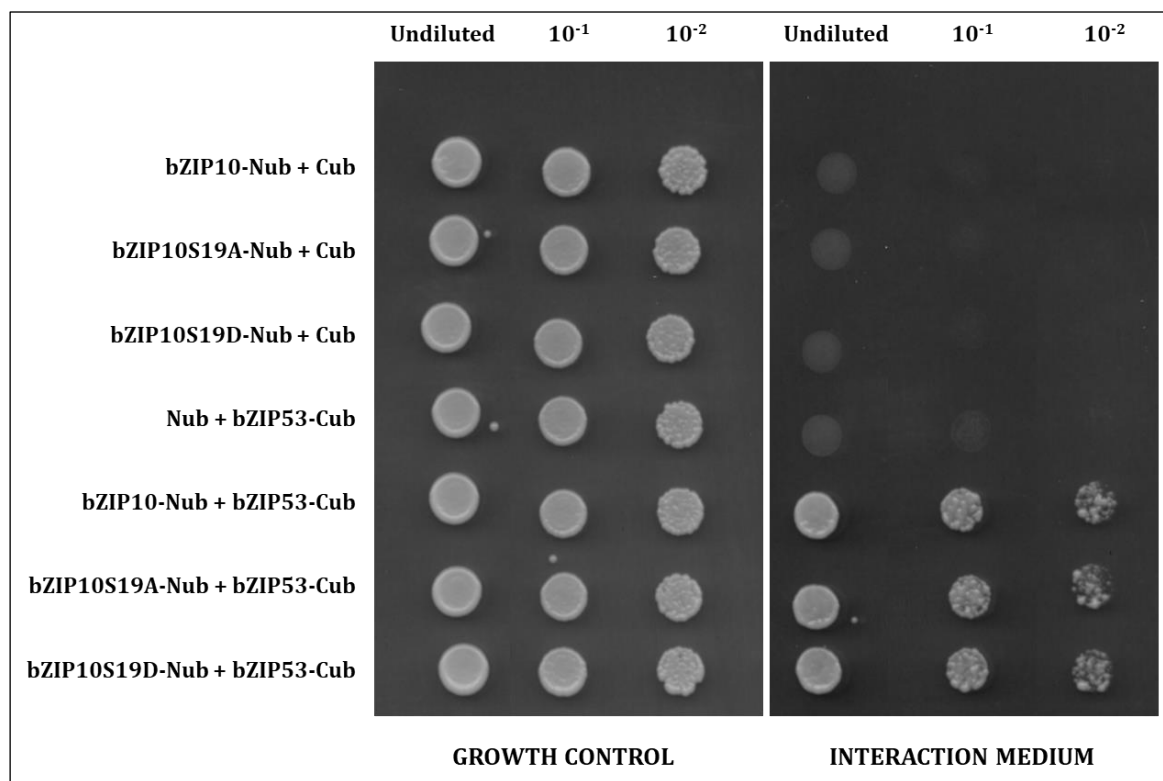


Figure 12: A representative image showing heterodimerization of bZIP53 with bZIP10 or one of its Ser19 mutants in yeast using the Split Ubiquitin System. Cub and Nub wherever mentioned in the image are the empty vector negative controls.

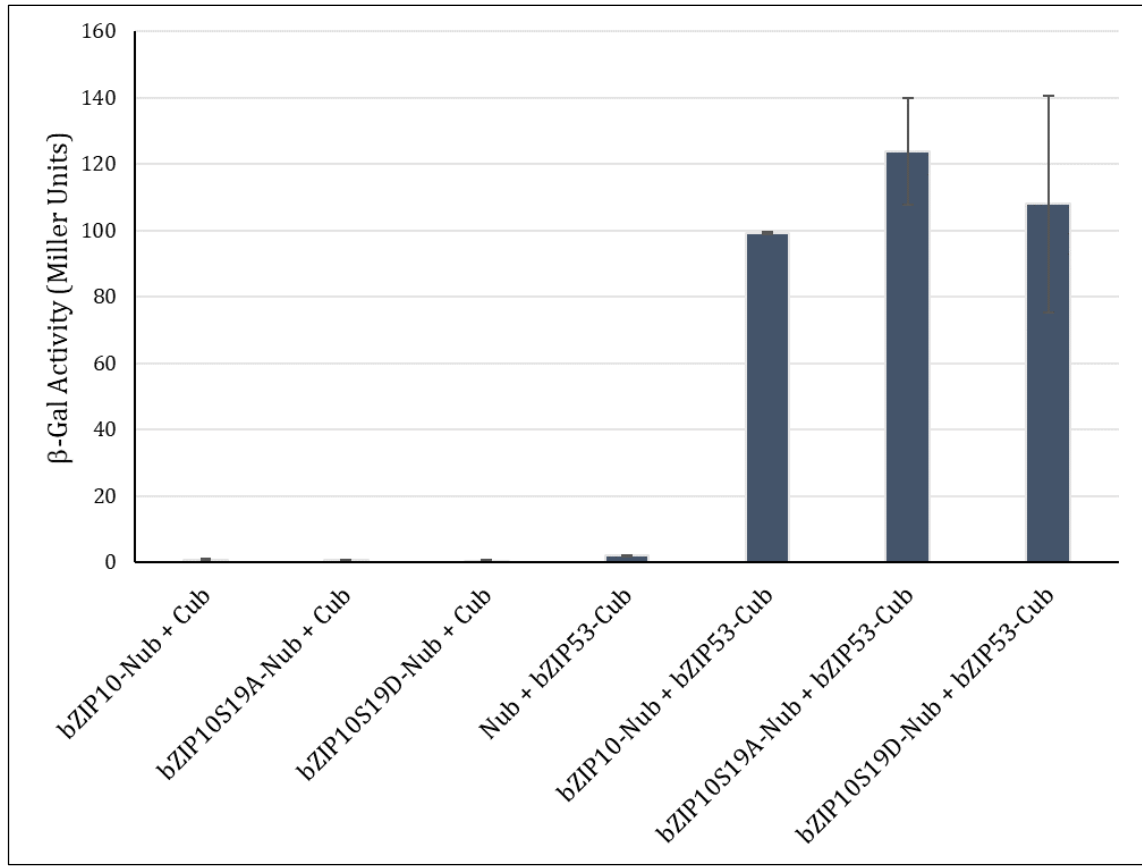


Figure 13: Split Ubiquitin Yeast 2-hybrid experiment to analyze the interaction of bZIP10 and its Ser mutants with bZIP53. Cub and Nub wherever mentioned alone in the graph are the empty vector negative controls. Statistical analysis was performed on four biological repeats.

4.1.3. Sub-cellular localization of bZIP10 phosphorylation mutants

The C-terminal fusion of bZIP10 with GFP proved to be functional in our reporter gene assay. Hence, the fusion proteins were also utilized for analyzing their sub-cellular localization. Either bZIP10 or one of its Ser19 mutants was co-transfected with mCherry-NLS (mCherry fused to a Nuclear Localization Signal and used as a nuclear marker) in *Arabidopsis* leaf mesophyll protoplasts prepared from *bzip10ko* line. As had been shown earlier (Kaminaka, Nake et al. 2006), bZIP10 localizes to the nucleus, with a weak cytoplasmic signal as well. Compared to the wild-type bZIP10, the bZIP10^{S19A} mutant showed stronger nuclear and weaker cytoplasmic signal, while bZIP10^{S19D} mutant showed a very strong cytoplasmic and a highly reduced nuclear signal (**Figure 14**).

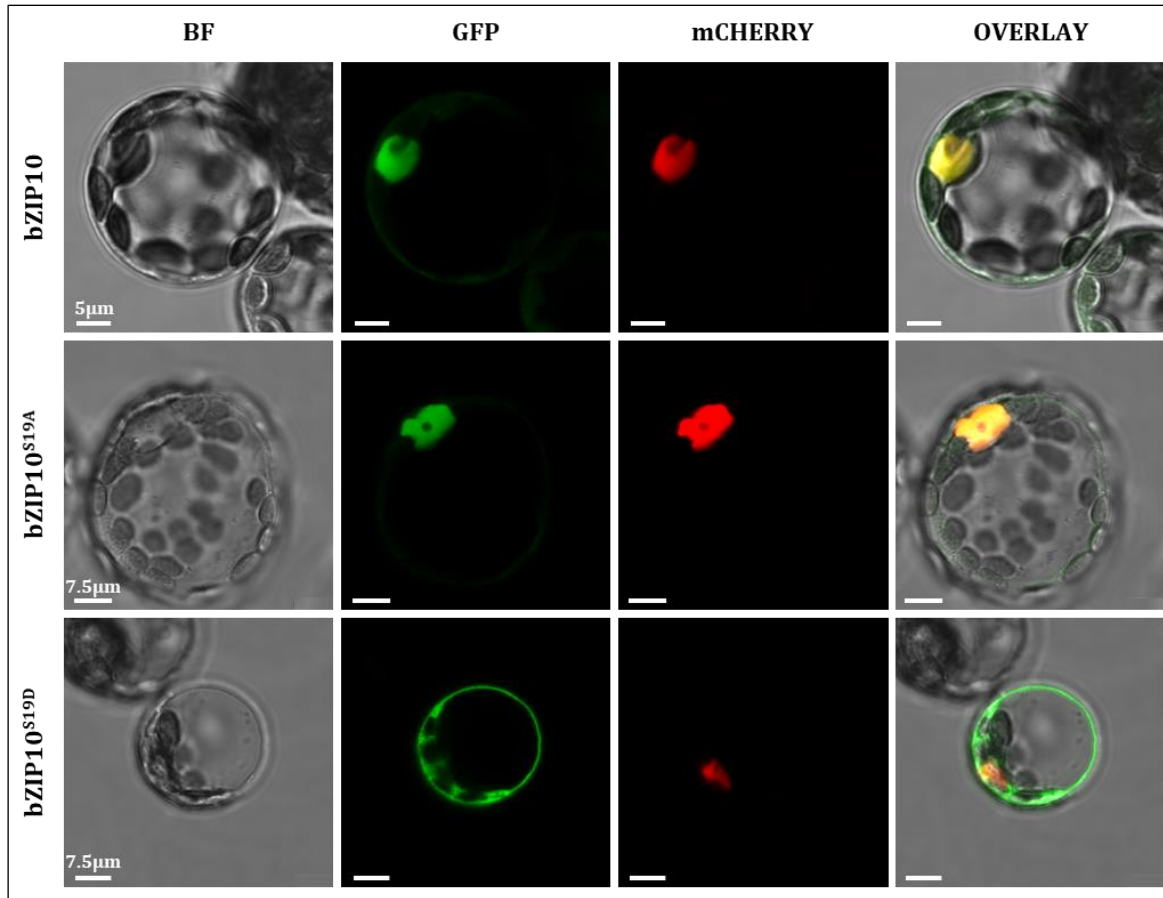


Figure 14: Subcellular localization of GFP tagged bZIP10, bZIP10^{S19A} and bZIP10^{S19D} in *Arabidopsis thaliana* leaf mesophyll protoplasts prepared from *bzip10ko* line. mCherry-NLS has been used as a nuclear marker.

As it is mentioned earlier, bZIP10 heterodimerizes with bZIP53, an S1-group Arabidopsis bZIP, to synergistically activate the expression of *pProDH1* and seed storage albumins (Weltmeier, Ehlert et al. 2006, Alonso, Onate-Sanchez et al. 2009). Unlike bZIP10, bZIP53 is detected only in the nucleus, which is in agreement with a previous study (Llorca, Berendzen et al. 2015). Interestingly, when bZIP10 or one of its Ser19 mutants was co-transfected with bZIP53-mCherry, bZIP10 and its Ser19 mutants displayed exclusively nuclear localization (**Figure 15**).

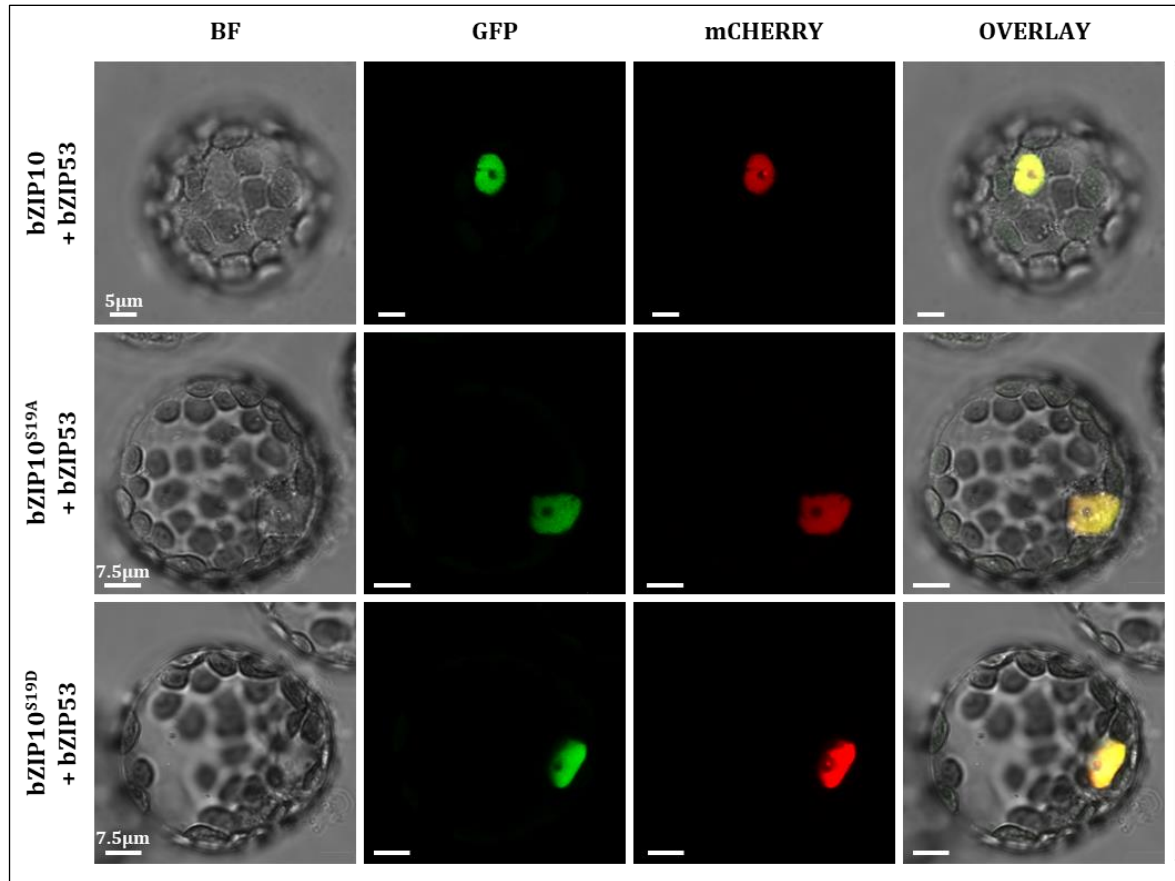


Figure 15: Subcellular localization of GFP tagged bZIP10, bZIP10^{S19A} and bZIP10^{S19D} with mCherry tagged bZIP53 in *Arabidopsis thaliana* leaf mesophyll protoplasts prepared from *bzip10ko* line.

The DBD of bZIP10 overlaps with the NLS. To determine if the cytoplasmic localization of bZIP10^{S19D} was due to a non-functional NLS caused by the mutated Ser residue, a GFP-tagged N-terminal deletion mutant of *bZIP10* (bZIP10 Δ 648) lacking the first 648 bp of its coding sequence was used. It has been reported that the first 105 amino acid residues of bZIP10 are required for its interaction with XPO1 (Kaminaka, Nake et al. 2006). Deletion of this N-terminal sequence removed the XPO1 interaction site in bZIP10, thereby making it easier to assess the functionality of its NLS. The Ser19 in its DBD was mutagenized to either Ala (bZIP10 Δ 648^{S19A}) or Asp (bZIP10 Δ 648^{S19D}). Either of these was at first co-transfected with mCherry-NLS in *Arabidopsis* leaf mesophyll protoplasts prepared from *bzip10ko* line. The bZIP10 Δ 648 mutant showed an exclusive nucleolar localization, and mutating the Ser19 to Ala or Asp did not lead to any change in its localization (**Figure 16**), thereby suggesting that mutating Ser19 to Ala or Asp did not impair the NLS. When

these constructs were co-transfected with C-terminally mCherry-tagged bZIP53, all the three mutants co-localized with bZIP53 in the nucleus (**Figure 17**).

Thus, the phosphorylation state of Ser19 residue in the DBD of bZIP10 seemed to be important for its sub-cellular localization, and presence of bZIP53 was enough to retain bZIP10 in the nucleus. The localization study corroborated the interaction data, i.e., the interaction of bZIP10 with bZIP53 is independent of the phosphorylation state of Ser19 in the DBD of bZIP10.

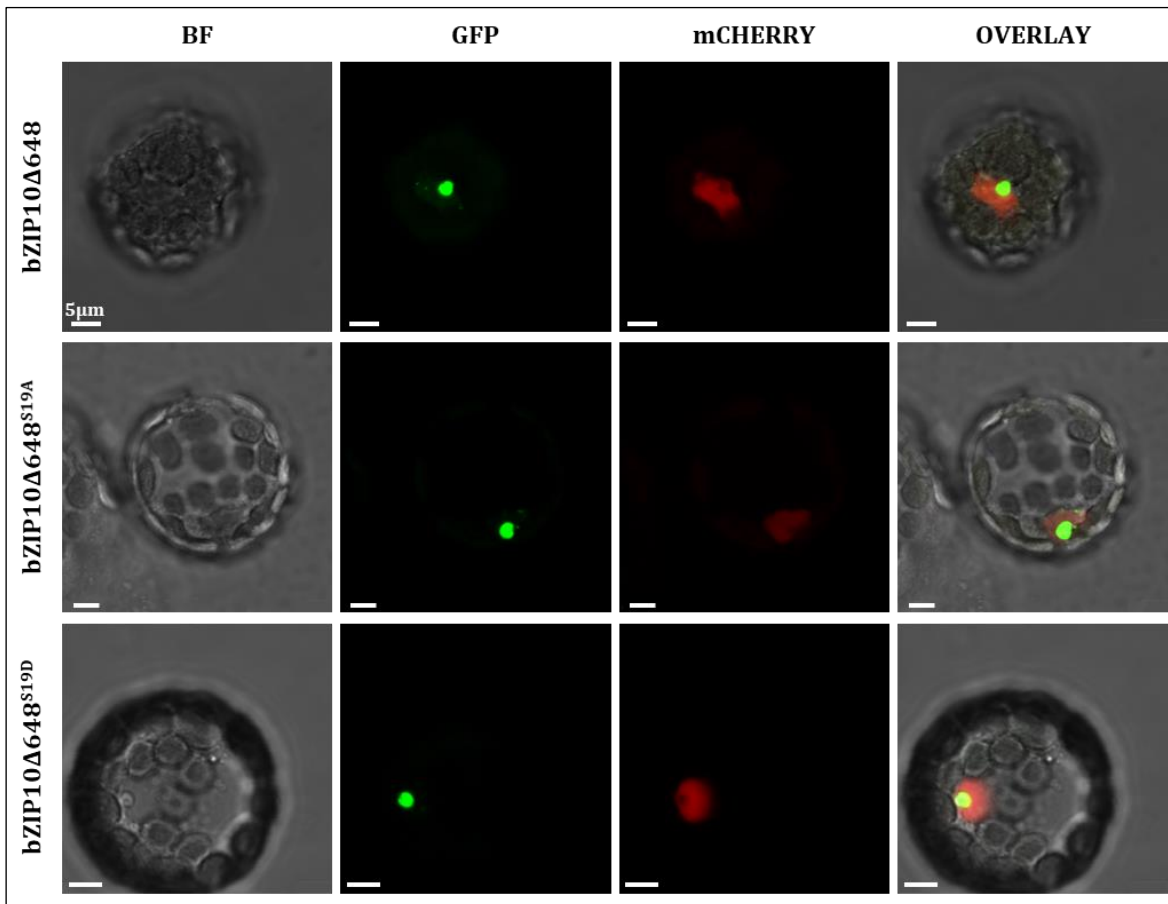


Figure 16: Subcellular localization of GFP tagged bZIP10Δ648, bZIP10Δ648^{S19A} and bZIP10Δ648^{S19D} in *Arabidopsis thaliana* leaf mesophyll protoplasts prepared from *bzip10ko* line. mCherry-NLS has been used as a nuclear marker.

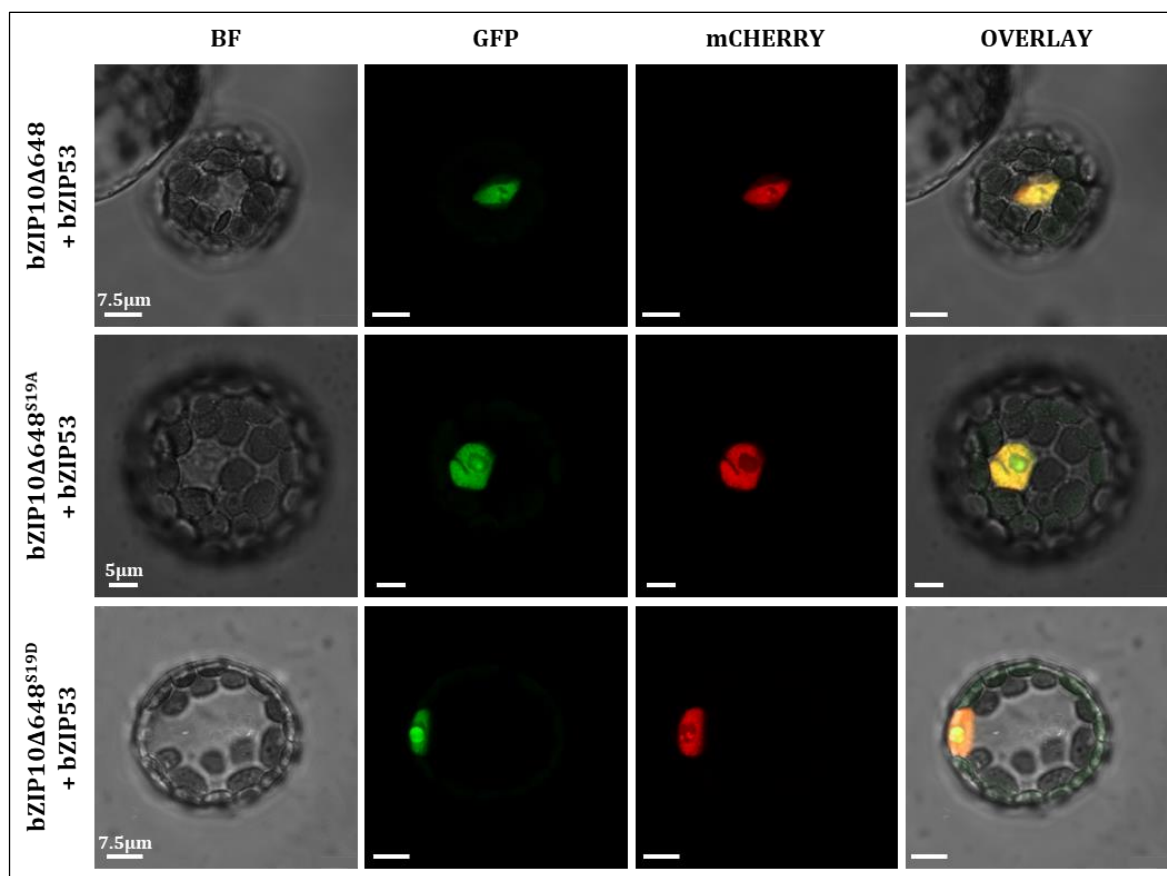


Figure 17: Subcellular localization of GFP tagged bZIP10Δ648, bZIP10Δ648^{S19A} and bZIP10Δ648^{S19D} with mCherry tagged bZIP53 in *Arabidopsis thaliana* leaf mesophyll protoplasts prepared from *bzip10ko* line.

4.2. Functional characterization of bZIP10

Our results show that substitution of Ser19 in the bZIP10 DBD with Asp leads to a strong reduction of bZIP10 transactivity, most likely due to the inability of bZIP10^{S19D} mutant and its heterodimers to bind to cognate DNA. The dimerization capacity of this mutant remains, however, comparable to the wild-type protein, thereby presumably forming a dominant negative form of bZIP10. The transgenic lines of *Arabidopsis thaliana* over-expressing C-terminally GFP-tagged bZIP10 (bZIP10-GFPox) and C-terminally GFP-tagged bZIP10 where Ser19 was mutated to Asp (bZIP10^{S19D}-GFPox, phospho-mimetic mutant) were generated and analyzed in further experiments. Due to the presence of conserved phosphorylatable residues at position 19 in the DBD across plant bZIPs and their involvement in the direct binding to DNA backbone [52], their potential phosphorylation leading to the attenuation of DNA binding and consequently their transactivity cannot be ruled out. Since there is a possibility of the bZIP10 regulation by reversible phosphorylation of Ser19, the absence of Ser19 in the DBD of bZIP10 might lead to constitutive DNA binding, consequently forming a dominant positive, DNA binding form of bZIP10. Therefore, the transgenic lines over-expressing C-terminal GFP-tagged bZIP10 where Ser19 was mutated to Ala (bZIP10^{S19A}-GFPox, phospho-ablative mutant) were generated as well. The homozygous lines were selected and the seeds of the fifth generation were used in further analyses.

It was shown earlier that bZIP10 positively mediates the plant basal defense responses and hypersensitive response (HR) upon *Hyaloperonospora parasitica* attack (Kaminaka, Nake et al. 2006). To gain insight into its role in the responses to a brighter spectrum of pathogens and herbivores, various pathogen assays were performed on bZIP10 transgenic lines, viz., bZIP10-GFPox, bZIP10^{S19A}-GFPox, bZIP10^{S19D}-GFPox, *bzip10ko*, and Col-0. Two independent transgenic lines of bZIP10-GFPox, bZIP10^{S19A}-GFPox, bZIP10^{S19D}-GFPox were used in the assays in order to avoid the false positives or negatives resulting from the t-DNA insertions.

4.2.1. *Mamestra brassicae* infection assay

This experiment was done in collaboration with Merel Steenberg and Dr. A. C. M. (Saskia) van Wees, Utrecht University, Netherlands. At first, the bZIP10 expression levels were analyzed at different time-points after infection with *Mamestra brassicae* (cabbage moth), a herbivore. The leaf material was harvested from infected (i) and uninfected (c) plants. As can be seen in **Figure 18**, the expression of bZIP10 transgene in bZIP10-GFPox, bZIP10^{S19A}-GFPox and bZIP10^{S19D}-GFPox is considerably higher than in Col-0 across all the time-points. Furthermore, there is no effect of *Mamestra* infection on bZIP10 transgene expression at all the time-points.

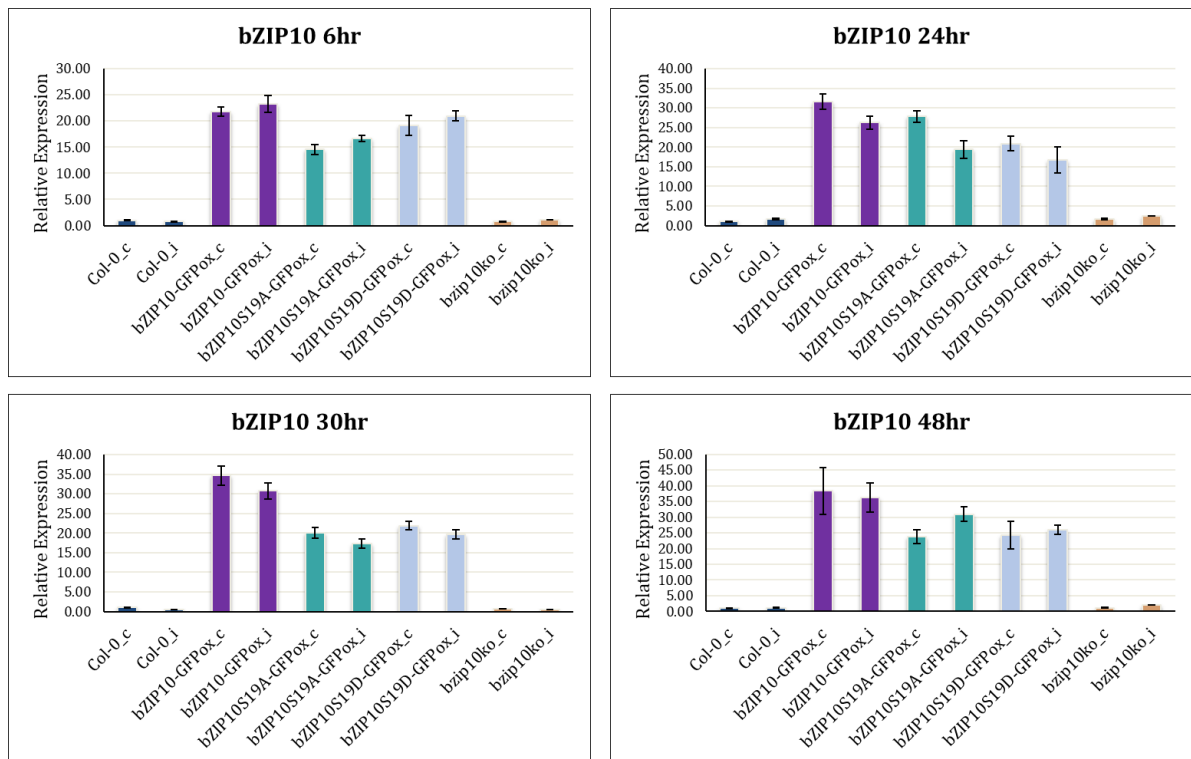


Figure 18: Expression of bZIP10 after *Mamestra brassicae* feeding on *Arabidopsis thaliana*, at the above mentioned time points. “c” refers to the control plant group whereas “i” refers to the infected plant group.

In order to analyze the bZIP10 dependent response of plants to *Mamestra*, the caterpillars were allowed to feed on Col-0, bZIP10-GFPox and *bzip10ko* and then weighed after 9 days of infection. The weight of the caterpillar indicated the susceptibility of the plant. The higher the weight, the more susceptible the plant is. It was observed that, when

compared to Col-0, bZIP10-GFPox was highly susceptible (p value $\leq 1 \times 10^{-4}$), whereas *bzip10ko* showed no difference. The same assay was performed with the phospho-ablative mutant bZIP10^{S19A}-GFPox and the phospho-mimetic mutant bZIP10^{S19D}-GFPox. As expected, the bZIP10^{S19A}-GFPox behaved similarly to the bZIP10-GFPox and showed high susceptibility (p value $\leq 1 \times 10^{-4}$) when compared to Col-0 while bZIP10^{S19D}-GFPox behaved similarly to *bzip10ko* and showed no difference to Col-0 (**Figure 19**). This assay was performed twice with similar outcome.

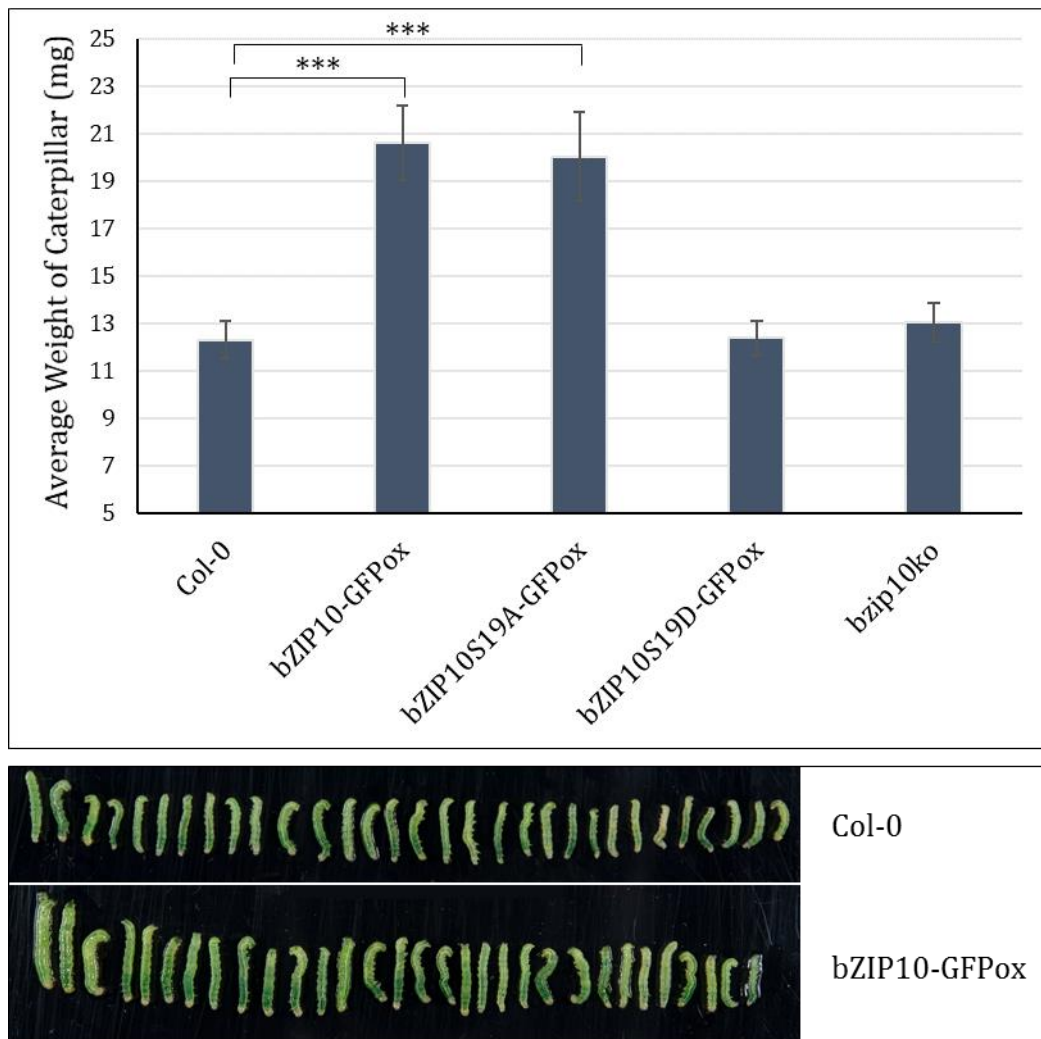


Figure 19: (Top) Weight of *Mamestra brassicae* feeding on *Arabidopsis thaliana* transgenic lines. (Bottom) Images of caterpillars that were fed on Col-0 and bZIP10-GFPox transgenic line respectively. *** denotes a significant change (p value ≤ 0.005). Representative data has been depicted.

It is known that herbivory induces the jasmonic acid (JA) defense pathway in plants. Upon insect attack, the JAZ proteins are de-repressed which leads to activation of JA-responsive genes (Pieterse, Van der Does et al. 2012). To investigate the transcriptional response of *Mamestra brassicae* feeding on *Arabidopsis thaliana*, some of these JA-responsive genes were used as markers and their expression was analyzed. For this purpose, RNA was isolated from the plant leaves harvested after 6 hours, 24 hours, 30 hours and 48 hours of *Mamestra brassicae* feeding, followed by reverse transcription-PCR (RT-PCR) with the primers of the following genes: *MYC2*, *VSP2*, *ERF1* and *ORA59*. The housekeeping gene EF-1 α (Elongation factor-1 α) was used for normalization. The MYC2-branch genes, *MYC2* and *VSP2*, showed induction across all the time-points measured in all the genotypes analyzed (**Figure 20**), indicating the non-involvement of bZIP10 in transcriptional regulation of these two genes.

The ERF-branch gene, *ERF1*, showed bZIP10 independent induction at time-points 24 h, 30 h and 48 h (**Figure 21**). At 6 h, *ERF1* seemed to be induced only in Col-0 and bZIP10ox (**Figure 21**). No change in the induction of *ORA59*, another ERF-branch gene, was detected in plants of all genotypes analyzed at 6 h and 30 h time-points. Interestingly, after 24 h of inoculation, the induction of *ORA59* in bZIP10^{S19D}-GFPox, *bzip10ko* and Col-0 plants was weaker than in bZIP10^{S19A}-GFPox, and especially in bZIP10-GFPox plants (**Figure 21**). Nevertheless, it should be mentioned that this difference was more prominent in two biological replicates, but not in the third. At 48 h, *ORA59* was only slightly induced across all the genotypes except Col-0 at a comparable level.

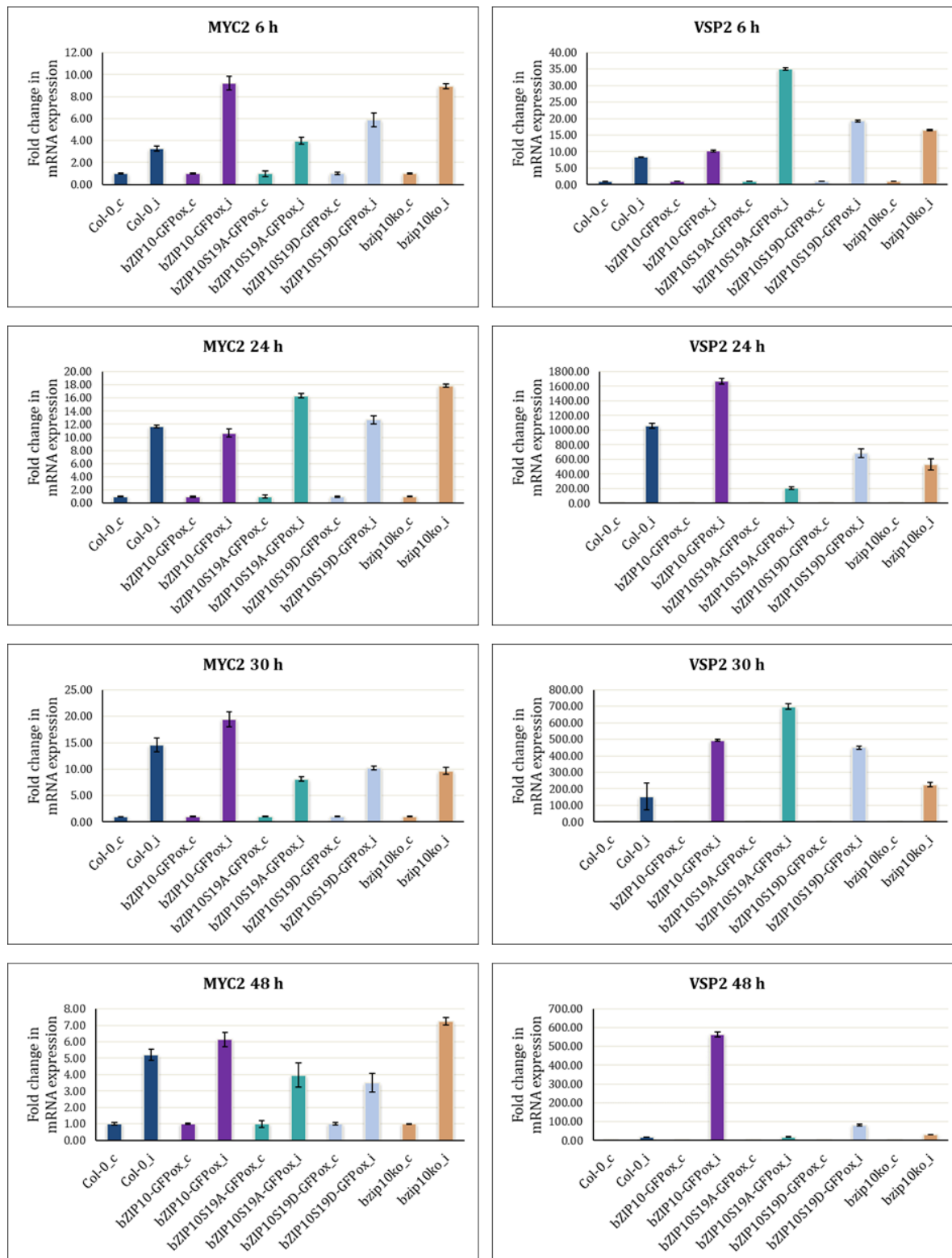


Figure 20: Representative data of the MYC2 and VSP2 expression changes after *Mamestra brassicae* feeding on *Arabidopsis thaliana*. The data are presented as fold change in the expression relative to the uninfected control, at the above mentioned time points. “c” refers to the control plant group whereas “i” refers to the infected plant group.

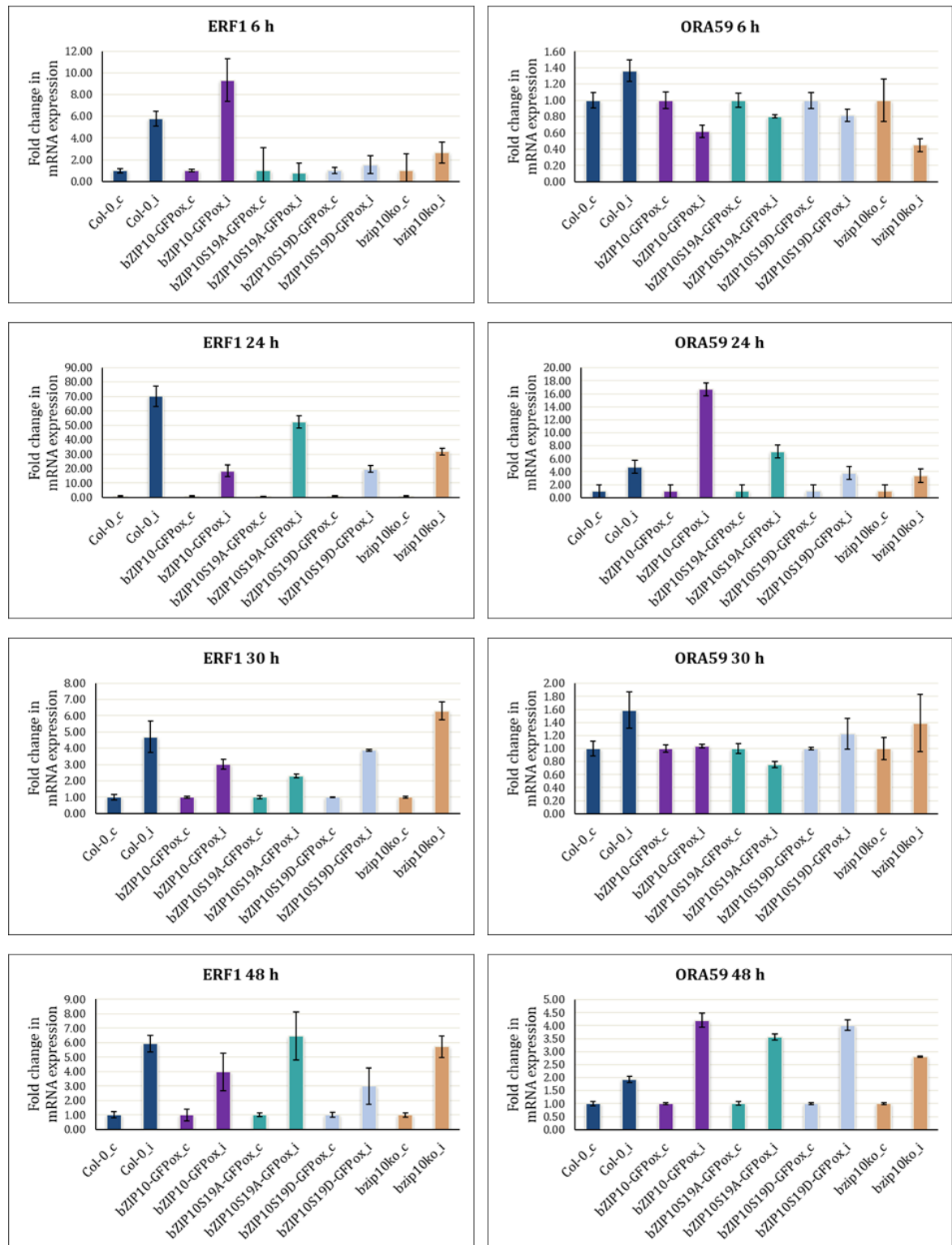


Figure 21: Representative data of the ERF1 and ORA59 expression changes after *Mamestra brassicae* feeding on *Arabidopsis thaliana*. The data are presented as fold change in the expression relative to the uninfected control, at the above mentioned time points. “c” refers to the control plant group whereas “i” refers to the infected plant group.

4.2.2. *Botrytis cinerea* infection assay

The response of the above mentioned lines was further examined towards the necrotrophic fungus *Botrytis cinerea*. The spores of the fungus were dropped on the leaves and monitored regularly. After 3-4 days of infection, the leaves were classified into different classes (I – IV) depending on the severity of the symptoms (Van Wees, Van Pelt et al. 2013). Although several biological repeats were performed, the growth rate of *Botrytis* in each assay differed dramatically being sometimes too fast and once too slow. Therefore, the data from only two assays containing all tested lines are presented here. Our results showed that, when compared to Col-0, bZIP10-GFPox and the mutant line bZIP10^{S19A}-GFPox showed more susceptibility (p value $\leq 5 \times 10^{-3}$) (**Figure 22A,B**) while *bzip10ko* and bZIP10^{S19D}-GFPox were more resistant (p value: 3×10^{-2}) (**Figure 22C**).

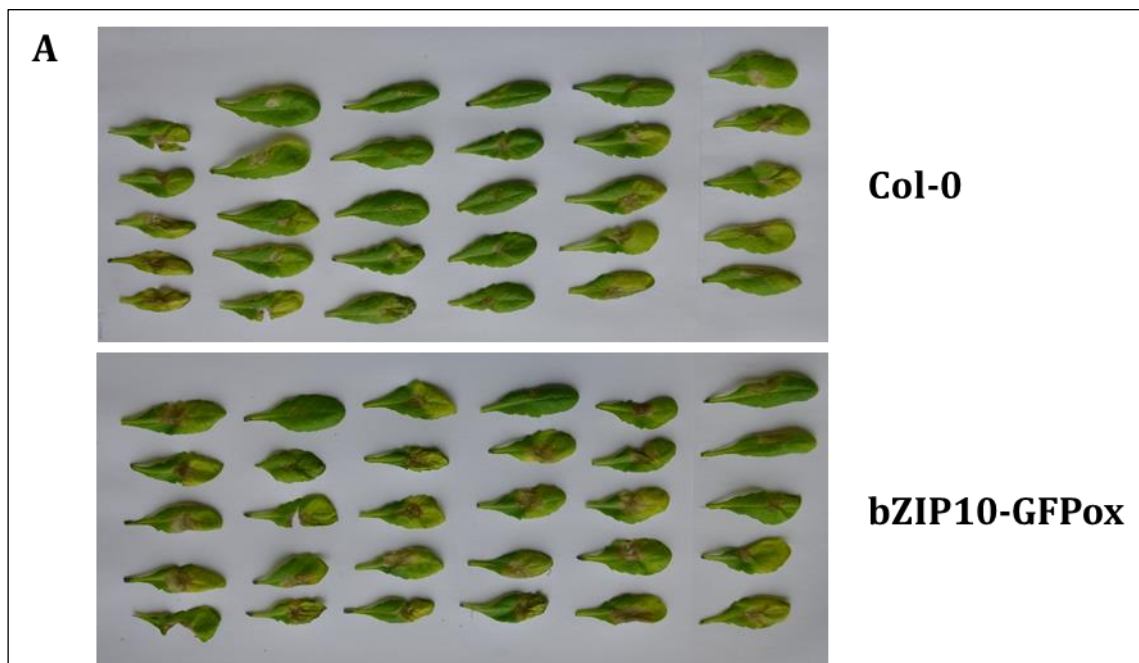


Figure 22A: Representative image showing susceptibility of bZIP10 transgenic lines to *Botrytis cinerea* infection. *Botrytis cinerea* infected leaves of 8 week-old Col-0 and bZIP10-GFPox four days post inoculation. Each column represents leaves from one plant.

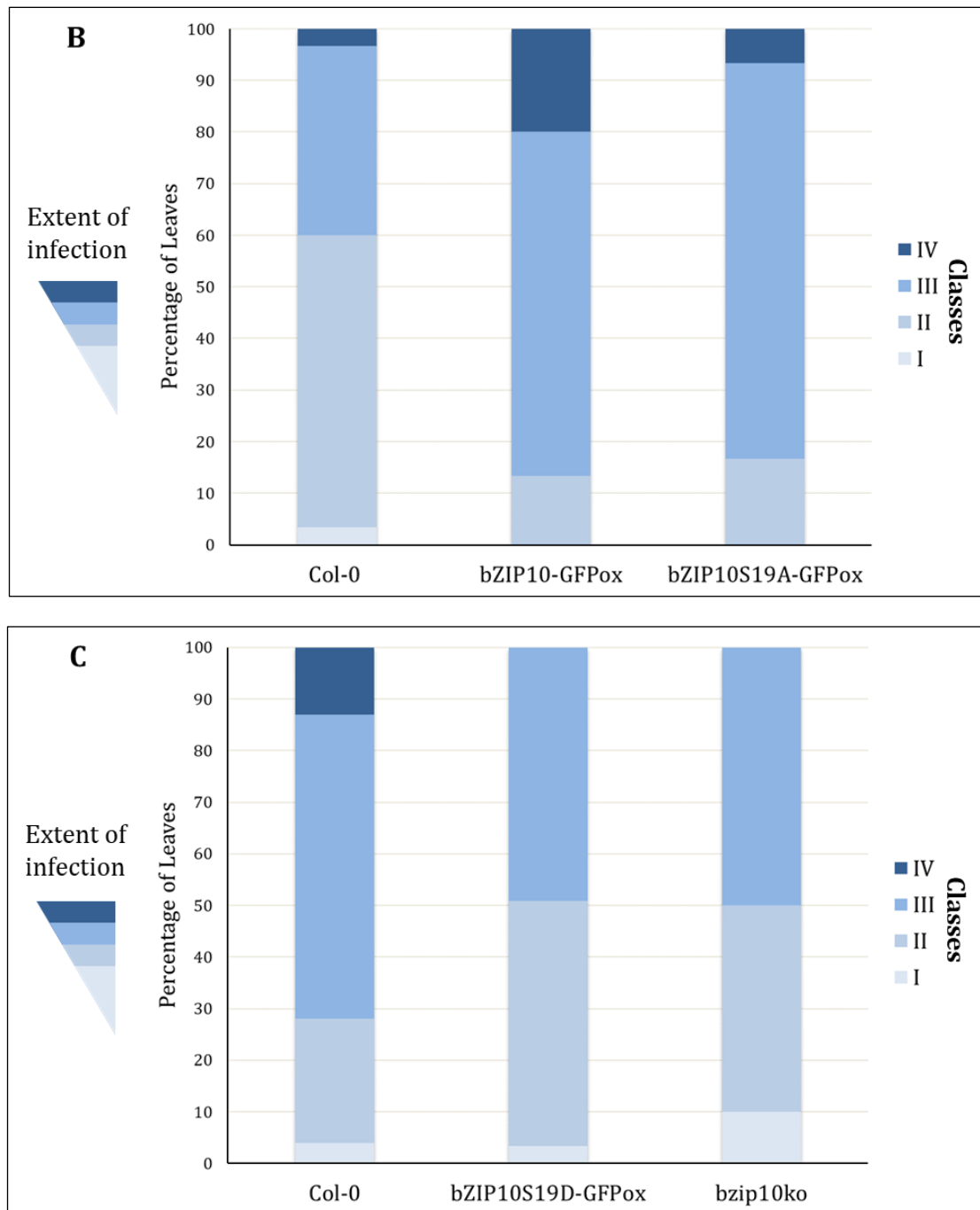


Figure 22: Representative images showing susceptibility of *bZIP10* transgenic lines to *Botrytis cinerea* infection. **(B), (C):** Representative graphs depicting the classification of plant susceptibility to the infection. The colour gradient from light to dark shows an increase in the extent of infection. Class I represents the least severity of infection while class IV represents the highest.

4.2.3. *Pseudomonas syringae* infection assay

This experiment was done in collaboration with Dr. Lorenzo Pedrotti, University of Wuerzburg, Germany. In addition to a herbivore and a necrotrophic pathogen, the effect of a hemi-biotrophic plant-pathogenic bacterium *Pseudomonas syringae* pv. *tomato* DC3000 (*Pst* DC3000) infection was tested on the above mentioned transgenic plant lines with Col-0 as a control. Biotrophic pathogens induce the salicylic acid (SA) defense pathway in plants (Pieterse, Van der Does et al. 2012). The bacteria were sprayed on the plant leaves, and then harvested after 0 day and 3 days of infection. The 0 day harvest showed that the bacteria were equally distributed among all tested lines (**Figure 23**). After 3 days of infection, bZIP10-GFPox showed higher resistance (p value ≤ 0.01) than Col-0 whereas *bzip10ko* was more susceptible (p value ≤ 0.05) to the infection. Here again, bZIP10^{S19A}-GFPox showed, similarly to bZIP10-GFPox, high resistance (p value ≤ 0.01) towards *Pst* DC3000 while bZIP10^{S19D}-GFPox showed more susceptibility (p value ≤ 0.05) when compared to Col-0 (**Figure 23**), resembling the *bzip10ko* phenotype. This assay was performed twice with similar outcome.

In conclusion, the overexpression of bZIP10-GFP or its phospho-ablative mutant form bZIP10^{S19A}-GFP caused enhanced susceptibility towards the herbivore *Mamestra brassicae* and the necrotrophic pathogen *Botrytis cinerea*, yet increased resistance towards the hemi-biotrophic pathogen *Pst* DC3000. The defense responses in *Arabidopsis thaliana* against herbivores and necrotrophs induce the jasmonic acid (JA) pathway, while the biotrophs induce the salicylic acid (SA) pathway (Pieterse, Van der Does et al. 2012). The above results suggest the involvement of bZIP10 in these responses. To determine whether bZIP10 functions upstream or downstream of SA and/or JA synthesis, the two hormones were quantified in the treated plants.

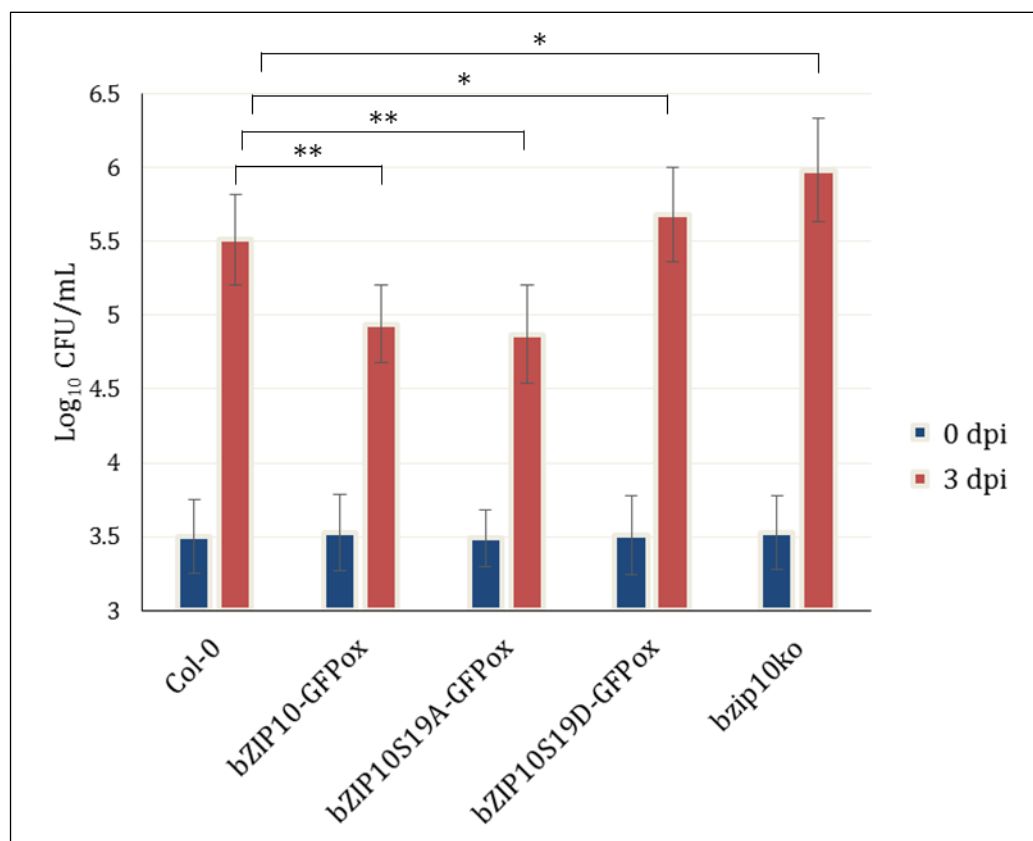


Figure 23: Susceptibility of bZIP10 transgenic lines to *Pst* DC3000 infection. The bacteria were harvested 0 days post infection (dpi) and 3 days post infection. * and ** denote a significant change (p value ≤ 0.05 and ≤ 0.01 respectively). Representative data has been depicted.

4.2.4. Hormone measurement

This experiment was done in collaboration with Dr. Joachim Kilian, Analytics, ZMBP, Tuebingen University. To investigate if bZIP10 is involved in SA or JA synthesis, Col-0, bZIP10-GFPox and *bzip10ko* lines were treated with either *Pst* DC3000 (to induce SA production) or *Botrytis cinerea* (to induce JA production), the leaves harvested and the plant hormones quantified. Upon 24h of *Pseudomonas* infection, the amount of salicylic acid in all the three lines tested was immensely higher (p value $\leq 1 \times 10^{-6}$) than in the mock treated samples. It was also observed that SA amount was higher (p value ≤ 0.05) in bZIP10-GFPox and *bzip10ko* (p value $\leq 8 \times 10^{-3}$) than in Col-0. All the three lines had similar amounts of SA in the mock treated controls (**Figure 24A**). Furthermore, there was also more (p value ≤ 0.05) production of abscisic acid (ABA) in the treated plants when compared to the mock treated samples. However, no significant differences were

seen between the different lines after infection. The amount of ABA in the three lines was similar in the mock treated controls as well (**Figure 24B**). Although bZIP10-GFPox and *bzip10ko* had higher SA levels than Col-0, there were no differences between the over-expressor and the knock out mutants of bZIP10, thus indicating that bZIP10 might not be involved in SA synthesis upon pathogen attack.

Upon 24h of *Botrytis* infection, only bZIP10-GFPox showed slightly increased (p value \leq 0.05) jasmonic acid amount when compared to the respective mock treated control. Although the difference in JA levels in Col-0 did not show a significant increase, it had the same tendency as in bZIP10-GFPox. There was no significant change in the JA amount in *bzip10ko* upon the treatment. However, the JA amount in treated *bzip10ko* was considerably lower (p value \leq 0.05) than in treated Col-0 (**Figure 25**), indicating that bZIP10 might be playing a role in the biosynthesis of JA in *Arabidopsis thaliana*. The JA levels in the mock treated controls were similar across the three genotypes.

Differences in the water content could lead to a change in the fresh weight of the leaves, which could give misleading results in the amount of hormone measured per gram of fresh weight. Therefore, the water content of the leaves was determined. In both these assays, the water content of the leaves was very similar.

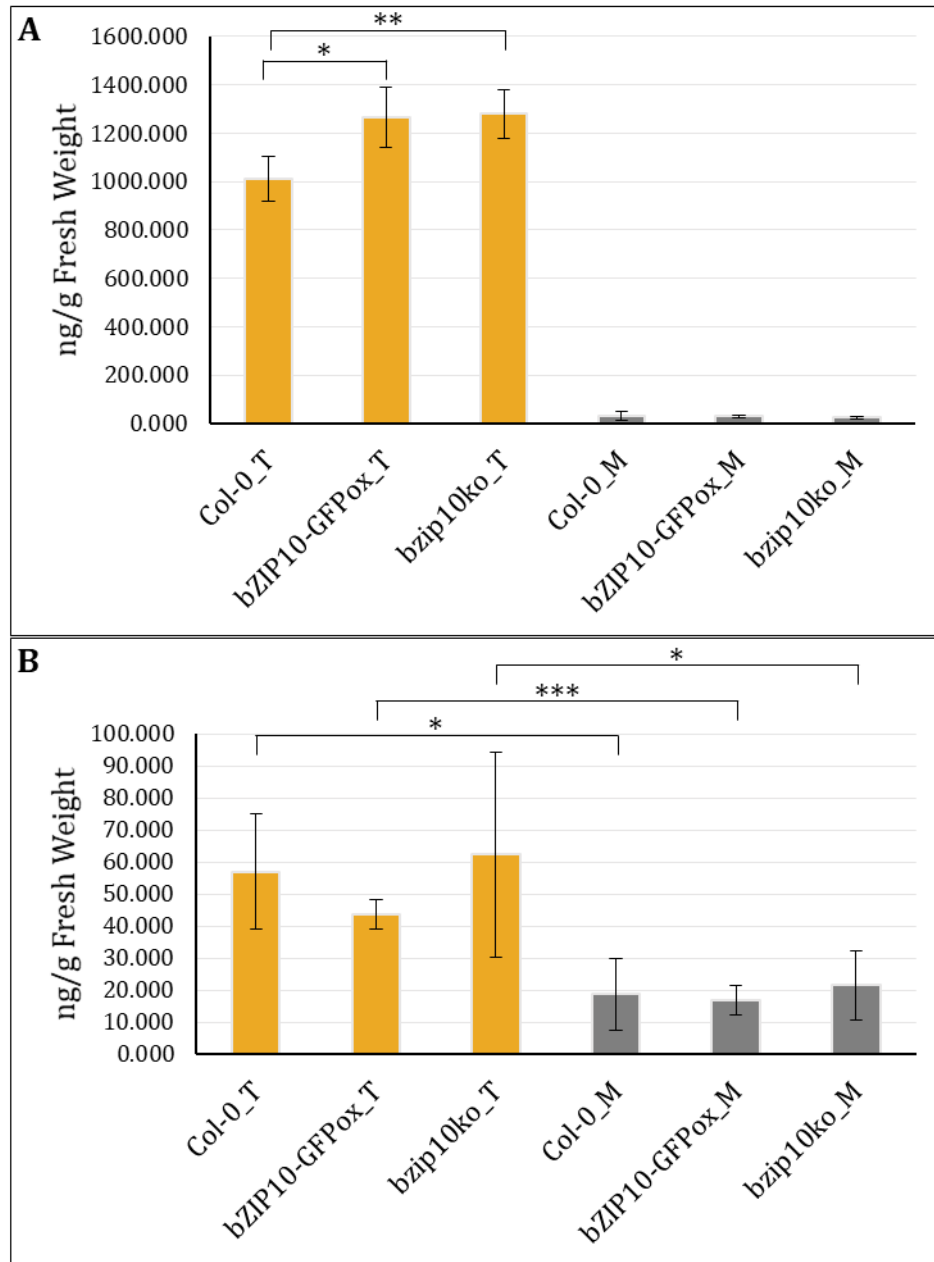


Figure 24: Hormone levels in bZIP10 transgenic lines upon after 24h Pst DC3000 infection; **(A)** Salicylic acid, **(B)** Absciscic acid. *, ** and *** denote a significant change (p value ≤ 0.05 , p value ≤ 0.01 and p value ≤ 0.0005 respectively). T: treated with Pst DC3000, M: mock treatment.

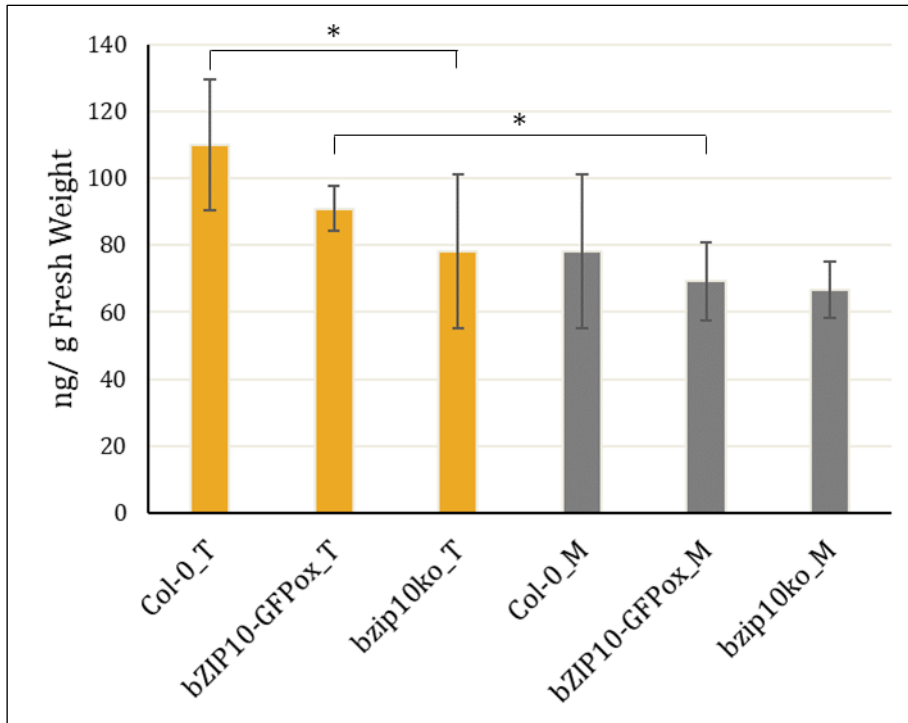


Figure 25: Jasmonic acid level in *bZIP10* transgenic lines upon 24h of *Botrytis cinerea* infection. * denotes a significant change (p value ≤ 0.05). T: treated with *Botrytis cinerea*, M: mock treatment.

4.2.5. Effect of SA on *bZIP10* transactivity

The mutant *bZIP10*^{S19D}-GFPox showed, similarly to *bzip10ko*, an antagonistic phenotype to the *bZIP10*-GFPox in *Pst* DC3000 pathogen assay (section 4.2.3.). However, the SA amount in *bZIP10*-GFPox and *bzip10ko* were comparable, independent of the infection. This might be indicative of increased responsiveness of *bZIP10*-GFPox lines to SA, and of its involvement in the SA signaling upon *Pst* DC3000 infection.

To investigate the effect of a biotrophic pathogen attack on *bZIP10* transactivation, the *Arabidopsis* leaf mesophyll protoplasts were treated with SA to mimic a biotrophic pathogen attack and the transactivation capacity of *bZIP10* analyzed. If not stated otherwise, the protoplasts prepared from *bzip10ko* line were used in all further experiments. At first, the appropriate concentration of SA to be used was determined. For this, *bZIP10* was co-transfected with *bZIP53*, *pProDH1::GUS* and the *35S::NAN* reporter (used for normalization) (Kirby and Kavanagh 2002) in the protoplasts and then treated with varying amounts of SA. When compared to the untreated control, the NAN activity

started to decrease with 75 μM SA, with 150 μM and 300 μM SA treatments exhibiting only about 30% and 15% activity respectively, indicating that these concentrations were lethal to the protoplasts. The NAN activity upon 100 μM SA treatment was comparable to that of 75 μM SA treatment (**Figure 26A**). The transactivation of bZIP10/bZIP53 heterodimers strongly increased upon 100 μM SA, as compared to the untreated protoplasts, and then started to decrease indicating that this effect may be due to the toxic effect of high SA concentration. Because 100 μM SA showed the largest change in reporter gene activity without killing the protoplasts (**Figure 26B**), this SA concentration was used for the treatment of the protoplasts.

Then, the influence of SA on the ability of bZIP10 and its mutated forms to activate the *ProDH1* promoter was analyzed. Either bZIP10-GFP or one of its Ser19 mutants was co-transfected with bZIP53-mCherry and *pProDH1::GUS* in the protoplasts. Upon treatment with SA, there was a strong increase (p value ≤ 0.05) in *pProDH1* transactivation by the heterodimers of bZIP10/bZIP53 and especially bZIP10^{S19A}/bZIP53, whereas the heterodimers of bZIP10^{S19D}/bZIP53 showed only a slight increase (p value ≤ 0.05), when compared to their respective mock treated controls (**Figure 27**). The SA-induced increase of *ProDH1::GUS* expression is bZIP-dependent since no increase was detected in the protoplasts transfected with *pProDH1::GUS* alone. These results indicated that in spite of the responsiveness of bZIP10 to SA, the Ser19 in the DBD did not seem to be involved in the regulation of this response.

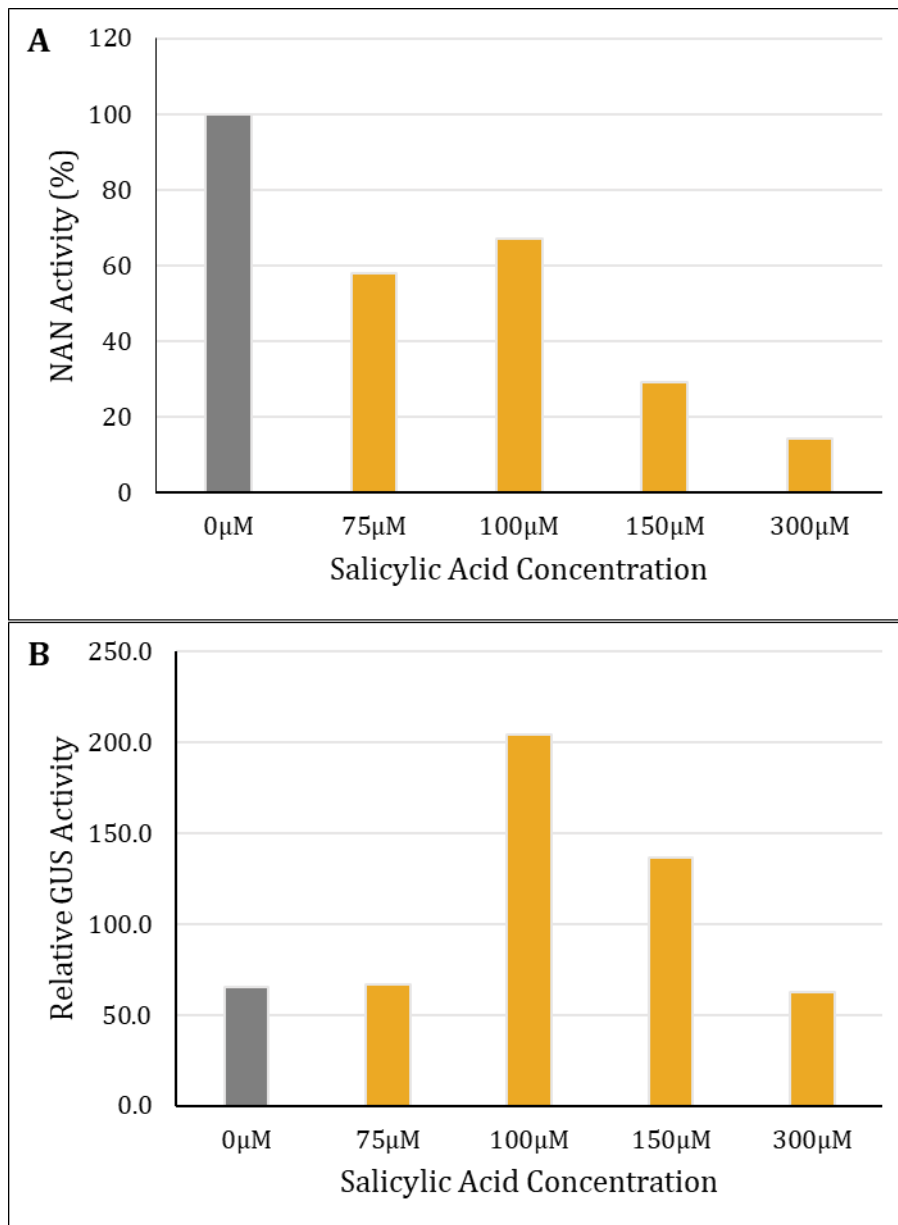


Figure 26: Reporter gene analysis in the protoplasts treated with SA. The *Arabidopsis thaliana* leaf mesophyll protoplasts prepared from *bzip10ko* line were transfected with *pProDH::GUS*, *bZIP10-GFP*, *bZIP53-mCherry* and *35S::NAN* and treated 6 h after transfection with different concentrations of SA. **(A)** Relative NAN activity **(B)** Relative GUS activity.

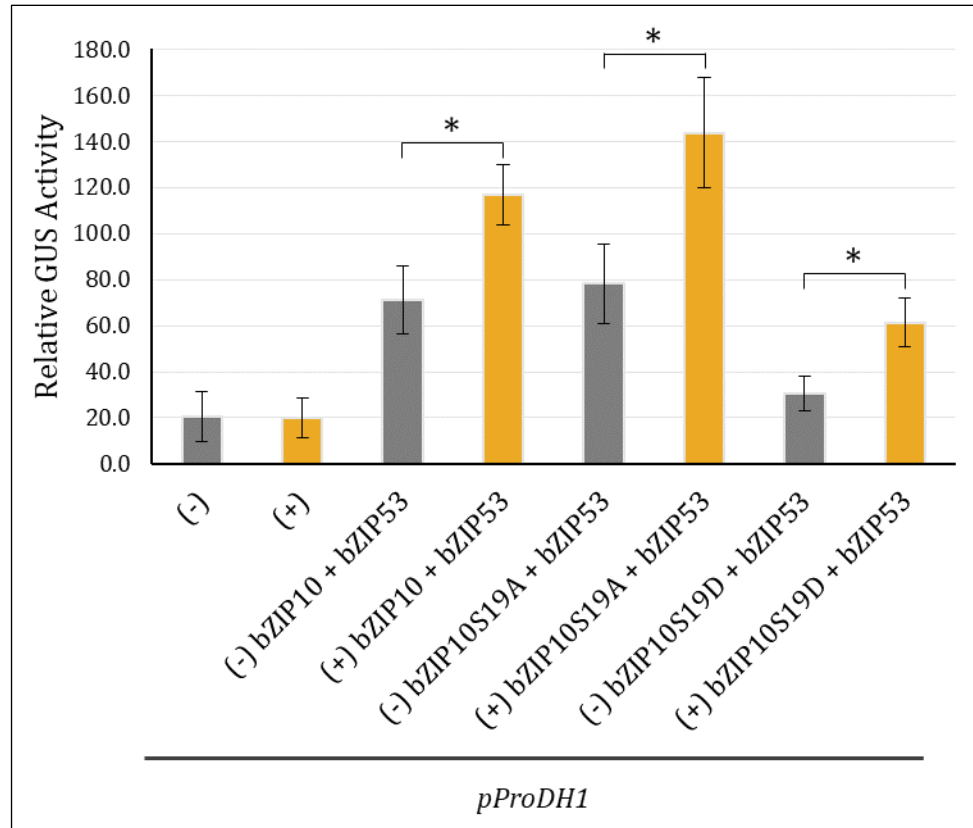


Figure 27: Relative GUS expression driven by pProDH1 promoter either alone or in the presence of bZIP10 or one of its Ser mutants and bZIP53, in *Arabidopsis thaliana* leaf mesophyll protoplasts prepared from *bzip10ko* line. The (+) denotes addition of 100 μ M salicylic acid and the (-) denotes mock treated control 6 h after transfection. * denotes a significant change (p value ≤ 0.05). Statistical analysis was performed on three biological repeats.

4.2.6. Effect of SA on bZIP10-dependent root growth

Next, it was investigated if bZIP10 responds to SA specifically upon pathogen attack or if it is involved in more general response to SA, by performing a root growth assay on *Arabidopsis thaliana* seedlings upon exogenous SA treatment. Seedlings of Col-0, bZIP10-GFPox and *bzip10ko* were grown on a solid agar media containing 50 μ M SA and the roots measured using ImageJ. Under control conditions, there were no differences in the root growth among the three lines (**Figure 28A,B**). After one week, root growth of all the lines grown on media containing SA was drastically reduced as compared to the respective control plants. However, root growth of all the three lines was similar in the presence of SA (**Figure 28A**). After two weeks, while *bzip10ko* showed root growth similar to Col-0, bZIP10-GFPox exhibited slightly longer roots than Col-0 in the control plants. Upon SA

treatment, root growth in all the three lines was highly inhibited (~ 61-65 % inhibition) as compared to the respective control plants, but in bZIP10-GFPox this inhibition was slightly weaker than in Col-0 and *bZIP10ko* (**Figure 28B**). It was not possible to measure the root length after three weeks because the roots outgrew the square petri plate. These results indicated that the responsiveness of bZIP10 to SA might not be limited to pathogen defense only.

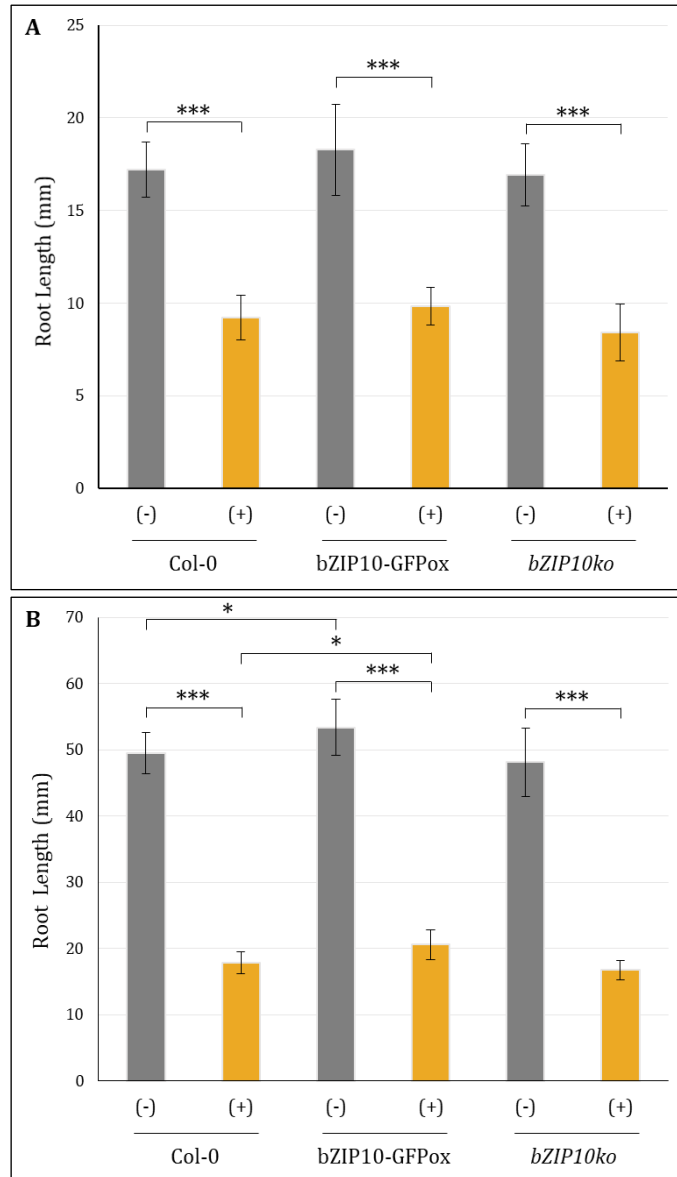


Figure 28: Root length measurements of *Arabidopsis thaliana* seedlings grown on solid media in the presence (+) or absence (-) of 50 μ M salicylic acid after **(A)** 1 week and **(B)** 2 weeks. * and *** denote a significant change (p value ≤ 0.05 and ≤ 0.005 respectively). Statistical analysis was performed on five biological repeats.

Earlier reports have shown that SA can modulate the redox status of a cell leading to the reduction of intermolecular disulfide bonds of NPR1 and intramolecular disulfide bonds of TGA1 and TGA4 transcription factors which is indispensable for the expression of defense genes (Despres, Chubak et al. 2003, Tada, Spoel et al. 2008). Also, the DNA binding of G-group bZIPs in *Arabidopsis thaliana* have been shown, *in vitro*, to be dependent on redox regulation of Cys residues (Shaikhali, Noren et al. 2012). Thus, plant bZIPs may act as sensor molecules receptive to cellular redox changes and regulate the expression of downstream target genes. In lieu of this and due to the fact that bZIP10 harbors three Cys residues in its amino acid sequence, we hypothesized that those Cys residues could play a role in the redox regulation of bZIP10. This hypothesis was tested in the further experiments.

4.3. Redox regulation of bZIP10

Sulfur containing amino acids, cysteine (Cys) and methionine, are known to be most easily oxidized (Bigelow and Squier 2011, Navrot, Finnie et al. 2011), and these amino acids can be reversibly oxidized inducing changes in the structure of protein, which can subsequently result in protein function modulation (Spadaro, Yun et al. 2010, Nagahara 2011). Although Cys sulfhydryls are generally known to be very reactive, it is their positional environment which actually controls their rate of oxidation, as well as its further impact on protein structure (Kim and Stites 2004). There are three Cys residues in the amino acid sequence of bZIP10, two towards the N-terminus (Cys102 and Cys130) and one towards the C-terminus (Cys409) (**Figure 3**). The *in silico* analysis of intrinsic disordered amino acids in bZIP10 using the PONDR-FIT algorithm (Xue, Dunbrack et al. 2010) revealed that the residues Cys102 and Cys409 are positioned in putatively disordered amino acid stretches (**Supplementary File 1**), which might be a pre-requisite for their accessibility for redox-dependent modification.

An N-terminal stretch of amino acids containing Cys130 in bZIP10 was found to be conserved throughout the eudicot plants. Although the eudicot C-group bZIPs form a different cluster when compared to their monocot counterparts (Nijhawan, Jain et al. 2008), Cys residue corresponding to the position 130 in bZIP10 from *Arabidopsis* was also found in rice bZIP ortholog. Furthermore, the amino acid sequence alignment of bZIP10 with the amino acid sequences of bZIPs from the moss *Physcomitrella patens* revealed the conservation of Cys at position 130 before the divergence of bryophytes and vascular plants (**Supplementary File 2**). Conservation of this cysteine residue across multiple plant lineages highlights the functional importance of this Cys residue and indicates that it might play an essential role in the plant molecular network.

Thus, the three Cys residues in bZIP10 were analyzed in further experiments for their involvement and importance in regulating bZIP10 activity upon oxidative stress.

4.3.1. MS-based proteomics analysis of bZIP10

4.3.1.1. Redox state analysis of bZIP10 cysteine residues.

All proteomics analyses were done in collaboration with the Proteome Centre Tuebingen (PCT), University of Tuebingen, Germany. To investigate if the Cys residues in bZIP10 were redox regulated, C-terminal GFP tagged bZIP10 was pulled down in the presence of NEM (N-ethylmaleimide) from bZIP10-GFPox transgenic lines of *Arabidopsis thaliana*. NEM can bind irreversibly to a reduced Cys residue in a protein, thereby preventing it from getting oxidized and can be easily identified on the mass spectrometer. Prior to mass spectrometry analysis the protein was reduced with DTT followed by irreversible carbamidomethylation of sulfhydryl groups with iodoacetamide. Therefore, a Cys residue labeled with NEM would indicate an *in vivo* reduced state of that Cys, and an absence of NEM (and correspondingly presence of carbamidomethyl group) would imply that it was oxidized.

To begin with, it was checked if NEM is indeed able to prevent proteins from getting oxidized using western blotting. Since intramolecular bonds make the protein structure more compact, the electrophoretic mobility of disulfide-containing protein is often higher than the mobility of the reduced one. Total cellular proteins were extracted from the leaves of bZIP10-GFPox plants in a denaturing buffer with DTT or without DTT and in the presence or absence of NEM. H₂O₂ was added to the denatured proteins to oxidize them. The proteins were then loaded on a polyacrylamide gel followed by western blotting using anti-GFP antibody. As can be seen in the **Figure 29**, under non-reducing conditions (i.e., lack of DTT) and in the absence of NEM, the lowest molecular weight protein band (highlighted in the dotted box, most probably free GFP) occurs as a single band which is most probably oxidized due to H₂O₂, while in the presence of NEM, two bands are visible for this protein. This could be the result of NEM blocking the reduced thiol groups of Cys residues due to which they could not be further oxidized by H₂O₂, and thus appearing as two bands, reduced and oxidized. Because H₂O₂ was added to the denatured protein, all Cys residues should have been exposed for oxidation by H₂O₂. Only a single band (reduced by DTT) of this protein is seen under the reducing conditions

(**Figure 29**). Similar in-gel band shifts under H_2O_2 treatment (**Figure 29**, shown with arrows) are also observed for bigger proteins in the absence of NEM. Instead, the resolution pattern of NEM-treated extract is more similar to the extract containing DTT. This demonstrated that labeling of Cys residues with NEM was successful.

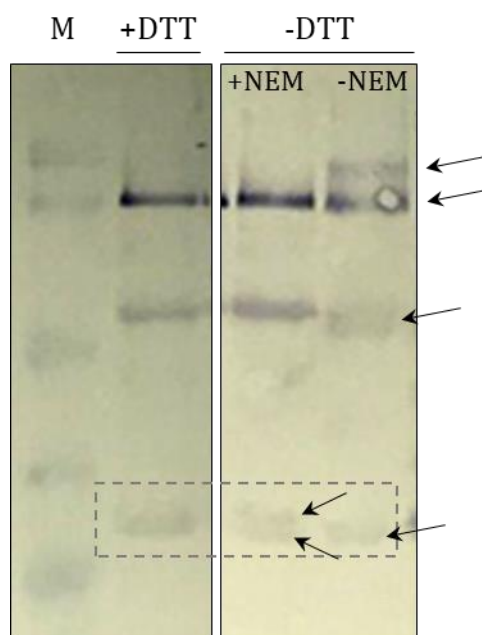


Figure 29: Western blot image of immunoprecipitated bZIP10 extracted under reducing (+DTT) and non-reducing conditions (-DTT) in the presence (+NEM) or absence (-NEM) of NEM. H_2O_2 was added to the protein extract prior to the gel loading.

Several pull-down experiments were performed, and the presence of immunoprecipitated GFP-tagged bZIP10 from each of the above-mentioned experiments was verified by western blot analysis (**Figure 30**). All proteins were submitted to the proteomics facility post pull-down, where they were briefly separated on a NuPAGE® Bis-Tris 4-12 % gradient polyacrylamide gel. This was then followed by in-gel digestion with trypsin and subsequent elution of the peptides from the gel. The samples were finally analyzed on the QExactive HF MS instrument (Thermo Fisher). The MS data was then analyzed for the presence of NEM labeled and NEM-unlabeled peptides.

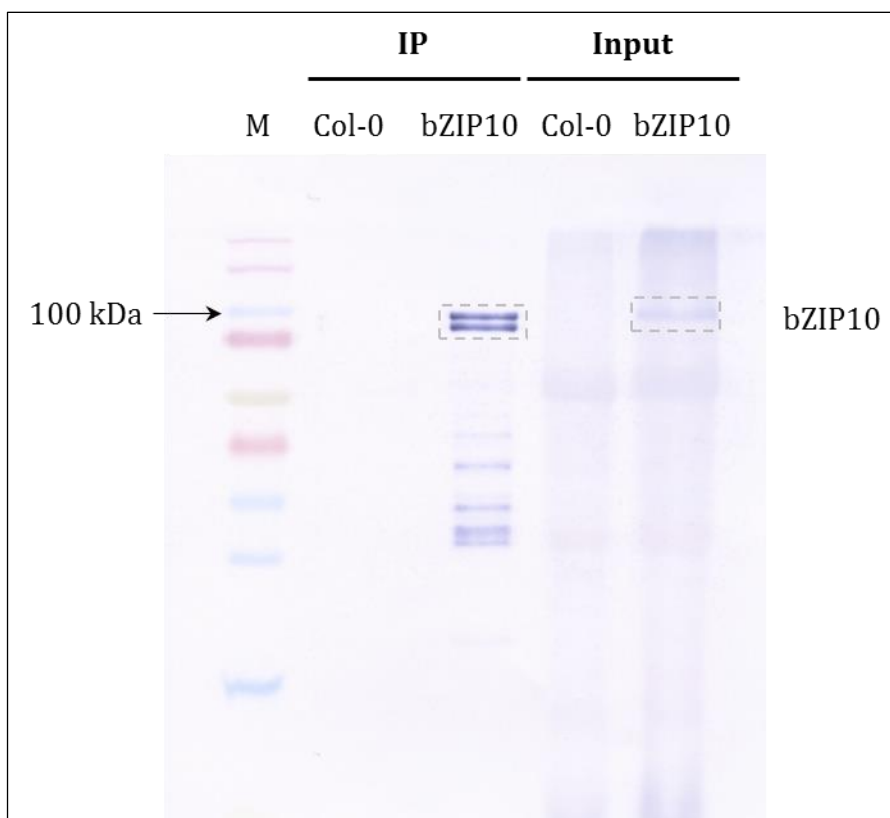


Figure 30: Representative example of the verification of the presence of an immunoprecipitated GFP tagged bZIP10 by western blot analysis (antibody: α -GFP). IP refers to the immunoprecipitated samples whereas Input refers to the same samples pre-IP.

At first, several pull-downs were performed with the leaf material harvested at two different time-points (morning and evening) to investigate if there is a difference in the reduced/oxidized state of Cys residues in bZIP10 depending on time of the day. A pool of NEM labeled and NEM-unlabeled peptides was found for the sites Cys102 and Cys130. Irrespectively of the harvesting time, in all the pull-downs the intensity peaks for NEM-unlabeled Cys102 and Cys 130 were much higher than for the NEM-labeled, what was interpreted as predominantly oxidized state of these residues *in vivo* (**Figure 31**). In contrast, the Cys409 was only identified as the NEM labeled form in these pull-downs. Due to a high frequency of Lys (K)/ Arg (R) residues (recognition sites for trypsin) around Cys409, the peptide containing this residue could be identified only upon missed cleavage. This was most probably the reason why its identification was not always successful. This is supported by the fact that these peptides were identified with an intensity value of zero, which points towards their low abundance in the respective

samples.

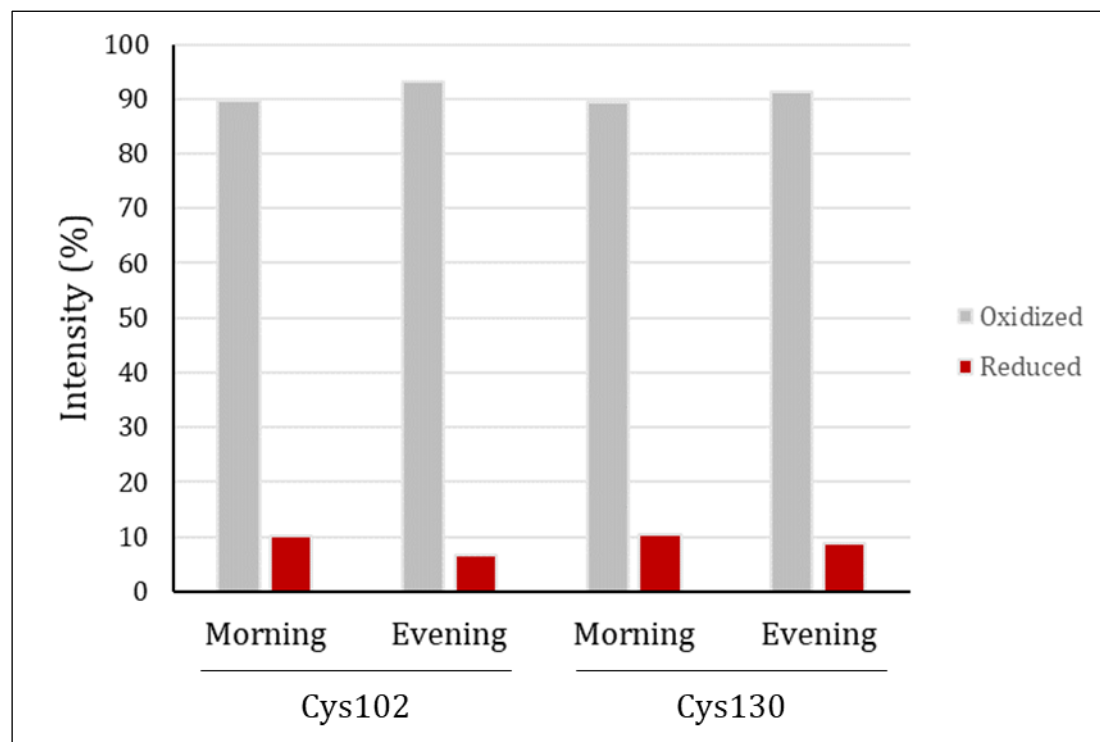


Figure 31: Representative plot depicting the relative intensities of bZIP10 peptides containing oxidized and reduced Cys residues, immunoprecipitated from bZIP10-GFPox leaf samples harvested in the morning or in the evening.

To analyze the possible effect of SA on the redox state of Cys residues, the bZIP10-GFP protein was pulled-down from the plants sprayed with 100 μ M SA for 5 h. A pool of NEM labeled and NEM-unlabeled peptides was found for the sites Cys102 and Cys130 upon SA treatment as well. As in the control conditions, the residue Cys130 was mostly found to be oxidized. The residue Cys102, however, exhibited an increase in its reduced state compared to the control conditions (**Figure 32**). Cys409 was not identified in this experiment most probably because of the reason mentioned above.

The **Table 1** lists all Cys-containing peptides identified by the proteomics analysis of bZIP10. All identified peptides (NEM-labeled and unlabeled) have a high Andromeda score and a good posterior error probability value. As negative controls, either Col-0 or plants overexpressing GFP protein driven by 35S promoter (eGFPox, Wachter et al., unpublished) were used.

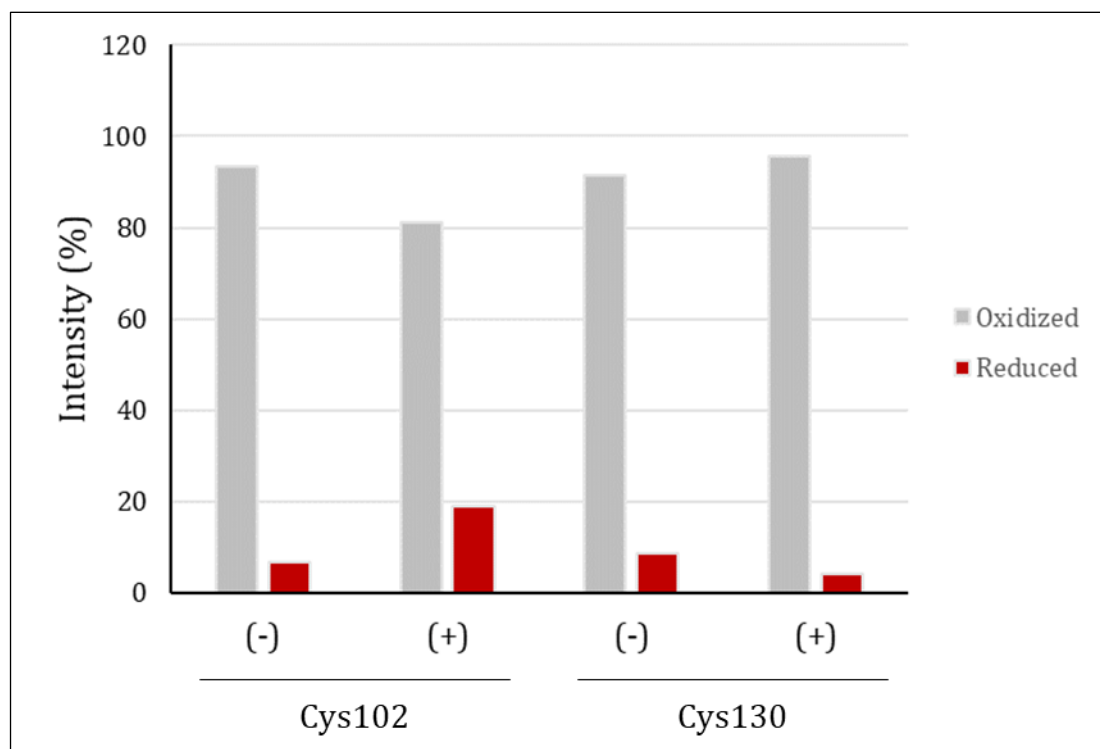


Figure 32: Column graph depicting the relative intensities of bZIP10 peptides containing oxidized and reduced Cys residues, immunoprecipitated from bZIP10-GFPox leaf samples harvested with (+) or without (-) 100 μ M salicylic acid treatment.

Table 1: Identified Cys-containing bZIP10 peptides

PEP	Score	Position	NEM-Modified	Peptide Sequence	Intensity Col-0	Intensity bZIP10 - GFPox (9AM)	Intensity bZIP10 - GFPox (4PM)
Control conditions							
7.56E-04	120.62	C409	Yes	C(NEM)VDKGGR	0	0	0
1.27E-04	99.069	C102	Yes	DSGNLDC(NEM)AAPMTTK	0	4.80E+07	2.24E+07
6.97E-21	180.95	C102	No	DSGNLDCAAPMTTK	0	2.61E+08	1.76E+08
1.15E-16	176.87	C130	Yes	LETEC(NEM)ATVVSLR	0	1.20E+07	2.72E+06
6.47E-06	128.85	C130	No	LETECATVVSLR	0	1.12E+08	4.81E+07

Table 1 continued

PEP	Score	Position	NEM-Modified	Peptide Sequence	Intensity eGFPox	Intensity eGFPox + SA	Intensity bZIP10 – GFPox + SA
SA treatment							
1.16E-05	162.1	102	Yes	DSGNLDC(NEM)AAPMTTK	0	0	4.47E+07
1.06E-03	76.156	102	No	DSGNLDCAAPMTTK	0	0	2.71E+08
2.77E-24	174.59	130	Yes	NKLETEC(NEM)ATVVSLR	0	0	8.09E+06
4.81E-05	98.676	130	No	NKLETECATVVSLR	0	0	1.52E+08

4.3.1.2. Post-translational modifications of bZIP10

To further characterize bZIP10, and to understand its possible post-translational regulation, the bZIP10 peptides were also checked for the presence of modifications such as phosphorylation or acetylation in the pull-down experiments described above.

Additionally, bZIP10 pull-down after *Botrytis cinerea* infection (24 hours) was included in this analysis because the phospho-mimicking, dominant negative mutant line bZIP10^{S19D}-GFPox showed resistance against the pathogen as compared to Col-0, while bZIP10-GFPox was more susceptible than Col-0 in *Botrytis* pathogen assay (see section 4.2.2.). Because the DBD of bZIP10 is rich in Arg (R) residues, LysC was chosen as the endoprotease in order to generate peptides of bZIP10 DBD.

The proteomics analysis revealed possible sites of phosphorylation and acetylation on bZIP10. **Table 2** lists the identified modified peptides. All phosphorylation and acetylation events were, however, only identified under control conditions, with an exception to Ser373. The residue Ser373 was additionally identified to be phosphorylated upon salicylic acid treatment. Upon *Botrytis* treatment, the DBD peptide of bZIP10 harboring the Ser19 residue, and thus any phosphorylation or acetylation event on it, could not be identified in the MS run. One small drawback of the shotgun proteomics methodology is that, based on the chemical composition of the peptides, not

all of them ionize and fly well in the mass spectrometer. All identified modified peptides had a high Andromeda score and a good posterior error probability value.

Table 2: Identified post-translationally modified peptides by proteomics

PEP	Score	Position	Localization Probability	Modified Peptide Sequence
PHOSPHO (STY) SITES				
1.71E-03	59.339	372	0.306	LGNNFAAPPSQTS(p)SPLQR
1.71E-03	59.339	373	0.564	LGNNFAAPPSQTSS(p)PLQR
1.71E-03	59.339	371	0.306	LGNNFAAPPSQT(p)SSPLQR
ACETYL (K) SITES				
2.99E-08	129.01	185	1.000	TGVSMK(ack)QVTSGSSR

4.3.2. Effect of oxidative stress on bZIP10 activity

The presence of NEM labeled and unlabeled Cys102 and Cys130 meant that there was a pool of bZIP10 molecules with either reduced or oxidized Cys102 and Cys130. The Cys residues getting reduced/oxidized indicate that these Cys residues might be playing a role in bZIP10 redox regulation. This hypothesis was further tested in the following experiments. The residue Cys409 was included in the analysis as well.

To test the transactivation capacity of bZIP10, two transient gene expression systems were tested: tobacco leaf cells and *Arabidopsis* leaf mesophyll protoplasts. It had been shown earlier that transient gene expression in tobacco leaves could be used for reporter gene studies (Wachter, Tunc-Ozdemir et al. 2007). All the constructs generated were successfully expressed in tobacco leaves; however, the outcome of the assay was not reproducible (**Supplementary Figure 1**). For the quantitative reporter gene assay to work properly, it is important that all the constructs are expressed in the same cell. Because this was not always the case in the tobacco system, it could have led to the

irreproducibility of the results of experimental repeats. Therefore, only the *Arabidopsis* leaf mesophyll protoplasts transformation system was used.

To examine if the oxidation of Cys residues in bZIP10 plays a role in its ROS-dependent regulation, three mutants of bZIP10 were used where either one, two or all the three Cys residues were substituted with Ala, namely, bZIP10^{C409A}, bZIP10^{C102,130A} and bZIP10^{C102,130,409A}, respectively.

For this experiment, the wild-type bZIP10 and its Cys mutants fused to HA-tag (*35S::HA-bZIP10*), and bZIP53 fused to GFP (*UBQ10::bZIP53-GFP*) were used. The residue Cys409 is towards the very end of C-terminus in a putative disordered amino acid region in bZIP10. We thought that big tags such as GFP at the C-terminus of bZIP10 might influence the conformation of this region containing Cys409. Furthermore, the N-terminus of bZIP10 has the XPO1 interaction site. Taking this into consideration, we decided to use a smaller tag towards the N-terminus of bZIP10 in order to avoid any specific conformational changes in bZIP10. The protoplasts were treated with H₂O₂ to induce oxidative stress in the cells. To begin with, the different H₂O₂ amounts were tested in order to determine the concentration of H₂O₂ to be used. bZIP10-HA was co-transfected with bZIP53-GFP, *pProDH1::GUS* and the *NAN* reporter (used for normalization) (Kirby and Kavanagh 2002) in the protoplasts and then treated with varying amounts of H₂O₂. As can be seen in the **Figure 33**, when compared to untreated control, the *NAN* activity started to decrease (**Figure 33A**) with 0.125 mM H₂O₂ but the *GUS* activity only changed after 0.25 mM H₂O₂ treatment (**Figure 33B**). The concentrations 0.4 mM and 0.5 mM turned out to be mostly lethal to the cells as seen from the *NAN* activity (**Figure 33A**). Hence, 0.3 mM H₂O₂ was chosen for treatment of the protoplasts.

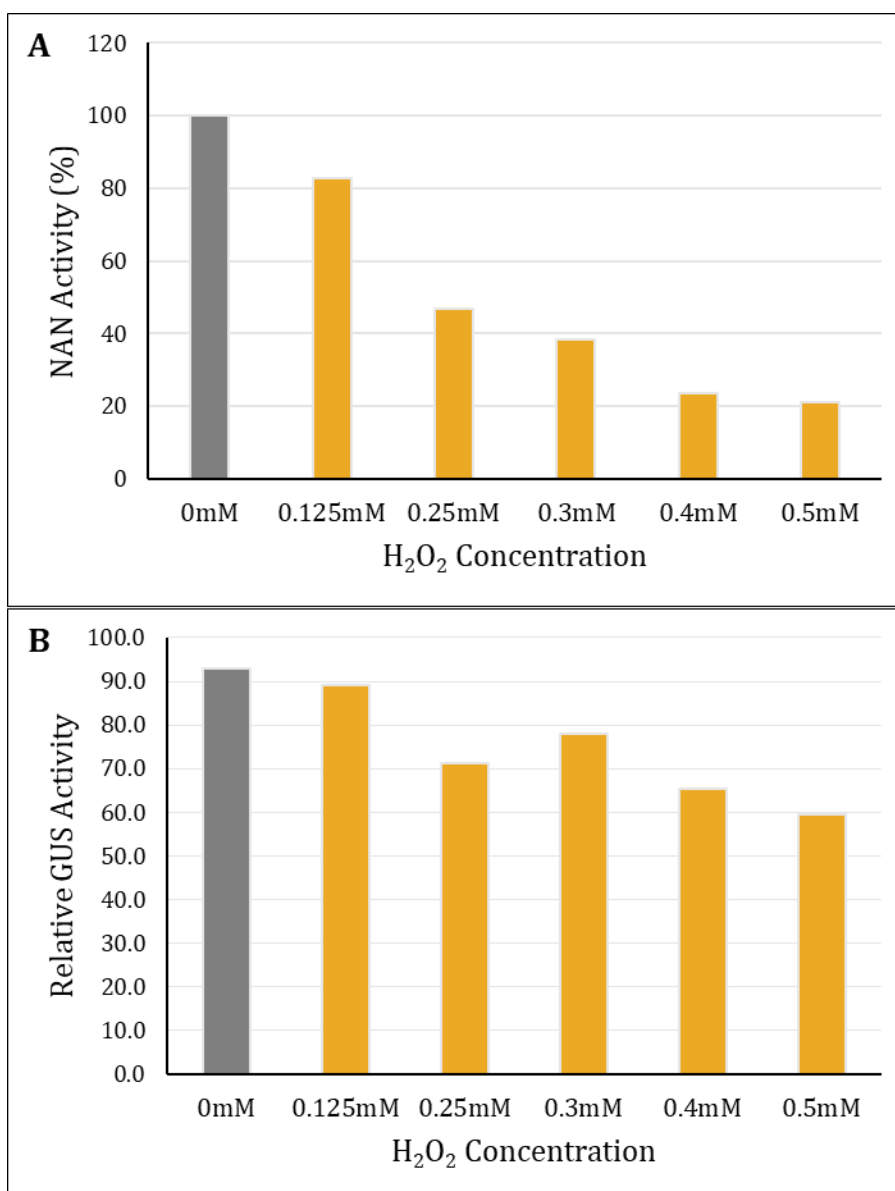


Figure 33: Reporter gene analysis in the protoplasts treated with H₂O₂. The *Arabidopsis thaliana* leaf mesophyll protoplasts prepared from *bzip10ko* line were transfected with *pProDH1::GUS*, *HA-bZIP10*, *bZIP53-mCherry* and *35S::NAN* and treated 6 h after transfection with different concentrations of H₂O₂. **(A)** Relative NAN activity **(B)** Relative GUS activity.

Upon co-transfection of either bZIP10 or one of its Cys mutants (bZIP10^{C409A}, bZIP10^{C102,130A} and bZIP10^{C102,130,409A}) with bZIP53 and *pProDH1::GUS* in the protoplasts, a synergistic activation of *pProDH1* was observed. The single Cys mutant bZIP10^{C409A} and the double Cys mutant bZIP10^{C102,130A} behaved similarly to the wild-type protein. However, there was a small decrease (p value: 1x10⁻⁵) in the transactivation capacity of

the triple Cys mutant bZIP10^{C102,130,409A} when compared to the wild-type bZIP10 (**Figure 34**).

Upon treatment with H₂O₂, bZIP10 showed a slight decrease (p value ≤ 0.05) in its transactivation capacity as compared to the mock treatment. On the contrary, the triple Cys mutant showed a minor increase (p value: 2x10⁻⁴) in the transactivation. The single and the double Cys mutant showed no significant change upon H₂O₂ treatment when compared to their respective mock treated control (**Figure 34**).

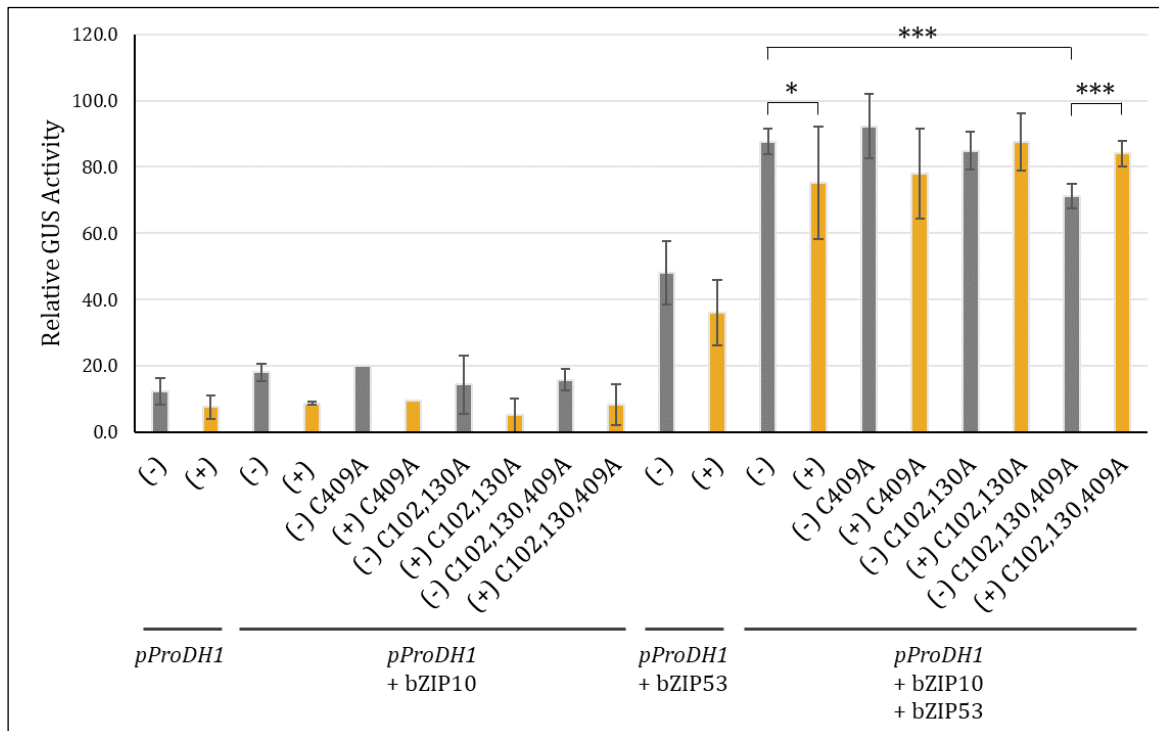


Figure 34: Relative GUS expression driven by pProDH1 promoter either alone or in the presence of bZIP10 or one of its Cys mutants and/or bZIP53, in *Arabidopsis thaliana* leaf mesophyll protoplasts prepared from *bzip10ko* line. The (+) denotes addition of 0.3 mM H₂O₂ and the (-) denotes mock treated control. The treatment was done 6 h after transfection. * and *** denote a significant change (p value ≤ 0.05 and ≤0.005 respectively). Statistical analysis was performed on at least four biological repeats.

4.3.3. Effect of oxidative stress on bZIP10 heterodimerization

Furthermore, the involvement of the Cys residues of bZIP10 in regulation of its heterodimer formation was analyzed by protoplast 2-hybrid. The wild-type bZIP10 and its Cys mutants, viz., bZIP10^{C409A}, bZIP10^{C102,130A} and bZIP10^{C102,130,409A} fused to the GAL4

Activation domain (AD) and the interaction partner bZIP53 fused to the GAL4 DNA-binding domain (BD) were used in this experiment. Either bZIP10 or one of its Cys mutants was co-transfected with bZIP53 and *GAL4-UAS::GUS* in *Arabidopsis* leaf mesophyll protoplasts. As can be seen in the **Figure 35**, none of the three Cys mutant versions of bZIP10 showed a significant difference in the heterodimerization capacity with bZIP53 when compared to wild-type bZIP10.

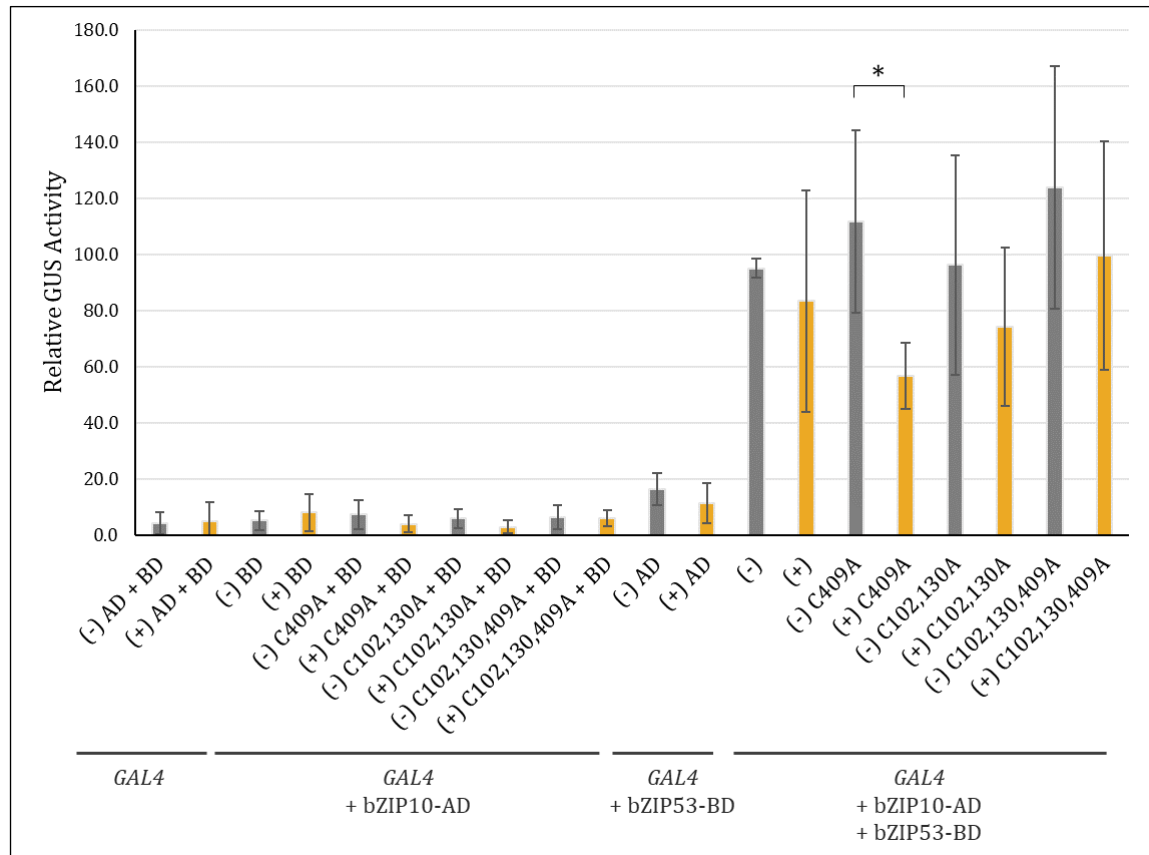


Figure 35: Relative GUS expression driven by GAL4 promoter either alone or in the presence of bZIP10-AD or one of its Cys mutants and/or bZIP53-BD, in *Arabidopsis thaliana* leaf mesophyll protoplasts prepared from *bzip10ko* line. AD and BD wherever mentioned alone in the graph (bar number 1-12 from left) are the empty vector negative controls. The (+) denotes addition of 0.3 mM H₂O₂ and the (-) denotes mock treated control. * denotes a significant change (p value ≤ 0.05). Statistical analysis was performed on at least five biological repeats.

Upon treatment with H₂O₂, the single Cys mutant bZIP10^{C409A} showed a decrease (p value $\leq 2 \times 10^{-2}$) in the heterodimer formation with bZIP53 in comparison to its respective mock treatment. The wild-type bZIP10, the double Cys mutant bZIP10^{C102,130A} and the triple Cys mutant bZIP10^{C102,130,409A} did not show any significant difference in the heterodimer

formation with bZIP53 when compared to their respective mock treatments. Besides normalization to the NAN signal, the overall GUS expression differed drastically from experiment to experiment. This obscured the identification of statistically significant differences between the heterodimers of wild-type bZIP10 and bZIP10^{C102,130,409A}. Nevertheless, in all the experiments, heterodimerization capacity of bZIP10^{C102,130,409A} after treatment was reduced as compared to its mock treated control. Therefore, although unexpected, the effect of H₂O₂ on the transactivation capacity of the heterodimers and on the heterodimerization itself was not similar.

4.3.4. Effect of oxidative stress on sub-cellular localization of bZIP10

The triple Cys mutant of bZIP10 behaved differently than the wild-type bZIP10 in the transactivation assay under oxidative stress, indicating that Cys residues might be important for functioning of bZIP10. In lieu of this, the triple Cys mutant of bZIP10 was further examined for its sub-cellular localization.

For the sub-cellular localization analysis, bZIP10 and its triple Cys mutant, bZIP10^{C102,130,409A}, fused to GFP at their C-termini were transfected in *Arabidopsis* leaf mesophyll protoplasts. In agreement with an earlier report (Kaminaka, Nake et al. 2006) and our data (see **Figure 14**), bZIP10 localized to the nucleus with a weak cytoplasmic signal (Kaminaka, Nake et al. 2006). However, bZIP10^{C102,130,409A} displayed a stronger cytoplasmic signal compared to the wild-type bZIP10 (**Figure 36**). The protoplasts were then treated with 0.5 mM H₂O₂ in order to induce oxidative stress in the cells but no difference could be seen in the localization pattern upon treatment with H₂O₂ (**Figure 36**). A higher concentration of H₂O₂ was used in this experiment than in the reporter gene assay because the treatment was done only for a short time. The protoplasts were examined every 10 minutes post treatment during 1 h. The images shown here are after 1 hour of H₂O₂ treatment.

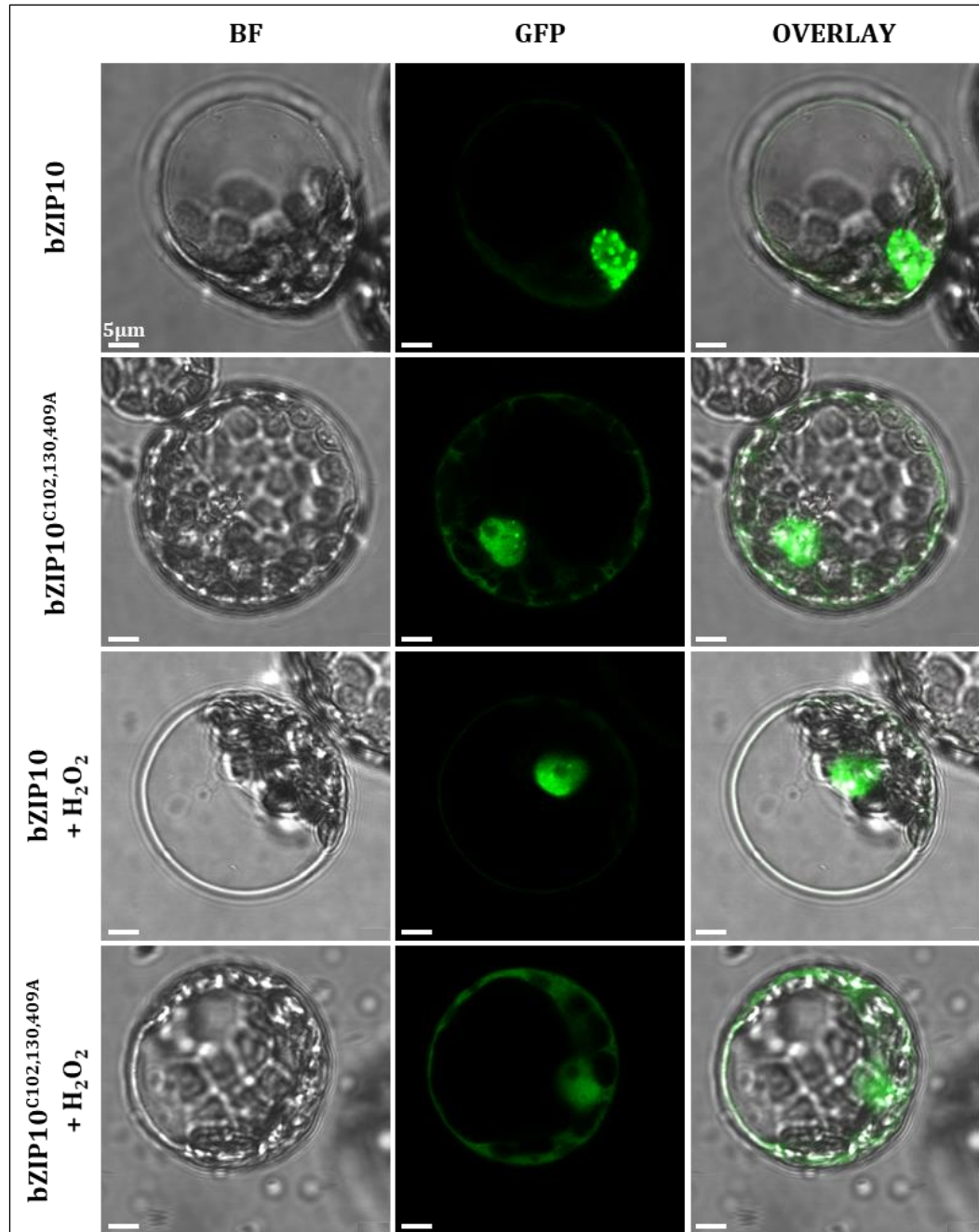


Figure 36: Subcellular localization of GFP tagged bZIP10 and bZIP10^{C102,130,409A} in *Arabidopsis thaliana* leaf mesophyll protoplasts prepared from *bzip10ko* line in the absence and presence of 0.5 mM H₂O₂ (1h).

4.3.5. LSD1 dependent sub-cellular localization of bZIP10

It had been shown that bZIP10 interacts specifically with LSD1. It was suggested that the transcriptional activity of bZIP10 could be controlled by LSD1 by regulating the

intracellular partitioning of bZIP10. Even though LSD1 does not directly bind to the DBD of bZIP10, it has been shown that this interaction inhibits the *in vitro* DNA-binding ability of bZIP10 (Kaminaka, Nake et al. 2006). Since the Cys409 is located in the protein domain indispensable for bZIP10's interaction with LSD1, it was examined if Cys-to-Ala substitutions could affect this interaction and the LSD1-dependent sub-cellular localization of bZIP10. For this analysis, LSD1 was fused to mCherry at its C-terminus under the control of 35S promoter and co-transfected with GFP-tagged bZIP10 or bZIP10^{C102,130,409A} in *Arabidopsis* leaf mesophyll protoplasts. The co-expression with LSD1 did not have any substantial effect on bZIP10 localization and both, the wild-type bZIP10 and its triple Cys mutant bZIP10^{C102,130,409A}, exhibited the same localization pattern as before (**Figure 37**). Considering that LSD1 antagonizes bZIP10 in ROS-induced cell death (Kaminaka, Nake et al. 2006), it could be possible that their sub-cellular localization was dependent on the ROS status of the cell. The protoplasts were therefore treated with 0.5 mM H₂O₂. However, no differences could be seen upon the treatment (**Figure 37**).

Because bZIP10 and LSD1 are present in both the compartments, the nucleus and the cytoplasm, an alternative approach for studying the effect of LSD1 on sub-cellular localization of bZIP10 was applied. The coding sequence of LSD1 was fused with an NLS or NES on either or both ends of LSD1 followed by a C-terminal mCherry tag, expressed under XVE estradiol inducible promoter, and transformed either in tobacco leaf cells or in *Arabidopsis* leaf mesophyll protoplasts. The idea was to spatially limit LSD1 to either nucleus or cytoplasm. It was expected that because of its interaction with LSD1, bZIP10 would also follow suit and would be retained in the same compartment as LSD1. It would then be easier to visualize the movement of bZIP10 upon various signals because the disruption of bZIP10-LSD1 interaction would lead to re-distribution of bZIP10. Unfortunately, the presence of NLS or NES did not limit LSD1 to the respective compartment (**Supplementary Figure 2**) and therefore, this approach to resolve LSD1 dependent localization of bZIP10 could not be used.

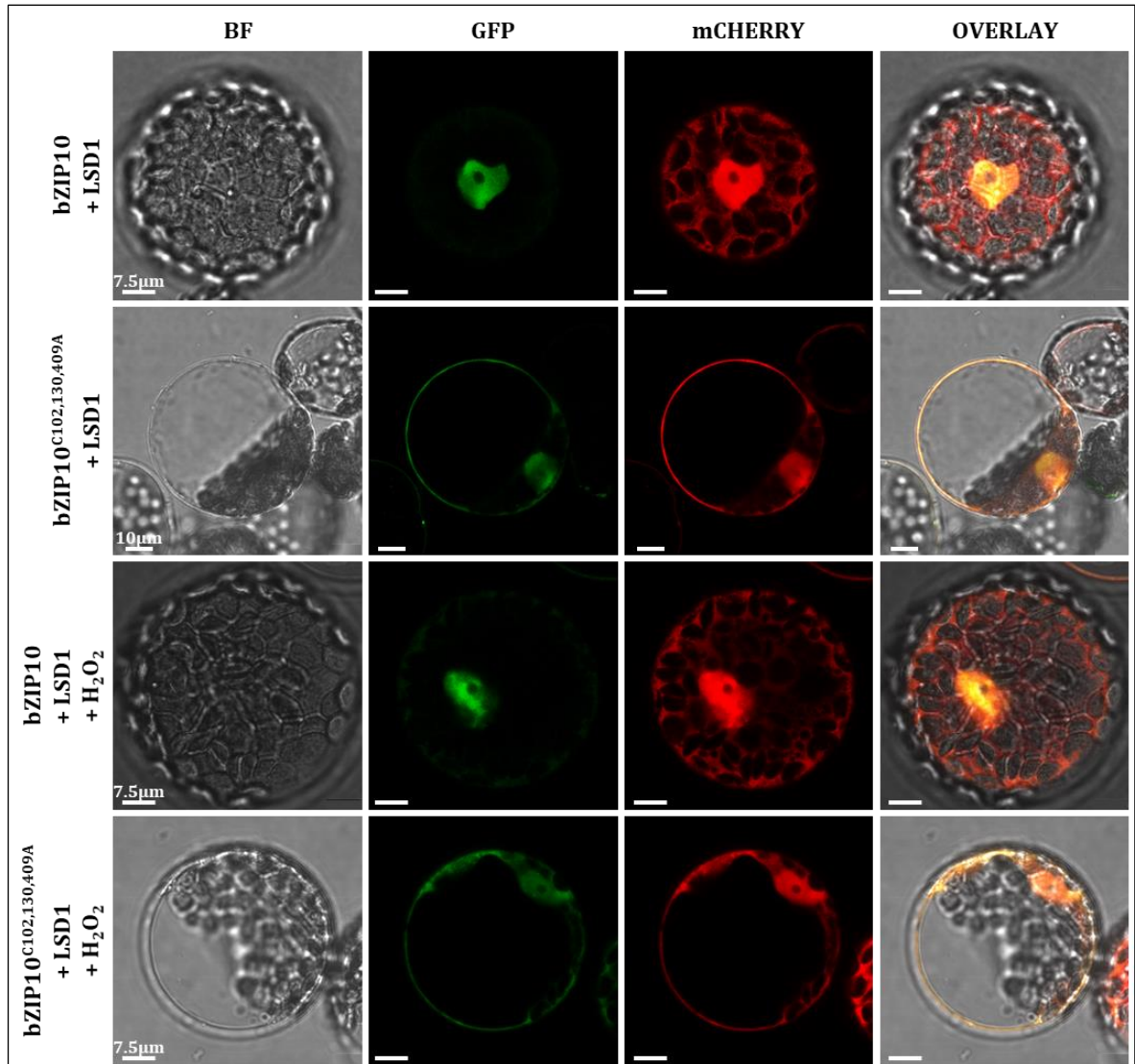


Figure 37: Subcellular localization of *bZIP10* and *bZIP10^{C102,130,409A}* along with *LSD1* in *Arabidopsis thaliana* leaf mesophyll protoplasts prepared from *bzip10ko* line in the absence and presence of 0.5 mM H_2O_2 . *bZIP10* is GFP tagged while *LSD1* has an mCherry tag.

4.3.6. Interaction of *bZIP10* and *LSD1* under oxidative stress

To test if *bZIP10*-*LSD1* interaction is influenced by oxidative stress, an Yeast 2-hybrid experiment was performed where *bZIP10* and its Cys mutants, viz., *bZIP10^{C409A}*, *bZIP10^{C102,130A}*, and a deletion mutant of *bZIP10* lacking the last 300 bp (*bZIP10 Δ 300*) were fused to the GAL4 Activation domain (AD). It had been shown earlier that the C-terminal part of *bZIP10* is required for its interaction with *LSD1* (Kaminaka, Nake et al. 2006). Removal of the last 300 bp from the coding sequence of *bZIP10* led to the deletion

of this interaction site, thus generating a bZIP10 mutant which could not interact with LSD1. LSD1 was fused to GAL4 DNA-binding domain (BD). To ensure the nuclear localization, LSD1 fused to NLS on both of its termini (NLS-LSD1-NLS) was used. Either bZIP10 or one of its above mentioned mutants was co-transformed with LSD1 in the yeast strain AH109 harboring the *lacZ* reporter gene expressed under GAL4 Upstream Activating Sequence (*GAL4-UAS::lacZ*), and then the reporter gene activity was measured by performing the β -Gal assay. The transformed yeast cells were treated with 0.5 mM H₂O₂ to induce oxidative stress in the cells. As can be seen in the figure, bZIP10 interacted with LSD1. This interaction was abolished by bZIP10 Δ 300 mutation which deletes the LSD1 binding site (Kaminaka, Nake et al. 2006), confirming that the method worked fine. There were no significant differences between the wild-type bZIP10 and either of its Cys mutants interacting with LSD1, irrespective of the presence or absence of H₂O₂ (**Figure 38**). The vector combinations 3238-AD and 2447-BD, and 3235-AD and 2441-BD are the negative and positive controls respectively.

Additionally, FRET-FLIM analysis was performed on bZIP10 and LSD1 in *Arabidopsis* leaf mesophyll protoplasts prepared from *bzip10/lsd1ko* line (double knock out line of bZIP10 and LSD1) to test their *in planta* interaction. For this purpose, bZIP10 fused at its C-terminus with GFP served as the donor molecule, while LSD1 was fused to mCherry at its C-terminus to serve as the acceptor molecule. Both the proteins were co-transfected and the fluorescence lifetime of GFP measured. For the negative control, bZIP10 was co-transfected with mCherry-NLS. A reduction of the fluorescence lifetime of donor molecule as compared to the negative control indicates a successful interaction. In addition, bZIP10 was fused to GFP followed by mCherry at its C-terminus, thus creating a fusion of donor and acceptor molecule which served as the positive control. A significant decrease (p value $\leq 2 \times 10^{-8}$) in the fluorescence lifetime of GFP indicates that bZIP10 interacted with LSD1 (**Figure 39**). The transfected protoplasts were then treated with 0.5 mM H₂O₂ to induce oxidative stress in the cells. The bZIP10-LSD1 interaction was unaffected by H₂O₂. I also tested the interaction between the triple Cys mutant bZIP10^{C102,130,409A} and LSD1. They interacted with each other irrespective of the presence or absence of H₂O₂ (**Figure 40**).

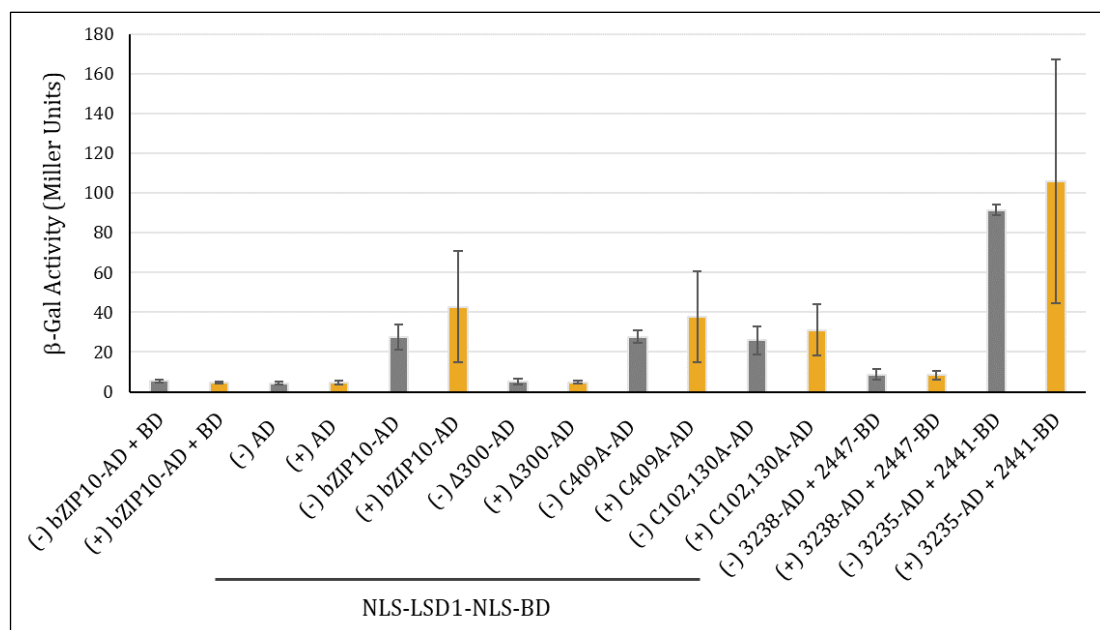


Figure 38: Yeast 2-hybrid experiment to analyze the interaction of bZIP10 and LSD1 under oxidative stress. AD and BD wherever mentioned alone in the graph (bar number 1-4 from left) are the empty vector negative controls. The (+) denotes addition of 0.5 mM H₂O₂ and the (-) denotes mock treated control. 3238-AD + 2447-BD and 3235-AD + 2441-BD are the negative and positive controls respectively. Statistical analysis was performed on three biological repeats.

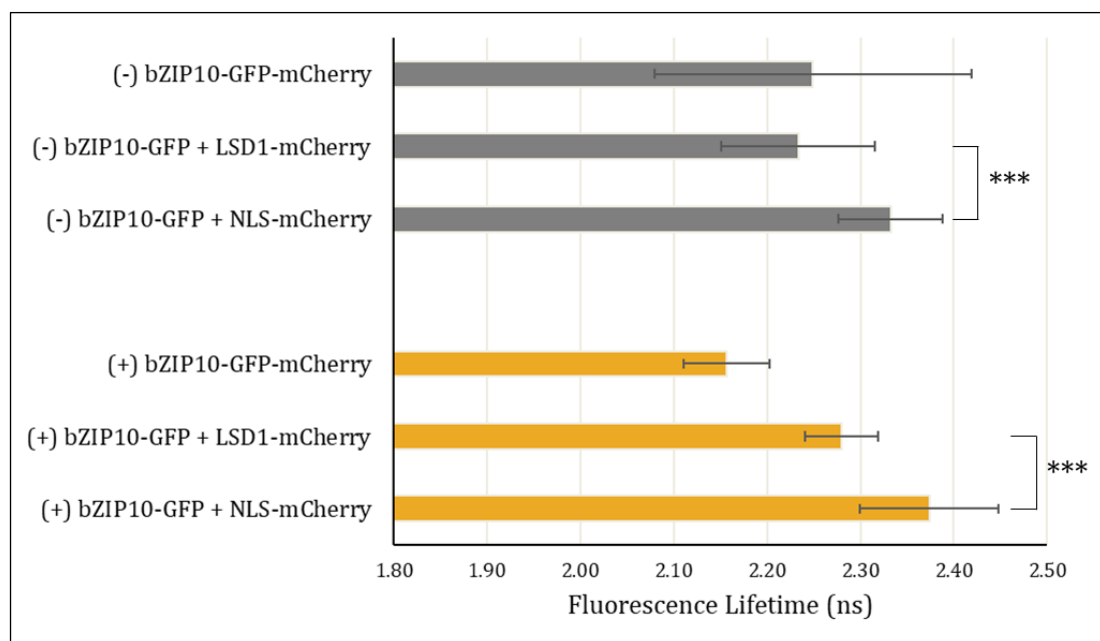


Figure 39: FRET-FLIM analysis of bZIP10 and LSD1 interaction in *Arabidopsis* leaf mesophyll protoplasts. bZIP10-GFP-mCherry is the positive control. The (+) denotes addition of 0.5 mM H₂O₂ and the (-) denotes mock treated control. *** denotes a significant change (p value ≤ 0.005). Statistical analysis was performed on fifteen measurements per sample. Representative data has been depicted.

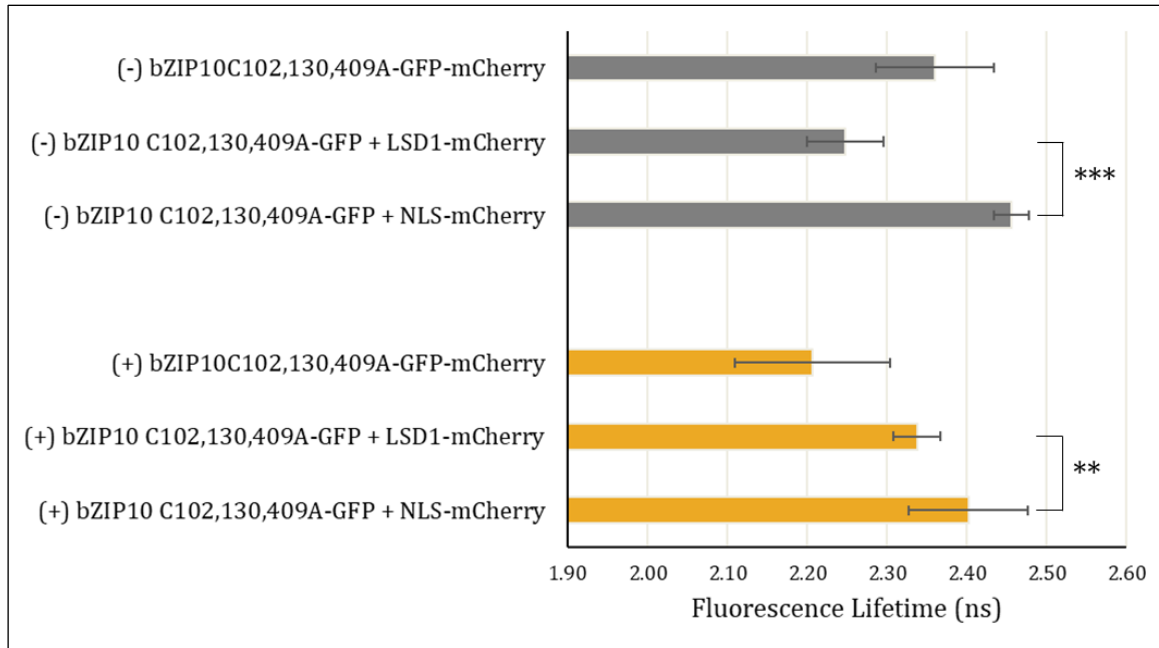


Figure 40: FRET-FLIM analysis of bZIP10^{C102,130,409A} and LSD1 interaction in Arabidopsis leaf mesophyll protoplasts. bZIP10^{C102,130,409A}-GFP-mCherry is the positive control. The (+) denotes addition of 0.5 mM H₂O₂ and the (-) denotes mock treated control. ** and *** denote a significant change (p value ≤ 0.01 and ≤ 0.005 respectively). Statistical analysis was performed on fifteen measurements per sample.

To summarize, two independent methods verified the bZIP10-LSD1 interaction which did not seem to be influenced neither by oxidative stress nor by Cys to Ala substitution in bZIP10.

4.3.7. Effect of LSD1 on bZIP10-bZIP53 transactivation capacity

There was a decrease in the transactivation of *pProDH1* by bZIP10-bZIP53 heterodimer upon treatment with H₂O₂ (see section 4.3.2.). Although the interaction of bZIP10 with LSD1 seems to be insensitive to oxidative stress, LSD1 could still regulate bZIP10 by interacting with bZIP10-bZIP53 heterodimer. To test if bZIP10-bZIP53 transactivation of *pProDH1* is affected by LSD1, Arabidopsis leaf mesophyll protoplasts prepared from *bzip10/lsd1ko* line were used. Either bZIP10 or one of its Cys mutants, viz., bZIP10^{C409A} and bZIP10^{C102,130,409A}, bZIP53 and *pProDH1::GUS* were co-transfected either with or without LSD1 in the protoplasts. The presence or absence of LSD1 did not affect *pProDH1* activation by bZIP10/bZIP53 heterodimers. As seen earlier in the case of reporter gene assay in *bzip10ko* protoplasts (see section 4.3.2.), the single Cys mutant bZIP10^{C409A}

behaved similarly to the wild-type protein, irrespective of the presence or absence of LSD1. Again comparable to the *bzip10ko* protoplasts, the triple Cys mutant bZIP10^{C102,130,409A} showed a significant decrease (p value ≤ 0.05) in the transactivation capacity in comparison to the wild-type bZIP10. However in the presence of LSD1, this decrease was abolished (**Figure 41**).

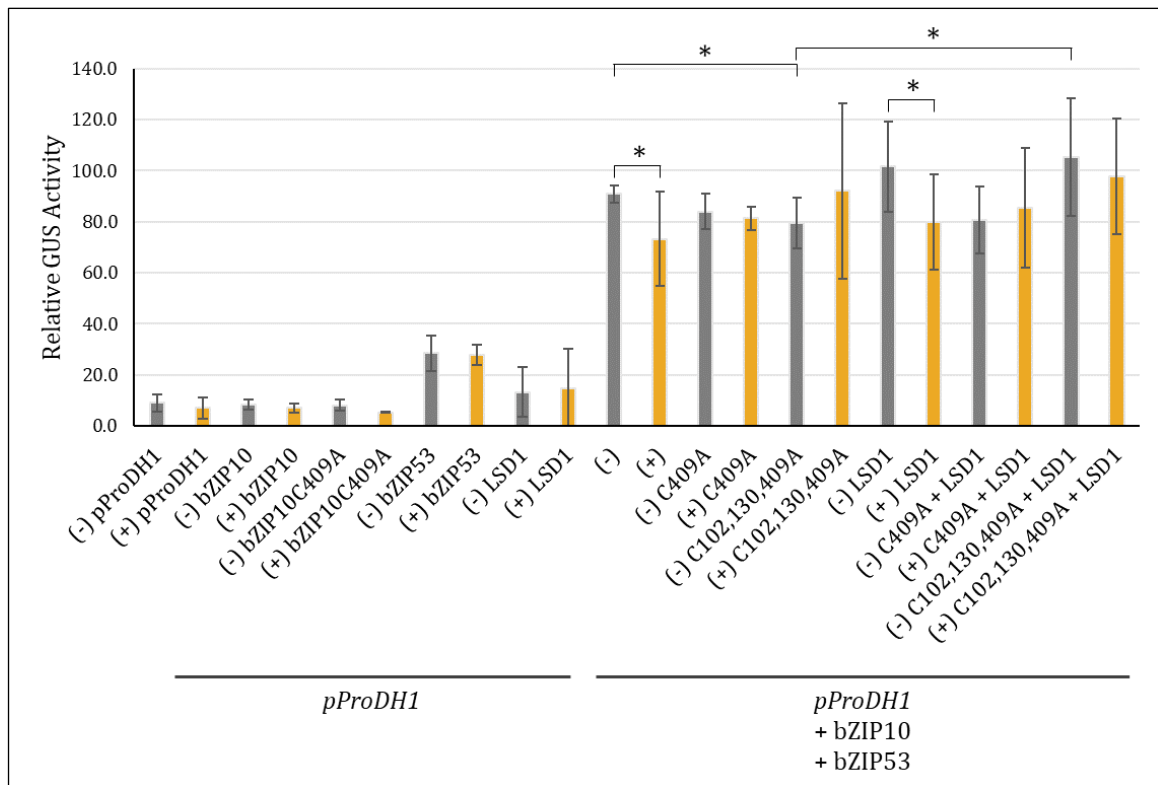


Figure 41: Relative GUS expression driven by *pProDH1* promoter either alone or in the presence of bZIP10 or one of its Cys mutants and/or bZIP53 and/or LSD1, in *Arabidopsis thaliana* leaf mesophyll protoplasts prepared from *bzip10-bsd1ko* line. The (+) denotes addition of 0.3 mM H₂O₂ and the (-) denotes mock treated control. * denotes a significant change (p value ≤ 0.05). Statistical analysis was performed on at least three biological repeats.

Next, it was tested if the presence or absence LSD1 had any effect on H₂O₂ dependent bZIP10-bZIP53 transactivation of *pProDH1*. Both in the presence and absence of LSD1, the transactivation capacity of bZIP10 was significantly decreased (p value ≤ 0.05) upon 0.3 mM H₂O₂ treatment. As seen earlier in the case of *bzip10ko* protoplasts, the single Cys mutant bZIP10^{C409A} showed no significant change in its transactivation capacity upon H₂O₂ treatment irrespective of the presence or absence of LSD1. Also, the triple Cys

mutant bZIP10^{C102,130,409A} showed no significant change in the transactivation capacity upon H₂O₂ treatment, both in the presence and absence of LSD1 (**Figure 41**).

Based on these data, it can be suggested that LSD1 does not influence the bZIP10/bZIP53-dependent activation of *pProDH1*.

4.4. Identification of direct targets of bZIP10

So far, only *ProDH1* promoter that contains the binding site for bZIP53, the dimerization partner of bZIP10, has been used in the reporter gene assays. The genomic sequences which can be directly recognized by bZIP10 are yet to be identified.

4.4.1 Screening for appropriate conditions and positive controls

To identify target genes of transcription factors *in vivo*, Chromatin Immunoprecipitation Sequencing (ChIP-Seq) is often used as a method of choice. However, it is a very complex method and optimization for individual transcription factors is a prerequisite. This includes testing variable duration of plant material fixation, DNA fragmentation, available antibody and subsequent immunoprecipitation of the protein-DNA complexes. For the method optimization, at least one DNA sequence recognized by bZIP10 is necessary as a positive control.

Apart from *ProDH1*, the earlier ChIP experiments have shown that bZIP1 and bZIP53 (both belonging to the S1-group bZIP) can bind *in vivo* to the promoter of the gene *ASN1* (Asparagine Synthetase 1) as well (Weltmeier, Ehlert et al. 2006, Dietrich, Weltmeier et al. 2011). Additionally, there was an increase in bZIP1 and bZIP53 transcripts after 4h extended night treatment. Also, it was shown that the accumulation of BCAT2 transcript in the dark is greatly enhanced by bZIP1 (Dietrich, Weltmeier et al. 2011). Because the C-group bZIPs including bZIP10 preferentially heterodimerize with the S1-group bZIPs leading to a synergistic activation of the target genes (Ehlert, Weltmeier et al. 2006), I analyzed the expression of these genes in bZIP10 transgenic lines.

For determining the conditions under which bZIP10 is most active, the following transgenic lines of *Arabidopsis thaliana* were used:

1. bZIP10-GFPox
2. bZIP10^{S19D}-GFPox

As mentioned earlier, proteins containing phosphorylation mimicking Ser19 to Asp substitution in their DBD are unable to bind to cognate DNA (Kirchler, Briesemeister et al. 2010). Thus, the bZIP10^{S19D}-GFPox transgenic line was chosen to verify the bZIP10

specificity of the target genes. The above-mentioned lines along with Col-0 were subjected to different treatments such as 0.5 M hydrogen peroxide (6 hours), 100 μ M salicylic acid (6 hours) and extended night (6 hours). The control plants were kept 6 h in light without any additional treatment. The leaves were harvested for RNA isolation followed by RT-PCR analysis with the primers for the following genes: *ASN1*, *ProDH1*, *ProDH2* and *BCAT2*. The housekeeping gene EF-1 α (Elongation factor-1 α) was used for normalization. In the control plants, only *ASN1* showed an increased expression in bZIP10-GFPox as compared to that in Col-0. *ProDH1* and *ProDH2* expression levels were similar in both bZIP10-GFPox and Col-0. The expression level of *BCAT2* was reduced in bZIP10-GFPox compared to Col-0. In bZIP10^{S19D}-GFPox, *ASN1*, *ProDH1* and *ProDH2* were expressed less than in bZIP10-GFPox whereas the expression of *BCAT2* was similar in both bZIP10-GFPox and bZIP10^{S19D}-GFPox. The expression of *bZIP10* transcript was also tested in all the three lines to verify the presence of bZIP10 transgene (**Figure 42**).

Upon H₂O₂ treatment, all the genes tested showed a decreased expression in both, bZIP10-GFPox and bZIP10^{S19D}-GFPox, as compared to that in Col-0 (**Figure 43**). The expression profiles of the tested genes upon salicylic acid treatment exhibited similar pattern as in the control plants in all the three lines analyzed (**Figure 44**). However, the difference in *ASN1* expression between bZIP10-GFPox and Col-0 plants was smaller than in the control plants. Surprisingly, the expression of *ProDH1* was at a comparable level in bZIP10-GFPox and Col-0 plants. Upon extended night treatment, both *ASN1* and *ProDH1* showed increased expression in bZIP10-GFPox compared to Col-0. At the same time, their expression was reduced in the bZIP10^{S19D}-GFPox line. Although *ProDH2* expression was also enhanced in bZIP10-GFPox as compared to Col-0, the increase in its transcript level was detected in bZIP10^{S19D}-GFPox as well. No difference could be seen in the expression of *BCAT2* in bZIP10-GFPox and Col-0 (**Figure 45**).

Out of the tested conditions, the extended night treatment exhibited the most specific increase in the expression of *ProDH1* and *ASN1* in bZIP10-GFPox. Therefore, the extended night treatment was selected as the treatment of choice for performing the ChIP-Seq experiment.

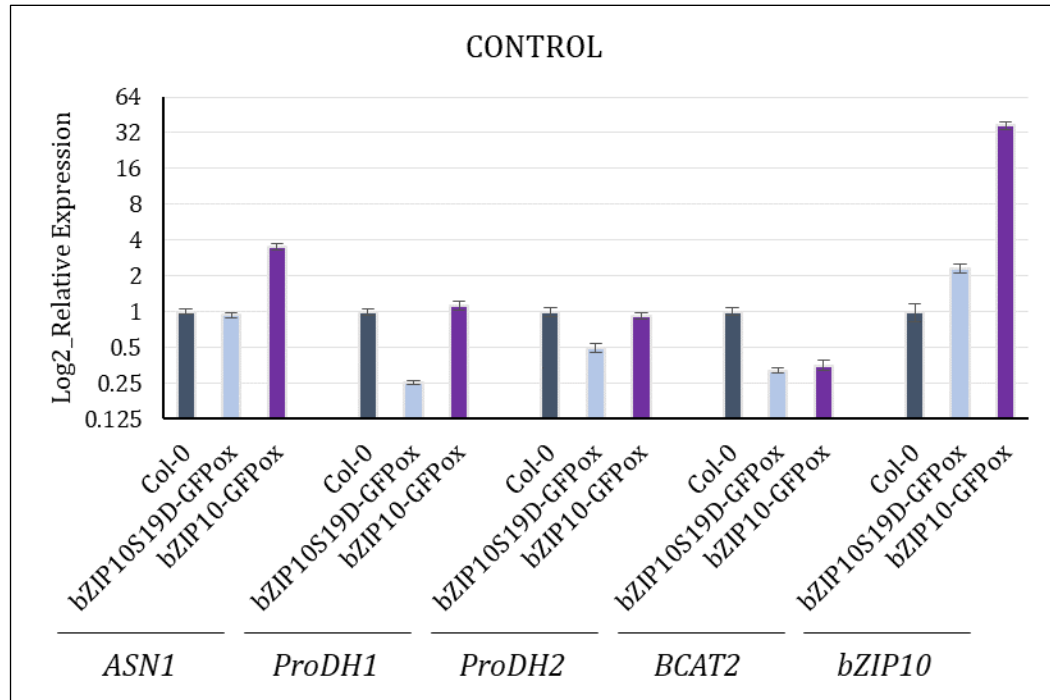


Figure 42: Expression of genes (*ASN1*, *ProDH1*, *ProDH2*, *BCAT2*, *bZIP10*) relative to *Col-0* in different transgenic lines (*Col-0*, *bZIP10^{S19D}ox*, *bZIP10ox*) of *Arabidopsis thaliana*, depicted in log₂ scale.

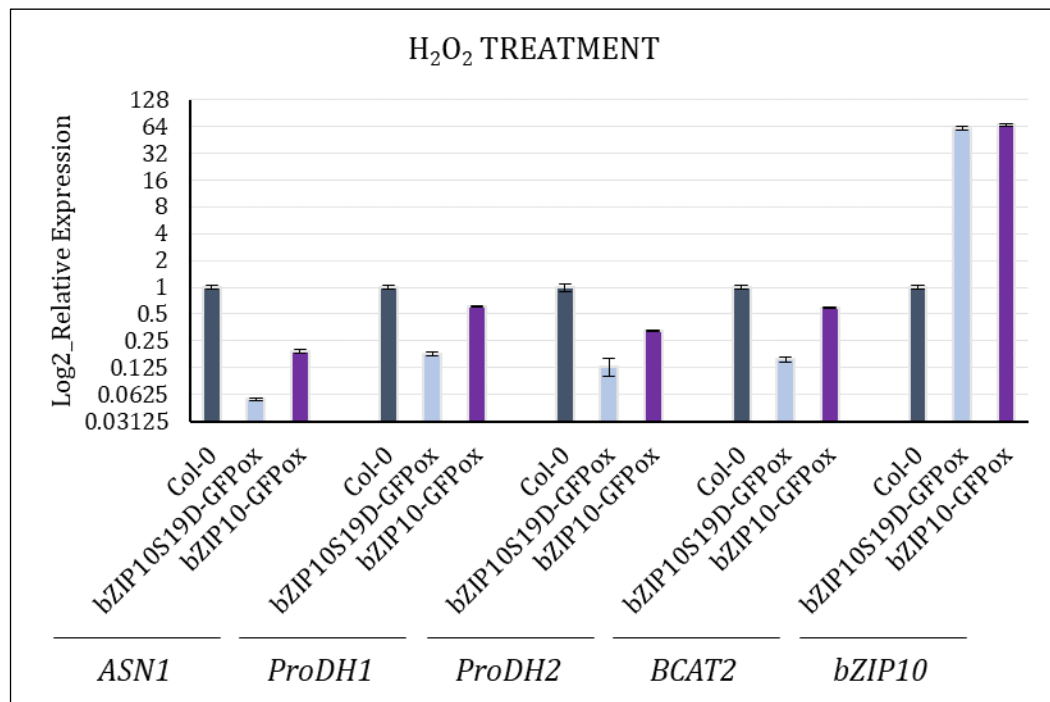


Figure 43: Expression of genes (*ASN1*, *ProDH1*, *ProDH2*, *BCAT2*, *bZIP10*) relative to *Col-0* in different transgenic lines (*Col-0*, *bZIP10^{S19D}ox*, *bZIP10ox*) of *Arabidopsis thaliana* after 6 h of H₂O₂ treatment, depicted in log₂ scale.

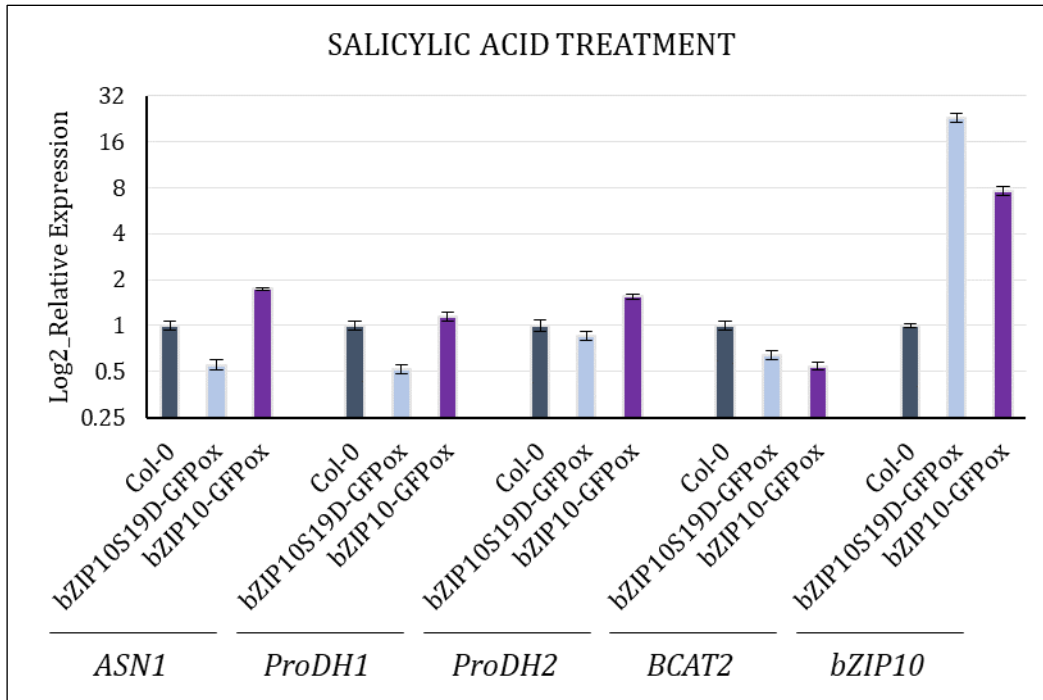


Figure 44: Expression of genes (*ASN1*, *ProDH1*, *ProDH2*, *BCAT2*, *bZIP10*) relative to *Col-0* in different transgenic lines (*Col-0*, *bZIP10^{S19D}ox*, *bZIP10ox*) of *Arabidopsis thaliana* after 6 h of SA treatment, depicted in log₂ scale.

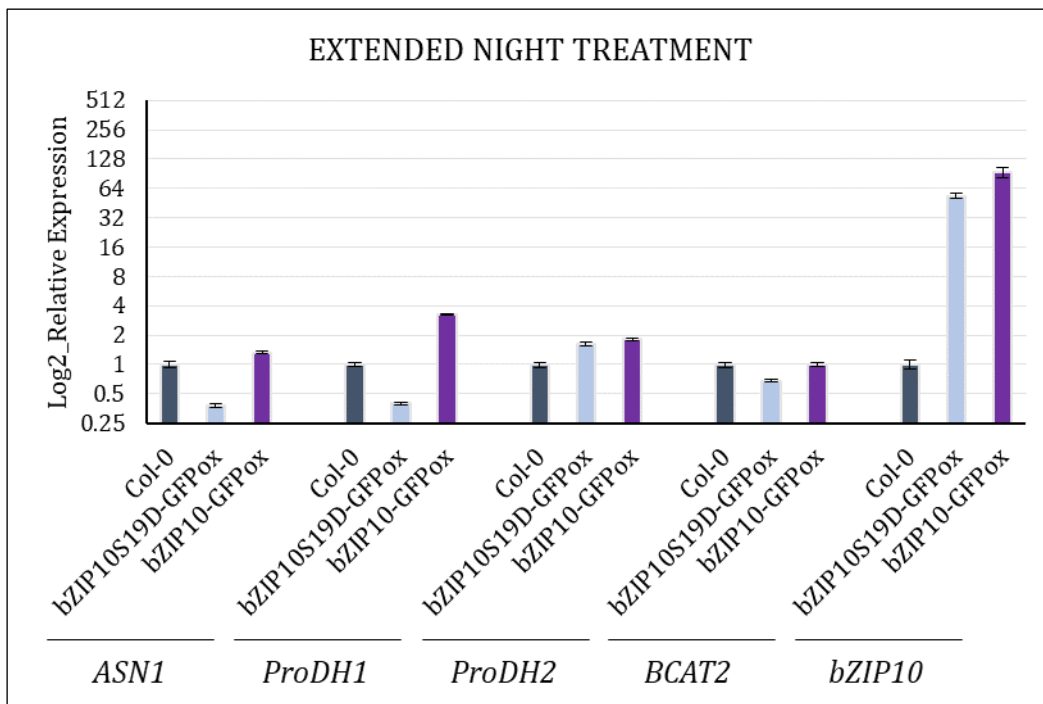


Figure 45: Expression of genes (*ASN1*, *ProDH1*, *ProDH2*, *BCAT2*, *bZIP10*) relative to *Col-0* in different transgenic lines (*Col-0*, *bZIP10^{S19D}ox*, *bZIP10ox*) of *Arabidopsis thaliana* after 6 h of extended night treatment, depicted in log₂ scale.

The next step was to optimize the sonication settings of the Branson probe sonicator such that the genomic DNA gets fragmented to about 200-500 bp. The samples were sonicated multiple number of times (4x, 6x and 8x times) and run on agarose gel to visualize the extent of fragmentation. As can be seen from the **Figure 46**, the required DNA fragmentation range was achieved after 8 times of sonication of the sample.

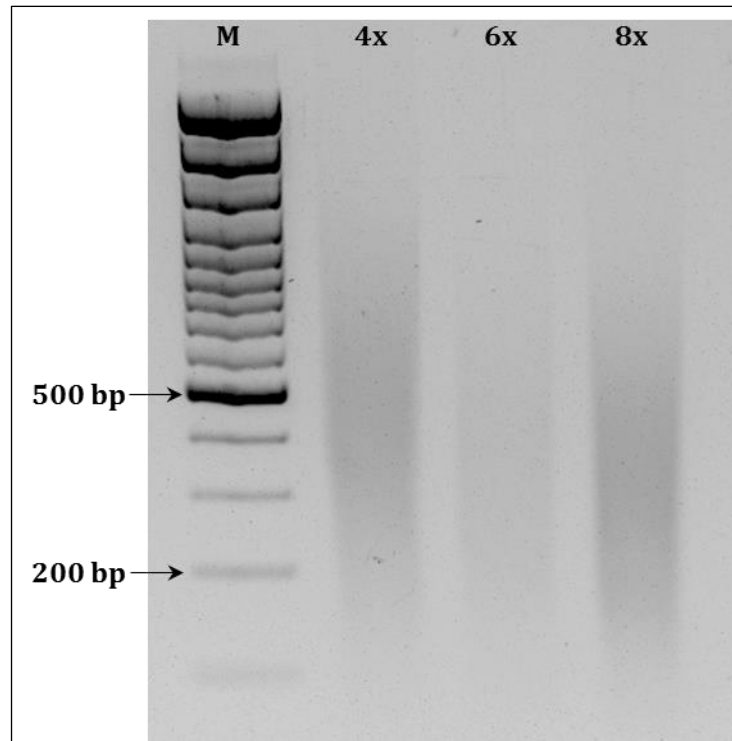


Figure 46: Visualization of the extent of DNA fragmentation after probe sonication. M: DNA ladder.

4.4.2. ChIP-qPCR pilot experiment

The plant material from bZIP10^{S19A}-GFPox and Col-0 was then harvested after the extended night treatment and fixed under green light using formaldehyde followed by genomic DNA isolation. The bZIP10^{S19A}-GFPox transgenic line was used because the absence of Ser19 in the DBD of bZIP10 might lead to a more stable DNA binding, consequently increasing the identification of bZIP10 target genes. The isolated DNA was then fragmented using the Branson probe sonicator followed by immunoprecipitation (IP). Before immunoprecipitation, a small aliquot of fragmented DNA was stored at -20 °C (this will be referred to as the input sample). After reverse cross-linking, the samples were checked for enrichment of the promoter sequences of the genes from the expression

analysis (see section 4.4.1.). For this purpose, quantitative-PCR (qPCR) was applied using the primers specifically designed against two different positions in the promoter region of the respective genes (**Figure 47**). The Actin primers were used for normalization. Unfortunately, very high level of contamination with *ProDH1* promoter sequence impaired the possibility of detection of its specific enrichment after immunoprecipitation. The contamination probably occurred due to the extensive application of this sequence in the reporter gene assays. As can be seen in the **Figure 48**, an enrichment of ASN1 could be seen in bZIP10^{S19A}-GFPox after immunoprecipitation. None of the other promoters analyzed were enriched after immunoprecipitation.

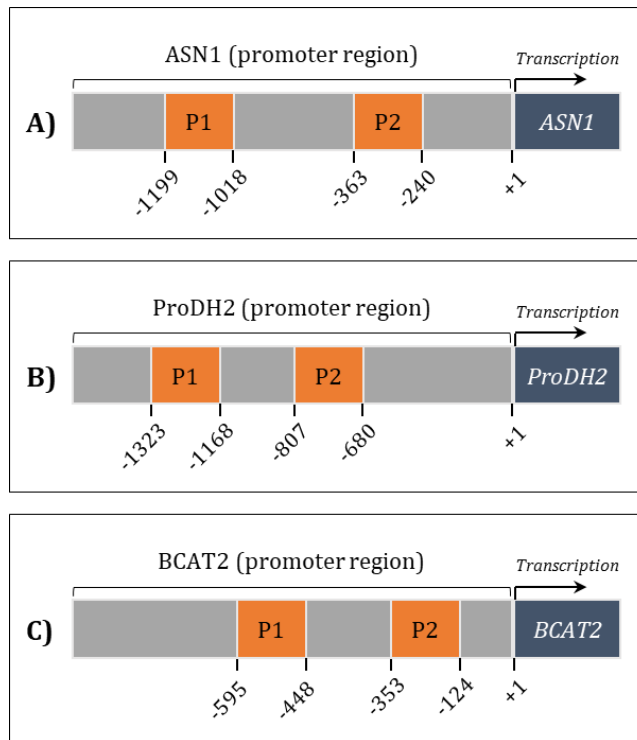


Figure 47: Schematic representation of the promoter regions of **(A)** ASN1, **(B)** ProDH2 and **(C)** BCAT2, indicating the positions where the primers (P1 and P2) were designed for ChIP-qPCR.

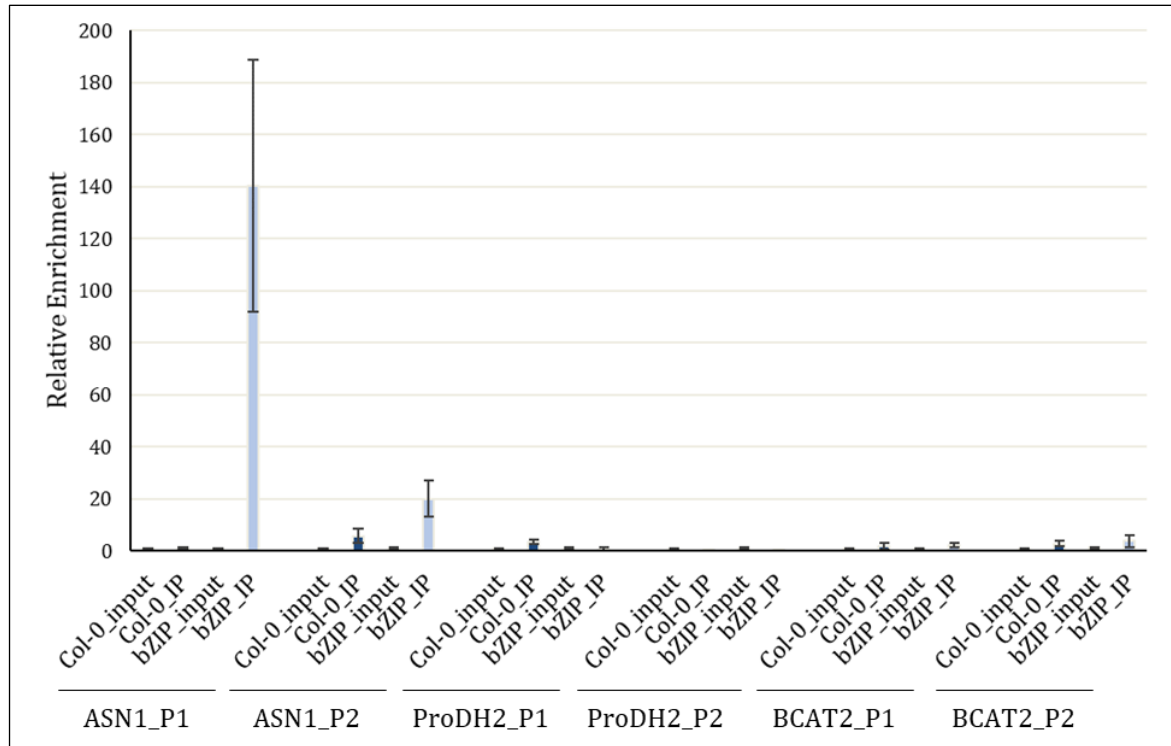


Figure 48: Relative enrichment of genes (*ASN1*, *ProDH2*, *BCAT2*) after ChIP-qPCR. P1 and P2 denote two different regions on the promoter for which primers were designed. *Col-0* is the control line and *bZIP* refers to *bZIP10^{S19A}-GFPox* transgenic line.

4.4.3. Chromatin Immunoprecipitation (ChIP-Seq)

For the identification of the other direct targets of bZIP10, the leaves from the following transgenic lines of *Arabidopsis thaliana* harvested under extended night (6 hours) were used:

1. bZIP10-GFPox
2. bZIP10^{S19A}-GFPox
3. eGFPox (this line was kindly provided by Dr. Andreas Wachter and used as a negative control)

In addition to the extended night treatment, *Pst* DC3000 infection (24 hours) was added as a treatment to bZIP10-GFPox because this line showed resistance against the pathogen as compared to *Col-0*, while the dominant negative mutant, bZIP10^{S19D}-GFPox was more susceptible than *Col-0* in *Pst* DC3000 pathogen assay (see section 4.2.3.).

After harvesting, the plant material was fixed under green light followed by genomic DNA isolation. These samples were fragmented using the Covaris sonicator (**Figure 49**) followed by immunoprecipitation. After reverse cross-linking, the samples were used for library preparation. Library preparation, the following library quality control analysis, and further sequencing and mapping of the reads to the *Arabidopsis thaliana* genome were done in collaboration with the Quantitative Biology Center (QBiC), Tuebingen University, Germany.

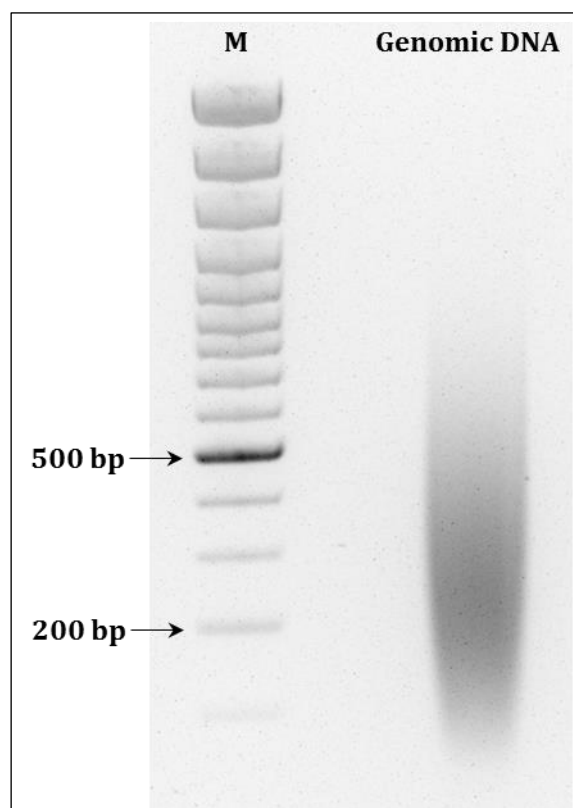


Figure 49: A representative image depicting the extent of DNA fragmentation after using a Covaris sonicator. M: DNA ladder.

4.4.3.1. Library quality check analysis

The finished libraries were run on Agilent High Sensitivity DNA chip using Agilent Technologies 2100 Bioanalyzer to verify the size distribution of each library. As can be seen in the **Figure 50**, the eGFPOx sample showed a nice size distribution from ~250-550 bp. However, for the other 3 samples, there were a couple of problems namely:

1. They exhibited an increased size distribution ranging from ~250 bp to >1000 bp followed by a tail of ~>5000 bp to >10,000 bp.
 2. There was a phantom peak at around 300 bp appearing before the main peak.
- Additionally, in the sample bZIP10^{S19A}-GFPox, there was a primer artifact peak at 150 bp. This primer artifact was removed before proceeding further (**Figure 51**). It looks as if the clean-up of the library caused a shift in the library size, but upon overlaying the electropherogram before and after the clean-up, no shift could be seen (data not shown).

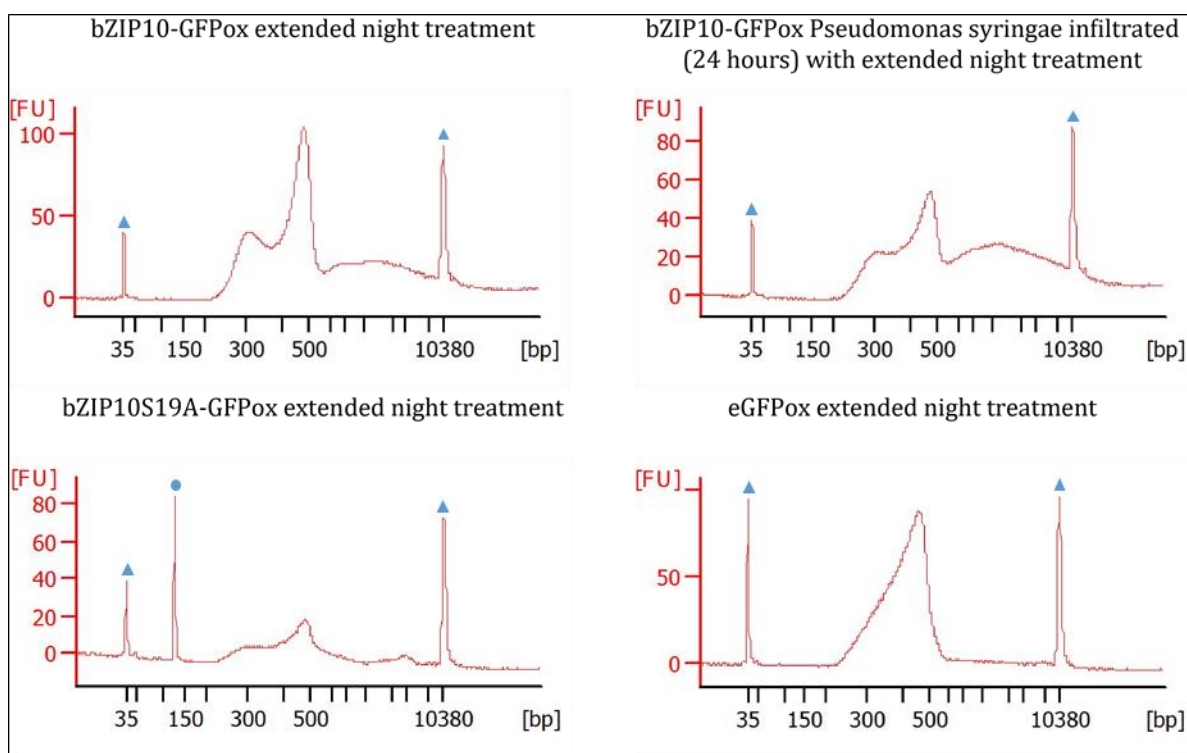


Figure 50: Quality check of the ChIP-DNA libraries run on the Bioanalyzer. The primer artifact is indicated with a circle on top of the respective peak and the DNA ladder peaks are indicated with triangles.

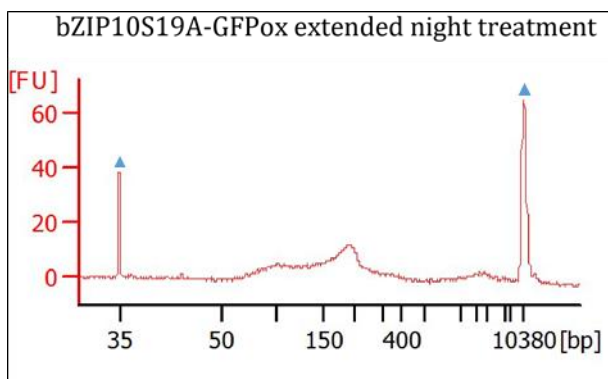


Figure 51: Quality check of bZIP10^{S19A}-GFPox ChIP-DNA library run on the Bioanalyzer after clean up. The triangles on top of the peaks represent the DNA ladder.

The libraries were then quantified using Qubit HS kit on Qubit Fluorometer (Thermo Fisher) and the results were as follows:

1. bZIP10-GFPox	0.16 ng/ μ L
2. bZIP10-GFPox <i>Pst</i> DC3000 infiltrated	0.521 ng/ μ L
3. bZIP10 ^{S19A} -GFPox	0.313 ng/ μ L
4. eGFPox	0.136 ng/ μ L

Because of the issues mentioned above, a pilot run on the Illumina MiSeq was done. The finished libraries were prepared for sequencing as per the Illumina kit (250 bp paired end) and pooled together (known as multiplexing) in equimolar ratios, followed by loading them on the MiSeq to be checked for their complexity. The output of the MiSeq run was as follows:

Sample	% reads identified
1. bZIP10-GFPox	32.4 %
2. bZIP10-GFPox <i>Pst</i> DC3000 infiltrated	49.6 %
3. bZIP10 ^{S19A} -GFPox	8.1 %
4. eGFPox	8.5 %

As is evident from the outcome, an imbalance is seen in number of reads obtained from the different samples. It was assumed for the data analysis that the reads obtained are single end in order to increase the number of the reads.

4.4.3.2. Quality control of the raw data

FastQC (<http://www.bioinformatics.babraham.ac.uk/projects/fastqc/>) was used for analyzing the quality of the raw data. The quality scores are plotted on the y-axis of the graph. Quality score represents the quality of the base call, the higher the better. The background of the plot is divided into three colours: green, orange and red representing the quality of the base call from very good (green) to poor (red). In general, an increase in read-length is accompanied by a decrease in sequencing quality leading to poor quality scores towards the end.

The quality of the raw data in this study was very similar for all the eight files (forward and reverse reads = 2 x 4 = 8 files). At around 150-160 bp of each read, a drop in the read quality is visible in the box-whisker plot drawn for each position (**Figure 52**). This plot indicates that there was a need of quality trimming at the 5' end of the reads.

4.4.3.3. Quality filtering

In the next step of data analysis, the tool CutAdapt (Martin 2011) was used for the quality filtering of the data. CutAdapt scans the next-generation sequencing (NGS) generated reads for adapter sequences, primers, poly-A tails and other unwanted sequences, and removes them. The over-represented adapter sequences were filtered out first. The reads which showed a match to typical over-represented Illumina adapters were identified using FastQC (<http://www.bioinformatics.babraham.ac.uk/projects/fastqc/>) and merged into a fasta file. The reads from the dataset were filtered out using this file (Quality filter 1). Only one over-represented adapter was found in this file:

```
>TruSeq Adapter, Index 1 (97 % over 35bp)
```

```
GATCGGAAGAGCACACGTCTGAACTCCAGTCACGTGAAACGATCTCGTAT
```

To address the problem of the low read quality per base (**Figure 52**), a second filter (Quality filter 2) was applied in order to cut off the low quality bases from the beginning and the end of the reads. This led to the optimization of the per base sequence quality (**Figure 53**).

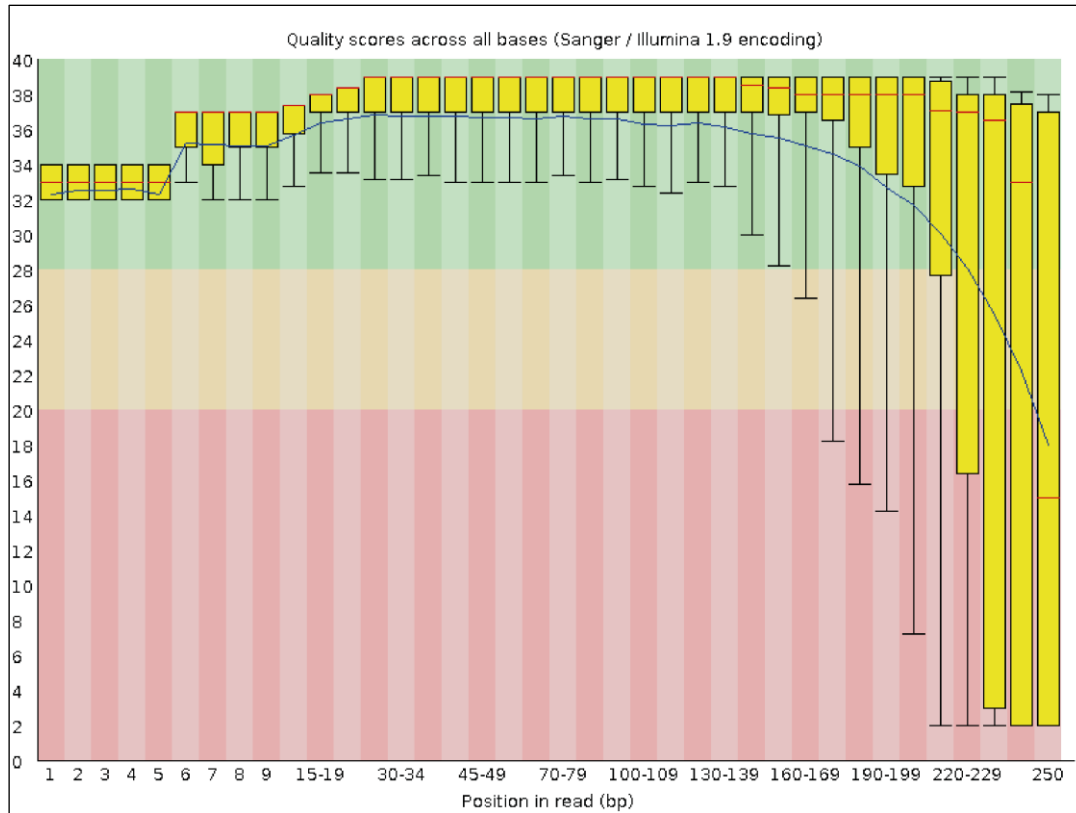


Figure 52: A representative box-whisker plot displaying the per base quality of the raw data. The red line corresponds to the median value, the yellow box signifies the inter-quartile range (25-75 %), the upper and lower whiskers denote the 10 % and 90 % points respectively, and the blue line is the mean quality.

Figure 54 shows the number of reads that were originally present and the reads after quality filtering. This plot reflects the same output as the MiSeq machine run itself, i.e. before the quality filtering was applied. The imbalance seen there is also seen here. In the MiSeq output, about 50 % of the reads were derived from bZIP10-GFPox (*Pst* DC3000 infiltrated) as is the case here: ~14 million reads for R1 and R2 were found for this sample in the original dataset. bZIP10-GFPox gave the second most identified reads with ~32 %, which can be seen here as well: 9 million forward and reverse reads present in the original dataset. The other samples (bZIP10^{S19A}-GFPox and eGFP-ox) contributed in the range of 8-8.5 % of the identified reads in the MiSeq output, which is also reflected here: 2.2 to 2.4 million reads for these two samples. In summary ~80 % of all the reads identified in the experiment were derived from two samples only, indicating the non-

equimolar pooling of the libraries (**Figure 54**).

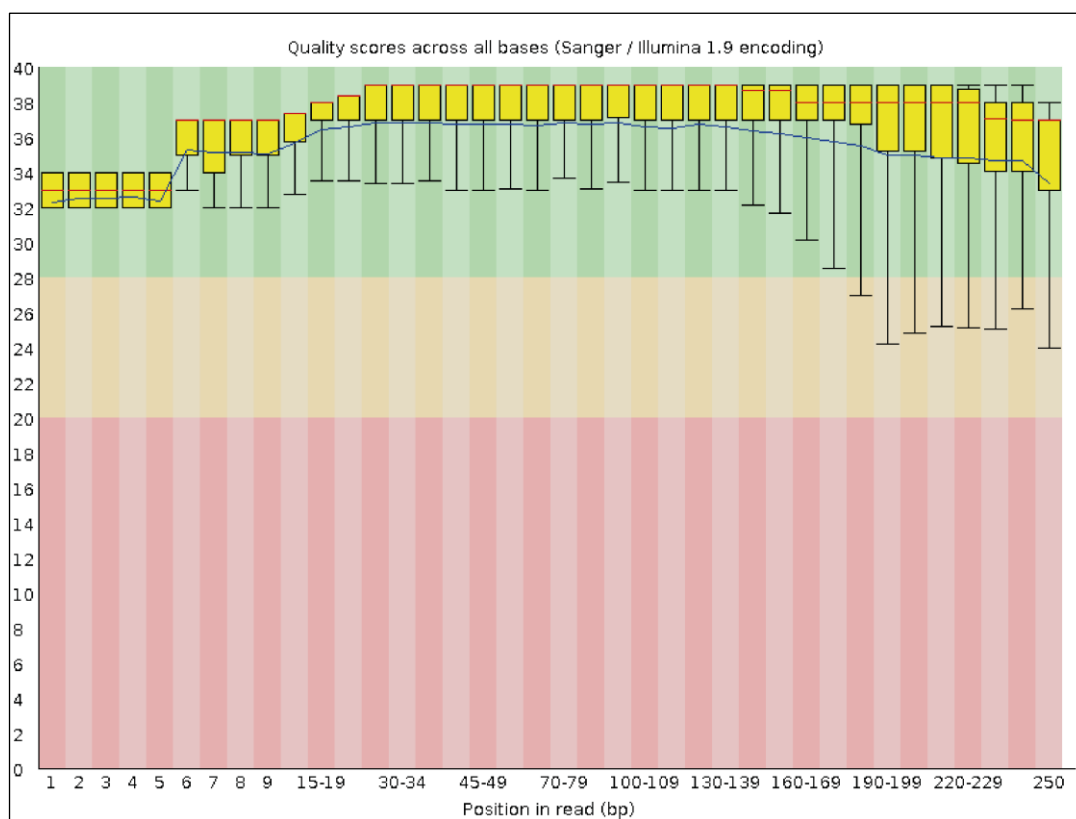


Figure 53: A box-whisker plot displaying the per base quality of the reads after removal of adapter and low quality bases. The red line corresponds to the median value, the yellow box signifies the inter-quartile range (25-75 %), the upper and lower whiskers denote the 10 % and 90 % points respectively, and the blue line is the mean quality.

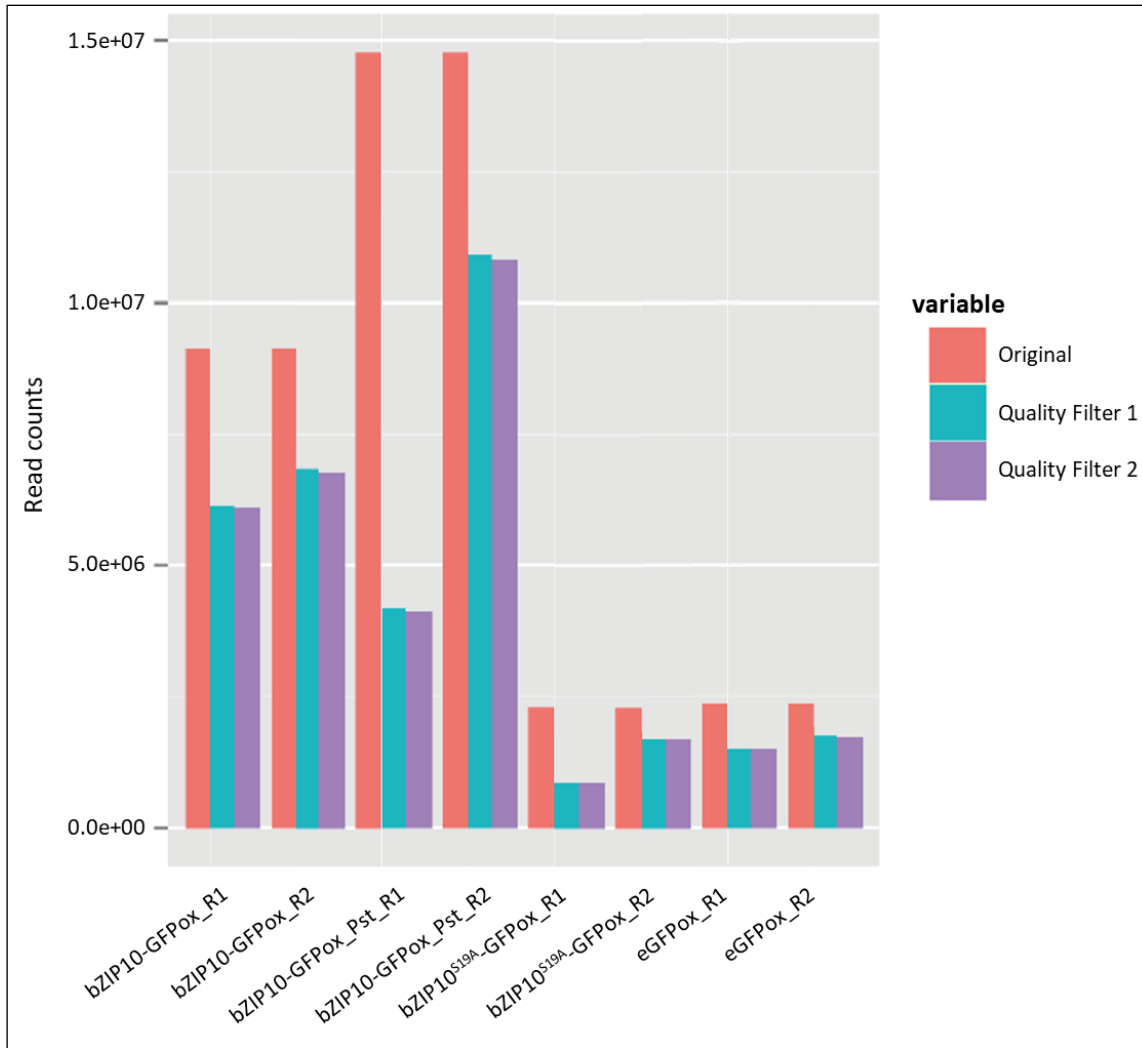


Figure 54: A plot representing the number of reads originally present (red), number of reads after adapter removal (Quality filter 1, blue bars), and the number of reads after adapter removal and removal of the low quality bases from the beginning and the end of the reads (Quality filter 2, violet bars). R1 denotes forward read and R2 denotes reverse read.

4.4.3.4. Mapping using Bowtie2 and Tophat2

The quality filtered reads were then fed into the sequence alignment tools Bowtie2 and Tophat2. It can be clearly seen from the plot that, despite (a) changing the tuning parameters for alignment using Bowtie2 (**Figure 55 A-B**) or Tophat2 (**Figure 55 C-D**) as the alignment tool, or (b) taking out the adapter sequences (**Figure 55 A and C**, blue bar from **Figure 54** was used as the input) and performing quality filtering of the reads (**Figure 55 B and D**, violet bar from **Figure 54** was used as the input), the alignment to the *Arabidopsis* TAIR10 genome was very low. At least 40 % of the reads showed

alignment to the human genome in majority of the samples. Only a small fraction mapped to *Arabidopsis thaliana*, *Escherichia coli* and *Saccharomyces cerevisiae*. Only sample 4 (eGFPOx) showed an alignment of ~50 % of the reads to the *Arabidopsis thaliana* genome (using Bowtie2).

The NRF (Non-Redundant Fraction) serves as a useful complexity metric for ChIP-Seq libraries. Defined as the number of positions in the genome that uniquely mappable reads map to, divided by the total number of uniquely mappable reads. The NRF value for good libraries should lie in the range of 0.8 for 10 million uniquely mapped reads (Landt, Marinov et al. 2012). In our experiment, as only ~100,000 reads mapped to the *Arabidopsis thaliana* genome on an average, the NRF value is expected to be around 0.008. However, it was in the range of 0.95, ~100 fold too large, for all the samples.

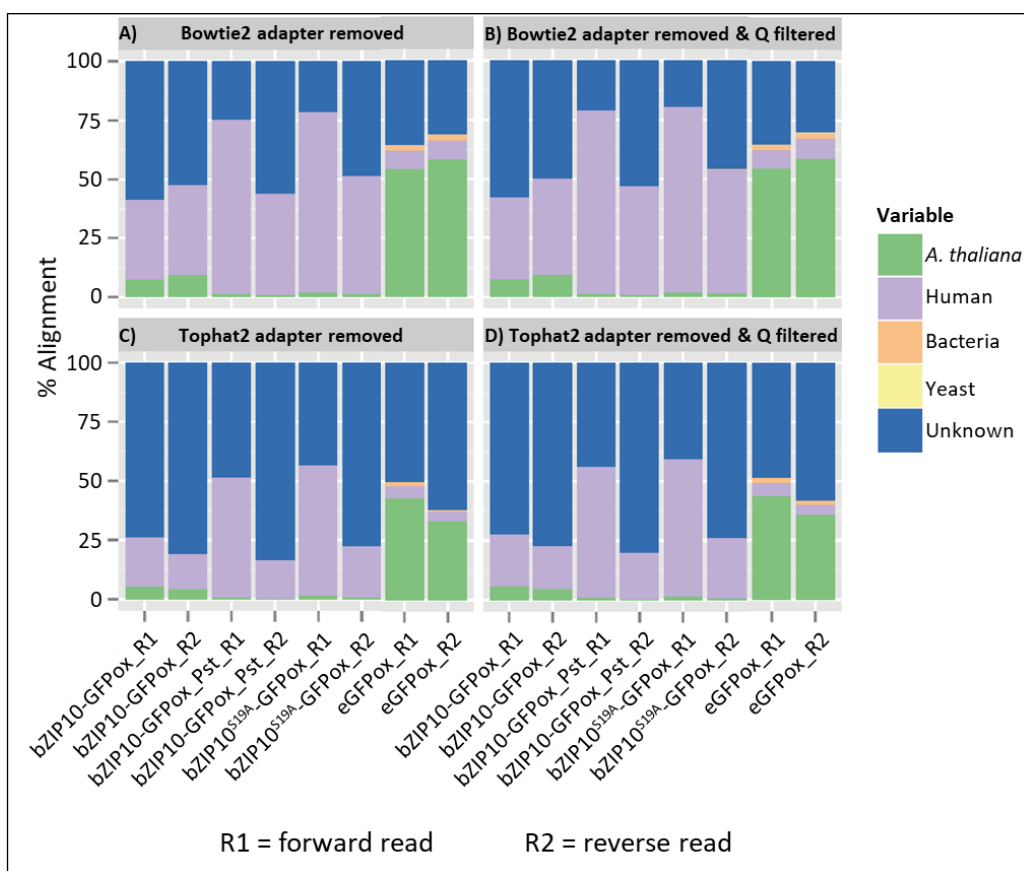


Figure 55: Mapping of the obtained reads using Bowtie2 and Tophat2 as the alignment tools. (A) and (C) show the mapping results for the reads with the adapter sequences removed using Bowtie2 and Tophat2 respectively. (B) and (D) show the mapping results for the quality filtered reads using Bowtie2 and Tophat2 respectively.

4.4.3.5. Analysis of the origin of the unmapped reads

Although a high percentage of the reads mapped to the human genome, there were also a lot of reads which were unknown. These unmapped reads (the blue bars in **Figure 55**) were extracted and combined to make a random subset of 1.5 million reads. This random subset was then used as a query in NCBI BLAST using the blastn algorithm and searched against the nucleotide database that contains non-redundant nucleotide sequences. Around 1,450,000 hits were successfully mapped (some sequences were still not found). As can be seen from the **Figure 56**, most of the sequences related closely to the human genome (1 million out of 1.5 million unmapped reads). Only a fraction of it (~260,000 reads) turned out to be of *Arabidopsis* origin.

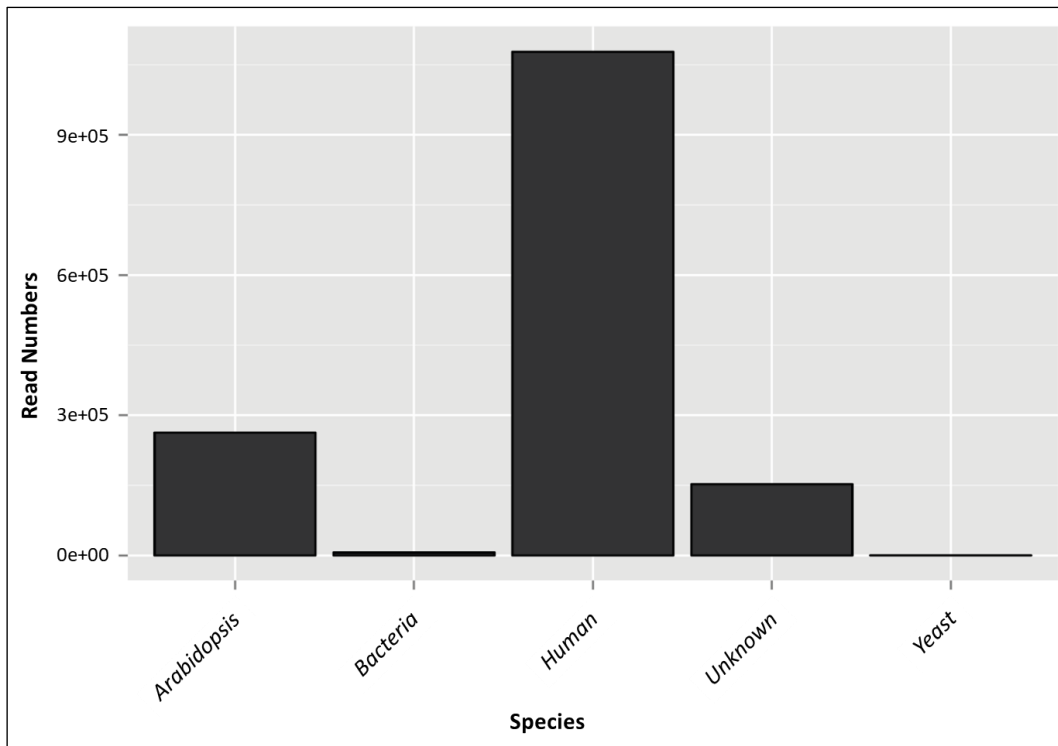


Figure 56: BLAST analysis of the reads that could not be mapped using Bowtie2 and Tophat2. The blue bars in **Figure 55** were used as the input.

In conclusion, this attempt of identifying the direct targets of bZIP10 was unfortunately not successful. Optimization of ChIP-Seq method for bZIP10 was a very time-intensive process. And it looked very promising after the pilot experiment where I did manage to identify *ASN1* as one of the possible direct targets of bZIP10. However, the total number

of reads obtained after sequencing was too low, along with their unequal distribution originating from certain samples. The outcome of the ChIP-Seq experiment, very disappointingly, did not turn out to be fruitful.

4.5. Proteomic screen for bZIP10 interaction partners

Screening of other interaction partners of bZIP10 was initiated in order to better understand the function of bZIP10 in *Arabidopsis thaliana*. Mass spectrometry based proteomic analysis was utilized for this purpose. *Arabidopsis* transgenic line bZIP10-GFPox was used for immunoprecipitation of bZIP10, and eGFPox and Col-0 were used as the negative control for these analyses. The following two pull-down experiments were carried out:

Experiment 1: bZIP10 pull-down under control conditions

Experiment 2: bZIP10 pull-down upon 100 μ M salicylic acid treatment (5 hours)

All proteins were submitted to the proteomics facility post pull-down and were processed further as mentioned in section 4.3.1.1. Approximately 300 proteins and 400 proteins were identified in Experiment 1 and Experiment 2 respectively with a good intensity (relative abundance) value, and exclusive only to the experimental samples and not identified in the respective controls. Identification of bZIP53, a known bZIP10 interaction partner, validated the experimental procedure. The **Supplementary Table** lists all the identified proteins that could be putative interaction partners of bZIP10 under control conditions and upon salicylic acid treatment respectively.

Compared to bZIP10-GFPox samples, much less proteins were identified in the pull-down from eGFPox. Among more than 300 proteins identified exclusively in the pull-down from bZIP10-GFPox, some promising protein sequences were found. For example, in the untreated sample, PP2A (type 2A protein phosphatases), CPK5/CPK6 (Calcium-dependent Protein Kinase 5/6), TRX3 (Thioredoxin H3) and TPL (TOPLESS) were identified. The possible role of these proteins in the regulation/function of bZIP10 is discussed further in section 5.5. of this thesis. In the SA treated sample, LOX2 (Lipoxygenase 2), CAT3 (Catalase 3) and β CA1 (Beta carbonic anhydrase 1) were among the identified potential interaction partners of bZIP10. Further experiments need to be done in order to verify the interaction of bZIP10 with these proteins.

Additionally, multiple chloroplast-localized proteins were identified in the bZIP10

samples. Since they were not found in the eGFPox- and Col-0-derived samples, which would otherwise indicate their unspecific binding either to GFP or antibody, we still do not have an explanation for this phenomenon.

5. Discussion

5.1. Regulation of bZIP10 by phosphorylation

The member of *Arabidopsis* C-group bZIP factors bZIP10 has been previously shown to function as a positive regulator of plant defense response to biotrophic pathogen *Hyaloperonospora parasitica* mainly by enhancing cell death in the LSD1-dependent manner (Kaminaka, Nake et al. 2006). Additionally, bZIP10 was reported to form heterodimer with S1-group bZIPs, and induce expression of ProDH1 and several seed endosperm-specific genes through heterodimerization with bZIP53 (Ehlert, Weltmeier et al. 2006, Weltmeier, Ehlert et al. 2006, Alonso, Onate-Sanchez et al. 2009, Weltmeier, Rahmani et al. 2009). Apart from this, very little is known about the mechanisms of bZIP10 molecular regulation as well as its possible involvement in broader spectrum of plant defenses and signal transduction. The functional characterization of bZIP transcription factors in general, and members of C- and S1-group in particular, is complicated due to their possible heterodimerization and redundancy. In addition, various post-translational modifications including phosphorylation have been reported for different bZIPs (Schutze, Harter et al. 2008). Therefore, the possibility of using dominant negative bZIP10 mutant was explored in my work. Crystallographic analysis of animal bZIPs have shown that the amino acid residue at position 19 in the DBD is the point of direct contact between the bZIP and DNA backbone (Fujii, Shimizu et al. 2000, Miller, Shuman et al. 2003). Accordingly, it may affect the protein-DNA binding affinity. In humans, this position is mainly occupied by Ser (35 %) or Cys (55 %), both of which can be post-translationally modified (Deppmann, Thornton et al. 2003). The phosphorylatable residue at position 19 is highly conserved in *Arabidopsis thaliana* bZIP factors as well. 66 genes out of 74 genes in the protein family have a conserved Ser residue at position 19. Two other phosphorylatable residues, Thr and Tyr, were present at this position in two and three genes respectively. Kirchler *et al.* predicted, based on a homology model, that Ser19 in the DBD of bZIP63 comes in the direct contact with the target DNA. Mutating the Ser19 to the phospho-mimicking Asp completely abolished the DNA binding activity of bZIP63 (Kirchler, Briesemeister et al. 2010), as well as the

activation of target gene (Kirchler 2014). Similarly, the heterodimers of bZIP53 with phospho-mimicking mutant bZIP10^{S19D} showed drastically reduced transactivation capacity. However, no difference could be seen in the heterodimer formation capacity of bZIP10 and its phosphorylation mutants with bZIP53. Instead, phospho-mimicking and phospho-ablative bZIP10 mutants show a difference in their localization pattern. The wild-type bZIP10 was found to be localized in the nucleus, with a weak cytoplasmic presence as well. While bZIP10^{S19A}-GFP displayed a strong nuclear signal, bZIP10^{S19D}-GFP was predominantly cytoplasmic. The cytoplasmic localization of bZIP10^{S19D} could be attributed to the presence of NES at its N-terminus, which was shown to be responsible for XPO1-dependent bZIP10 nuclear export (Schutze, Harter et al. 2008). Analysis of localization of the bZIP10^{S19D} mutant lacking the XPO1 interaction site revealed that the cytoplasmic localization of the phospho-mimicking mutant is not due to the disruption of its NLS. It is possible that bZIP10^{S19D} could get transported to the nucleus, but it still fails to bind to the DNA, as is seen in the transactivation assay and, as a consequence, is more easily exported to the cytoplasm. Interestingly, in the presence of nuclear-localized bZIP53, all the three versions of bZIP10 show a complete nuclear localization, indicating that the interaction of bZIP10 with bZIP53 prevents the nuclear export of bZIP10. The endogenous level of bZIP53 may not be enough to account for the over-expressed bZIP10. It is probably because of this reason that the complete nuclear localization of bZIP10 is observed only in the presence of over-expressed bZIP53.

It has been reported earlier that phosphorylation can affect the sub-cellular localization of a protein (Brunet, Park et al. 2001, Macian, Lopez-Rodriguez et al. 2001) and prevent its binding to DNA (Mahoney, Shuman et al. 1992, Whitmarsh and Davis 2000). For example, it has been shown that in *Arabidopsis thaliana*, the brassinosteroid responsive transcription factor BZR1 (Brassinazole Resistant 1) is translocated to the nucleus upon phosphorylation with the BIN2 (Brassinosteroid Insensitive 2), a GSK-3 like kinase. The authors also showed that PP2A-type phosphatases mediated de-phosphorylation of BZR1 led to its nuclear translocation (Ryu, Kim et al. 2007). Similarly, the animal bZIP transcription factor BATF (Basic leucine zipper transcriptional factor ATF-like) has been shown to be phosphorylated on several residues, including Ser43 (which corresponds to

the position 19 in the DBD). The authors showed that the phospho-mimicking mutant BATF^{S43A} was able to dimerize with Jun proteins but the heterodimer displayed an inability to bind to the DNA (Deppmann, Thornton et al. 2003). In analogy, the probable importance of phosphorylation of this Ser residue in regulation of bZIP10 cannot be excluded. The wild-type bZIP10 shows both, nuclear and cytoplasmic localization probably because of a pool of phosphorylated and non-phosphorylated bZIP10. Since the phospho-ablative mutant bZIP10^{S19A} could not be phosphorylated at this position, it shows a very strong nuclear localization. On the other hand, the phospho-mimicking mutant bZIP10^{S19D}, which could not be de-phosphorylated, predominantly displays cytoplasmic signal.

Based on the above-described results, it appears that phosphorylation-mimicking Ser19Asp substitution is inhibiting the activity of bZIP10 by either restricting it to the cytoplasm and/or rendering it unable to bind to DNA. Taking into account that the dimerization with S1-group partner is, however, not disrupted, the ectopic expression of bZIP10^{S19D} in the wild-type background should lead to the interruption of bZIP10-dependent transcription, thus working as the dominant negative mutation.

5.2. The antagonistic role of bZIP10 in the *Arabidopsis* defense responses

Kaminaka *et al* showed the involvement of bZIP10 in defense response of *Arabidopsis thaliana* against the biotrophic fungi *Hyaloperonospora parasitica* (Kaminaka, Nake et al. 2006). In an attempt to find out the role of bZIP10 in plant defense responses to a brighter spectrum of pathogens and herbivores, the transgenic and mutant lines of *Arabidopsis thaliana* over-expressing bZIP10 and its phosphorylation mutants were subjected to treatment with different pathogens such as caterpillars of the herbivore *Mamestra brassicae*, the necrotroph *Botrytis cinerea* and the hemi-biotroph *Pst* DC3000. It is known that, with some exceptions, biotrophs induce the SA-defense pathway while the herbivores and necrotrophs induce the JA-defense pathway in plants (Berens, Berry et al. 2017), and that these two pathways are antagonistic to each other (Pieterse, Van der Does et al. 2012). Similar to the data on biotrophic fungi *Hyaloperonospora parasitica* (Kaminaka, Nake et al. 2006), bZIP10-GFPox showed increased resistance against *Pst* DC3000 with *bzip10ko* being hyper-sensitive to this pathogen. This indicates that bZIP10 plays a positive role in the defense response against biotrophic pathogens. . On the contrary, *bzip10ko* and dominant negative bZIP10^{S19D}-GFPox plants were observed to be much more resistant than Col-0 (as described previously in section 4.2.2.) against the infection with necrotrophic fungus *Botrytis*, while bZIP10-GFPox and bZIP10^{S19A}-GFPox showed higher susceptibility. Further on, the transgenic lines bZIP10-GFPox and bZIP10^{S19A}-GFPox also showed an increased susceptibility against *Mamestra* feeding suggesting the negative role of bZIP10 in the responses to herbivores and necrotrophic pathogens. The observed phenotypes in this study point towards the possible involvement of bZIP10 either in synthesis of one of the defense hormones or in their signaling crosstalk.

In the JA measurement assay, only a slight increase in JA production was found after 24 h *Botrytis* infection, indicating that the duration of the treatment could have been too short. The amount of JA in *Botrytis* infected *bzip10ko* was lower than that in Col-0 and bZIP10-GFPox. JA production in Col-0 and bZIP10-GFPox was not significantly different

from each other. However, JA levels in bZIP10-GFPox and Col-0 was slightly higher than in their respective mock-treated controls. Increasing the duration of the infection or the concentration of *Botrytis* spores used for inoculation may provide a better insight into the role of bZIP10 in JA biosynthesis. Nevertheless, it can be hypothesized that bZIP10 could be involved in the inhibition of JA-defense signaling pathway downstream to JA synthesis. Over-expression of bZIP10 inhibits the JA-defense pathway more than in Col-0, thereby rendering a more susceptible phenotype. In *bzip10ko*, the absence of bZIP10 probably lifts up the inhibition, causing the JA-defense pathway to be constitutively active, thus making the plants more resistant than Col-0. Since this pathway is constitutively active, a negative feedback loop is perhaps triggered targeting JA production, causing low amounts to be produced since JA would not be required anymore to activate this signaling cascade.

Unlike the case with *Botrytis*, the amount of SA was found to be greatly elevated in Col-0 24 h post *Pst* DC3000 infection, which is in agreement with the previous reports (Vlot, Dempsey et al. 2009, Zheng, Spivey et al. 2012). The SA amount in bZIP10-GFPox and *bzip10ko* was also significantly higher than in their respective mock treated controls and in Col-0, thereby indicating that bZIP10 may not be involved in the production or accumulation of SA upon pathogen infection, and that it most probably functions downstream to the SA biosynthesis pathway. The increased SA level in bZIP10-GFPox correlates with its increased resistance towards *Pst* DC3000. However, even with the increased amounts of SA in *bzip10ko*, the plants were more susceptible to *Pst* DC3000 than Col-0. One possible explanation for this could be that the *bzip10ko* plants are unable to perceive SA. Until now, three proteins NPR1, NPR3 and NPR4 (all three members of Non-expressor of Pathogenesis-Related Genes family) are known to be the SA receptors in *Arabidopsis thaliana*, with NPR1 being the transcriptional co-activator and the master regulator of SA dependent defense response (Seyfferth and Tsuda 2014). In total, about 30 SABPs (SA-Binding Proteins) have been identified, either by purification methodologies (Chen, Silva et al. 1993, Durner and Klessig 1995, Slaymaker, Navarre et al. 2002, Kumar and Klessig 2003, Vlot, Liu et al. 2008), or by high-throughput genome-wide screening (Tian, von Dahl et al. 2012, Manohar, Tian et al. 2014), thereby indicating

that more than a few receptors are involved in SA-mediated responses (Klessig, Tian et al. 2016). Nevertheless, the transcriptional reprogramming mediated by SA is not completely explainable by these SABPs.

In an earlier report, the amount of ProDH1 has been shown to increase upon SA treatment in *Arabidopsis*. The authors also suggested that this increase was due to its transcriptional activation owing to the accumulation of *ProDH1* transcript (Cecchini, Monteoliva et al. 2011). In our study, treatment with SA led to a strong increase in the transactivation of *ProDH1* promoter by bZIP10 (and its phospho-ablative mutant bZIP10^{S19A})/bZIP53 heterodimer in *Arabidopsis* protoplast assay, while bZIP10^{S19D}/bZIP53 heterodimers displayed only a slight increase of the same. However, the possibility that this could have been an effect on bZIP53, and not bZIP10, cannot be excluded. In a very recent study, it was demonstrated that ProDH1 and ProDH2 are required to mount defense against avirulent *Pseudomonas syringae*, where loss of either of them resulted in hyper-sensitivity against the pathogen (Rizzi, Cecchini et al. 2017). This is in agreement with the observed phenotypes against *Pst* DC3000 infection in our study as well. It is possible that bZIP10 is another SA-binding protein, not yet identified to be interacting with SA. Another possibility is that SA does not bind directly to bZIP10 but indirectly affects its function. This, however, needs to be tested further.

Apart from its crucial role in plant defense responses, SA also regulates plant developmental processes such as flowering time (Martinez, Pons et al. 2004), root growth (Jones 2009) and senescence (Buchanan-Wollaston, Page et al. 2005), and physiological processes such as photosynthesis (Mateo, Funck et al. 2006). The root growth assay in our study indicates that the responsiveness of bZIP10 to SA may not be restricted to plant defense responses. However, unlike in SA-dependent immune response, it appears that bZIP10 is functioning antagonistically to SA-mediated root inhibition. Our results show that upon SA treatment of *Arabidopsis* seedlings, the root growth inhibition was slightly, but significantly, less pronounced in bZIP10-GFPox as compared to Col-0. The *bzip10ko* mutant did not show an increased root inhibition when compared to Col-0, which could be attributed to the redundancy often seen among bZIPs. It has been reported earlier that SA-mediated root inhibition is independent of NPR1

signaling. On the contrary, the author suggested the NPR1 signaling may actually counteract the inhibitory effect of SA on root growth (Jones 2009). It is possible that bZIP10 is part of this signaling cascade and thus, aids in SA-dependent pathogen defense responses but antagonizes the SA-mediated inhibition of root elongation.

In addition to SA, the amount of ABA in the three genotypes was found to be slightly elevated in *Pst* DC3000 treated plants when compared to their respective mock treated controls. It has been shown earlier that for stomata closure after *Pst* DC3000 infection, ABA biosynthesis is required and the subsequent closing of stomata is SA-dependent (Melotto, Underwood et al. 2006). The absence of differences in ABA levels among the three genotypes points towards the non-involvement of bZIP10 in ABA biosynthesis in response to *Pst* DC3000. Two methods of *Pst* DC3000 infection were tested- syringe infiltration (**Supplementary Figure 3**) and spray inoculation (**Figure 23**). Both the methods yielded similar phenotypic outcome, indicating that the resistance of bZIP10-GFPox is not because of the differences in stomatal closure between Col-0 and bZIP10-GFPox.

As has been mentioned earlier, the JA defense pathway is comprised of two branches: the JA and ABA regulated MYC-branch, and the JA and ET regulated ERF-branch. Furthermore, the MYC branch regulating the wounding and herbivore defense response has been reported to be antagonistic to the ERF branch regulating the defense responses against the necrotrophs (Pieterse, Van der Does et al. 2012, Wasternack and Hause 2013). It has been shown that *Pieris rapae* (a specialist herbivore of brassicaceous species) feeding on *Arabidopsis thaliana* induces the MYC-branch of JA signaling pathway. The authors reported activation of *MYC2* and *VSP2* in Col-0 after 6 hours of the caterpillar feeding. They also analyzed the expression of *ORA59* (ERF-branch gene) in Col-0 upon *Pieris* feeding and observed very slight induction of *ORA59* at 24 h and 30 h time-points (Verhage, Vlaardingerbroek et al. 2011). To my knowledge, no reports have been published demonstrating the transcriptional response of *Mamestra brassicae* feeding on *Arabidopsis thaliana*. In our study, the expression pattern of *MYC2*, *VSP2* and *ORA59* in Col-0 is in agreement with the previous report mentioned above (Verhage, Vlaardingerbroek et al. 2011), thus validating the experimental set-up used in our study.

MYC2 and *VSP2* (MYC-branch genes), both were induced in all the bZIP10 transgenic and mutant lines analyzed, indicating the non-involvement of bZIP10 in the regulation of these two genes. Additionally, the expression of ERF-branch genes, *ERF1* and *ORA59*, upon *Mamestra* feeding was also analyzed in this experiment. *ERF1* was induced in all the genotypes analyzed at time-points 24 h, 30 h and 48 h. At 6 h, it did seem to be induced only in bZIP10-GFPox and to some extent in Col-0. At 24 hours time-point, *ORA59* was induced in bZIP10-GFPox and bZIP10^{S19A}-GFPox more than in the other lines, indicating that bZIP10 could possibly be involved in regulating the expression of *ORA59*. On the other hand, the similar induction of *ORA59* in the mutant lines, bZIP10^{S19D}-GFPox and *bzip10ko*, and in Col-0 clearly implies the existence of other factors, taking over the role in *ORA59* regulation.

As it is mentioned above, the ERF-branch of JA defense pathway is antagonized by the MYC-branch regulating defense against herbivory (Pieterse, Van der Does et al. 2012). This antagonism occurs downstream to *ERF1* (Lorenzo, Chico et al. 2004), which could explain the increased levels of *ERF1*. Induction of *ERF1* in all the genotypes indicates that bZIP10 is not involved in the regulation of *ERF1*. Similar to *ERF1*, *ORA59* is also known to regulate the ERF-branch of JA defense signaling pathway against necrotrophic pathogens (Pieterse, Van der Does et al. 2012). It has been shown that the plants where ERF-branch is not suppressed are more attractive to the herbivore *Pieris rapae* (Kazan and Manners 2013). This can also explain the hyper-sensitivity of bZIP10-GFPox and bZIP10^{S19A}-GFPox towards *Mamestra* in this study.

In conclusion, overexpression of bZIP10 in *Arabidopsis* plants caused an increased susceptibility against *Mamestra* and *Botrytis*, while exhibiting an increased resistance against *Pst* DC3000. The lines overexpressing bZIP10^{S19D} phospho-mimicking protein form in the Col-0 background indeed demonstrated dominant negative phenotype being comparable with *bzip10ko* plants. On the other hand, ectopic expression of the phospho-ablative bZIP10^{S19A} form rendered plants similar in their responses to bZIP10 over-expressor. Due to the differences in the phenotype of different transgenic and mutant lines of bZIP10 subjected to different biotic stresses, the involvement of bZIP10 in the defense responses towards these stresses is quite apparent. Further analyses need to be

done in order to pinpoint the exact function of bZIP10 in these responses. Nevertheless, it does appear that bZIP10 is positively regulating the SA-mediated defenses while indirectly down regulating the JA-mediated defense pathway, and thereby facilitating the cross talk between SA- and JA-defense pathways in *Arabidopsis thaliana*.

5.3. Redox regulation of bZIP10

Reactive Oxygen Species (ROS) can lead to modification of proteins that is dependent on the chemical properties and sensitivities of certain amino acids. A number of amino acids are known to be oxidized, such as tryptophan, tyrosine, histidine, cysteine and methionine. Of these, the sulfur containing amino acids, cysteines (Cys) and methionines, are the most easily oxidized (Bigelow and Squier 2011, Navrot, Finnie et al. 2011). These amino acids can be reversibly oxidized inducing changes in the structure of a protein, which can subsequently result in protein function modulation (Spadaro, Yun et al. 2010, Nagahara 2011). Such a protein can act as a sensor molecule of the redox status of the cell. For example, YAP1 (AP-1-like transcription factor), a bZIP transcription factor that regulates the oxidative stress response in *Saccharomyces cerevisiae*, is one such protein which acts as a redox sensor. In the native state, YAP1 localizes to both cytoplasm and nucleus. Upon oxidative stress, a reversible intramolecular disulphide bond formation occurs between certain Cys residues in YAP1, which leads to masking of the NES in the protein. This results in constriction of YAP1 to the nucleus and activation of the downstream genes (Wood, Storz et al. 2004).

A NEM-labeling approach was used to determine if the Cys residues in bZIP10 are regulated by redox changes in the cell. The residues Cys 102 and Cys130 were found to be predominantly in the oxidized state, irrespective of the harvesting time. Upon SA treatment, while Cys130 mostly remained oxidized, an increase in the reduced state of Cys102 was observed. These results are in agreement with the PONDR-FIT analysis of bZIP10 amino acid sequence which revealed that the residue Cys102, and not Cys130, is positioned in intrinsically disordered region which might make it more accessible for post-translational modifications. The positionally conserved residue Cys130 was predicted to be in the structured region. The lack of considerable change in its oxidized/reduced state in our mass spectrometric analysis indicates its unavailability for further modification, most probably due to its involvement in structural integrity of bZIP10. The third Cys residue in bZIP10, Cys409, was also predicted to be in the intrinsically disordered region. We could identify only the NEM-labeled peptide containing Cys409. Due to the presence of Lys (K)/ Arg (R) residues (recognition sites for

trypsin) around Cys409, its identification in the mass spectrometric analysis was not always successful.

Apart from bZIP10 peptides, we also identified NEM-labeled and unlabeled peptides of other proteins, thus indicating the reliability of the method. For example, the peptides of β CA1 (Beta carbonic anhydrase 1), also known as SABP3 (Salicylic acid binding protein 3), and GLDP1 (Glycine dehydrogenase 1) were identified in both NEM-labeled (reduced) and unlabeled (oxidized) form. The reduced/oxidized ratio of β CA1 was similar across the different measurements (**Supplementary Figure 4A**). The drastic fluctuations in reduced/oxidized ratio of GLDP1 indicated that it is probably highly sensitive to the redox changes in the cells (**Supplementary Figure 4B**).

The proteomic analysis also revealed the residues Thr371, Ser372 and Ser373 as being possibly phosphorylated, and the residue Lys185 as being potentially acetylated. Further experiments have to be conducted in order to understand the implication of these modified sites. Published reports have shown regulation of other bZIPs by post-translation modifications such as phosphorylation in their DBD (Mair, Pedrotti et al. 2015, Smykowski, Fischer et al. 2015). Like phosphorylation, acetylation is another crucial and reversible post-translational modification known to modulate enzyme activity, protein-protein interactions and protein-DNA interactions (Yang and Seto 2008), to name a few. To my knowledge, only three reports of *Arabidopsis* leaves lysine acetylome are published to date (Finkemeier, Laxa et al. 2011, Wu, Oh et al. 2011, Hartl, Fussl et al. 2017), in none of which, an acetylation event on bZIP10 was detected. For the first time, in this study we report the identification of an acetylation event on Lys185 in bZIP10. It has been shown earlier that acetylation of WRKY transcription factors in *Arabidopsis thaliana* renders them inactive and unable to bind to the DNA (Le Roux, Huet et al. 2015). Similarly, it could be speculated that acetylation of bZIP10 could modulate its DNA binding activity. Unlike in the case of WRKY transcription factors where the acetylation was seen in the DNA binding domain, bZIP10 acetylation was 28 amino acids N-terminal to its DBD. It is still plausible that acetylation could cause- 1) a change in protein structure/folding or 2) an interaction with another protein, thus affecting

bZIP10's DNA-binding capacity. Further experiments need to be conducted to confirm this hypothesis and to understand the importance of this acetylation event.

The peptide containing the DBD of bZIP10 could not be identified. Because the DBD of bZIP10 is rich in the Arg residue, digestion with trypsin (cleaves at the C-terminus of Arg and Lys residues) prior to the mass spectrometric analysis led to generation of such small peptides that could not be identified in the mass spectrometer. For the peptides of DBD to be identified, and especially the Ser19 phosphorylation state, the enzyme LysC was used for digestion of proteins prior to the mass spectrometric analysis. Although we did identify several bZIP10-specific peptides, unfortunately the peptide containing the DBD of bZIP10 could still not be identified. This could have happened because of the amino acid composition of the peptides (possessing positively charged side chains) resulting in their sub-optimal ionization and ability to fly in the mass spectrometer.

Because of the indication derived from the proteomic analysis that the Cys residues in bZIP10 might be playing a role in its redox based regulation, bZIP10 was analyzed for its transactivation capacity in transiently transformed *Arabidopsis* leaf mesophyll protoplasts prepared from *bzip10ko* mutant line. Out of the three Cys mutant combinations tested, only the heterodimers of triple Cys mutant (bZIP10^{C102,130,409A}) displayed a decrease in transactivation, while the heterodimers of the other two Cys mutants behaved like wild-type bZIP10. In the sub-cellular localization assay, the bZIP10^{C102,130,409A} mutant exhibited a stronger cytoplasmic signal than bZIP10 wild-type protein, which correlates with the reduced transactivation capacity of its heterodimers in the transactivation assay. Upon treatment with H₂O₂, the heterodimers of wild-type bZIP10 showed reduced transactivation of *pProDH1* as compared to its mock treated control. This reduction in the transactivation activity was absent in the heterodimers of single Cys mutant (bZIP10^{C409A}) and the double Cys mutant (bZIP10^{C102,130A}) upon H₂O₂ treatment when compared to their respective mock treated controls. The heterodimers of triple Cys mutant exhibited a slight increase in transactivation upon treatment with H₂O₂. However, no differences could be seen in the localization pattern of neither bZIP10 nor bZIP10^{C102,130,409A} upon this treatment. Although it seems that Cys modification could possibly be important for the sub-cellular localization of bZIP10, quantifying it by

transient transformation in protoplasts is not sensitive enough. This problem can be circumvented by generating transgenic lines of *Arabidopsis* stably transformed with genomic construct of bZIP10 under its native promoter or with the use of a switchable fluorescent protein. Unfortunately, even after several attempts made to generate the transgenic lines, no positive transformants could be obtained. Based on the transactivation assay results, it seems that all the three Cys residues in bZIP10 might be important for its regulation as none of the three Cys mutant combinations tested behaved like the wild-type bZIP10.

The protoplast two-hybrid experiment revealed that the decrease in transactivation capacity of heterodimers of bZIP10 upon H₂O₂ treatment was not because of its reduced dimerization with bZIP53, thus indicating that either conformational change of bZIP10 itself or another protein, not yet known, might be involved in this regulation. Upon H₂O₂ treatment, bZIP10^{C409A} and bZIP10^{C102,130,409A} mutants did show a decrease in their heterodimerization with bZIP53 but this was not accompanied by a decrease in their activity in the transactivation assay, possibly indicating the involvement of another protein that is regulating bZIP10's activity. As a possible candidate, the SA receptor NPR1 might be proposed for this role. As mentioned earlier, salicylic acid has been known to cause a change in the cellular redox state (Tada, Spoel et al. 2008), which leads to the reduction of intermolecular disulfide bonds between the Cys residues of NPR1. This activated NPR1 then interacts with TGA factors, D-group bZIPs, to activate the defense gene expression and establish SAR (Systemic Acquired Resistance). It has been shown that TGA1 and TGA4 can form intramolecular disulfide bridges and that reduction of these Cys residues is indispensable for their interaction with NPR1. SA has been shown to be able to reduce these Cys residues and thereby facilitating the NPR1-TGA interaction (Despres, Chubak et al. 2003).

It has been reported in an earlier study that LSD1 interacts with bZIP10, and that this interaction caused bZIP10 cytoplasmic retention and inhibited the DNA binding ability of bZIP10 *in vitro* (Kaminaka, Nake et al. 2006). Therefore, we hypothesized that LSD1 could be regulating the redox-dependent localization and activity of bZIP10. The localization with LSD1 under H₂O₂ treatment was analyzed. However, no differences in

sub-cellular localization pattern of bZIP10 and its triple Cys mutant bZIP10^{C102,130,409A} could be seen neither without nor upon H₂O₂ treatment in the presence of LSD1. Very strong fluorescent signal was observed both in the cytoplasm and in the nucleus due to LSD1-mCherry overexpression. I also tried to clone *LSD1* driven by its own promoter but in spite of utilizing different cloning approaches, this task could not be accomplished.

The interaction of bZIP10 with LSD1 was further analyzed under the influence of oxidative stress. No differences could be seen between bZIP10 and bZIP10^{C102,130,409A} mutant with respect to their interaction with LSD1 in the presence or absence of H₂O₂, as indicated via yeast two-hybrid and FRET-FLIM. In the transactivation assay performed in *Arabidopsis* leaf mesophyll protoplast prepared from *bzip10ko* line, LSD1 could have had an effect on the transactivation capacity of bZIP10/bZIP53 heterodimer. In order to analyze this, the transactivation assay was repeated in *Arabidopsis* leaf mesophyll protoplasts prepared from *bzip10/lsd1ko* line with wild-type bZIP10, its single Cys mutant (bZIP10^{C409A}) and its triple Cys mutant (bZIP10^{C102,130,409A}). Both in the presence and absence of H₂O₂, a similar pattern (as in the case of *bzip10ko* protoplasts) was obtained, with the only exception that there was no change in the transactivation capacity of the triple Cys mutant bZIP10^{C102,130,409A} upon H₂O₂ treatment compared to its mock. In the presence of LSD1 (expressed exogenously), this pattern remained the same except that the triple Cys mutant bZIP10^{C102,130,409A} also behaved like the wild-type bZIP10. Upon H₂O₂ treatment, only wild-type bZIP10 showed a decrease in the transactivation capacity while both the Cys mutants showed no effect. Thus it appears that LSD1 is not involved in the transactivation of *pProDH1* by bZIP10/bZIP53 heterodimers.

ABI3 (Abscisic Acid Insensitive 3), have also been reported to interact with bZIP10/bZIP53 heterodimer and enhance the activation of the target genes (Alonso, Onate-Sanchez et al. 2009). ABI3 could be another possible candidate regulating the activity of bZIP10. It will be interesting to perform the transactivation assays and the protoplast two-hybrid assays in *Arabidopsis* leaf mesophyll protoplasts prepared from *bzip10/abi3* double knock out mutant line to examine if ABI3 has any effect on the heterodimer formation between Cys mutants of bZIP10 and bZIP53 or their transactivation capacity.

To elucidate the involvement of Cys-based redox regulation of bZIP10, it will be interesting to analyze the Cys to Ala mutants of the S1-group bZIPs, all five of which have either one or two C-terminus Cys residue that may be involved in the inter-molecular disulfide bond formation with Cys409 in bZIP10. The Cys mutant of bZIP53, bZIP53^{C146A} displayed decreased heterodimerization with bZIP10 in a protoplast two-hybrid experiment (preliminary data, data not shown). The corresponding Cys mutants of all the five S1-group bZIPs have been generated and their analyses is in the pipeline.

5.4. Identification of ASN1 as a direct target of bZIP10

Different treatments were performed in order to find out the condition when bZIP10 is the most active. It looks like *ProDH2* and *BCAT2* could be controlled by bZIP10 in the control conditions, however, this is not the case in none of the other conditions tested. The absence of enrichment of these two genes in the ChIP-qPCR confirms our results.

In the control plants, over-expression of bZIP10 did not seem to have any effect on the expressions of *ProDH1* and *ProDH2* as compared to Col-0 under control conditions. We observed an increase in *ProDH1* activation by bZIP10/bZIP53 heterodimers in the *Arabidopsis* protoplast assay; however, this increased *ProDH1* expression was absent in bZIP10-GFPox line relative to Col-0. In the protoplast assay, the increase in *ProDH1* activation was seen in the presence of both, bZIP10 and bZIP53. However, when bZIP10 was expressed alone, no such increase was seen (**Figure 10**). As mentioned earlier, the S1-group bZIPs are translationally repressed by sucrose in a process known as SIRT (Sucrose Induced Repression of Translation) (Dietrich, Weltmeier et al. 2011). Because the gene expression was analyzed in the leaves harvested during the day, the presence of sugars in the cells would have led to the absence of bZIP53. This could explain the similar expression level of *ProDH1* in bZIP10-GFPox and Col-0. On the contrary, under prolonged dark conditions, the expression of *ProDH1* was higher in bZIP10-GFPox and lower in bZIP10^{S19D}-GFPox, when compared to Col-0, which indicates the involvement of bZIP10 in the regulation of this gene upon the extended night treatment. Out of all the tested conditions, the extended night treatment displayed the most specific response in the expression of some of the genes analyzed, which also fits well with SIRT regulation of S1 bZIPs.

In the bZIP10^{S19D}-GFPox line, a weaker *ProDH1* and *ProDH2* expression was observed as compared to that in bZIP10-GFPox, thereby confirming the dominant negative nature of the bZIP10^{S19D} mutation. The decreased expression of *ProDH1* upon H₂O₂ treatment is in agreement with our transactivation assays in *Arabidopsis* protoplasts.

The increased expression of *ASN1* in bZIP10ox line, as compared to Col-0, indicates that bZIP10 might be directly involved in the induction of *ASN1*. Its similar expression in bZIP10^{S19D}-GFPox line and Col-0 under light (control) conditions could be attributed to its co-activation by bZIP1 or bZIP53, which have been shown to be able to bind to the promoter of *ASN1* (Weltmeier, Ehlert et al. 2006, Dietrich, Weltmeier et al. 2011). As mentioned above, these S1-group proteins are, most probably, absent or present at a very low level in the light-growing plants. *ASN1* have been shown to be involved in the starvation response and is regulated by the members of C/S1 bZIP network. Because the S1-group bZIPs demonstrate SIRT, the extended night-induced *ASN1* levels correlate with the protein levels of S1-group bZIPs (Dietrich, Weltmeier et al. 2011).

Indeed, only *ASN1* was enriched in the immunoprecipitated sample compared to its input control. For our ChIP experiment, the plants were kept in dark for extended period before performing ChIP, and thus the identification of *ASN1* also correlates well. These data clearly support the suggestion that *ASN1* promoter is, one of the direct target genes of bZIP10. None of the other promoters analyzed were enriched after immunoprecipitation.

The *ASN1* gene encodes a glutamine-dependent enzyme asparagine synthetase which converts glutamine (Gln) to asparagine (Asn) (Lam, Peng et al. 1994, Lam, Wong et al. 2003). Asn is an ideal metabolite for nitrogen transportation and storage because of two properties: the nitrogen to carbon ratio in Asn is higher (compared to Gln), and it is relatively inert (compared to Glu, Asp and Gln) (Lam, Wong et al. 2003). Nitrogen mobilization and storage plays an important role in normal growth and development of plants. During seed germination, the photosynthetic machinery of seedlings is built from the nitrogen derived from the seed storage proteins. Also, nitrogen from senescent tissues is transported to other developing parts of the plant where it can be utilized in several biosynthetic processes (Olea, Perez-Garcia et al. 2004). Apart from its role in carbon/nitrogen metabolism in plants, asparagine synthetase has been proposed to impart resistance to plants against biotrophic pathogens by facilitating host cell death. This strategy, however, may not work against the necrotrophs and make the plants susceptible (Seifi, De Vleeschauwer et al. 2014). This invasion-triggered senescence, known as the slash and burn defense strategy, comprises of transportation of ammonium

(generated by catabolism of amino acids) in the form of Asn or Gln, away from the infected site. This could either lead to the conservation of the nitrogen content of the host or deprive the pathogen of its nutrients (Seifi, Van Bockhaven et al. 2013). In a previous report, it has been shown that an early induction of asparagine synthetase in pepper is important for resistance against the hemibiotroph *Xanthomonas campestris* pv. *vesicatoria* while its later induction correlated with the susceptibility of the plants. Similar results were obtained upon infecting transgenic *Arabidopsis* plants, which over-expressed pepper asparagine synthetase, with *Pseudomonas syringae* and the biotroph *Hyaloperonospora arabidopsidis* (Hwang, An et al. 2011). The phenotypic outcomes obtained in our pathogen assays against *Pseudomonas syringae* and *Botrytis cinerea* correlate well with the above-mentioned defense strategy. Hence it appears that bZIP10 could be involved in the defense responses against pathogens via its regulation of *ASN1*. Nevertheless, further experimentation needs to be done in order to confirm this.

5.5. Target gene identification attempt by Chromatin

Immunoprecipitation (ChIP-Seq)

With the pilot experiment being successful with the identification of *ASN1* as a direct target gene of bZIP10, we then proceeded further. *ASN1* was an educated guess, but there could be more direct targets of bZIP10. To identify those, ChIP-Seq was performed to identify those targets.

The analysis of the prepared DNA libraries on Agilent High Sensitivity DNA chip using Agilent Technologies 2100 Bioanalyzer revealed a nice size distribution from ~250-550 bp for the eGFPox sample (control). However, the following problems were encountered in the remaining samples:

1. There was a phantom peak appearing before the main peak, at around 300 bp.
2. They exhibited an increased size distribution ranging from ~250 bp to >1000 bp followed by a tail of ~>5000 bp to >10,000 bp.

A PCR artifact can cause a double peak in a library sample but that cannot be the case here because usually the first peak is half the size of the second one. Here, the main peak is around 500 bp and the phantom peak is at 300 bp. So it cannot be a PCR artifact. This double peak could be caused by over amplification of DNA during the final PCR step. The most likely explanation for this could be that two strands of DNA that do not match in the middle got annealed together resulting in a strange run on the Bioanalyzer chip. However, this was not a concern because the DNA is denatured before loading for sequencing.

The tailing effects in library preparations can be a consequence of incomplete shearing of DNA in the Bioanalyzer, when a large amount of DNA is being used for shearing. Indeed, because of the low amount of DNA obtained after immunoprecipitation, a larger size range was used in elution from the Blue Pippin. Also, this could have happened due to too many PCR cycles leading to over amplification of DNA during the library preparation, which may cause the double peaks as well. One way to circumvent this problem could be to perform less PCR cycles during the library preparation.

A single end 150 bp sequencing run is normally sufficient for ChIP-Seq. However, because of the above issues with the quality of the prepared libraries, a 250 bp paired end test sequencing run was performed on the MiSeq. This had several advantages:

1. Longer reads provide a more comprehensive view of the DNA fragments.
2. Problems such as resolving splicing, structural re-arrangement, *de novo* assembly of repetitive regions are taken care of with the longer reads. It also improves mapping in general.
3. Longer reads help in more specific removal of PCR duplicates, and offer better estimation of average fragment length distribution.
4. It is easier to differentiate between the signal and noise in the downstream peak calling analysis of the paired end sequencing generated strand specific-reads because a true signal will comprise of two equal magnitude peaks on the complementary strands.
5. In case the ChIP-Seq is being performed in the highly repetitive region of the genome, it is possible to anchor the read pairs generated from paired end sequencing in a non-repetitive region of the genome, consequently leading to more reliable final mapping.
6. The ability of identifying the relative positions of the reads in the genome is improved by paired end sequencing.

For the data analysis, the reads obtained were assumed to be single end in order to increase the number of reads. The plan was to perform the paired end read mapping after obtaining successful results from this analysis.

Upon plotting the number of reads that were originally present and quality filtered, the same imbalance is seen as in the case of MiSeq run. The initial sequence analysis verified the readout of the MiSeq run: the reads are derived disproportionately from certain samples. In summary, ~80 % of all the reads identified in the experiment are derived from two samples only (bZIP10-GFPox (*Pst* DC3000 infiltrated) and bZIP10-GFPox), indicating the non-equimolar pooling of the libraries resulting in an imbalanced multiplex library. This might be ascribed to the low concentration inputs for the library preparation, with its concomitant high pipetting errors.

The quality filtered reads were mapped using two different alignment tools: Bowtie2 and Tophat2. Irrespective of the alignment tool used, most of the reads do not align to the *Arabidopsis thaliana* TAIR10 genome. In majority of the samples, the reads predominantly align to the human genome, with only a small fraction mapping to *Arabidopsis thaliana*, *Escherichia coli* and *Saccharomyces cerevisiae*. Only the eGFOox sample showed an alignment of ~50 % of the reads to the *Arabidopsis thaliana* genome (using Bowtie2), which correlates nicely with its good library quality. The NRF value being ~100 fold too large indicated the identification of only a small set of uniquely mapped regions on the genome, without covering most of it. This is in consonance with the result that most of the reads do not map to the *Arabidopsis thaliana* genome.

Even after a successful pilot experiment, the outcome of ChIP-Seq experiment was not as expected. The major problems were the low number of sequencing reads and their unequal distribution originating from certain samples. Both the problems could be ascribed to the low amount of DNA obtained after chromatin immunoprecipitation, hence the method needs further optimization so as to increase the amount of immunoprecipitated DNA for library preparation. In this case here, GFP-Trap_MA (magnetic agarose beads with anti-GFP nanobody immobilized on them, from ChromoTek) was used for immunoprecipitation of the fragmented cross-linked genomic DNA because of its ease of use and good results in the immunoprecipitation of GFP tagged bZIP10 for the proteomic analysis (see section 4.3.1.). It is possible that GFP tagged bZIP10 already bound to DNA is not able to bind to the nanobody. Therefore it might help to change the antibody for immunoprecipitation of chromatin bound GFP tagged bZIP10. The anti-GFP antibody from Abcam has been successfully used previously for immunoprecipitating chromatin bound GFP tagged proteins (Liu, Gao et al. 2016, Kim and Sung 2017). Alternatively, instead of GFP tagged bZIP10, an HA tagged version of bZIP10 could be used. Being a smaller tag than GFP, HA tag may incur less steric hindrance and therefore possibly result in its better binding to the antibody.

Based on a previous report (Watson, Kitching et al. 2000), an alternative approach to identify the direct genomic targets of bZIP10 could also be applied. The linker ligated, fragmented genomic DNA from *Arabidopsis thaliana* could be incubated with bZIP10 and

an appropriate antibody. After elution of bZIP10 bound DNA fragments from the antibody, the recovered fragments could be sub-cloned for sequencing and further analysis. This approach has been used to successfully identify the genomic target sequences of WRKY53 transcription factor (Miao, Laun et al. 2004).

5.6. Proteomic screen for bZIP10 interaction partners

For a better understanding of the function of bZIP10 in *Arabidopsis thaliana*, a proteomics-based interaction screen was carried out. More than 200 proteins were identified as putative bZIP10 interactors, the physiological relevance of which needs to be tested by further experimentation. However, some of them need a special mention. For example, LOX2 (lipoxygenase 2), CAT3 (catalase 3) and β CA1 (Beta carbonic anhydrase 1) were identified as putative bZIP10 interaction partners upon SA treatment.

LOX2 has been reported to be involved in the wounding response in *Arabidopsis* leaves by being responsible for the wound-induced biosynthesis of JA (Wasternack and Hause 2013). It has also been shown to function downstream to MYC2 in the JA-defense signaling pathway (Bu, Jiang et al. 2008). Previously in section 5.2, the possible role of bZIP10 in the regulation of JA-defense pathway has been discussed. Based on that hypothesis, it can be speculated that bZIP10 mediated inhibition of JA-defense signaling pathway could be a result of its interaction with LOX2. However, as mentioned earlier, this interaction needs to be confirmed by performing further experiments.

In a report published earlier, LSD1 was shown to interact with all the three catalases (CAT1, CAT2 AND CAT3) in *Arabidopsis* and thereby regulating the HR induced cell death (Li, Chen et al. 2013). The authors reported that binding of LSD1 to catalases enhanced their activity and that in the *lsd1* mutant, reduced catalase activity led to an increase in pathogen induced cell death. Furthermore, they also demonstrated that LSD1 and catalases regulated HR cell death require SA accumulation (Li, Chen et al. 2013). LSD1 and bZIP10 have been known to be functioning antagonistic to each other, with LSD1 negatively regulating the ROS-induced cell death and HR response in *Arabidopsis* and vice versa for bZIP10 (Kaminaka, Nake et al. 2006). LSD1 could do this by interacting with catalases and enhancing their activity which in turn reduce the hydrogen peroxide levels in the cells. To my knowledge, the mechanism by which the interaction of LSD1 and catalases influences their activity is not known yet. We found, in our proteomic analysis, that bZIP10 could be interacting with CAT3 upon SA treatment. Although this interaction needs to be confirmed, it can be speculated that, working antagonistic to LSD1, bZIP10

interacts with CAT3 and reduces its activity leading to an increase in hydrogen peroxide levels in the cells causing cell death. This could be another possible explanation for the hyper-sensitivity of *bzip10ko* mutant to *Pst* DC3000. It has been discussed in section 5.1 that bZIP10 is possibly functioning downstream to SA biosynthesis in SA-defense pathway. It has been reported that SA can bind to CAT2 and inhibit its activity consequently leading to the inhibition of auxin accumulation and JA biosynthesis (Yuan, Liu et al. 2017). The interaction of bZIP10 with CAT3 could have the same implications. Although the authors also showed that *cat1* and *cat3* mutants did not affect IAA and JA biosynthesis, but this could have happened because the expression of all the three catalases in *Arabidopsis*, and SA and JA biosynthesis are regulated by the circadian rhythm, with *CAT2* being the morning-phased gene, and *CAT1* and *CAT3* being the evening-phased genes (Mwimba and Dong 2017).

β CA1, also known as SABP3 (Salicylic acid binding protein 3), has been shown to be involved in mounting the defense against avirulent *Pst* DC3000(*avrB*). The *sabp3* mutants displayed enhanced growth of the pathogen as compared to the wild-type (Wang, Feechan et al. 2009). Although identified as a chloroplastic protein in our analyses, it has been reported recently that, among others, the cytosolic version of this protein is also produced from the *β CA1* gene in *Arabidopsis*. Recently, SABP3 has been shown to be involved in the perception of SA as well as to interact with NPR1, thereby implicating it in the SA-mediated plant defense responses (Medina-Puche, Castello et al. 2017).

Among others, CPK5/CPK6 (Calcium-dependent Protein Kinase 5/6), TRX3 (Thioredoxin H3), TPL (TOPLESS) and PP2A (type 2A protein phosphatases) were identified as the potential bZIP10 interaction partners in the untreated sample. In plants, certain members of CPK family have been shown to be involved in plant defense responses. CPK5 (and its closely related CPK6), along with CPK4 and CPK11, in *Arabidopsis thaliana* were found to be involved in FLS2 (flagellin sensitive 2) mediated innate immune signaling (Boudsocq, Willmann et al. 2010). Furthermore, it was shown that CPK5, upon activation by pathogen associated molecular pattern (PAMP) stimuli, signaling conferred salicylic acid mediated resistance to plants against *Pst* DC3000 (Dubiella, Seybold et al. 2013). Most interestingly, however, the C-group bZIPs have been shown to be phosphorylated

by different members of the CPK family. The residue Ser11 in the DBD of all the four members of C-group bZIPs was found to be phosphorylated by CPK6 *in vitro*. Upon analyzing the *in vivo* interaction of CPK6 with the C-group bZIPs, CPK6 specifically interacted only with bZIP10. However, no *in vitro* phosphorylation at Ser19 residue in the DBD of bZIP10 was detected (Kirchler 2014). The identification of CPK5/6 in our bZIP10 interaction screen points towards the integrity of the experimental set-up employed in this screen.

TRX-H3 are the reductases which, upon changes in the cellular redox status by salicylic acid produced in response to pathogen attack, reduce the inter-molecular cysteine disulfide bonds in NPR1 leading to its monomerization and subsequently activation of PR genes (Pieterse, Van der Does et al. 2012). The TPL co-repressor is known to be involved in numerous plant processes such as floral transition, hormonal responses, and biotic and abiotic stress responses (Causier, Ashworth et al. 2012). For example, it is recruited by the adaptor protein NINJA (Novel Interactor of JAZ) to repress the activation of JA defense pathway in the absence of a stimulus (Pieterse, Van der Does et al. 2012). Similarly to TPL, PP2A is also known to be implicated in various plant processes such as root growth, light signaling, stress signaling and hormone signaling (Uhrig, Labandera et al. 2013).

All the above-mentioned putative interaction partners of bZIP10 are known to play a role in, among others, the stress responses in plants. As mentioned earlier, although the interaction of these proteins with bZIP10 requires further verification, this proteomic screen provide valuable clues regarding the function and regulation of bZIP10.

6. Conclusion

The functional importance of bZIP10 in the regulation of the plant biotic stress responses and its possible mode of regulation has been elucidated in this thesis. The major conclusions of this study are as follows:

1. The analyses of the phospho-mimicking and phospho-ablative mutant forms of bZIP10 indicate that the Ser19Asp mutation in the DBD of bZIP10 inhibits the activity of bZIP10 by preventing it from binding to DNA and limiting it to the cytoplasm. This mutation, however, does not affect the heterodimerization of bZIP10 with the S1-group partner. Thus, this mutation can be used to generate a dominant negative form of bZIP10, which will form heterodimers but will not initiate the transcription of bZIP10-dependent genes. This can be used as a tool to circumvent the problem of redundancy in the bZIP factors.
2. For the functional characterization of bZIP10, the transgenic lines of *Arabidopsis* over-expressing bZIP10 and its phosphorylation mutant forms were generated and used in the pathogen assays. These assays indicate that bZIP10 is involved in the positive regulation of SA-mediated defense against biotrophic pathogens. On the other hand, it might be acting as a negative regulator of JA-mediated defense responses, and thus be participating in the SA-JA cross talk.
3. The mass spectrometry based analyses of the Cys residues in bZIP10 indicates that under ambient (control) conditions, the N-terminal residues are predominantly oxidized. It seems that salicylic acid may cause a shift towards a more reduced state of Cys102, however a quantitative proteomics analysis is required to verify this possibility. The importance of potentially redox-regulated thiols for the proper protein function is demonstrated by the altered transactivity of bZIP10 upon substitution of Cys residues: the induction of *ProDH1* by the heterodimers of bZIP10 Cys mutants with bZIP53 was reduced in control conditions but in contrast to wild-type bZIP10, increased during hydrogen peroxide treatment. Yet, the observed changes in the transactivation do not

seem to correlate with the capacity of bZIP10 Cys mutants to form heterodimers with bZIP53.

4. The ChIP-qPCR and gene expression analyses identified *ASN1* as a possible direct genomic target of bZIP10. The phenotypic outcome of our pathogen assays is in agreement with the earlier reported phenotypic outcome of pathogen assays performed with the *Arabidopsis* plants containing modified levels of *ASN1*. This indicates that the bZIP10-dependent regulation of defense responses may occur, at least partially, via its regulation of *ASN1* activity.

5. The mass spectrometry based proteomics screen identified several candidates as putative bZIP10 interactors. Among others, there are proteins known to be involved in the defense responses in *Arabidopsis*. This screen thus provides valuable data for further study regarding the regulation and function of bZIP10.

7. References

- Abe, M., Y. Kobayashi, S. Yamamoto, Y. Daimon, A. Yamaguchi, Y. Ikeda, H. Ichinoki, M. Notaguchi, K. Goto and T. Araki (2005). "FD, a bZIP protein mediating signals from the floral pathway integrator FT at the shoot apex." *Science* **309**(5737): 1052-1056.
- Akter, S., J. Huang, C. Waszczak, S. Jacques, K. Gevaert, F. Van Breusegem and J. Messens (2015). "Cysteines under ROS attack in plants: a proteomics view." *J Exp Bot* **66**(10): 2935-2944.
- Albertos, P., M. C. Romero-Puertas, K. Tatematsu, I. Mateos, I. Sanchez-Vicente, E. Nambara and O. Lorenzo (2015). "S-nitrosylation triggers ABI5 degradation to promote seed germination and seedling growth." *Nat Commun* **6**: 8669.
- Alonso, R., L. Onate-Sanchez, F. Weltmeier, A. Ehlert, I. Diaz, K. Dietrich, J. Vicente-Carbajosa and W. Droge-Laser (2009). "A pivotal role of the basic leucine zipper transcription factor bZIP53 in the regulation of Arabidopsis seed maturation gene expression based on heterodimerization and protein complex formation." *Plant Cell* **21**(6): 1747-1761.
- Alves, M. S., S. P. Dadalto, A. B. Goncalves, G. B. De Souza, V. A. Barros and L. G. Fietto (2013). "Plant bZIP transcription factors responsive to pathogens: a review." *Int J Mol Sci* **14**(4): 7815-7828.
- Amorim, L. L. B., R. da Fonseca Dos Santos, J. P. B. Neto, M. Guida-Santos, S. Crovella and A. M. Benko-Iseppon (2017). "Transcription Factors Involved in Plant Resistance to Pathogens." *Curr Protein Pept Sci* **18**(4): 335-351.
- Arabidopsis Genome Initiative (2000). "Analysis of the genome sequence of the flowering plant Arabidopsis thaliana." *Nature* **408**(6814): 796-815.
- Baena-Gonzalez, E., F. Rolland, J. M. Thevelein and J. Sheen (2007). "A central integrator of transcription networks in plant stress and energy signalling." *Nature* **448**(7156): 938-942.
- Begara-Morales, J. C., B. Sánchez-Calvo, M. Chaki, R. Valderrama, C. Mata-Pérez, F. J. Corpas and J. B. Barroso (2016). Protein S-Nitrosylation and S-Glutathionylation as Regulators of Redox Homeostasis During Abiotic Stress Response. *Redox State as a Central Regulator of Plant-Cell Stress Responses*. D. Gupta, J. Palma and F. Corpas, Springer, Cham.
- Begara-Morales, J. C., B. Sanchez-Calvo, M. Chaki, R. Valderrama, C. Mata-Perez, M. N. Padilla, F. J. Corpas and J. B. Barroso (2016). "Antioxidant Systems are Regulated by Nitric Oxide-Mediated Post-translational Modifications (NO-PTMs)." *Front Plant Sci* **7**: 152.
- Berens, M. L., H. M. Berry, A. Mine, C. T. Argueso and K. Tsuda (2017). "Evolution of Hormone Signaling Networks in Plant Defense." *Annu Rev Phytopathol* **55**: 401-425.
- Bigelow, D. J. and T. C. Squier (2011). "Thioredoxin-dependent redox regulation of cellular signaling and stress response through reversible oxidation of methionines." *Mol Biosyst* **7**(7): 2101-2109.
- Boudsocq, M., M. R. Willmann, M. McCormack, H. Lee, L. Shan, P. He, J. Bush, S. H. Cheng and J. Sheen (2010). "Differential innate immune signalling via Ca(2+) sensor protein kinases." *Nature* **464**(7287): 418-422.
- Breathnach, R. and P. Chambon (1981). "Organization and expression of eucaryotic split genes coding for proteins." *Annu Rev Biochem* **50**: 349-383.
- Brunet, A., J. Park, H. Tran, L. S. Hu, B. A. Hemmings and M. E. Greenberg (2001). "Protein kinase SGK mediates survival signals by phosphorylating the forkhead transcription factor FKHL1 (FOXO3a)." *Mol Cell Biol* **21**(3): 952-965.
- Bu, Q., H. Jiang, C. B. Li, Q. Zhai, J. Zhang, X. Wu, J. Sun, Q. Xie and C. Li (2008). "Role of the Arabidopsis thaliana NAC transcription factors ANAC019 and ANAC055 in regulating jasmonic acid-signaled defense responses." *Cell Res* **18**(7): 756-767.
- Buchanan-Wollaston, V., T. Page, E. Harrison, E. Breeze, P. O. Lim, H. G. Nam, J. F. Lin, S. H. Wu, J. Swidzinski, K. Ishizaki and C. J. Leaver (2005). "Comparative transcriptome analysis reveals

- significant differences in gene expression and signalling pathways between developmental and dark/starvation-induced senescence in Arabidopsis." *Plant J* **42**(4): 567-585.
- Buratowski, S. (1994). "The basics of basal transcription by RNA polymerase II." *Cell* **77**(1): 1-3.
- Buratowski, S., S. Hahn, L. Guarente and P. A. Sharp (1989). "Five intermediate complexes in transcription initiation by RNA polymerase II." *Cell* **56**(4): 549-561.
- Caarls, L., C. M. Pieterse and S. C. Van Wees (2015). "How salicylic acid takes transcriptional control over jasmonic acid signaling." *Front Plant Sci* **6**: 170.
- Causier, B., M. Ashworth, W. Guo and B. Davies (2012). "The TOPLESS interactome: a framework for gene repression in Arabidopsis." *Plant Physiol* **158**(1): 423-438.
- Cecchini, N. M., M. I. Monteoliva and M. E. Alvarez (2011). "Proline dehydrogenase contributes to pathogen defense in Arabidopsis." *Plant Physiol* **155**(4): 1947-1959.
- Chen, Z., H. Silva and D. F. Klessig (1993). "Active oxygen species in the induction of plant systemic acquired resistance by salicylic acid." *Science* **262**(5141): 1883-1886.
- Cheng, H., W. Deng, Y. Wang, J. Ren, Z. Liu and Y. Xue (2014). "dbPPT: a comprehensive database of protein phosphorylation in plants." *Database (Oxford)* **2014**: bau121.
- Choi, H., J. Hong, J. Ha, J. Kang and S. Y. Kim (2000). "ABFs, a family of ABA-responsive element binding factors." *J Biol Chem* **275**(3): 1723-1730.
- Choudhury, F. K., R. M. Rivero, E. Blumwald and R. Mittler (2017). "Reactive oxygen species, abiotic stress and stress combination." *Plant J* **90**(5): 856-867.
- Correa, L. G., D. M. Riano-Pachon, C. G. Schrago, R. V. dos Santos, B. Mueller-Roeber and M. Vincentz (2008). "The role of bZIP transcription factors in green plant evolution: adaptive features emerging from four founder genes." *PLoS One* **3**(8): e2944.
- Couturier, J., K. Chibani, J. P. Jacquot and N. Rouhier (2013). "Cysteine-based redox regulation and signaling in plants." *Front Plant Sci* **4**: 105.
- Cremers, C. M. and U. Jakob (2013). "Oxidant sensing by reversible disulfide bond formation." *J Biol Chem* **288**(37): 26489-26496.
- Davis, S. J. and R. D. Vierstra (1998). "Soluble, highly fluorescent variants of green fluorescent protein (GFP) for use in higher plants." *Plant Mol Biol* **36**(4): 521-528.
- Dempsey, D. A. and D. F. Klessig (2017). "How does the multifaceted plant hormone salicylic acid combat disease in plants and are similar mechanisms utilized in humans?" *BMC Biol* **15**(1): 23.
- Deppmann, C. D., T. M. Thornton, F. E. Utama and E. J. Taparowsky (2003). "Phosphorylation of BATF regulates DNA binding: a novel mechanism for AP-1 (activator protein-1) regulation." *Biochem J* **374**(Pt 2): 423-431.
- Despres, C., C. Chubak, A. Rochon, R. Clark, T. Bethune, D. Desveaux and P. R. Fobert (2003). "The Arabidopsis NPR1 disease resistance protein is a novel cofactor that confers redox regulation of DNA binding activity to the basic domain/leucine zipper transcription factor TGA1." *Plant Cell* **15**(9): 2181-2191.
- Dietrich, K., F. Weltmeier, A. Ehlert, C. Weiste, M. Stahl, K. Harter and W. Droge-Laser (2011). "Heterodimers of the Arabidopsis transcription factors bZIP1 and bZIP53 reprogram amino acid metabolism during low energy stress." *Plant Cell* **23**(1): 381-395.
- Djamei, A., A. Pitzschke, H. Nakagami, I. Rajh and H. Hirt (2007). "Trojan horse strategy in Agrobacterium transformation: abusing MAPK defense signaling." *Science* **318**(5849): 453-456.
- Dubiella, U., H. Seybold, G. Durian, E. Komander, R. Lassig, C. P. Witte, W. X. Schulze and T. Romeis (2013). "Calcium-dependent protein kinase/NADPH oxidase activation circuit is required for rapid defense signal propagation." *Proc Natl Acad Sci U S A* **110**(21): 8744-8749.
- Durner, J. and D. F. Klessig (1995). "Inhibition of ascorbate peroxidase by salicylic acid and 2,6-dichloroisonicotinic acid, two inducers of plant defense responses." *Proc Natl Acad Sci U S A* **92**(24): 11312-11316.

- Dynlacht, B. D., T. Hoey and R. Tjian (1991). "Isolation of coactivators associated with the TATA-binding protein that mediate transcriptional activation." *Cell* **66**(3): 563-576.
- Edison, A. S., R. D. Hall, C. Junot, P. D. Karp, I. J. Kurland, R. Mistrik, L. K. Reed, K. Saito, R. M. Salek, C. Steinbeck, L. W. Sumner and M. R. Viant (2016). "The Time Is Right to Focus on Model Organism Metabolomes." *Metabolites* **6**(1).
- Ehlert, A., F. Weltmeier, X. Wang, C. S. Mayer, S. Smeeckens, J. Vicente-Carbajosa and W. Droge-Laser (2006). "Two-hybrid protein-protein interaction analysis in Arabidopsis protoplasts: establishment of a heterodimerization map of group C and group S bZIP transcription factors." *Plant J* **46**(5): 890-900.
- Fancy, N. N., A. K. Bahlmann and G. J. Loake (2017). "Nitric oxide function in plant abiotic stress." *Plant Cell Environ* **40**(4): 462-472.
- Finkemeier, I., M. Laxa, L. Miguet, A. J. Howden and L. J. Sweetlove (2011). "Proteins of diverse function and subcellular location are lysine acetylated in Arabidopsis." *Plant Physiol* **155**(4): 1779-1790.
- Foster, R., T. Izawa and N. H. Chua (1994). "Plant bZIP proteins gather at ACGT elements." *FASEB J* **8**(2): 192-200.
- Frankel, A. D. and P. S. Kim (1991). "Modular structure of transcription factors: implications for gene regulation." *Cell* **65**(5): 717-719.
- Fujii, Y., T. Shimizu, T. Toda, M. Yanagida and T. Hakoshima (2000). "Structural basis for the diversity of DNA recognition by bZIP transcription factors." *Nat Struct Biol* **7**(10): 889-893.
- Fujita, Y., M. Fujita, R. Satoh, K. Maruyama, M. M. Parvez, M. Seki, K. Hiratsu, M. Ohme-Takagi, K. Shinozaki and K. Yamaguchi-Shinozaki (2005). "AREB1 is a transcription activator of novel ABRE-dependent ABA signaling that enhances drought stress tolerance in Arabidopsis." *Plant Cell* **17**(12): 3470-3488.
- Grefen, C., P. Obrdlik and K. Harter (2009). "The determination of protein-protein interactions by the mating-based split-ubiquitin system (mbSUS)." *Methods Mol Biol* **479**: 217-233.
- Hardtke, C. S., K. Gohda, M. T. Osterlund, T. Oyama, K. Okada and X. W. Deng (2000). "HY5 stability and activity in Arabidopsis is regulated by phosphorylation in its COP1 binding domain." *EMBO J* **19**(18): 4997-5006.
- Hartl, M., M. Fussl, P. J. Boersema, J. O. Jost, K. Kramer, A. Bakirbas, J. Sindlinger, M. Plochinger, D. Leister, G. Uhrig, G. B. Moorhead, J. Cox, M. E. Salvucci, D. Schwarzer, M. Mann and I. Finkemeier (2017). "Lysine acetylome profiling uncovers novel histone deacetylase substrate proteins in Arabidopsis." *Mol Syst Biol* **13**(10): 949.
- Higashi, K., Y. Ishiga, Y. Inagaki, K. Toyoda, T. Shiraishi and Y. Ichinose (2008). "Modulation of defense signal transduction by flagellin-induced WRKY41 transcription factor in Arabidopsis thaliana." *Mol Genet Genomics* **279**(3): 303-312.
- Holmberg, C. I., S. E. Tran, J. E. Eriksson and L. Sistonen (2002). "Multisite phosphorylation provides sophisticated regulation of transcription factors." *Trends Biochem Sci* **27**(12): 619-627.
- Hu, P., W. Zhou, Z. Cheng, M. Fan, L. Wang and D. Xie (2013). "JAV1 controls jasmonate-regulated plant defense." *Mol Cell* **50**(4): 504-515.
- Hu, Y., Q. Dong and D. Yu (2012). "Arabidopsis WRKY46 coordinates with WRKY70 and WRKY53 in basal resistance against pathogen *Pseudomonas syringae*." *Plant Sci* **185-186**: 288-297.
- Hwang, I. S., S. H. An and B. K. Hwang (2011). "Pepper asparagine synthetase 1 (CaAS1) is required for plant nitrogen assimilation and defense responses to microbial pathogens." *Plant J* **67**(5): 749-762.
- Ishida, S., T. Yuasa, M. Nakata and Y. Takahashi (2008). "A tobacco calcium-dependent protein kinase, CDPK1, regulates the transcription factor REPRESSION OF SHOOT GROWTH in response to gibberellins." *Plant Cell* **20**(12): 3273-3288.

- Izawa, T., R. Foster and N. H. Chua (1993). "Plant bZIP protein DNA binding specificity." *J Mol Biol* **230**(4): 1131-1144.
- Jakoby, M., B. Weisshaar, W. Droge-Laser, J. Vicente-Carbajosa, J. Tiedemann, T. Kroj, F. Parcy and Z. I. P. R. G. b (2002). "bZIP transcription factors in Arabidopsis." *Trends Plant Sci* **7**(3): 106-111.
- Johnson, P. F. and S. L. McKnight (1989). "Eukaryotic transcriptional regulatory proteins." *Annu Rev Biochem* **58**: 799-839.
- Jones, A. M. (2009). Plant-pathogen interactions: microbial pathogenesis, plant immunity and plant-pathogen crosstalk. Doctor of Philosophy, University of California, Berkeley.
- Kaminaka, H., C. Nake, P. Epple, J. Dittgen, K. Schutze, C. Chaban, B. F. Holt, 3rd, T. Merkle, E. Schafer, K. Harter and J. L. Dangl (2006). "bZIP10-LSD1 antagonism modulates basal defense and cell death in Arabidopsis following infection." *EMBO J* **25**(18): 4400-4411.
- Katagiri, F., E. Lam and N. H. Chua (1989). "Two tobacco DNA-binding proteins with homology to the nuclear factor CREB." *Nature* **340**(6236): 727-730.
- Kazan, K. and J. M. Manners (2013). "MYC2: the master in action." *Mol Plant* **6**(3): 686-703.
- Kim, D. H. and S. Sung (2017). "The Binding Specificity of the PHD-Finger Domain of VIN3 Moderates Vernalization Response." *Plant Physiol* **173**(2): 1258-1268.
- Kim, Y. H. and W. E. Stites (2004). "Oxidation of buried cysteines is slow and an insignificant factor in the structural destabilization of staphylococcal nuclease caused by H₂O₂ exposure." *Amino Acids* **27**(2): 175-181.
- Kirby, J. and T. A. Kavanagh (2002). "NAN fusions: a synthetic sialidase reporter gene as a sensitive and versatile partner for GUS." *Plant J* **32**(3): 391-400.
- Kirchler, T. (2014). The regulation of bZIP63 through posttranslational phosphorylation and protein-protein interaction. Doctor of Philosophy, Tuebingen University.
- Kirchler, T., S. Briesemeister, M. Singer, K. Schutze, M. Keinath, O. Kohlbacher, J. Vicente-Carbajosa, M. Teige, K. Harter and C. Chaban (2010). "The role of phosphorylatable serine residues in the DNA-binding domain of Arabidopsis bZIP transcription factors." *Eur J Cell Biol* **89**(2-3): 175-183.
- Klessig, D. F., M. Tian and H. W. Choi (2016). "Multiple Targets of Salicylic Acid and Its Derivatives in Plants and Animals." *Front Immunol* **7**: 206.
- Koornneef, A., A. Leon-Reyes, T. Ritsema, A. Verhage, F. C. Den Otter, L. C. Van Loon and C. M. Pieterse (2008). "Kinetics of salicylate-mediated suppression of jasmonate signaling reveal a role for redox modulation." *Plant Physiol* **147**(3): 1358-1368.
- Kramer, U. (2015). "Planting molecular functions in an ecological context with Arabidopsis thaliana." *Elife* **4**.
- Kumar, D. and D. F. Klessig (2003). "High-affinity salicylic acid-binding protein 2 is required for plant innate immunity and has salicylic acid-stimulated lipase activity." *Proc Natl Acad Sci U S A* **100**(26): 16101-16106.
- Lam, H. M., S. S. Peng and G. M. Coruzzi (1994). "Metabolic regulation of the gene encoding glutamine-dependent asparagine synthetase in Arabidopsis thaliana." *Plant Physiol* **106**(4): 1347-1357.
- Lam, H. M., P. Wong, H. K. Chan, K. M. Yam, L. Chen, C. M. Chow and G. M. Coruzzi (2003). "Overexpression of the ASN1 gene enhances nitrogen status in seeds of Arabidopsis." *Plant Physiol* **132**(2): 926-935.
- Landt, S. G., G. K. Marinov, A. Kundaje, P. Kheradpour, F. Pauli, S. Batzoglou, B. E. Bernstein, P. Bickel, J. B. Brown, P. Cayting, Y. Chen, G. DeSalvo, C. Epstein, K. I. Fisher-Aylor, G. Euskirchen, M. Gerstein, J. Gertz, A. J. Hartemink, M. M. Hoffman, V. R. Iyer, Y. L. Jung, S. Karmakar, M. Kellis, P. V. Kharchenko, Q. Li, T. Liu, X. S. Liu, L. Ma, A. Milosavljevic, R. M. Myers, P. J. Park, M. J. Pazin, M. D. Perry, D. Raha, T. E. Reddy, J. Rozowsky, N. Shores, A. Sidow, M. Slattery, J. A. Stamatoyannopoulos, M. Y. Tolstorukov, K. P. White, S. Xi, P. J. Farnham, J. D. Lieb, B. J. Wold and

- M. Snyder (2012). "ChIP-seq guidelines and practices of the ENCODE and modENCODE consortia." *Genome Res* **22**(9): 1813-1831.
- Le Roux, C., G. Huet, A. Jauneau, L. Camborde, D. Tremousaygue, A. Kraut, B. Zhou, M. Levailant, H. Adachi, H. Yoshioka, S. Raffaele, R. Berthome, Y. Coute, J. E. Parker and L. Deslandes (2015). "A receptor pair with an integrated decoy converts pathogen disabling of transcription factors to immunity." *Cell* **161**(5): 1074-1088.
- Li, B., X. Meng, L. Shan and P. He (2016). "Transcriptional Regulation of Pattern-Triggered Immunity in Plants." *Cell Host Microbe* **19**(5): 641-650.
- Li, Y., L. Chen, J. Mu and J. Zuo (2013). "LESION SIMULATING DISEASE1 interacts with catalases to regulate hypersensitive cell death in Arabidopsis." *Plant Physiol* **163**(2): 1059-1070.
- Liu, G., S. Gao, H. Tian, W. Wu, H. S. Robert and Z. Ding (2016). "Local Transcriptional Control of YUCCA Regulates Auxin Promoted Root-Growth Inhibition in Response to Aluminium Stress in Arabidopsis." *PLoS Genet* **12**(10): e1006360.
- Liu, L., F. M. Sonbol, B. Huot, Y. Gu, J. Withers, M. Mwimba, J. Yao, S. Y. He and X. Dong (2016). "Salicylic acid receptors activate jasmonic acid signalling through a non-canonical pathway to promote effector-triggered immunity." *Nat Commun* **7**: 13099.
- Liu, Y. and C. He (2017). "A review of redox signaling and the control of MAP kinase pathway in plants." *Redox Biol* **11**: 192-204.
- Llorca, C. M., K. W. Berendzen, W. A. Malik, S. Mahn, H. P. Piepho and U. Zentgraf (2015). "The Elucidation of the Interactome of 16 Arabidopsis bZIP Factors Reveals Three Independent Functional Networks." *PLoS One* **10**(10): e0139884.
- Llorca, C. M., M. Potschin and U. Zentgraf (2014). "bZIPs and WRKYs: two large transcription factor families executing two different functional strategies." *Front Plant Sci* **5**: 169.
- Lorenzo, O., J. M. Chico, J. J. Sanchez-Serrano and R. Solano (2004). "JASMONATE-INSENSITIVE1 encodes a MYC transcription factor essential to discriminate between different jasmonate-regulated defense responses in Arabidopsis." *Plant Cell* **16**(7): 1938-1950.
- Lupas, A. (1996). "Coiled coils: new structures and new functions." *Trends Biochem Sci* **21**(10): 375-382.
- Macian, F., C. Lopez-Rodriguez and A. Rao (2001). "Partners in transcription: NFAT and AP-1." *Oncogene* **20**(19): 2476-2489.
- Mahoney, C. W., J. Shuman, S. L. McKnight, H. C. Chen and K. P. Huang (1992). "Phosphorylation of CCAAT-enhancer binding protein by protein kinase C attenuates site-selective DNA binding." *J Biol Chem* **267**(27): 19396-19403.
- Mair, A., L. Pedrotti, B. Wurzinger, D. Anrather, A. Simeunovic, C. Weiste, C. Valerio, K. Dietrich, T. Kirchler, T. Nagele, J. Vicente Carbajosa, J. Hanson, E. Baena-Gonzalez, C. Chaban, W. Weckwerth, W. Droge-Laser and M. Teige (2015). "SnRK1-triggered switch of bZIP63 dimerization mediates the low-energy response in plants." *Elife* **4**.
- Manohar, M., M. Tian, M. Moreau, S. W. Park, H. W. Choi, Z. Fei, G. Friso, M. Asif, P. Manosalva, C. C. von Dahl, K. Shi, S. Ma, S. P. Dinesh-Kumar, I. O'Doherty, F. C. Schroeder, K. J. van Wijk and D. F. Klessig (2014). "Identification of multiple salicylic acid-binding proteins using two high throughput screens." *Front Plant Sci* **5**: 777.
- Mao, P., M. Duan, C. Wei and Y. Li (2007). "WRKY62 transcription factor acts downstream of cytosolic NPR1 and negatively regulates jasmonate-responsive gene expression." *Plant Cell Physiol* **48**(6): 833-842.
- Martin, M. (2011). "Cutadapt Removes Adapter Sequences From High-Throughput Sequencing Reads." *EMBnet.journal* **17**(1): 10-12.
- Martinez, C., E. Pons, G. Prats and J. Leon (2004). "Salicylic acid regulates flowering time and links defence responses and reproductive development." *Plant J* **37**(2): 209-217.

- Mateo, A., D. Funck, P. Muhlenbock, B. Kular, P. M. Mullineaux and S. Karpinski (2006). "Controlled levels of salicylic acid are required for optimal photosynthesis and redox homeostasis." *J Exp Bot* **57**(8): 1795-1807.
- Medina-Puche, L., M. J. Castello, J. V. Canet, J. Lamilla, M. L. Colombo and P. Tornero (2017). "beta-carbonic anhydrases play a role in salicylic acid perception in Arabidopsis." *PLoS One* **12**(7): e0181820.
- Melotto, M., W. Underwood, J. Koczan, K. Nomura and S. Y. He (2006). "Plant stomata function in innate immunity against bacterial invasion." *Cell* **126**(5): 969-980.
- Meshi, T. and M. Iwabuchi (1995). "Plant transcription factors." *Plant Cell Physiol* **36**(8): 1405-1420.
- Miao, Y., T. Laun, P. Zimmermann and U. Zentgraf (2004). "Targets of the WRKY53 transcription factor and its role during leaf senescence in Arabidopsis." *Plant Mol Biol* **55**(6): 853-867.
- Mignolet-Spruyt, L., E. Xu, N. Idanheimo, F. A. Hoeberichts, P. Muhlenbock, M. Brosche, F. Van Breusegem and J. Kangasjarvi (2016). "Spreading the news: subcellular and organellar reactive oxygen species production and signalling." *J Exp Bot* **67**(13): 3831-3844.
- Miller, M., J. D. Shuman, T. Sebastian, Z. Dauter and P. F. Johnson (2003). "Structural basis for DNA recognition by the basic region leucine zipper transcription factor CCAAT/enhancer-binding protein alpha." *J Biol Chem* **278**(17): 15178-15184.
- Mone, Y., D. Monnin and N. Kremer (2014). "The oxidative environment: a mediator of interspecies communication that drives symbiosis evolution." *Proc Biol Sci* **281**(1785): 20133112.
- Mur, L. A., P. Kenton, R. Atzorn, O. Miersch and C. Wasternack (2006). "The outcomes of concentration-specific interactions between salicylate and jasmonate signaling include synergy, antagonism, and oxidative stress leading to cell death." *Plant Physiol* **140**(1): 249-262.
- Mwimba, M. and X. Dong (2017). "The CAT(2) Comes Back." *Cell Host Microbe* **21**(2): 125-127.
- Nagahara, N. (2011). "Intermolecular disulfide bond to modulate protein function as a redox-sensing switch." *Amino Acids* **41**(1): 59-72.
- Navrot, N., C. Finnie, B. Svensson and P. Hagglund (2011). "Plant redox proteomics." *J Proteomics* **74**(8): 1450-1462.
- Nijhawan, A., M. Jain, A. K. Tyagi and J. P. Khurana (2008). "Genomic survey and gene expression analysis of the basic leucine zipper transcription factor family in rice." *Plant Physiol* **146**(2): 333-350.
- Olea, F., A. Perez-Garcia, F. R. Canton, M. E. Rivera, R. Canas, C. Avila, F. M. Cazorla, F. M. Canovas and A. de Vicente (2004). "Up-regulation and localization of asparagine synthetase in tomato leaves infected by the bacterial pathogen *Pseudomonas syringae*." *Plant Cell Physiol* **45**(6): 770-780.
- Pabo, C. O. and R. T. Sauer (1992). "Transcription factors: structural families and principles of DNA recognition." *Annu Rev Biochem* **61**: 1053-1095.
- Phillips, T. (2008). "Regulation of Transcription and Gene Expression in Eukaryotes." *Nature Education* **1**(1): 199.
- Phillips, T. and L. Hoopes (2008). "Transcription factors and transcriptional control in eukaryotic cells." *Nature Education* **1**(1): 119.
- Pieterse, C. M., D. Van der Does, C. Zamioudis, A. Leon-Reyes and S. C. Van Wees (2012). "Hormonal modulation of plant immunity." *Annu Rev Cell Dev Biol* **28**: 489-521.
- Ptashne, M. (1988). "How eukaryotic transcriptional activators work." *Nature* **335**(6192): 683-689.
- Ram, H. and S. Chattopadhyay (2013). "Molecular interaction of bZIP domains of GBF1, HY5 and HYH in Arabidopsis seedling development." *Plant Signal Behav* **8**(1): e22703.

- Ramegowda, V., U. S. Gill, P. N. Sivalingam, A. Gupta, C. Gupta, G. Govind, K. N. Nataraja, A. Pereira, M. Udayakumar, K. S. Mysore and M. Senthil-Kumar (2017). "GBF3 transcription factor imparts drought tolerance in *Arabidopsis thaliana*." *Sci Rep* **7**(1): 9148.
- Riechmann, J. L., J. Heard, G. Martin, L. Reuber, C. Jiang, J. Keddie, L. Adam, O. Pineda, O. J. Ratcliffe, R. R. Samaha, R. Creelman, M. Pilgrim, P. Broun, J. Z. Zhang, D. Ghandehari, B. K. Sherman and G. Yu (2000). "Arabidopsis transcription factors: genome-wide comparative analysis among eukaryotes." *Science* **290**(5499): 2105-2110.
- Rizzi, Y. S., N. M. Cecchini, G. Fabro and M. E. Alvarez (2017). "Differential control and function of *Arabidopsis* ProDH1 and ProDH2 genes on infection with biotrophic and necrotrophic pathogens." *Mol Plant Pathol* **18**(8): 1164-1174.
- Ryu, H., K. Kim, H. Cho, J. Park, S. Choe and I. Hwang (2007). "Nucleocytoplasmic shuttling of BZR1 mediated by phosphorylation is essential in *Arabidopsis* brassinosteroid signaling." *Plant Cell* **19**(9): 2749-2762.
- Schutze, K., K. Harter and C. Chaban (2008). "Post-translational regulation of plant bZIP factors." *Trends Plant Sci* **13**(5): 247-255.
- Seifi, H., D. De Vleeschauwer, A. Aziz and M. Hofte (2014). "Modulating plant primary amino acid metabolism as a necrotrophic virulence strategy: the immune-regulatory role of asparagine synthetase in *Botrytis cinerea*-tomato interaction." *Plant Signal Behav* **9**(2): e27995.
- Seifi, H. S., J. Van Bockhaven, G. Angenon and M. Hofte (2013). "Glutamate metabolism in plant disease and defense: friend or foe?" *Mol Plant Microbe Interact* **26**(5): 475-485.
- Seyfferth, C. and K. Tsuda (2014). "Salicylic acid signal transduction: the initiation of biosynthesis, perception and transcriptional reprogramming." *Front Plant Sci* **5**: 697.
- Shaikhali, J., L. Noren, J. de Dios Barajas-Lopez, V. Srivastava, J. Konig, U. H. Sauer, G. Wingsle, K. J. Dietz and A. Strand (2012). "Redox-mediated mechanisms regulate DNA binding activity of the G-group of basic region leucine zipper (bZIP) transcription factors in *Arabidopsis*." *J Biol Chem* **287**(33): 27510-27525.
- Slaymaker, D. H., D. A. Navarre, D. Clark, O. del Pozo, G. B. Martin and D. F. Klessig (2002). "The tobacco salicylic acid-binding protein 3 (SABP3) is the chloroplast carbonic anhydrase, which exhibits antioxidant activity and plays a role in the hypersensitive defense response." *Proc Natl Acad Sci U S A* **99**(18): 11640-11645.
- Smykowski, A., S. M. Fischer and U. Zentgraf (2015). "Phosphorylation Affects DNA-Binding of the Senescence-Regulating bZIP Transcription Factor GBF1." *Plants (Basel)* **4**(3): 691-709.
- Spadaro, D., B. W. Yun, S. H. Spoel, C. Chu, Y. Q. Wang and G. J. Loake (2010). "The redox switch: dynamic regulation of protein function by cysteine modifications." *Physiol Plant* **138**(4): 360-371.
- Spoel, S. H., J. S. Johnson and X. Dong (2007). "Regulation of tradeoffs between plant defenses against pathogens with different lifestyles." *Proc Natl Acad Sci U S A* **104**(47): 18842-18847.
- Suckow, M., B. von Wilcken-Bergmann and B. Muller-Hill (1993). "Identification of three residues in the basic regions of the bZIP proteins GCN4, C/EBP and TAF-1 that are involved in specific DNA binding." *EMBO J* **12**(3): 1193-1200.
- Tabata, T., H. Takase, S. Takayama, K. Mikami, A. Nakatsuka, T. Kawata, T. Nakayama and M. Iwabuchi (1989). "A protein that binds to a cis-acting element of wheat histone genes has a leucine zipper motif." *Science* **245**(4921): 965-967.
- Tachibana, T., S. Okazaki, A. Murayama, A. Naganuma, A. Nomoto and S. Kuge (2009). "A major peroxiredoxin-induced activation of Yap1 transcription factor is mediated by reduction-sensitive disulfide bonds and reveals a low level of transcriptional activation." *J Biol Chem* **284**(7): 4464-4472.
- Tada, Y., S. H. Spoel, K. Pajerowska-Mukhtar, Z. Mou, J. Song, C. Wang, J. Zuo and X. Dong (2008). "Plant immunity requires conformational changes [corrected] of NPR1 via S-nitrosylation and thioredoxins." *Science* **321**(5891): 952-956.

- Tian, M., C. C. von Dahl, P. P. Liu, G. Friso, K. J. van Wijk and D. F. Klessig (2012). "The combined use of photoaffinity labeling and surface plasmon resonance-based technology identifies multiple salicylic acid-binding proteins." *Plant J* **72**(6): 1027-1038.
- Tjian, R. and T. Maniatis (1994). "Transcriptional activation: a complex puzzle with few easy pieces." *Cell* **77**(1): 5-8.
- Tome, F., T. Nagele, M. Adamo, A. Garg, C. Marco-Llorca, E. Nukarinen, L. Pedrotti, A. Peviani, A. Simeunovic, A. Tatkiewicz, M. Tomar and M. Gamm (2014). "The low energy signaling network." *Front Plant Sci* **5**: 353.
- Tun, N. N., C. Santa-Catarina, T. Begum, V. Silveira, W. Handro, E. I. Floh and G. F. Scherer (2006). "Polyamines induce rapid biosynthesis of nitric oxide (NO) in *Arabidopsis thaliana* seedlings." *Plant Cell Physiol* **47**(3): 346-354.
- Uhrig, R. G., A. M. Labandera and G. B. Moorhead (2013). "Arabidopsis PPP family of serine/threonine protein phosphatases: many targets but few engines." *Trends Plant Sci* **18**(9): 505-513.
- Van Wees, S. C., J. A. Van Pelt, P. A. Bakker and C. M. Pieterse (2013). "Bioassays for assessing jasmonate-dependent defenses triggered by pathogens, herbivorous insects, or beneficial rhizobacteria." *Methods Mol Biol* **1011**: 35-49.
- Verhage, A., I. Vlaardingerbroek, C. Raaymakers, N. M. Van Dam, M. Dicke, S. C. Van Wees and C. M. Pieterse (2011). "Rewiring of the Jasmonate Signaling Pathway in *Arabidopsis* during Insect Herbivory." *Front Plant Sci* **2**: 47.
- Vlot, A. C., D. A. Dempsey and D. F. Klessig (2009). "Salicylic Acid, a multifaceted hormone to combat disease." *Annu Rev Phytopathol* **47**: 177-206.
- Vlot, A. C., P. P. Liu, R. K. Cameron, S. W. Park, Y. Yang, D. Kumar, F. Zhou, T. Padukkavidana, C. Gustafsson, E. Pichersky and D. F. Klessig (2008). "Identification of likely orthologs of tobacco salicylic acid-binding protein 2 and their role in systemic acquired resistance in *Arabidopsis thaliana*." *Plant J* **56**(3): 445-456.
- Wachter, A., M. Tunc-Ozdemir, B. C. Grove, P. J. Green, D. K. Shintani and R. R. Breaker (2007). "Riboswitch control of gene expression in plants by splicing and alternative 3' end processing of mRNAs." *Plant Cell* **19**(11): 3437-3450.
- Wang, Y. Q., A. Feechan, B. W. Yun, R. Shafiei, A. Hofmann, P. Taylor, P. Xue, F. Q. Yang, Z. S. Xie, J. A. Pallas, C. C. Chu and G. J. Loake (2009). "S-nitrosylation of AtSABP3 antagonizes the expression of plant immunity." *J Biol Chem* **284**(4): 2131-2137.
- Wasternack, C. and B. Hause (2013). "Jasmonates: biosynthesis, perception, signal transduction and action in plant stress response, growth and development. An update to the 2007 review in *Annals of Botany*." *Ann Bot* **111**(6): 1021-1058.
- Waszczak, C., S. Akter, S. Jacques, J. Huang, J. Messens and F. Van Breusegem (2015). "Oxidative post-translational modifications of cysteine residues in plant signal transduction." *J Exp Bot* **66**(10): 2923-2934.
- Watson, D. K., R. Kitching, C. Vary, I. Kola and A. Seth (2000). "Isolation of target gene promoter/enhancer sequences by whole genome PCR method." *Methods Mol Biol* **130**: 1-11.
- Weisshaar, B., G. A. Armstrong, A. Block, O. da Costa e Silva and K. Hahlbrock (1991). "Light-inducible and constitutively expressed DNA-binding proteins recognizing a plant promoter element with functional relevance in light responsiveness." *EMBO J* **10**(7): 1777-1786.
- Weiste, C., L. Pedrotti, J. Selvanayagam, P. Muralidhara, C. Froschel, O. Novak, K. Ljung, J. Hanson and W. Droge-Laser (2017). "The *Arabidopsis* bZIP11 transcription factor links low-energy signalling to auxin-mediated control of primary root growth." *PLoS Genet* **13**(2): e1006607.
- Weltmeier, F., A. Ehlert, C. S. Mayer, K. Dietrich, X. Wang, K. Schutze, R. Alonso, K. Harter, J. Vicente-Carbajosa and W. Droge-Laser (2006). "Combinatorial control of *Arabidopsis* proline dehydrogenase transcription by specific heterodimerisation of bZIP transcription factors." *EMBO J* **25**(13): 3133-3143.

- Weltmeier, F., F. Rahmani, A. Ehlert, K. Dietrich, K. Schutze, X. Wang, C. Chaban, J. Hanson, M. Teige, K. Harter, J. Vicente-Carbajosa, S. Smeeckens and W. Droge-Laser (2009). "Expression patterns within the Arabidopsis C/S1 bZIP transcription factor network: availability of heterodimerization partners controls gene expression during stress response and development." *Plant Mol Biol* **69**(1-2): 107-119.
- Whitmarsh, A. J. and R. J. Davis (2000). "Regulation of transcription factor function by phosphorylation." *Cell Mol Life Sci* **57**(8-9): 1172-1183.
- Wood, M. J., G. Storz and N. Tjandra (2004). "Structural basis for redox regulation of Yap1 transcription factor localization." *Nature* **430**(7002): 917-921.
- Wu, F. H., S. C. Shen, L. Y. Lee, S. H. Lee, M. T. Chan and C. S. Lin (2009). "Tape-Arabidopsis Sandwich - a simpler Arabidopsis protoplast isolation method." *Plant Methods* **5**: 16.
- Wu, X., M. H. Oh, E. M. Schwarz, C. T. Larue, M. Sivaguru, B. S. Imai, P. M. Yau, D. R. Ort and S. C. Huber (2011). "Lysine acetylation is a widespread protein modification for diverse proteins in Arabidopsis." *Plant Physiol* **155**(4): 1769-1778.
- Xu, Z. Y., S. Y. Kim, Y. Hyeon do, D. H. Kim, T. Dong, Y. Park, J. B. Jin, S. H. Joo, S. K. Kim, J. C. Hong, D. Hwang and I. Hwang (2013). "The Arabidopsis NAC transcription factor ANAC096 cooperates with bZIP-type transcription factors in dehydration and osmotic stress responses." *Plant Cell* **25**(11): 4708-4724.
- Xue, B., R. L. Dunbrack, R. W. Williams, A. K. Dunker and V. N. Uversky (2010). "PONDR-FIT: a meta-predictor of intrinsically disordered amino acids." *Biochim Biophys Acta* **1804**(4): 996-1010.
- Yang, X. J. and E. Seto (2008). "Lysine acetylation: codified crosstalk with other posttranslational modifications." *Mol Cell* **31**(4): 449-461.
- Yoshida, T., Y. Fujita, K. Maruyama, J. Mogami, D. Todaka, K. Shinozaki and K. Yamaguchi-Shinozaki (2015). "Four Arabidopsis AREB/ABF transcription factors function predominantly in gene expression downstream of SnRK2 kinases in abscisic acid signalling in response to osmotic stress." *Plant Cell Environ* **38**(1): 35-49.
- Yuan, H. M., W. C. Liu and Y. T. Lu (2017). "CATALASE2 Coordinates SA-Mediated Repression of Both Auxin Accumulation and JA Biosynthesis in Plant Defenses." *Cell Host Microbe* **21**(2): 143-155.
- Zaffagnini, M., M. De Mia, S. Morisse, N. Di Giacinto, C. H. Marchand, A. Maes, S. D. Lemaire and P. Trost (2016). "Protein S-nitrosylation in photosynthetic organisms: A comprehensive overview with future perspectives." *Biochim Biophys Acta* **1864**(8): 952-966.
- Zheng, M., F. Aslund and G. Storz (1998). "Activation of the OxyR transcription factor by reversible disulfide bond formation." *Science* **279**(5357): 1718-1721.
- Zheng, X. Y., N. W. Spivey, W. Zeng, P. P. Liu, Z. Q. Fu, D. F. Klessig, S. Y. He and X. Dong (2012). "Coronatine promotes *Pseudomonas syringae* virulence in plants by activating a signaling cascade that inhibits salicylic acid accumulation." *Cell Host Microbe* **11**(6): 587-596.
- Zhou, Q., T. G. Boyer and A. J. Berk (1993). "Factors (TAFs) required for activated transcription interact with TATA box-binding protein conserved core domain." *Genes Dev* **7**(2): 180-187.

8. List of Publications

1. Tomé F, Nägele T, Adamo M, **Garg A**, Marco-Llorca C, Nukarinen E, Pedrotti L, Peviani A, Simeunovic A, Tatkiewicz A, Tomar M, Gamm M.
The low energy signaling network.
Front Plant Sci. 2014 Jul 17;5:353.

9. Curriculum Vitae

PERSONAL INFORMATION

Name: Abhroop Garg

Date of Birth: 2nd September 1985

Nationality: Indian

EDUCATIONAL QUALIFICATIONS

09/2011 - Present	PhD Student in Biology Zentrum für Molekularbiologie der Pflanzen, Eberhard Karls Universität, Tübingen, Germany
09/2008 – 08/2009	MSc Industrial and Commercial Biotechnology Newcastle University, Newcastle upon Tyne, UK.
01/2004 – 12/2007	Bachelor of Technology (Biotechnology) S.V.B.P. University of Science and Technology, Meerut, India

RESEARCH EXPERIENCE

09/2009 – 07/2010	Guest member of staff, Newcastle Institute for Research on Environment and Sustainability (NIREs), UK.
08/ 2010 – 01/2011	Internship Newcastle University Proten and Proteome Analysis (NUPPA), UK.

10. Acknowledgements

First and foremost I would like to express my gratitude to my supervisor Dr. Christina Chaban for believing in me and giving me the opportunity to work on such an interesting topic. My research would not have been completed successfully without your constant guidance and support, especially during the times when things did not work well.

I would like to thank Prof. Dr. Klaus Harter for his ever-friendly nature, constant guidance and support that has enabled me to grow as a scientist. I would additionally like to thank Prof. Dr. Klaus Harter and Prof. Dr. Ulrike Zentgraf for taking the time to evaluate my thesis. I cannot think of any better place to be other than ZMBP to have done my PhD, around such wonderful and supportive people who inspired me to excel in my research. I would also like to thank my all the examiners on my defense panel - Prof. Dr. Klaus Harter, Prof. Dr. Ulrike Zentgraf, Prof. Dr. Gabriel Schaaf and Dr. Laura Ragni, firstly for their valuable time and most importantly for accommodating my request at such a short notice. I would be ever grateful for their helpfulness.

A big thank you to Ms. Charlotte Consuelo Rehm for going out of her way in helping me with my visa application, accommodation and initial bureaucratic processes in Tuebingen when I first reached Germany, and also for helping me throughout my PhD. It was very kind of her.

I would like to give a special thanks to all the “MERIT” members, students and PI’s alike, for their ever useful inputs, the various successful collaborations, the organization of workshops and training activities, and last but not the least for the fun times during as well as outside the MERIT program.

The Avengers group needs a special mention here – I thank Tobi, Jochen and Sven very much for helping me during my research work with interesting ideas, suggestions, sometimes annoying questions and of course, for their friendship.

I would like to thank all the members of my lab, past and present – Kerstin Haible, Christel Mattern, Petra Neumann, Anne, Rebecca, Heunes and Juan for providing such an amazing fun working environment and for all the useful discussions, help and support during my research work. It has been incredible to work with them, not to mention the parties after

work. Additionally, I would like to thank Christel and Kerstin for all their help with some of my experiments and making my research go quicker and smoother.

I would also like to thank my friends and colleagues at ZMBP who made my life inside and outside the lab a bit easier. A special thanks to Marcella, Arvid, Deb, Nargis, Niklas, and Joachim.

I am grateful to all my collaborators- Dr. Wees, Ms. Merel Steenbergen, Dr. Lorenzo Pedrotti, Dr, Stefan Czernel, Christa Lanz, Dr. Joachim Kilian, Dr. Boris Macek and Dr. Mirita Franz, for their invaluable help.

A big special thanks to Philipp and Margaux, not only for their suggestions, help and ideas at work, but also for their invaluable friendship and support during my time in Tuebingen; and additionally for all the fun trips we have had together. They will be missed the most!

I am thankful to all my friends in Tübingen (Prateek, Bala, Janani, Siva, Anurag, Anjali, Martina, Prajwal, Ruchika, *etc*) and back home for all the amazing memories.

I cannot thank Vaishnavi enough, for bearing with me, for encouraging me and for providing the emotional and mental support during the ups and downs of this journey. This would have been very, very difficult if it wasn't for her.

And last but not the least, I am extremely thankful to my mother, my father and my sister Ginni, for their never-ending support throughout all these years.